UC Berkeley
UC Berkeley Electronic Theses and Dissertations

Title
The Downstream Geomorphic Effects of Dams: A Comprehensive and Comparative Approach

Permalink
https://escholarship.org/uc/item/1f8612f9

Author
Minear, Justin Toby

Publication Date
2010

Peer reviewed|Thesis/dissertation

eScholarship.org Powered by the California Digital Library
University of California

The Downstream Geomorphic Effects of Dams:
A Comprehensive and Comparative Approach

by

Justin Toby Minear

A dissertation submitted in partial satisfaction of the

requirements for the degree of

Doctor of Philosophy

in

Landscape Architecture and Environmental Planning

in the

Graduate Division

of the

University of California, Berkeley

Committee in charge:

Professor G. Mathias Kondolf, Chair
Professor William E. Dietrich
Professor Vincent H. Resh
Professor Joseph R. McBride

Fall 2010

The Downstream Geomorphic Effects of Dams:
A Comprehensive and Comparative Approach

Copyright © 2010

Justin Toby Minear

Table of Contents

Acknowledgements

I am indebted to many people at Berkeley but first and foremost among them, I would like to thank Matt Kondolf and Bill Dietrich for their support and advice. While Matt and Bill have distinct approaches to advising and geomorphology, I appreciate that they both care deeply about their students and the natural world. Matt's insights into the fields of geomorphology and restoration lead me down many fruitful intellectual paths and he has been supportive and patient with my attempts to forge new paths in those woods. Bill Dietrich has been an exemplary model as a teacher and scholar – his ability to quickly expose fundamental issues in scientific arguments is a wonder that I constantly will attempt to attain through my professional life. His personal pursuit of peerless scholarship, quantitative rigor and clarity of thought and word has opened my mind to what excellent science is all about.

I am deeply indebted to my committee members for their thoughtful feedback and assistance through the course of my studies. Vince Resh is a constant well of positive support and encouragement – I wish I could take him with me when I go. Joe McBride has given very helpful advice, particularly in the planning stages of this study. Many thanks to the field helpers that assisted with field work.

I would like to thank the CalFed-Sea Grant Program for their generous support over the course of several years when I was a CalFed Science Fellow (U-04-SC-005). Many thanks also to the Beatrix Farrand Fund at U.C. Berkeley for providing funds to improve Chapter 4.

Many thanks to the editors at Water Resources Research, in which an excerpt from Chapter 2 was published last year. I am indebted to reviewers William Renwick and Greg Morris and an anonymous reviewer for their comments, Bob Stallard and Dave Mixon for sharing the RESIS-II database and insights regarding data quality, Blair Greimann and Cope Willis for sharing reservoir sedimentation data, and Jim Kirchner for advice on statistical approaches.

On a personal level, I could not have done this without the love and support of my wife, Sarah Thomas. She is a marvel and lights up my life.

Abstract

The Downstream Geomorphic Effects of Dams:
A Comprehensive and Comparative Approach

by

Justin Toby Minear

Doctor of Philosophy in Landscape Architecture and Environmental Planning

University of California, Berkeley

Professor G. Mathias Kondolf, Chair

Large dams commonly alter the natural regimes of hydrologic and sediment processes that are critical for the maintenance of native instream and riparian communities, often affecting landscapes hundreds of kilometers from the dam. California has over 1,400 large dams, some of which have been in place for over 100 years. As a consequence, the legacy of large dam construction has greatly altered California's natural hydrologic and sediment processes.

Previous attempts to estimate the effects of multiple large dams on sediment processes have ignored two key factors for large spatial and temporal modeling: sediment trapping due to multiple dams in the same watershed and decreasing sediment trapping as reservoirs fill. Here, I develop a spreadsheet-based model that incorporates both factors. Using California as a case study, measured sedimentation rates first were used to estimate sediment yields for distinct geomorphic regions and the rates then were applied to unmeasured reservoirs by region. The results of the model show that statewide reservoirs have likely filled with 2.1 billion m^3 of sediment to date, decreasing total reservoir capacity by 4.5%. In addition, approximately 200 reservoirs have likely lost more than half their initial capacity to sedimentation.

Fourteen of the fifteen major tributaries to the Sacramento-San Joaquin river system in California are dammed by "foothill" dams, very large dams situated at the base of the mountain fronts. Constructed primarily in the 1940s-1970s, the foothill dams include some of the largest dams in the United States. In addition to blocking access to migrating endangered salmonids, the dams have further altered downstream hydrologic and sediment processes by changing flow-duration and frequencies and releasing sediment-free flows. There has been no comprehensive effort to evaluate the long-term changes in magnitude and frequency of sediment transport downstream of these dams, despite hundreds of millions of dollars spent on restoration efforts. In this study, I evaluate the different effects of the foothill dams on downstream rivers using hydrologic

analyses of pre- and post-dam flows, calculations of bedload transport from an extensive literature search and field data, and field observations using gravel tracer and monitored cross sections from water year 2006 (WY2006) to test the results of the bedload transport calculations. From the results of the hydrologic analysis, the average reduction in the 2-year return interval flow for the dams is 65%, however, there is a wide range in the results, with some post-dam flows remaining equal to pre-dam magnitudes, particularly at larger return intervals. Using topographic data and tracer gravel collected during water year 2006, extensive gravel movement was observed downstream of the dams, indicating that even after 50+ years of operation, the riverbeds below the dams are continuing to transport sediment and still are responding to the cessation in supply. From the calculation of bedload transport for each of the major tributaries, post-dam annual bedload transport has fallen by an average of 45%, with total bedload of particles greater than 8mm decreasing by 42%. Some rivers, while having reductions in flood flows, had increases in bedload transport downstream of the dam, primarily due to increases in medium-magnitude medium-frequency events. Bedload is still transported at high rates for most sites, with eleven of the fourteen rivers transporting more than 100,000 m^3 / yr in the post-dam period. Effective discharge in these channels is difficult to determine due to confounding factors, however, the majority of the rivers have a high-percentage of total bedload transported at discharges larger than the 5-year return interval suggesting that higher discharge events tend to dominate the channel response.

A sediment budget was constructed for both coarse and total sediment for each of the fourteen major tributaries to the Sacramento-San Joaquin river system downstream of the major "foothill" dams. The methods used to construct the sediment budget include a reservoir sedimentation model, bedload transport equations, and suspended and bedload measurements from gaging stations. The results of the sediment budget indicate a volume of approximately 244 million m^3 of sediment is trapped behind dams in the upper watersheds, and 4.0 million m^3 is trapped by the dams each year. With the exception of the mainstem Sacramento River, very little bedload material is supplied by smaller tributaries to the gravel-bed reaches downstream of the foothill dams. Ten of the fourteen rivers do not have enough supply from small tributaries to meet the calculated average annual bedload transport. Several of the rivers (Putah Creek, the Mokelumne River, and the San Joaquin River) may be strongly affected by small tributaries downstream of the dams because they have relatively large watersheds downstream of the dams and highly reduced post-dam transport ability. Approximately 267,000 m^3 of gravel has been artificially augmented into Sacramento-San Joaquin tributaries downstream of the foothill dams through 2004. While gravel augmentation projects have been extensive on six of the rivers, they are minimal or absent on the other eight rivers. Overall, gravel is augmented at only 3.7% of the post-dam bedload transport capacity, however, some rivers with highly reduced flows have had gravel augmented at rates that approach the post-dam gravel transport rate, primarily due to the large post-dam reduction in bedload transport.

Chapter 1: Introduction

Natural regimes of hydrologic and geomorphic processes are critical for the maintenance of native instream and riparian communities (Poff and Ward 1989, Gregory et al. 1991, Poff et al. 1997). High flows disturb river channels, banks, and floodplains, thereby generating new landforms and areas for colonization by both riparian and instream communities (Gregory et al. 1991). Thus at any one time, due to geomorphic disturbance, a river has a suite of habitat types each occupied by different species assemblages forming a diverse patchwork of species and habitats (Resh et al. 1988, Naiman and Decamps 1997). Native riparian plants, such as cottonwoods, and instream organisms depend on natural flow regimes because they have life-history strategies that are timed to exploit the timing and magnitude of natural flow events (Poff and Ward 1989, Naiman and Decamps 1997, Mahoney and Rood 1998).

Large dams, due to their capacity to store large amounts of water, have the potential to disrupt the natural flow regime and sediment supply in downstream rivers, thus altering the physical template on which instream and riparian communities depend (Petts 1979, Petts 1984, Williams and Wolman 1984, Collier et al. 1996, Richter et al. 1996, Grant et al. 2003). The most common downstream hydrologic effects of large dams are decreased magnitude and frequency of high flows, increased duration and magnitude of low flows, decreased connectivity between the channel and floodplain, altered timing of flow during the year, and altered temperature regimes (Ward and Stanford 1979, Petts 1984, Collier et al. 1996, Nilsson and Berggren 2000). The dam-induced reduction in scouring peak flows and an increase in low flows often allows vegetation to encroach onto previous streambed surfaces (Wilcock et al. 1996, Surian 1999), thereby further reducing instream habitat and sediment supply. Recruitment of riparian vegetation has been found to decrease below dams for certain riparian species, such as cottonwoods, that depend on occasional disturbance and consistent stage reduction through the seed germination period (Mahoney and Rood 1998, Everitt 1995, Johnson 2002, Nakamura and Shin 2001). Riparian and instream communities typically respond to the alteration of natural flow by shifting towards less diverse communities, often with high numbers of invasive species (Ward and Stanford 1979, Petts 1984). Native instream communities in regions with high inter- and intra-annual variation in climate, like California, are particularly susceptible to dam-induced flow alterations compared to communities in more temperate regions (Gasith and Resh 1999, Poff and Ward 1989).

In addition to altering flow regimes, large dams trap all coarse sediment and nearly all of the fine sediment within their upstream reservoirs (Brune 1953). This sediment trapping starves downstream channels of both bedload and suspended sediment supply, resulting in bed incision as material is excavated from the bed (Gilbert 1917, Williams and Wolman 1984, Kondolf 1997, Vericat and Batalla 2006), and often causes a concurrent bed material coarsening (Williams and Wolman 1984, Petts 1979, Dietrich et al. 1989). Incision of the river bed may further decouple the river channel from its surrounding floodplain (Williams and Wolman 1984). The dam-related changes in sediment supply and transport can extend for hundreds of kilometers downstream of the dam and takes decades for the river to fully respond to post-dam conditions (Williams and Wolman 1984, Andrews 1984, Hazel et al. 2006). The biological effects of dam-related sediment trapping can include reduction in spawning gravel supply for salmonids (Kondolf and Matthews 1993), reduction in fine-sediment deposits (Hazel et al. 2006) utilized by riparian tree seedlings, and increased instream light penetration, which can increase the standing stock of benthic algae and macrophyte communities (Lowe 1979).

Large dams in California

In California, extensive dam construction has occurred over the last century and a half, with currently over 1,400 large dams in the state (Figure 1). Dam construction in California peaked in the 1960s and 1970s, with the construction of the massive "foothill" dams, located on the major tributaries to the Sacramento-San Joaquin river system, in the foothills between the mountains and the alluvial Central Valley (Figure 2). These foothill dams include some of the largest dams in the United States. The location of these dams, intercepting water and sediment mountain regions before it reaches the plains, has greatly reduced sediment supply to the lower rivers. Fourteen of the fifteen major tributaries to the Sacramento-San Joaquin river system have been dammed by foothill dams, with only one remaining relatively undammed major river, the Cosumnes River.

Biologically, one of the most destructive effects of the foothill dams was the blocking of access to upstream habitat for native salmonids, such as the Chinook salmon (Yoshiyama et al. 1996) and Steelhead trout (Lindley et al. 2006). Seventy to ninety percent of the available upstream habitat was blocked by the foothill dams on most river systems (Yoshiyama et al. 1996, Lindley et al. 2006), leaving less than thirty percent available downstream of the dams, primarily in the Middle Sacramento River and its undammed tributaries. Unfortunately, much of the remaining habitat (downstream of the dams) does not contain suitable habitat for certain species and seasonal runs of salmon, particularly spring run Chinook (Yoshiyama et al. 1996). The remaining habitat downstream of the dams continues to degrade with time as the dams alter flow regimes and sediment supply (Kondolf and Swanson 1993, Kondolf and Matthews 1993). In addition to the reduction in spawning gravels as they are flushed downstream (Kondolf and Matthews 1993), many of the rivers in the Sacramento-San Joaquin river system report fine sediment problems, primarily associated with the reduction in gravel mobility and the infiltration of fine sediment into the spawning gravel (Vyverberg et al. 1997, Horner et al. 2004, Kondolf et al. 2001). Many of the salmon species in the Sacramento-San Joaquin river system have consequently been listed as threatened or endangered (Calfed 2000a,b).

In response to the declining fish populations in the downstream rivers and concurrent fish declines in the Sacramento-San Joaquin delta, the state of California and the federal government have embarked on a series fish rehabilitation programs. Notable programs include the Four Pumps program, the Anadromous Fisheries Recovery Program, CalFed, and the current Delta Stewardship Council. Hundreds of millions of dollars have been spent on restoration activities downstream of the dams to recover these fish species. The restoration activities have stopped further declines of most of the fish stocks, however, the current fish populations are a fraction of their historical numbers and still are considered vulnerable to extinction (CalFed 2000a,b).

A major critique of the fish restoration efforts undertaken to date has been the absence of a basin-wide comprehensive plan to effectively revitalize these fish species and to determine the best use of restoration funds. The only previous comprehensive plan, the CalFED Ecosystem Restoration Program Plan (CalFed 2000a,b) evaluated the biology of the fish populations extensively, but its assessment of underlying changes to hydrology, sediment supply and geomorphology was rudimentary. The recent study by the U.S. Army Corps of Engineers (USACE 2002), while called the “Comprehensive Study”, only addresses the effects of flows, primarily for levee stability. As a result of the lack of a comprehensive plan, many of the restoration projects in the Sacramento-San Joaquin river system, while being well-planned and scientifically-based at a site level, have been planned and implemented in a piece-meal way. Given limited restoration funds, a comprehensive framework of the changes that have occurred downstream of the dams, combined with strategic, targeted restoration projects will achieve the most “bang for the buck”.

Objectives of this dissertation

In this dissertation, I address several large-scale questions concerning the long-term effects of large dams in California, particularly their effects on the gravel-bed reaches of Sacramento-San Joaquin river system. In Chapter 2, I tackle the issue of reservoir sedimentation and the lifetime of dams as they fill. In California, many dams are often located in the same watershed, raising a thorny issue: how can sediment yields be calculated with multiple trapping effects of large dams within the same watershed, particularly as they fill over time? In response to this question, I develop a reservoir sedimentation model (“3W” model) that accounts for the trapping of dams in the same watershed, while also accounting for the decrease in trap efficiency as the dams fill over time. Using the 3W model, I calculate long-term sediment yields and estimate the state-wide sediment trapping and the infilling of dams from 1849 to present and project the rates up to the year 2200.

Given the varied operation of the foothill dams in the Sacramento-San Joaquin river system (Figures 3, 4), it is likely that the response of the downstream gravel-bed rivers also will vary. Of particular interest, particularly due to the biological repercussions to salmonid species, is the question: how have the dam-induced changes in flow altered bedload transport in the regions downstream of the dams? In Chapter 3, I investigate the long-term effects of flow alteration on bedload transport and bed conditions downstream of the foothill dams in the Sacramento-San Joaquin river system. Using a combination of field data and previously published data from a variety of sources, I develop bedload transport curves for the gravel-bed rivers downstream of the dams. With the bedload transport curves, I examine the changes between pre- and post-dam annual bedload transport, the total bedload deficit and the magnitude and frequency of bedload transport.

For rivers downstream of large dams, a major factor influencing the post-dam channel response is the rate and volume of sediment supply from downstream tributaries, particularly compared to the pre-dam sediment supply rate and the post-dam transport rate (Williams and Wolman 1984, Schmidt and Rubin 1995, Grant et al. 2003). In Chapter 4, I address the issue of sediment supply to the downstream rivers in the Sacramento-San Joaquin river system using a sediment budget approach. Gravel augmentation volumes and rates are collected and compared to the post-dam bedload transport capacity using the grain size distribution of the current river bed as well as an ideal gravel augmentation grain size distribution.

References

Brune, G.M., 1953. Trap Efficiencies of Reservoirs. Trans. Am. Geoph. Union 34(3), 407-418.

CalFed Bay-Delta Program, 2000a. Ecosystem Restoration Program Plan, Volume I: Ecological Attributes of the San Francisco Bay-Delta Watershed. CalFed Bay-Delta Program, Final Programmatic EIS/EIR Technical Appendix.

CalFed Bay-Delta Program, 2000b. Ecosystem Restoration Program Plan, Volume II: Ecological Management Zone Visions. CalFed Bay-Delta Program, Final Programmatic EIS/EIR Technical Appendix.

California Division of Safety of Dams (CDSD), 2007. Electronic database of dams and reservoirs in California, damsafety.water.ca.gov, accessed April 2007.

Collier M, Webb RH, and JC Schmidt, 1996. A Primer on the Downstream Effects of Dams. U.S.G.S. Circular 1126. Menlo Park, CA. 94p.

Dietrich, W.E., Kirchner, J.W., Ikeda, H., and F. Iseya, 1989. Sediment supply and the development of the coarse surface layer in gravel-bedded rivers. Nature 340(6230), 215-217.

Everitt, B.L., 1995. Hydrologic factors in regeneration of Fremont Cottonwood along the Fremont River, Utah. in J.E. Costa et al. (eds.), Natural and Anthropogenic Influences in Fluvial Geomorphology (the Wolman Volume). American Geophysical Union, Geophysical Monograph 89. Washington, D.C. pp. 197-208.

Gasith, A., and V.H. Resh, 1999. Streams in Mediterranean Climate Regions: Abiotic influences and biotic responses to predictable seasonal events. Annual Review of Ecology and Systematics 30, 51-81.

Gilbert, G.K., 1917. Hydraulic-mining Debris in the Sierra Nevada. United States Geological Survey, Professional Paper 105. 107p.

Grant, G.E., Schmidt, J.C. and S.L. Lewis, 2003. A Geological Framework for Interpreting Downstream Effects of Dams on Rivers. In Grant, G.E. and J.E. O'Connor (eds), *A Peculiar River*. Water Science and Application 7. American Geophysical Union, San Francisco. Pp. 209-226.

Gregory, S.V., Swanson, F.J., McKee, W.A., and K.W. Cummins, 1991. An ecosystem perspective of riparian zones. Bioscience 41(8): 540-551.

Hazel, J.E., Topping, D.J., Schmidt, J.C., and M. Kaplinski, 2006. Influence of a dam on fine-sediment storage in a canyon river. Journal of Geophysical Research 111, F01025, doi:10.1029/2004JF000193.

Horner, T., Titus, R., and M. Brown, 2003. American River gravel studies 2004: Phase 3 gravel assessment on the Lower American River. 93p.

Johnson, W.C., 2002. Riparian vegetation diversity along regulated rivers: contribution of novel and relict habitats. Freshwater Biology 47: 749-759.

Kondolf, G.M. and W.V.G. Matthews, 1993. Management of Coarse Sediment on Regulated Rivers. California Water Resources Center, University of California, Report no. 80. 128p.

Kondolf, G.M., 1997. Hungry water: effects of dams and gravel mining on river channels. *Environmental Management*. 21(4), 533-551.

Kondolf, G.M., and M.L. Swanson, 1993. Channel adjustments to reservoir construction and instream gravel mining, Stony Creek, California. Environmental Geology and Water Science 21, 256-269.

Lindley, S.T., Schick, R.S., Agrawal, A., Goslin, M., Pearson, T.E., Mora, E., Anderson, J.J., May, B., Greene, S., Hanson, C., Low, A., McEwan, D., MacFarlane, R.B., Swanson, C., and J.G. Williams, 2006. Historical population structure of Central Valley Steelhead and its alteration by dams. San Francisco Estuary and Watershed Science, February 2006. 19p.

Lowe, R.L., 1979. Phytobenthic ecology and regulated streams. In Ward, J.V., and J.A. Stanford (eds.), *The Ecology of Regulated Streams*. Plenum Press, New York. Pp. 25-34.

Mahoney, J.M., and S.B. Rood, 1998. Streamflow requirements for Cottonwood seedling recruitment – an integrative model. Wetlands 18(4), 634-645

Naiman, R.J. and H. Decamps, 1997. The ecology of interfaces: riparian zones. Annual Review of Ecology and Systematics 28, 621-658.

Nakamura, F. and N. Shin, 2001. The downstream effects of dams on the regeneration of tree species in Northern Japan. In Dorava, Montgomery, Palcsak and Fitzpatrick (eds.) *Geomorphic Processes and Riverine Habitat*. American Geophysical Union, Water Science and Application 4. pp 173-183.

Nilsson, C. and K. Berggren, 2000. Alterations of riparian ecosystems caused by river regulation. Bioscience 50(9), 783-792.

Petts, G.E., 1979. Complex response of river channel morphology subsequent to reservoir construction. Progress in Physical Geography 3(3), 329-362.

Petts, G.E., 1984. *Impounded Rivers: Perspectives for Ecological Management*. John Wiley and Sons, New York. 326 p.

Poff, N.L., Allan, J.D., Bain, M.B., Karr, J.R., Prestegaard, K.L., Richter, B.D., Sparks, R.E., and J.C. Stromberg, 1997. The natural flow regime: a paradigm for river conservation and restoration. Bioscience 47(100), 769-784.

Poff, N.L., and J.V. Ward, 1989. Implications of streamflow variability and predictability for lotic community structure: a regional analysis of streamflow patterns. Canadian Journal of Fisheries and Aquatic Sciences 46, 1805-1818.

Resh, V.H., Brown, A.V., Covich, A.P., Gurtz, M.E., Li, H.W., Minshall, G.W., Reice, S.R., Sheldon, A.L., Wallace, J.B., and R.C. Wissmar, 1988. The role of disturbance in stream ecology. Journal of the North American Benthological Society 7(4), 433-455.

Richter, B.D., Baumgartner, J.V., Powell, J., and D.P. Braun, 1996. A method for assessing hydrologic alteration within ecosystems. Conservation Biology 10, 1163-1174.

Schmidt, J.C., and D.M. Rubin, 1995. Regulated streamflow, fine-grained deposits, and effective discharge in canyons with abundant debris fans. In J.E. Costa et al. (eds.), *Natural and Anthropogenic Influences in Fluvial Geomorphology (the Wolman Volume).* American Geophysical Union, Geophysical Monograph 89. Washington, D.C. pp. 177-195.

Surian, N., 1999. Channel changes due to river regulation: The case of the Piave River, Italy. Earth Surface Processes and Landforms 24, 1135-1151.

United States Army Corps of Engineers (USACE), 2002. Sacramento and San Joaquin River Basins, California, Comprehensive Study, Interim Report.

Vericat, D., and R.J. Batalla, 2006. Sediment transport in a large impounded river: The lower Ebro, NE Iberian Peninsula. Geomorphology 79, 72-92.

Vyverberg, K., Snider, B., and R.G. Titus, 1997. Lower American River Chinook Salmon Spawning Habitat Evaluation, October 1994. California Department of Fish and Game, Environmental Services Division. 44p.

Ward, J.V. and J.A. Stanford, 1983. The intermediate-disturbance hypothesis: an explanation for biotic diversity patterns in lotic ecosystems. In Fontaine, T.D. and S.M. Bartell (eds.), Dynamics of Lotic Ecosystems. Ann Arbor Science Publishers, Ann Arbor, Michigan. Pp. 355-395.

Ward, J.V., and J.A. Stanford (eds.), 1979. *The Ecology of Regulated Streams*. Plenum Press, New York. 398p.

Wilcock, P.R., Kondolf, G.M., Matthews, W.V.G., and A.F. Barta, 1996. Specification of sediment maintenance flows for a large gravel-bed river. Water Resources Research 32(9), 2911 – 2921.

Williams, G.P. and M.G. Wolman, 1984. Downstream Effects of Dams on Alluvial Rivers. U.S. Geological Survey Professional Paper 1286. U.S. Government Printing Office, Washington. 83 p.

Wolman, M.G., and R Gerson, 1978. Relative scales of time and effectiveness of climate in watershed geomorphology. Earth Surface Processes 3, 189-208.

Yoshiyama, R.M., Gerstung, E.R., Fisher, F.W., and P.B. Moyle, 1996. Historical and present distribution of Chinook salmon in the Central Valley drainage of California. In Sierra Nevada Ecosystem Project final report to Congress. Centers for Water and Wildland Resources, University of California, Davis. Volume 3, p 309-361.

Figures

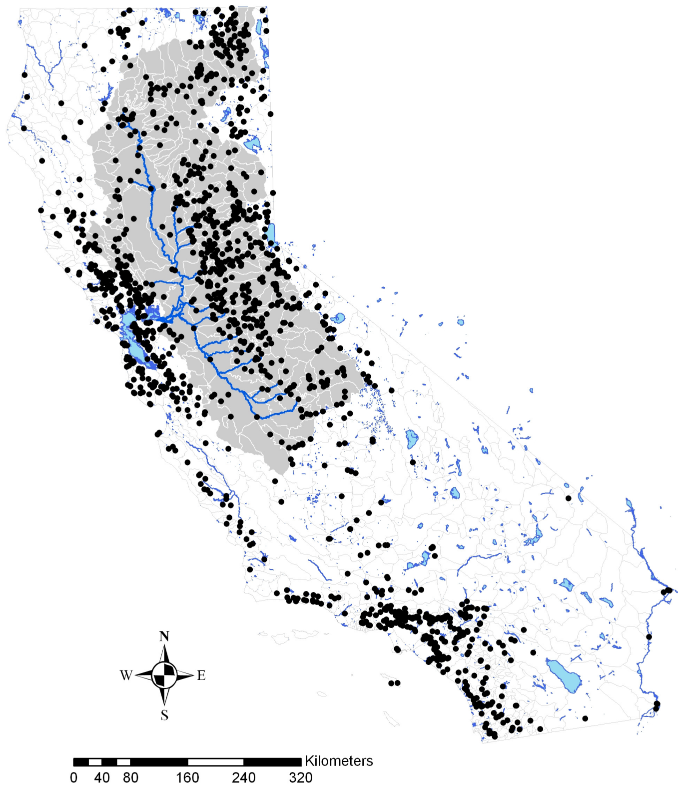

Figure 1. Map of the large dams (black circles) in California (source data CDSD 2007). Shaded area is the Sacramento-San Joaquin watershed, with major tributaries.

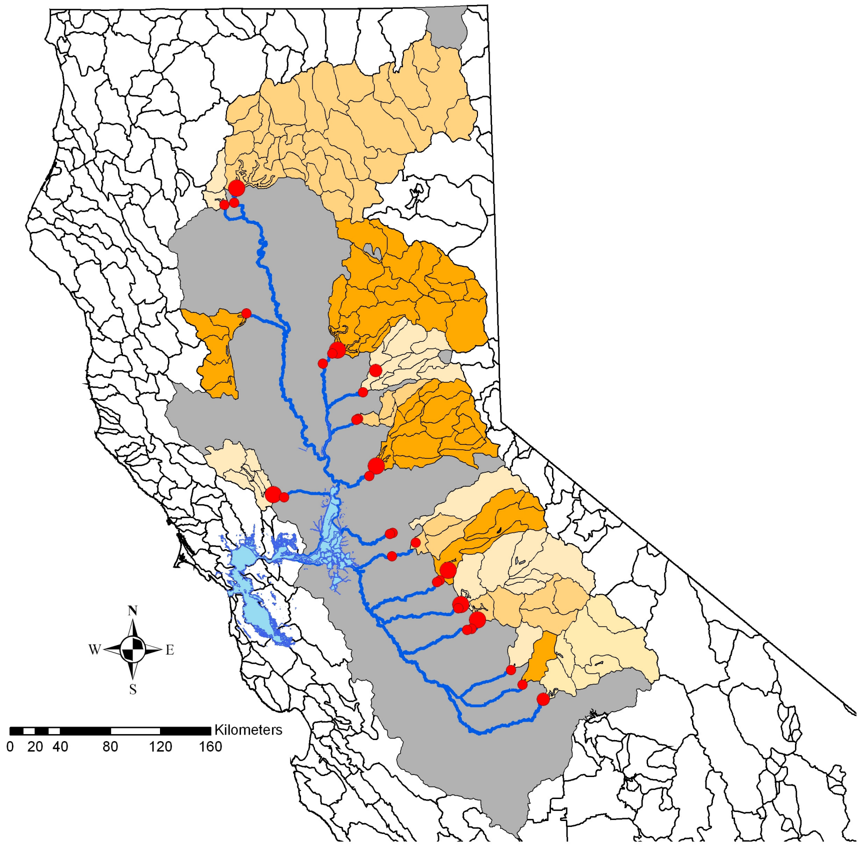

Figure 2. Map of the fourteen foothill dams and their reregulating dams in the Sacramento-San Joaquin river system (source data CDSD 2007), also includes the dams on the Chowchilla and Fresno Rivers, though these were not studied in the present effort. Gray-shaded area downstream of the dams is the undammed watersheds, orange- and yellow-shaded areas are the watersheds upstream of the foothill dams.

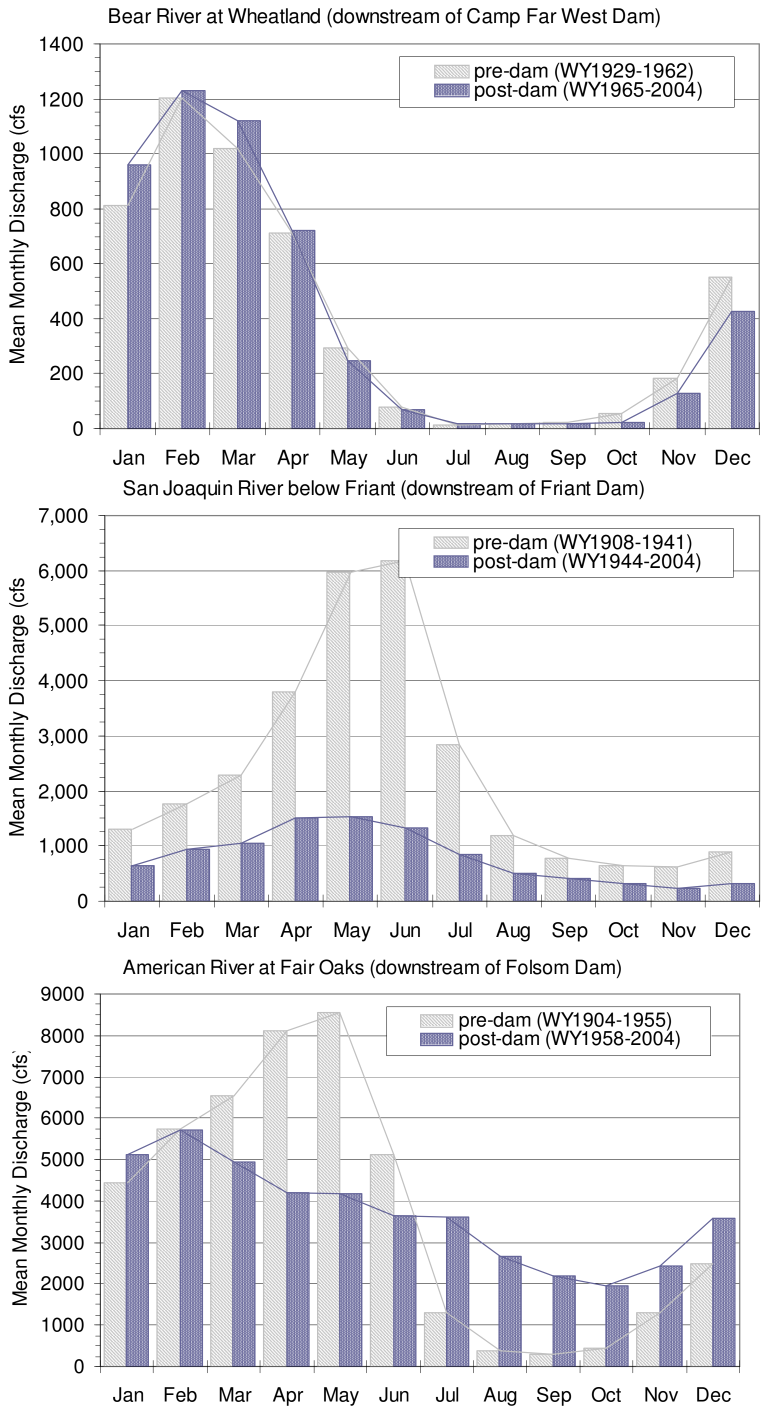

Figure 3a-c. Plots of monthly pre- and post-dam water discharge for the Bear River (top), San Joaquin River (middle), and American River (bottom). Note the differences in flow alteration between the different dams.

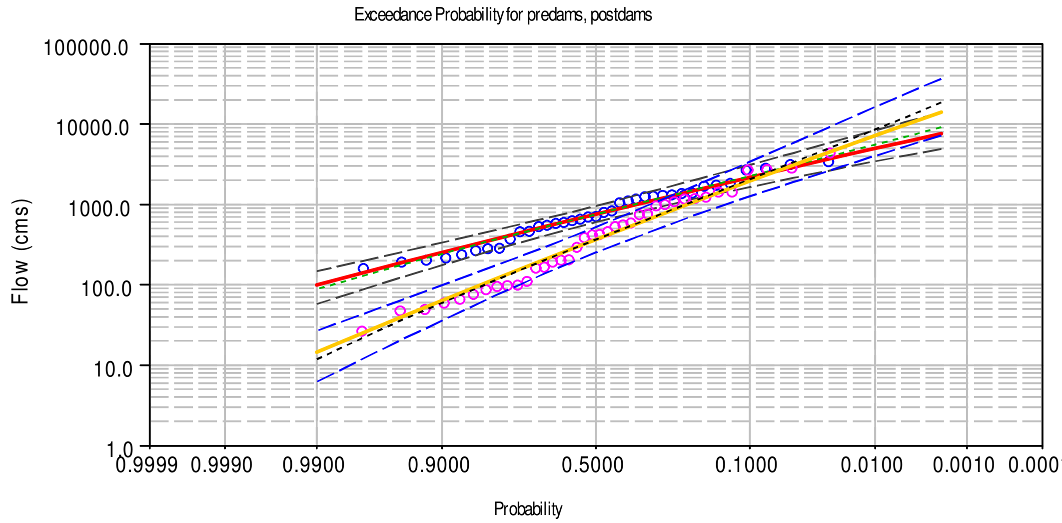

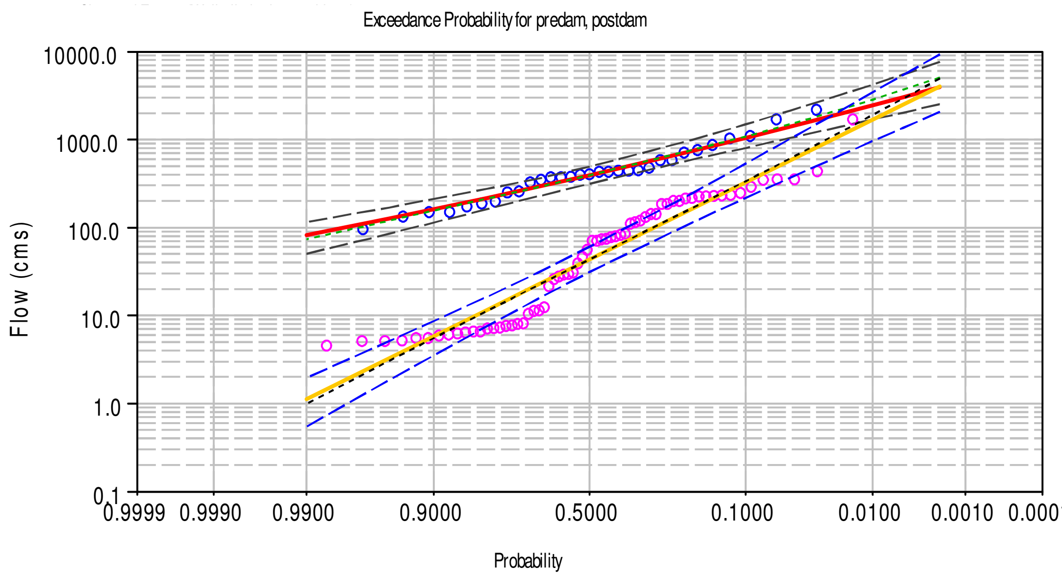

Figure 4. Differences in pre-dam and post-dam flood frequency reduction for the Yuba River (top), and the San Joaquin River (bottom). In both graphs, the top curves are the pre-dam flood frequencies and the bottom curves are the post-dam flood frequencies (in each grouping, the top line is the +95% confidence interval, middle line is the mean, and the bottom line is the -95% confidence intervals). The flood frequencies for 2-year and larger flows (probability < 0.5) on the Lower Yuba River have not been significantly affected by dams. In contrast, on the San Joaquin River, nearly all flood frequencies have been significantly reduced compared to the pre-dam state, in some cases they are reduced by more than a factor of 10.

Chapter 2: Estimating reservoir sedimentation rates at large spatial and temporal scales: A case study of California

Abstract

Previous reservoir sedimentation models have ignored two key factors for large spatial and temporal modeling of multiple reservoirs: trapping by upstream dams and decreasing sediment trapping as reservoirs fill. A spreadsheet-based model was developed that incorporates both factors. Using California as a case study, measured sedimentation rates were used to estimate sediment yields for distinct geomorphic regions and applied those rates to unmeasured reservoirs by region. Statewide reservoirs have likely filled with 2.1 billion m^3 of sediment to date, decreasing total reservoir capacity by 4.5%. About 200 reservoirs have likely lost more than half their initial capacity to sedimentation.

Introduction

Reservoir sedimentation is a serious problem in many regions with high sediment yield, particularly in geologically active regions such as California. Small-capacity reservoirs in rapidly eroding mountain regions are most vulnerable to sedimentation problems. The costs of dealing with accumulated sediments can be prohibitively expensive and, for some dam removals, have been the greatest component of dam decommissioning costs (e.g., U.S. Bureau of Reclamation 2006). Even before reservoirs fill completely with sediment, sediment within the reservoir can reduce usable capacity, interfere with outlet works, damage turbines, and cause backwater flooding upstream (Morris and Fan 1998). Reservoirs filled with sediment may be at greater risk during earthquakes because accumulated sediment deposits are denser than water and may exert greater force against the dam during seismic shaking (Chen and Hung 1993). Reservoir sediments are also a significant global sink for carbon and other important nutrients (Vorosmarty et al. 2003, Stallard 1998). In addition, the trapped sediment is not available for downstream economic and ecological benefits, such as beach replenishment (Willis and Griggs 2003) or salmonid habitat, and release of sediment-starved water commonly causes bed incision in the downstream channel, which can result in downstream stream bank erosion, infrastructure damage, and drawdown of the alluvial water table (Williams and Wolman 1984, Kondolf 1997).

In the design and maintenance of most reservoirs, little thought has been given to sustaining reservoir functions as capacity is progressively lost to sedimentation. Instead, most reservoirs are designed with extra capacity to be able to absorb sediment inputs without losing reservoir function over the planned lifetime of the dam, which is typically 50 years (Morris and Fan 1998). The loss of reservoir capacity from sedimentation is difficult to offset with construction of new reservoirs because reservoirs have already been constructed at most viable sites in the developed world (Morris and Fan 1998).

Maintaining reservoir capacity into the future will require that we address capacity losses from sedimentation, which requires tools to predict sedimentation rates and to identify reservoirs vulnerable to rapid sedimentation.

Existing reservoir sedimentation models are not able to model large temporal or spatial scale patterns of sedimentation involving multiple dams, primarily due to the extensive data requirements of the models. Current sedimentation models include process-based models that operate at small temporal and spatial scales (i.e. single watersheds and a short range of years) and require data such as yearly or daily hydrologic records, detailed reservoir bathymetry, and sediment grain size distributions (e.g. Ackers and Thompson 1987, Sundborg 1992, Lajczak 1996, Tarela and Menendez 1999, Rowan et al. 2000). Similarly, geographic information system (GIS) based large spatial scale models estimate sedimentation on the basis of land use and/or hydrologic data (Verstraeten et al. 2003, Vorosmarty et al. 2003), which are lacking for most areas, particularly for historical periods. In addition, applying these process-based models without calibration can result in modeled sediment yields diverging from measured sediment yield rates by orders of magnitude (Trimble 1999).

Most importantly, existing reservoir sedimentation models do not account for two important factors: the effects of trapping by upstream reservoirs and changes in the rate of sediment retention, known as the trap efficiency, over time as reservoirs fill. As upstream reservoirs are built, they can reduce sediment yield to downstream reservoirs. This effect is particularly important in areas with numerous reservoirs within the same watershed, as exemplified by the 57 reservoirs on the American River and tributaries upstream of Folsom Reservoir, California (California Division of Safety of Dams (CDSD), Electronic database of dams and reservoirs in California, 2004, available at http://www.water.ca.gov/damsafety/).

Temporally variable trap efficiency, the percentage of the incoming sediment trapped by a reservoir, is an important factor to include in sedimentation models when the time scale of the model is approaching the time scales at which appreciable changes occur in reservoir capacity because of reservoir sedimentation. For bed load sediment, trap efficiency is 100% (except in very small diversion or low-head navigation dams) but for suspended sediment trap efficiency varies roughly with the ratio of reservoir capacity to river inflow: large reservoirs typically approach 100% and small reservoirs are less efficient, with trap efficiency decreasing over time as sedimentation reduces capacity (Brune 1953). Previous reservoir sedimentation models have either not incorporated trap efficiency (Dendy et al. 1973), thereby implicitly assuming 100% trap efficiency, or have used constant trap efficiency less than 100% (Taylor 1983, Renwick et al. 2005, Vorosmarty et al. 2003).

In this study, I develop a new spreadsheet-based model that iteratively calculates sediment yield, accounting for trapping by upstream reservoirs and changing trap efficiency with time. As a case study, the model was applied to California, where a large number of the state's 1391 dams are in areas of high sediment yield. Dozens of small reservoirs in the state have already experienced significant capacity loss, and the population of reservoirs is aging: more than half are more than 50 years old, and at least 170 are more than a century old (Figure 1).

Methods

The approach used here consists of two parts: (1) a determination of sediment yield by geomorphic region from measured reservoir sedimentation rates and (2) the application of this sediment yield rate to unmeasured reservoirs in each region.

2.1. Determining sediment yield by geomorphic region

To capture the pronounced regional variations in sediment yield, geomorphic regions were delineated, as those defined by the California Geological Survey (CGS) (2002) on the basis of similar climate, relief, geology, and vegetation (Table 1 and Figure 2a). To determine sediment yield by region, reservoir sedimentation data was compiled from Dendy and Champion (1973, 1978), Federal Interagency Sedimentation Committee (FISC) (1992), Willis and Griggs (2003), Kondolf and Matthews (1993), and unpublished data of B. Greimann, U.S. Bureau of Reclamation (personal communication, 2005). Remarkably few reservoirs in California have been subject to sedimentation surveys, with the number of surveys declining since the mid-20th century (Figure 3). Three reservoirs were excluded (Matilija, San Clemente, and Englebright) that have been proposed for removal and have good sedimentation data to use to test the model.

To locate the reservoirs, an initial assessment was performed of the Reservoir Sedimentation Information System (RESIS) (Steffen 1996), which organized data from Dendy and Champion (1973, 1978) and FISC (1992) into a computerized database, later updated (as RESIS-II) with an automated location program that attempted to match coordinate data from each of the reservoirs, with approximately 75% success (Stallard et al. 2001). The RESIS-II database had inconsistencies in reported drainage areas and spelling of reservoir names (Stallard et al. 2001), errors in reservoir location, and duplicate entries with conflicting data. Instead, the reservoir sedimentation records were matched to the database of the CDSD, which regulates the 1391 dams in the state that exceed a threshold size of 7.7 m high and 18,500 m^3 storage capacity or 1.8 m high and 61,700 m^3 storage capacity. Initially, 214 reservoirs were identified with sedimentation records, from which the records were removed for debris basins (89) and dry flood-control-only reservoirs (19) because they are dry most of the year and would have different trap efficiencies. Also excluded were diversion dams (1) and reservoirs that lacked essential data, such as age or size (2). This left 103 reservoirs, for which the locations could be determined for 69 by matching the name, stream, size, and construction date to the CDSD database. The remaining 34 reservoirs were not used because their location could not be confidently determined.

Using Universal Transverse Mercator (UTM) coordinates in the CDSD database, the locations of all dams (measured and unmeasured) were plotted on a GIS map of California and dendritic diagrams were compiled relating reservoirs to others upstream and downstream. Superimposing geomorphic regions of California (from CGS, 2002) onto the larger GIS map, each reservoir was assigned to one of the regions on the basis of its catchment's dominant geomorphic region. 189 dams were excluded from the CDSD database since they lacked drainage area, year completed, or UTM coordinates, leaving 1202 dams. Overlaid on a GIS layer of reservoirs and lakes, the CDSD dams typically plotted within tens of meters of where the hydrography data set displayed the appropriate lake or reservoir. There were significant differences between the CDSD and the National Inventory of Dams (NID) databases, despite the fact that the California entries in the NID were supposedly compiled from CDSD data. Hundreds of dams appeared in one but not the other database. The source of this discrepancy was not obvious.

2.2. Estimating sediment yield rates by geomorphic region

The following equation from Brown (1944) was used to calculate trap efficiency, expressed in S.I. units:

$$C_{a,t} = 1 - 1 / [1 + (0.00021 \text{ x } K_{a,t-1} / W_a)] \qquad (1)$$

where $C_{a,t}$ is trap efficiency (expressed as a decimal percent) of reservoir a at time step t; $K_{a,t-1}$ is reservoir capacity (m^3) of reservoir a at time step t - 1, calculated by equation (5); and W_a is drainage area (km^2) of reservoir a. The Brown equation was chosen instead of the better known Brune curve (Brune 1953) because the Brune relation requires water inflow data, which were available for only about 20% of the reservoirs.

To calculate the sediment yield from a basin with a reservoir that has a sedimentation record, a coupled worksheet model was constructed to calculate the weighted watershed area (adjusted for upstream construction of reservoirs and trapping effects) for a reservoir of interest, while taking into account trap efficiency for all reservoirs in the basin and construction of upstream reservoirs. For the first worksheet, a set of formulas were created, three versions of which are shown here for each time step (a year in this case), to take into account trap efficiency as well as upstream reservoirs:

$$A'_{a,t} = \{C_{a,t}[A_a - (A'_b + A'_c + \ldots)]\}, \qquad (2)$$

$$A'_{b,t} = \{C_{b,t}[A_b - A'_c]\}, \qquad (3)$$

$$A'_{c,t} = \{C_{c,t}A_c\} \qquad (4)$$

This set of equations represents the weighted watershed area (*A'*) for a single time step for a set of reservoirs along a single mainstream. In the equation, *A'* is the weighted watershed area (km^2) during the time step; *C* is trap efficiency (decimal), calculated from Brown's (1944) equation (1); *A* is the drainage area (not sediment contributing area) (km^2); subscripts a, b, and c denote different reservoirs: in this case reservoir a is farthest downstream and c is upstream of b; and subscript t denotes current time step (yearly in this case). If reservoirs b and c were on separate streams and not in line with each other, the formula to use for reservoir b would be equation (4).

For the first part of the study, to determine the sediment yield rates for reservoirs with measured sedimentation rates, two populations of reservoirs were differentiated: measured and unmeasured. Since the infill rates and sediment yield are not known a priori for the unmeasured reservoirs, the initial trap efficiency was used as the single value for unmeasured reservoirs upstream of the measured reservoir of interest. For the measured reservoirs, since both initial and final trap efficiency could be calculated, a linear interpolation was used between them to determine trap efficiency for the intervening years. For the second part of the study, in which the sediment yield rates were applied to calculate reservoir sedimentation in unmeasured reservoirs, trap efficiency was calculated from the Brown (1944) curve on a yearly basis as described in equation (1).

The following equation was used to determine the volumetric sediment yield for a single measured reservoir:

$$Y = X_a \,/\, \mathrm{sum}_{(t\ start\ to\ t\ finish)}(A'_a) \qquad (5)$$

where *Y* is the sediment yield of the basin ($m^3\ km^{-2}$ per time step), X_a is the amount of sediment accumulated in reservoir a (m^3), $\mathrm{sum}_{(t\ start\ to\ t\ finish)}$ is the sum over the years of the sedimentation survey from which X_a is derived, and A'_a is calculated from equations (2), (3), and (4) above. Here *Y* is a volumetric sediment yield, not sediment yield by weight, since it has not been corrected for the density of the sediment in the reservoirs.

2.3. Estimating reservoir sedimentation in unmeasured reservoirs

For the second part of the study, estimating reservoir sedimentation in unmeasured reservoirs, the calculated volumetric sediment yield values was used for each geomorphic region from the first part of the study, applying the median sediment yield as well as the 25th and 75th quartiles (Table 1). Geomorphic regions lacking measured reservoirs (Modoc, Cascade, Basin and Range, and Mojave Desert), were assigned yields from nearby regions.

A coupled three-worksheet (3W) model was constructed, similar to the model for estimating sediment yield, linking yearly time steps of varying trap efficiency, reservoir capacity, and reservoir sedimentation rate. For the first worksheet of the 3W model, a set of formulas was created, three of which are shown here, to calculate reservoir sedimentation in a given reservoir for each time step (a year in this case), taking into account trap efficiency as well as upstream reservoirs:

$$R_{a,t} = \{C_{a,t-1}[A_a Y - (R_b + R_c + R_c + \ldots)]\}, \qquad (6)$$

$$R_{b,t} = \{C_{b,t-1}[A_b Y - (R_c)]\}, \qquad (7)$$

$$R_{c,t} = \{C_{c,t-1}[A_c Y]\} \qquad (8)$$

This set of equations represents the reservoir sedimentation R for a single time step for a set of reservoirs along a single mainstream. In the equation, R is the amount of sediment (m^3) trapped during the time step; C is trap efficiency (decimal), in this case calculated in the second worksheet from Brown's (1944) equation (1); A is the reservoir's drainage area (not just the area below upstream dams) (km^2); Y is sediment yield (m^3 km^{-2} per time step); subscripts a, b, and c denote different reservoirs: in this case reservoir a is farthest downstream and c is upstream of b; and subscript t denotes current time step (yearly in this case), while subscript t - 1 represents the previous time step. If reservoirs b and c were on separate streams and not in line with each other, the formula to use for reservoir b would be equation (8). To determine the total amount of sediment deposited, R was summed for the period of interest.

In the second worksheet, trap efficiency was calculated for each reservoir using the Brown (1944) curve, equation (1) in section 2.2, with the capacity term, K, calculated in the third worksheet. The third worksheet calculates the reservoir capacity to reflect the amount of sediment deposited in the reservoir during the previous time step:

$$K_t = K_{t-1} - R_t \qquad (9)$$

where K is reservoir capacity (m^3), subscripts t and t - 1 denote the current and previous time step, and R (m^3) is the calculated value from equations (6), (7), and (8) above.

Reservoir sediment was assumed to all have the same density, 960 kg m^{-3}, the median value from Dendy and Champion (1973, 1978) and FISC (1992), after comparing reported values of density among geomorphic regions. The linked 3W worksheets used to determine both steps of this study (estimating sediment yield from measured reservoirs and estimating reservoir sedimentation in unmeasured reservoirs) can be found in the auxiliary material for this paper stored at the University of California, Water Resources Center Archives.

2.4. Uncertainty and limitations of the model

Many variables influence sediment deposition within a reservoir, including flow, relative pool height, sediment supply from upstream, and sediment size and distribution, which vary regionally with geology, geomorphic delivery processes, land use history, fires, and climatic cycles. The approach used here assumed that similar processes occur within geomorphic regions and that these processes are constant through time, which is a simplification necessary for computation. Thus, this model is appropriate for detecting regional trends and highlighting reservoirs potentially at risk of sedimentation but would not give accurate estimates of sedimentation within individual reservoirs.

For this study, the assumption was that the surface sediment samples from Dendy and Champion (1973, 1978) and FISC (1992) were representative of the sediment density found throughout each individual reservoir, but in reality sediment density can vary in a single reservoir with sample location and depth and how composite sediment density is calculated for the reservoir (e.g., Snyder et al. 2006). For the 3W model, the median sediment density of 960 kg m-3 from Dendy and Champion (1973, 1978) and FISC (1992) (taken primarily from grab samples at the top layer of sediment) was applied to all geomorphic regions in the study since there was little statistical evidence to support using a different value, but densities could certainly vary among and within regions.

Results

The median sediment yield in the state is 180m^3 km^{-2} yr^{-1}, with the highest yield (520m^3 km^{-2} yr^{-1}) in the Transverse Ranges and the lowest (89 m^3 km^{-2} yr^{-1}) in the Central Valley. Although compilations of sediment yield data typically show smaller yields from larger basins (Walling 1983), no such trend was apparent in this small data set. Total annual sediment accumulated in California reservoirs through the year 2008 is estimated to be 2.1 billion m^3, representing a decrease of 4.5% of the state's total reservoir storage capacity of 47.2 billion m^3. Extrapolated to year 2200, the cumulative sedimentation is predicted to reach 7.1 billion m^3 (15% of statewide capacity) (Figure 4).

The 3W model predicted that at present, over 120 reservoirs have capacities reduced to less than 25% of original capacity and almost 190 reservoirs have less than 50% of original capacity remaining (Figure 2b). These include not only small diversion dams and debris basins but also several moderate-sized reservoirs with well-known sedimentation problems, including San Clemente, Searsville, Jameson, Gibraltar, Matilija, and Century reservoirs.

Comparing the 3W model results against sedimentation data for three well-studied reservoirs exposed some discrepancies, as should be expected when using a median or mean sediment yield value. San Clemente Reservoir on the Carmel River decreased in reservoir capacity from 1.76 million m^3 in 1921 to 154,000 m^3 in 2000 (Coastal Conservancy 2007), a difference of 1.62 million m^3. The 3W model predicted 1.65 million m^3 of sediment, close to the measured loss of capacity. Englebright Dam on the

Yuba River was built in 1941 with an initial reservoir capacity of 86 million m^3. The 3W model estimated that Englebright Reservoir should have 5.6 million m^3 of sediment on the basis of regional trends, but Childs et al. (2003) estimated the volume of sediment in the reservoir at 21.9 million m^3. This discrepancy may be explained by the fact that the measured reservoirs that were used to develop the sediment yield rate for the Sierra Nevada do not include many from the hydraulically-mined region. Englebright Dam was built specifically as a debris basin to trap sediment from hydraulic mining upstream, much of which remains in tributaries and continues to move down into the reservoir (James 2005). As such, the catchment sediment yield of the Yuba River and other historic mining regions is likely much higher than elsewhere in the Sierra Nevada. Matilija Dam on Matilija Creek (Ventura River) was built in 1949 with a capacity of 8.66 million m^3, which decreased to 5.45 million m^3 in 1967 when the dam was lowered out of safety concerns arising from structural deterioration (U.S. Bureau of Reclamation 2006). Matilija Dam had approximately 615,000 m^3 of storage remaining in 1999, with the reservoir nearly full of 4.5 million m^3 of sediment trapped (U.S. Bureau of Reclamation 2006). The 3W model estimated 3.2 million m^3 of deposited sediment, or approximately 70% of the observed reservoir sedimentation.

Discussion

When creating reservoir sedimentation models, it is important to take into account trapping by upstream reservoirs and incorporating variable trap efficiency in areas with numerous dams in the same watershed. Without taking into account upstream reservoirs, the total drainage area impounded by dams in California would appear to be 906,000 km^2 (over 2 times the area of the state). However, after correcting for reservoirs in upstream watersheds using the 3W model, the impounded drainage area drops to 186,000 km^2 46% of the state). The results of the 3W model were compared against two simple reservoir sedimentation models, both of which did not account for trapping by upstream reservoirs and assumed either perfect trap efficiency or set trap efficiency to the static initial value. The two simpler models overpredicted reservoir sedimentation rates compared to the 3W model by 416% and 161%, respectively, up to the year 2008 (Figure 4).Without accounting for upstream dams or trap efficiency, total sedimentation in the year 2200 would be projected to be 33.1 billion m^3, or two thirds of the state's reservoir capacity, much higher than the volume projected by the 3W model (7.1 billion m^3).

While the median rates of sediment yield were chosen to estimate sedimentation in unmeasured reservoirs for this study, a valid critique is that median rates are an overly conservative estimate and ignore some of the high rates of sedimentation observed in a few of the measured reservoirs (Figure 5). Some of the high rates of sedimentation observed in the measured reservoirs are associated with the effects of fires, which can increase sediment yields by up to 10-80 times for the year immediately following the fire (Krammes 1969, Rice 1982). The effects of fire on sediment yields is a complex process, the effects of which depend on a variety of factors including extent and intensity of the fire and the intensity and timing of rainfall following the fire (Moody and Martin 2001). In general, sediment yield rates decrease quickly after the first year, with yields returning to pre-fire rates within four to ten-years, likely related to vegetation regrowth (Rice 1982, Moody and Martin 2001). For this particular study, median rates were chosen to estimate rates of reservoir infilling since they most closely represented the rates affecting the majority of reservoirs (i.e. relatively few reservoirs would be expected to be influenced by large-scale fires). Given the long return period of large-scale fires (on the order of 30-200 years depending on the region), the use of mean rates would most likely produce sediment yields that would be more typical of long-term landscape sediment yields.

The 3W model as well as future reservoir sedimentation models could be improved by a statistical analysis of the Brown (1944) and Brune (1953) sediment trapping data since these curves are still recommended in standard reservoir engineering textbooks (Vanoni 2006). The Brown and Brune equations were derived by fitting the data by eye and, as such, no meaningful statistical information can be gleaned from them. A brief statistical analysis was performed during the course of this current study and found that compared to the original data, both Brown and Brune's equations produce residuals that have a trend and are not homoschedastic. An improvement of generalized trap efficiency equations would be a valuable contribution to the field. An expansion or evaluation of the quality of their data set also would be warranted. In California, a welcome addition to the current reservoir sedimentation database would be additional sedimentation surveys, particularly in geomorphic regions that have not been well studied such as the Siskiyou, Mojave Desert, and Modoc Plateau regions.

Conclusion

Sediment accumulated in reservoirs creates costly problems for dam operation and ultimate decommissioning. Many of the dams on the landscape can be viewed as future maintenance problems, which will become more urgent as they fill with sediment and lose capacity. In addition, the carbon stored within reservoir sediments has been shown to be a significant sink of terrestrial carbon (Stallard 1998). Given that most reservoirs have not been surveyed for sedimentation, managers could benefit from a tool with which to identify at a regional level those reservoirs at higher risk of filling in the near future so that problems can be anticipated and countermeasures can be explored and implemented such as installation of upstream sediment traps, sediment pass-through, flushing, or mechanical removal.

The 3W model presented here is the first such model to estimate reservoir sedimentation at a large number of reservoirs while taking into account the effect of reduced sediment input due to trapping by upstream dams, important in rivers with multiple dams. The model serves to identify reservoirs vulnerable to sedimentation problems by virtue of their size and regional sediment yields and which may be likely candidates for either removal or sediment management. This study indicates that sedimentation rates are small relative to overall storage capacity statewide, but some individual reservoirs have been affected because of their small capacities and high sediment yields of their catchments. The model correctly identified several small reservoirs that have been recognized as having filled (or nearly so) with sediment and identified several others that are likely to experience such problems in the near future, which have important implications given the high costs of dredging or decommissioning such structures. While a state-level study was completed here, the 3W model could be applied equally well to individual watersheds with varying sediment yields. By anticipating which reservoirs are most vulnerable to capacity loss from sedimentation, the 3W model approach is a tool with which managers can identify reservoirs at risk and can implement countermeasures where feasible and warranted to avoid the costs of sediment-filled reservoirs.

References

Ackers, P., and G. Thompson, 1987. Reservoir sedimentation and influence of flushing. in Sediment Transport in Gravel-Bed Rivers, edited by C. R. Thorne, J. C. Bathurst, and R. D. Hey, pp. 845– 868, John Wiley, Chichester, U. K.

Brown, C. B., 1944. Discussion, in Sedimentation in Reservoirs. edited by B. J. Witzig, Trans. Am. Soc. Civ. Eng., 109, 1047– 1106.

Brune, G. M., 1953. Trap efficiencies of reservoirs. Eos Trans. AGU, 34(3), 407.

California Division of Safety of Dams (CDSD), 2005. Electronic database of dams and reservoirs in California, damsafety.water.ca.gov, accessed April 2005.

California Geological Survey (CGS), 2002. California geomorphic provinces. Note 36, 13 pp., Calif. Geol. Surv., Sacramento.

Chen, B., and T. Hung, 1993. Dynamic pressure of water and sediment on rigid dam, J. Eng. Mech., 119(7), 1411 – 1433, doi:10.1061/(ASCE)0733- 9399(1993)119:7(1411).

Childs, J. R., N. P. Snyder, and M. A. Hampton, 2003. Bathymetric and geophysical surveys of Englebright Lake, Yuba-Nevada Counties, California. U.S. Geol. Surv. Open File Rep., 03-383, 20 pp.

Coastal Conservancy, 2007. San Clemente Dam removal project technical assistance. Rep. 07-004-01, 7 pp., Calif. State Coastal Conserv., Oakland.

Dendy, F. E., and W. A. Champion, 1973. Summary of reservoir sediment deposition surveys made in the United States through 1970. Misc. Publ. 1266, 88 pp., U.S. Dep. Of Agric., Washington, D. C.

Dendy, F. E., and W. A. Champion, 1978. Sediment deposition in U.S. reservoirs: Summary of data reported through 1975. Misc. Publ. 1362, 68 pp., U.S. Dep. of Agric., Washington, D. C.

Dendy, F. E., W. A. Champion, and R. B. Wilson, 1973. Reservoir sedimentation surveys in the United States, in Man-Made Lakes: Their Problems and Environmental Effects. Geophys. Monogr. Ser., vol. 17, edited by W. C. Ackermann et al., pp. 349– 357, AGU,Washington, D. C.

Federal Interagency Sedimentation Committee (FISC), 1992. Sediment deposition in U.S. reservoirs: Summary of data reported 1981–85. 62 pp., U.S. Interagency Advis. Comm. on Water Data, Reston, Va.

James, L. A., 2005. Sediment from hydraulic mining detained by Englebright and small dams in the Yuba basin. Geomorphology, 71(1–2), 202–226, doi:10.1016/j.geomorph.2004.02.016.

Kondolf, G. M., 1997. Hungry water: Effects of dams and gravel mining on river channels. Environ. Manage. N. Y., 21(4), 533– 551, doi:10.1007/s002679900048.

Kondolf, G. M., and W. V. G. Matthews, 1993. Management of coarse sediment in regulated rivers of California (December 1, 1991). Tech. Completion Rep. W-748, 123 pp., Cent. for Water Resour., Univ. of Calif., Berkeley.

Krammes, J.S., 1969. Hydrologic significance of the granitic parent material of the San Gabriel Mountains, California. Ph.D. dissertation, Oregon State University, Hydrology.

Lajczak, A., 1996. Modelling the long-term course of non-flushed reservoir sedimentation and estimating the life of dams. Earth Surf. Processes Landforms, 21, 1091–1107, doi:10.1002/(SICI)1096-9837(199612)21:12<1091::AID-ESP653>3.0.CO;2-2.

Moody, J.A. and Martin, D.A., 2001. Initial hydrologic and geomorphic response following a wildfire in the Colorado Front Range. Earth Surface Processes and Landforms 26, 1049-1070.

Morris, G. L., and J. Fan, 1998. Reservoir Sedimentation Handbook. 898 pp., McGraw-Hill, New York.

Renwick, W. H., S. V. Smith, J. D. Bartley, and R. W. Buddemeir, 2005. The role of impoundments in the sediment budget of the conterminous United States. Geomorphology, 71(1–2), 99–111, doi:10.1016/j.geomorph.2004.01.010.

Rice, R.M., 1982. Sedimentation in the Chaparral: How do you handle unusual events? In: F.J. Swanson, R.J. Janda, T. Dunne and D.N. Swanston (eds.), Sediment Budgets and Routing in Forested Drainage Basins. U.S. Forest Service, pp. 39-49.

Rowan, J. S., L. E. Price, C. P. Fawcett, and P. C. Young, 2000. Reconstructing historic reservoir sedimentation rates using data-based mechanistic modeling. Phys. Chem. Earth, Part B, 26(1), 77 – 82, doi:10.1016/S1464-1909(01)85018-8.

Snyder, N. P., S. A. Wright, C. N. Alpers, L. E. Flint, C. W. Holmes, and D. M. Rubin, 2006. Reconstructing depositional processes and history from reservoir stratigraphy: Englebright Lake, Yuba River, northern California. J. Geophys. Res., 111, F04003, doi:10.1029/2005JF000451.

Stallard, R. F., 1998. Terrestrial sedimentation and the carbon cycle: Coupling weathering and erosion to carbon burial. Global Biogeochem. Cycles, 12(2), 231– 257, doi:10.1029/98GB00741.

Stallard, R. F., D. Mixon, and D. A. Kinner, 2001. RESIS-II: Making the reservoir survey information system complete and user friendly. Paper presented at the Seventh Federal Interagency Sedimentation Conference, Subcomm. on Sediment., Reno, Nev.

Steffen, L. J., 1996. A reservoir sedimentation survey information system—RESIS. Paper presented at the Sixth Federal Interagency Sedimentation Conference, Subcomm. on Sediment., Las Vegas, Nev.

Sundborg, A., 1992. Lake and reservoir sedimentation prediction and interpretation. Geogr. Ann., Ser. A, 74(2 – 3), 93 – 100, doi:10.2307/521287.

Tarela, P. A., and A. N. Menendez, 1999. A model to predict reservoir sedimentation. Lakes Reservoirs Res. Manage., 4, 121 – 133, doi:10.1046/j.1440-1770.1999.00087.x.

Taylor, B. D., 1983. Sediment yields in coastal southern California. J. Hydraul. Eng., 109(1), 71 – 85, doi:10.1061/(ASCE)0733-9429(1983)109:1(71).

Trimble, S. W., 1999. Decreased rates of alluvial sediment storage in the Coon Creek basin, Wisconsin, 1975– 1993. Science, 285(5431), 1244–1246, doi:10.1126/science.285.5431.1244.

U.S. Bureau of Reclamation, 2006. Hydrology, hydraulics, and sediment studies for the Matilija Dam Ecosystem Restoration Project, Ventura, CA. Draft report, 323 pp., Sediment. and River Hydraul. Group, Denver, Colo.

Vanoni, V. A., 2006. Sedimentation Engineering. Am. Soc. Of Civ. Eng., Reston, Va. 418 pp.

Verstraeten, G., J. Poesen, J. de Vente, and X. Koninckx, 2003. Sediment yield variability in Spain: A quantitative and semiqualitative analysis using reservoir sedimentation rates. Geomorphology, 50(4), 327 – 348, doi:10.1016/S0169-555X(02)00220-9.

Vorosmarty, C. J., M. Meybeck, B. Fekete, K. Sharma, P. Green, and J. P.M. Syvitski, 2003. Anthropogenic sediment retention: Major global impact from registered river impoundments. Global Planet. Change, 39, 169– 190, doi:10.1016/S0921-8181(03)00023-7.

Walling, D. E., 1983. The sediment delivery problem. J. Hydrol., 65, 209–237, doi:10.1016/0022-1694(83)90217-2.

Williams, G. P., and M. G. Wolman, 1984. Downstream effects of dams on alluvial rivers. U.S. Geol. Surv. Prof. Pap., 1286, 83 pp.

Willis, C. M., and G. B. Griggs, 2003. Reductions in fluvial sediment discharge by coastal dams in California and implications for beach sustainability. J. Geol., 111, 167–182, doi:10.1086/3459

Figures

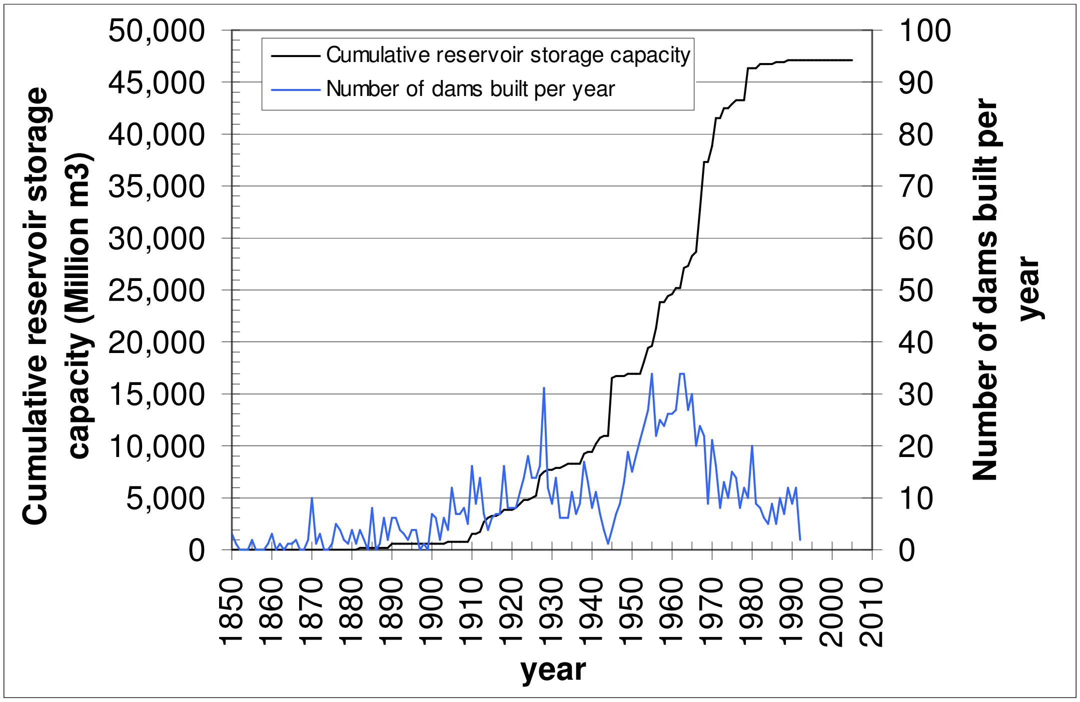

Figure 1. Graph showing the cumulative reservoir storage capacity and number of dams built per year in California (source, CDSD dataset 2004).

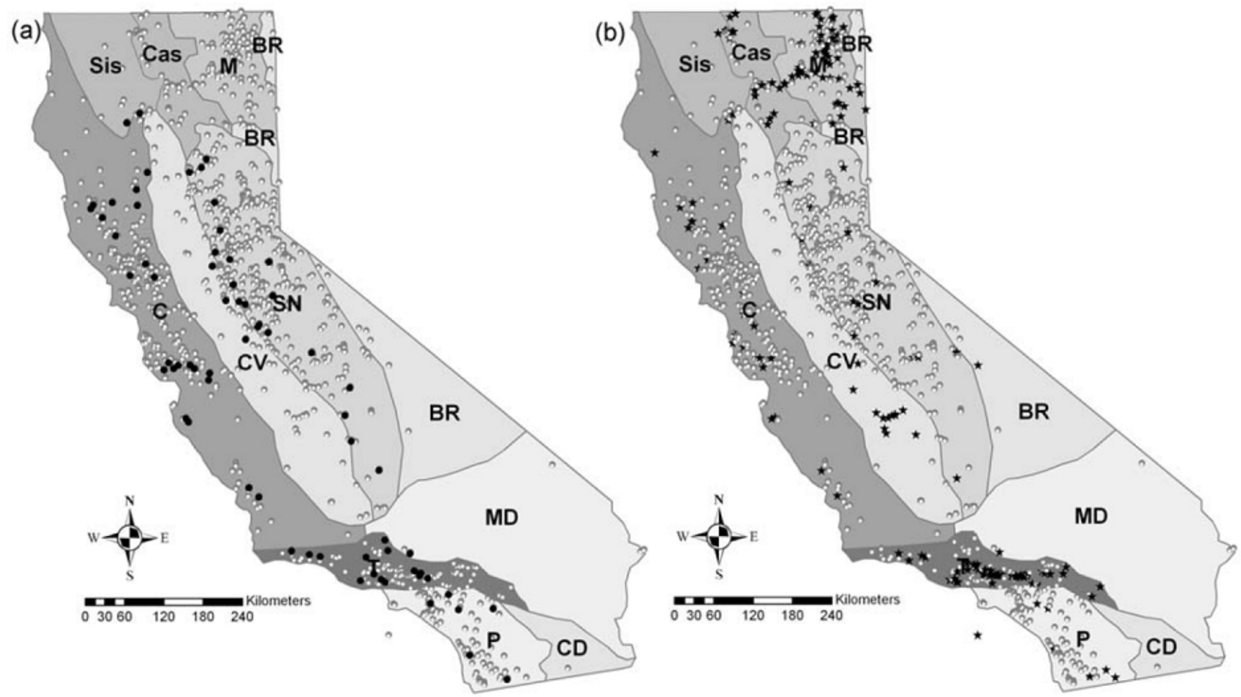

Figure 2. Reservoirs and geomorphic regions of California. (a) Reservoirs with measured sedimentation rates used in this study are shown with solid circles; others are shown with open circles. Geomorphic regions (from CGS 2002) with higher median sediment yields are shown in darker shades; lower yield areas are shown in lighter shades. (b) Reservoir sedimentation predicted by the 3W model: open circles, >50% of capacity remaining; solid stars, <50% capacity due to sedimentation. The extent of the state extends from 32.50_N to 42.00_N and from 114.13_W to 124.40_W.

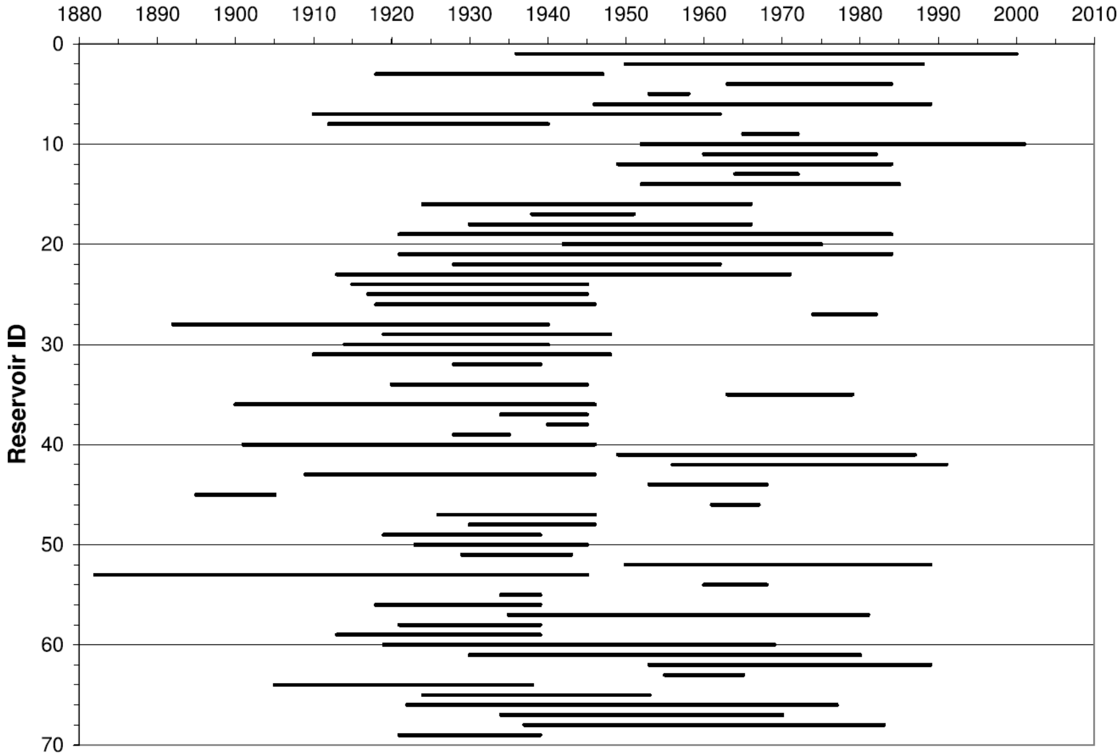

Figure 3. Period of reservoir sedimentation surveys in California. Note the sparseness of data for the latter part of the 20th century. Numbers on the y axis correspond to the reservoir identification numbers held on file at the University of California, Berkeley, Water Resources Center Archives.

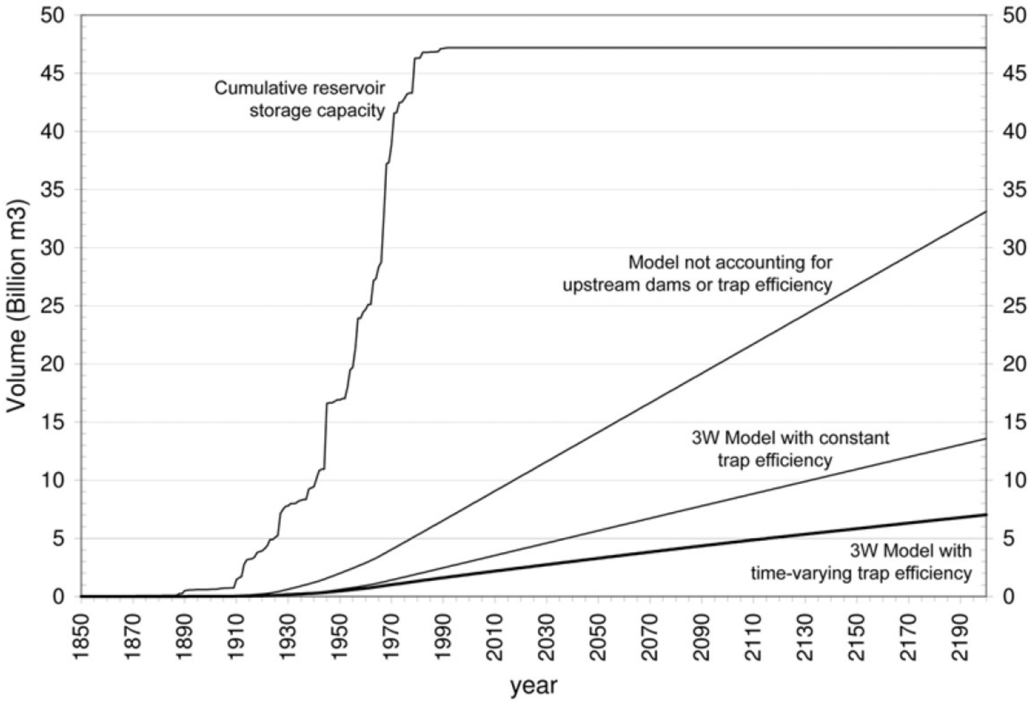

Figure 4. Cumulative reservoir capacity and estimates of reservoir sedimentation. Shown are long-term reservoir sedimentation accumulation predicted by the 3W model and predictions by simplified sedimentation models that do not account for multiple upstream dams or temporally variable trap efficiencies.

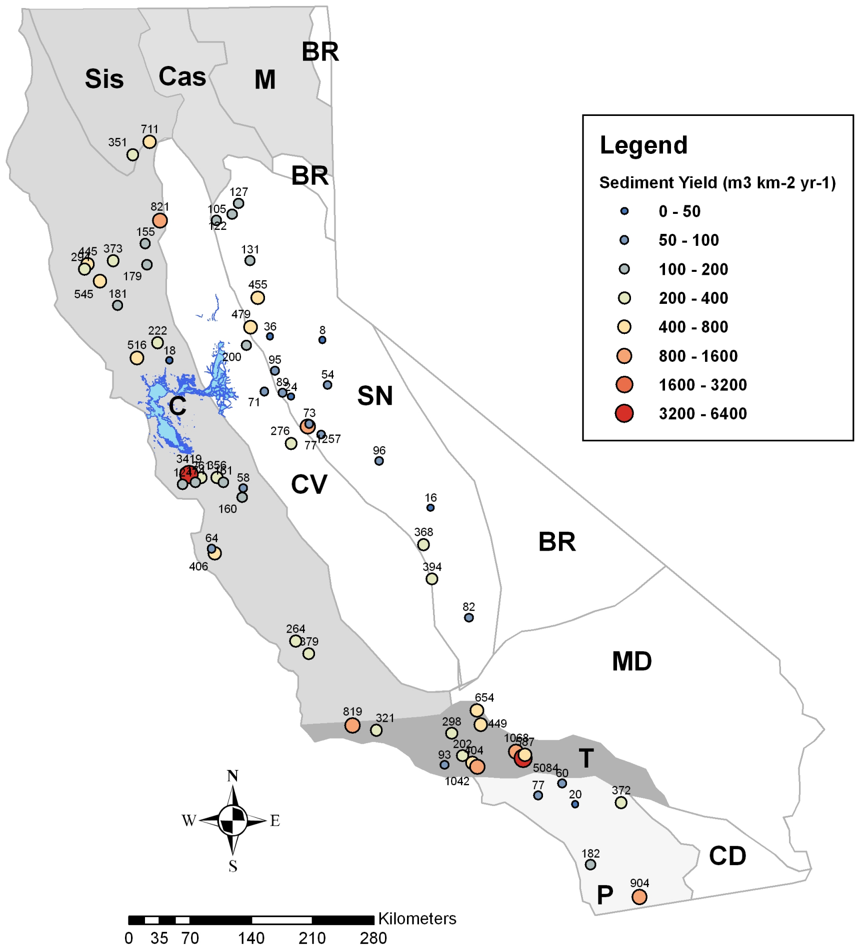

Figure 5. Map of California showing measured reservoir sedimentation rates. Note the several high sedimentation rates spread throughout the state.

Tables

Table 1. Reservoirs and Reservoir Sediment Yields by Geomorphic Region in California[a]

Geomorphic Region	Abbreviation	Number of Reservoirs: Total	Number of Reservoirs: Surveyed Reservoirs	Sediment Yield (m^3 km^{-2} yr^{-1}): Median	25% of Median	75% of Median	Minimum	Maximum	Mean	Standard Error	Median Denudation Rate (mm yr^{-1})
Coastal	C	370	23	262	160	406	19	3,419	417	142	
Central Valley	CV	18	4	89	36	234	24	277	120	55	0.032
Siskiyou	Sis	94	2	531	351	711	351	711	531	180	0.192
Peninsular	P	425	6	130	50	505	21	905	270	137	0.047
Sierra Nevada	SN	166	19	97	73	369	8	1,257	219	67	0.035
Transverse	T	127	12	519	304	986	93	5,085	919	389	0.188

Regions Without Sedimentation Data	Abbreviation	Number of Reservoirs: Total	Number of Reservoirs: Surveyed Reservoirs	Estimated Sediment Yield (m^3 km^{-2} yr^{-1})
Modoc	M	107	ND	531
Mojave Desert	MD	11	ND	97
Cascade	Cas	41	ND	531
Basin and Range	BR	17	ND	97
Colorado Desert	CD	3	ND	130
Colorado River	CR	3	ND	not used

[a]Capacity data from individual reservoirs used to determine sedimentation rates available at http://www.lib.berkeley.edu/WRCA/. We excluded the Colorado River geomorphic unit from this study because the river originates outside California and only a small portion of the state drains to the Colorado. ND indicates no reservoir sedimentation data used (either none reported or none meeting minimum standards for use in study). Estimated sediment yields are for regions with no data interpolated from nearby regions.

Table 2. Measured reservoir sedimentation rates in California. See text for a list of the sources used to compile the table.

ID	DWR ID	NID ID	Reservoir	Geomorphic Region	Stream	Source Drainage Area (km^2)	Year storage began	Initial capacity (10^6 m^3)	Year last survey	End capacity (10^6 m^3)	Period (years)
1	72-004	CA00289	**Almaden**	**C**	Guadalupe	31	1936	2.467	2000	1.956	64
2	72-009	CA00294	**Anderson**	**C**	Coyote	500	1950	112.617	1988	109.870	38
3	740-000	CA00723	**Atascadero Park Lake**	**C**	Atascadero Creek	3	1918	0.185	1947	0.168	29
4	9000-102	CA10102	**Black Butte**	**C**	Stony Ck	1,911	1963	197.437	1984	177.446	21
5	411-000	CA00574	**Catacoula (Bar 49)**	**C**	Maxwell Creek	2	1953	0.226	1958	0.223	5
6	72-002	CA00287	**Coyote**	**C**	Coyote Ck	311	1946	30.307	1989	28.289	43
7	9000-145	CA10145	**East Park**	**C**	Little Stony Creek	263	1910	62.784	1962	60.367	52
8	651-000	CA00694	**Hawkins**	**C**	N. Fk. Los Viboras Creek	10	1912	0.677	1940	0.656	28
9	1011-002	CA00828	**Highland Creek Dam**	**C**	Highland Creek	35	1965	3.990	1972	3.946	7
10	72-008	CA00293	**Lenihan**	**C**	Los Gatos Creek	96	1952	30.960	2001	23.490	49
11	23-002	CA00156	**Loch Lomond (Newell Creek)**	**C**	Newell Cr	21	1960	10.608	1982	10.551	22
12	642-004	CA00692	**Los Padres**	**C**	Carmel R	117	1949	3.825	1984	2.382	35
13	1002-004	CA00794	**Matanzas**	**C**	Matanzas	30	1964	1.850	1972	1.740	8
14	9000-201	CA10201	**Mendocino**	**C**	Russian R	272	1952	113.279	1985	109.306	33
15	7-000	CA00102	**Milliken**	**C**	Milliken Creek	27	1924	2.467	1958	2.452	34
16	2036-000	CA00406	**Morris**	**C**	Davis Creek	13	1924	1.011	1966	0.793	42
17	77-000	CA00299	**North Fork**	**C**	Pacheco Creek	171	1938	7.158	1951	7.038	13
18	382-000	CA00560	**Ridgewood (Walker)**	**C**	Walker Creek	15	1930	0.386	1966	0.266	36
19	642-000	CA00689	**San Clemente**	**C**	Carmel R	324	1921	0.956	1984	0.390	63
20	9000-202	CA10202	**Santa Margarita Lake (Salinas)**	**C**	Salinas River	290	1942	31.824	1975	28.370	33
21	97-101	CA00398	**Scott**	**C**	Eel R	746	1921	116.488	1984	99.583	63
22	9000-194	CA10194	**Stony Gorge**	**C**	Stony Creek	515	1928	61.674	1962	59.404	34
23	622-004	CA00679	**Williams Reservoir**	**C**	Los Gatos Creek	14	1913	0.243	1971	0.133	58
24	1499-000	CA00845	**Copperopolis**	**CV**	Penney Creek	5	1915	0.327	1945	0.324	30
25	571-000	CA00655	**Gilmore**	**CV**	Trib. Of Mormon Slough	13	1917	0.714	1945	0.691	28

26	73-000	CA00296	**Magalia**	**CV**	Little Butte Creek	21	1918	4.586	1946	4.500	28
27	666-000	CA01097	**Mustang**	**CV**	Mustang Cr	30	1974	1.077	1982	1.018	8
28	817-000	CA00763	**Lake Hemet**	**P**	Trib. San Jacinto River	171	1892	17.269	1940	14.434	48
29	8-003	CA00108	**Lake Hodges**	**P**	San Diequito River	785	1919	45.147	1948	41.299	29
30	81-003	CA00305	**Mockingbird Canyon**	**P**	Mockingbird Canyon	30	1914	1.233	1940	1.185	26
31	8-005	CA00110	**Morena**	**P**	Cottonwood Creek	290	1910	82.356	1948	72.693	38
32	818-000	CA00765	**Railroad Canyon**	**P**	San Jacinto River	1,860	1928	15.071	1939	14.844	11
33	75-000	CA00298	**Santiago Creek**	**P**	Santiago Creek	163	1931	30.837	1948	30.640	17
34	2220-002	CA01027	**Lake Rainbow (Misselbeck)**	**SIS**	N.Fk. Cottonwood Cr.	31	1920	5.304	1945	5.040	25
35	9000-190	CA10190	**Spring Creek**	**SIS**	Spring Creek	40	1963	6.882	1979	6.436	16
36	97-061	CA00379	**Bear River**	**SN**	Bear River	74	1900	8.279	1946	8.252	46
37	469-000	CA00611	**Big Canyon Creek**	**SN**	Big Canyon Creek	14	1934	0.247	1945	0.242	11
38	454-000	CA00601	**Blodgett**	**SN**	Trib, Cosumnes River	8	1940	0.318	1945	0.313	5
39	61-009	CA00249	**Combie (Van Geisen)**	**SN**	Bear River	337	1928	10.540	1935	9.670	7
40	95-003	CA00337	**Crane Valley**	**SN**	N. Fk. San Joaquin River	141	1901	56.012	1946	55.541	45
41	93-006	CA00329	**Cresta**	**SN**	N. Fk. Feather R	4,869	1949	5.105	1987	2.886	38
42	9000-148	CA10148	**Folsom**	**SN**	American River	4,882	1956	1245.817	1991	1205.05 6	35
43	9000-307	CA10307	**Hume**	**SN**	Ten Mile Creek	63	1909	1.739	1946	1.706	37
44	9000-106	CA10106	**Isabella Reservoir**	**SN**	Kern River	5,372	1953	665.667	1968	659.248	15
45	68-002	CA00278	**La Grange**	**SN**	Tuolumne River	3,888	1895	2.876	1905	1.317	10
46	9000-114	CA10114	**Lake Kaweah (Terminus)**	**SN**	Kaweah River	1,450	1961	184.528	1967	181.444	6
47	58-002	CA00240	**Lake McClure (Old Exchequer)**	**SN**	Merced River	2,660	1926	356.476	1946	352.339	20
48	97-073	CA00387	**Lyons**	**SN**	S. Fk. Stanislaus River	176	1930	6.784	1946	6.705	16
49	1034-000	CA00863	**Old Bullards Bar**	**SN**	North Yuba River	1,243	1919	38.855	1939	35.639	20
50	68-007	CA00281	**Old Don Pedro**	**SN**	Tuolumne River	2,593	1923	356.476	1945	350.637	22
51	31-004	CA00164	**Pardee**	**SN**	Mokelumne River	1,002	1929	259.031	1943	258.023	14
52	93-007	CA00330	**Rock Creek**	**SN**	N. Fk. Feather R	4,587	1950	5.427	1989	2.527	39
53	496-000	CA00620	**Salt Springs**	**SN**	Rock Creek	53	1882	15.949	1945	15.662	63

			Valley								
54	9000-113	CA10113	**Success Lake**	**SN**	Tule River	1,018	1960	106.277	1968	103.218	8
55	6-031	CA00088	**Bouquet Canyon**	**T**	Bouquet Creek	33	1934	45.022	1939	44.943	5
56	6-004	CA00067	**Chatsworth**	**T**	Trib. Los Angeles River	14	1918	12.489	1939	12.430	21
57	32-005	CA00190	**Cogswell (San Gabriel #2)**	**T**	San Gabriel River	102	1935	15.888	1981	11.201	46
58	6-007	CA00070	**Encino**	**T**	Encino Creek	4	1921	3.983	1939	3.959	18
59	6-008	CA00071	**Fairmont**	**T**	Antelope Valley River	7	1913	9.235	1939	9.119	26
60	11-000	CA00138	**Gibraltar**	**T**	Santa Ynez	559	1919	18.867	1969	11.908	50
61	34-002	CA00211	**Jameson Lake (Juncal)**	**T**	Santa Ynez River	36	1930	8.331	1980	0.037	50
62	9000-136	CA10136	**Lake Cachuma (Bradbury)**	**T**	Santa Ynez River	1,080	1953	252.708	1989	234.866	36
63	1005-000	CA00805	**Lake Piru (Santa Felicia)**	**T**	Piru Creek	1,101	1955	124.828	1965	121.782	10
64	765-000	CA00736	**Lake Sherwood**	**T**	Triunfo Creek	41	1905	3.540	1938	3.419	33
65	57-000	CA00237	**Little Rock**	**T**	Little Rock Creek	176	1924	5.674	1953	0.007	29
66	32-007	CA00192	**Live Oak**	**T**	Live Oak Creek	6	1922	0.305	1977	0.032	55
67	35-005	CA00216	**Morris Reservoir**	**T**	San Gabriel River	547	1934	48.496	1970	37.109	36
68	32-019	CA00200	**San Gabriel Dam No 1**	**T**	San Gabriel River	526	1937	65.799	1983	54.552	46
69	6-025	CA00083	**Stone Canyon**	**T**	Stone Canyon Creek	4	1921	9.865	1939	9.805	18

Chapter 3: Magnitude, Frequency and Duration: Sediment mobilization downstream of dams in the Sacramento-San Joaquin river system of California

Abstract

Large dams commonly alter the natural regimes of hydrologic and geomorphic processes that are critical for the maintenance of native instream and riparian communities. Much of the previous research on the long-term geomorphic effects of dams has been conducted on sand-bedded streams, often within only two decades of dam closure. Less is known about the long-term effects on gravel-bedded streams, which likely respond over longer timeframes. In the Sacramento-San Joaquin river system, excellent flow and good geomorphic datasets exist for the gravel-bedded streams immediately downstream of the largest "foothill" dams, with 50-year pre- and post-dam data as well as hundreds of agency and consulting reports. There has been no comprehensive effort to evaluate the long-term changes in magnitude and frequency of bedload transport downstream of these dams, despite hundreds of millions of dollars spent on restoration efforts. In this study, bedload transport is calculated to estimate the long-term downstream effects of these dams using data from an extensive data and literature search combined with supplemental data collected during this study, including topographic data and gravel tracer from the water year 2006. The average reduction in the 2-year return interval flow for the dams is 65% (ranging from 34% to 95%), however, there is a larger range for other return intervals, with some post-dam flows remaining equal to pre-dam magnitudes, particularly at larger return intervals. The results of the tracer gravels show extensive gravel movement downstream of the dams, indicating that even after 50+ years of operation, the riverbeds below the dams are continuing to transport sediment and are continuing to respond to the cessation in sediment supply. Post-dam annual bedload transport has fallen by an average of 45%, with bedload transport of particles greater than 8mm decreasing by 42%. Some rivers, while having reductions in flood flows, had increases in bedload transport downstream of the dam, primarily due to increases in medium-magnitude medium-frequency events. Bedload transport is still transported at large volumes (>100,000 m^3 / yr) for most sites. Effective discharge in these channels is difficult to determine due to confounding factors such as instream gravel mining and historical gold mining, however, the majority of the rivers have a high-percentage of total bedload being transported at discharges larger than the 5-year return interval. This result suggests that higher discharge events are now controlling channel response, instead of high frequency low-magnitude events.

Introduction

Importance of the natural flow regime

Natural regimes of hydrologic and geomorphic processes are critical for the maintenance of native instream and riparian communities (Poff and Ward 1989, Gregory et al. 1991, Poff et al. 1997). High flows disturb river channels, banks, and floodplains, thereby generating new landforms and areas for colonization by both riparian and instream communities (Gregory et al. 1991). Thus at any one time, due to geomorphic disturbance, a river has a suite of habitat types each occupied by different species assemblages forming a diverse patchwork of species and habitats (Naiman and Decamps 1997). Native riparian plants, such as cottonwoods, and instream organisms depend on natural flow regimes because they have life-history strategies that are timed to exploit the predictive timing and magnitude of natural flow events (Poff and Ward 1989, Naiman and Decamps 1997, Mahoney and Rood 1998).

Detrimental effects of large dams on the natural flow and sediment regime

Large dams, due to their capacity to store large amounts of water, have the potential to disrupt the natural flow regime and sediment supply in downstream rivers, and thus alter the physical template on which instream and riparian communities depend (Petts 1979, Petts 1984, Williams and Wolman 1984, Collier et al. 1996, Richter et al. 1996, Grant et al. 2003). The most common downstream hydrologic effects of large dams are decreased magnitude and frequency of high flows, increased duration and magnitude of low flows, decreased connectivity between the channel and floodplain, altered timing of flow during the year, and altered temperature regimes (Ward and Stanford 1979, Petts 1984, Collier et al. 1996, Nilsson and Berggren 2000). Reduction in scouring peak flows and an increase in low flows often allows vegetation to encroach onto previous streambed surfaces (Wilcock et al. 1996, Surian 1999), thereby reducing instream habitat and sediment supply. Recruitment of riparian vegetation has been found to decrease significantly below dams for certain riparian species, such as cottonwoods, that depend on occasional disturbance and consistent stage reduction through the seed germination period (Mahoney and Rood 1998, Everitt 1995, Johnson 2002, Nakamura and Shin 2001). Native instream communities in regions, like California, with high inter- and intra-annual variation in climate are particularly susceptible to dam-induced flow alterations compared to communities in more temperate regions (Gasith and Resh 1999, Poff and Ward 1989). Riparian and instream communities typically respond to the alteration of natural flow by shifting towards less diverse communities, often with high numbers of invasive species (Ward and Stanford 1979, Petts 1984).

In addition to altering flow regimes, large dams trap all coarse sediment and nearly 100% of the fine sediment within their upstream reservoirs (Brune 1953). This sediment trapping starves downstream channels of both bedload and suspended sediment supply, resulting in bed incision as material is excavated from the bed (Gilbert 1917, Williams and Wolman 1984, Kondolf 1997, Vericat and Batalla 2006), and often causes a concurrent bed material coarsening (Williams and Wolman 1984, Petts 1979, Dietrich et al. 1989). Incision of the river bed may further decouple the river channel from its surrounding floodplain (Williams and Wolman 1984). The dam-related changes in sediment supply and transport can extend for hundreds of kilometers downstream (Williams and Wolman 1984, Andrews 1984). Biological effects of dam-related sediment trapping can include reduction in spawning gravel supply for salmonids (Kondolf and Matthews 1993), reduction in fine-sediment deposits (Hazel et al. 2006) utilized by riparian tree seedlings, and increased instream light penetration, which can increase the standing stock of benthic algae and macrophyte communities (Lowe 1979).

Much of the previous research on the effects of dams on the magnitude and frequency of downstream geomorphic processes has occurred on what were previously sand-bedded streams (e.g. Williams and Wolman 1984, Andrews 1984, Schmidt and Rubin 1995). Less is known about the long-term (e.g. 50+ year) geomorphic response of gravel-bedded streams to regulation. In particular, the higher threshold of mobility in gravel-bedded systems results in less-mobile beds compared to sand-bedded streams, in which sand mobilizes at relatively low shear stresses and can move as both bedload and suspended load. Gilvear (2004) found that the gravel-bedded Spey River, Scotland, responded to regulation primarily by narrowing and was still adjusting its bed 60 years later. The Trinity River in Northwestern California (Wilcock et al. 1996) is one of the few well-studied regulated gravel-bedded streams and exhibits some of the unique factors affecting regulated gravel-bedded streams. Due to flow diversion out of the Trinity Basin and into the Sacramento-San Joaquin system, the transporting ability of the Trinity has been reduced such that the primary adverse effects are the deposition of sand and fine sediment into the main channel from tributaries and the development of deltas at major tributary junctions (Wilcock et al. 1996, Milhous 1997). Additionally, sediment trapped by the dam and riparian encroachment onto the previous gravel bar surfaces have greatly reduced gravel supply, resulting in a decrease of bar topography (Scott McBain, McBain and Trush, pers. comm.) and a lack of suitable spawning and rearing habitat for salmonids (Wilcock et al. 1996).

The Sacramento-San Joaquin river system of California has been extensively dammed during the last century, with 619 dams in the watershed large enough to be regulated by the California Division of Dams (jurisdictional CDSD dams are larger than: 7.62 m in height and 18,500 m^3 in volume or 1.83 m in height and 61,600 m^3 in volume, CDSD 2005) (Figure 1). 42% of the Sacramento-San Joaquin watershed, including nearly all of the high-elevation areas, which have the highest precipitation, is now contained behind the major “foothill” dams (Figure 2). The foothill dams, located at the mountain fronts as the rivers decrease slope, include some of the largest dams in the world, with a range of dam sizes, periods of operation and operating styles (CDSD 2005). The construction of these dams has greatly affected the downstream gravel-bedded rivers, including altering the magnitude and frequency of the natural flow regime and greatly reducing sediment supply (Porterfield et al. 1978, CDWR 1981, Kondolf and Matthews 1993, Singer and Dunne 2004). There is some evidence that the channels downstream of the dams are continuing to evolve, despite the passing of 40- to 70-years since dam closure, including grain size coarsening (Figure 3) (CDWR 2004a), vegetation encroachment (Vick 1995, Kondolf et al. 1996), and incision. Incision, while difficult to pin down using point locations such as USGS gaging stations, has been observed in the range of 1-4m for the reaches downstream of several of the dams (James 1991, 1997, Cain 1997, Kondolf and Swanson 1993, Fairman 2007), suggesting that these reaches are still adjusting to the effects of dam closure, although the continuing incision through historical mining sediment may be a confounding factor in some rivers (James 1991, 1997). In addition to blocking upstream access to 82% of salmonid habitat (Yoshiyama et al. 1996), the dams in the Sacramento-San Joaquin river system have continued to degrade the remaining downstream habitat, such that, present salmonid stocks are much reduced compared to historical population levels (Sommer et al. 2001, Williams 2001). Restoration efforts of these threatened and endangered fish runs is a major motivation for the restoration of the rivers downstream of the major foothill dams (CalFed 2000a,b).

Only sparse information exists regarding the dam-related alteration to bedload transport frequencies and magnitudes downstream of the dams in the Sacramento-San Joaquin river system, despite hundreds of reports and restoration projects and hundreds of millions of dollars spent on restoration efforts. The few data that do exist and are pertinent to bedload transport in the Sacramento-San Joaquin river system are interspersed among the agency and consulting reports. To date, there has been no systematic review or compilation of the available river specific geomorphic information. The last compilation effort, the CalFed Ecosystem Restoration Program Plan (CalFed 2000a,b), did not adequately address geomorphic issues, a fact that has been widely recognized. A synthesis of the existing data and compilation into bedload transport estimates would be a significant contribution to the understanding and restoration of these rivers.

Objectives

The primary objective of this study is to evaluate the bedload transport downstream of the dams on the fourteen major dammed tributaries in the Sacramento-San Joaquin river system and to compare the long-term effects of dams on bedload transport. The questions of interest for this chapter include: What are the current rates of bedload transport? Are the channels downstream of the dams still adjusting to dam closure (i.e. is bedload transport still occurring and how frequently)? What has been the effect of the long-term (50+year) dam regulation on the bedload transport in the streams below the dams?

Site Description

The Sacramento-San Joaquin River System

The Sacramento-San Joaquin river system is located approximately 150 kilometers inland of the Pacific Ocean and connects to the coast via the San Francisco Delta and San Francisco Bay, eventually exiting through the Golden Gate (Figure 2). The Sacramento River drains the northern part of the valley, and the San Joaquin River drains from the south. Both the Sacramento and San Joaquin receive waters from the western-side of the Sierra Nevada Mountains, as well as the eastern-side of the Coast Ranges. Runoff from the Coast Ranges is primarily dominated by winter-storm events (Jones et al. 1972), while the runoff from the Sierra Nevada is dominated by a combination of snowmelt and winter-storm events. Summer months in California's Mediterranean climate have little precipitation, and the majority of precipitation occurs in a relatively small time period between November and April.

The Sacramento-San Joaquin has had other human-caused historical influences in addition to dam construction. One of the largest impacts was hydraulic mining that occurred during the gold rush of the 1850s-1890s (Gilbert 1917), the effects of which continued into the early 1900s (James 1999) (Figure 4). The impacts of hydraulic mining are detailed by Gilbert in his classic 1917 study, where he estimated approximately 2,360 $x10^6$ m^3 of sediment was excavated from the Sierra Nevada tributaries (primarily Yuba, Bear, and American with lesser impacts on Feather and some of the southern tributaries), with 203 $x10^6$ m^3 still deposited in the stream channels of the Sierras, and 405 $x10^6$ m^3 deposited in piedmont deposits at base of the foothills. Many of these deposits today are still in place upstream of the foothill dams (James 1989). Gilbert (1917) proposed that even in his time the main aggradational effects of hydraulic mining had passed, a hypothesis that has since been revised by James (1997) to reflect the slow moving tail of the lag deposits left behind by the original sediment wave. Englebright Dam on the Yuba River, one of the smallest foothill dams, was commissioned specificially as a retention dam to halt downstream progression of the hydraulic mining sediment (James 2005, Childs et al. 2003).

Other important factors influencing the geomorphology downstream of the foothill dams include gold dredging on piedmont and instream that occurred in the mid-1900s and was particularly active on the San Joaquin tributaries, Clear Creek and the Yuba and Bear Rivers (Clark 1969, Vick 1995, Kondolf and Matthews 1993). Instream and floodplain gravel mining (1930s-1990s) have been a more recent but significant source of gravel and sand removal in many of the rivers, with extraction rates in some cases exceeding annual sediment loads by two or more orders of magnitude (Kondolf and Matthews 1993, Kondolf and Swanson 1993). Levee construction and bank hardening has also occurred in the region, particularly on the Lower Sacramento and Lower Feather (USACE 2002).

There are fourteen major foothill dams in the Sacramento-San Joaquin river system (Figure 2). Many of the foothill dams in the Sacramento-San Joaquin river system have smaller reregulation dams downstream, which serve several purposes, including rerouting water from the larger dams into canals, providing stable downstream flows, or are connected to hydroelectric operations. Several of the foothill dams are second generation dams, as they have replaced older structures located near the same site, often with a significant increase in capacity. For example, New Don Pedro dam with a capacity of 2.5 billion m^3 was built in 1971 to replace the original Don Pedro dam built in 1926 with a capacity of 358 million m^3.

Methods

Since there are fourteen major dammed tributaries in the Sacramento-San Joaquin river system, it was not within the cost or time-frame of this study to directly measure bedload transport in each river. Instead, I calculate bedload transport in each river here using bedload transport equations supported with field studies and tracer gravel observations during WY2006. The background data used in the bedload transport calculations were compiled from an extensive literature search through hundreds of agency and consultant reports and is in itself a useful contribution to any future bedload management in the Sacramento-San Joaquin system.

After the extensive literature search, it was determined that seven of the major tributaries had none or sparse geomorphic information about them. As such, these tributaries were targeted for field work (Table 1). It is hoped that data collected from the current study will help to increase future research and decision-making on these little-studied tributaries. Appendix B contains the pertinent field data and compiled data used in calculations by this study. The seven tributaries not directly studied have had some level of geomorphic evaluation and restoration projects on them though nearly all were lacking data on bedload transport data. The two exceptions are Clear Creek, which has had extensive sampling and studies related to bedload transport (McBain and Trush and GMA 1999, McBain and Trush 2001). The Upper Sacramento River has also had only limited bedload sampling and calculations (see Singer and Dunne 2004 and Singer 2008), which is surprising given the attention given to the middle and lower reaches (Brice 1977, Michelli et al. 2004, Singer and Dunne 2004) as well as to sediment export to the Sacramento-San Joaquin Delta downstream (Porterfield 1980, McKee et al. 2002, Singer and Dunne 2004, Wright and Schoelhamer 2004, among many others).

A review of historical photographs from the Water Resources Center Archive was undertaken to determine the bed conditions in the Sacramento-San Joaquin river system before the dams were built, however, only a few pre-dam photographs were discovered. For the rivers heavily affected by hydraulic mining on the east-side of the Sacramento Valley, the pre-mining historical grain size will likely never be known since few photographs exist of that time. On the few major rivers with photographs from pre-dam periods, gravel was seen or inferred from the geomorphic features present (e.g. gravel bars).

For the hydrologic analyses, flow gages downstream of the dams were located in U.S.G.S. records and from the California Data Exchange Center (CDEC). Gaging records of defunct gages that were flooded by dam construction were also located and collected as these often had the best record of pre-dam hydrology. The year of dam completion and one year after completion were removed from the record as these were likely to be influenced by dam construction activities and the subsequent filling of the reservoir. The complete list of the gages used in the following hydrologic analyses is listed in Table 2.

For each of the selected gages, I used average monthly flows to determine changes in the annual distribution of flows, average daily flow data to determine changes in the cumulative distribution, and instantaneous peak flows to estimate flood frequencies. The United States Army Corps of Engineers (USACE) HEC-SSP software was used to determine the flood frequency analysis using U.S.G.S. Bulletin 17B procedures (USGS 1982). Results were plotted in HEC-SSP using a Weibull plotting position, and can be found in Appendix A. The majority of stream gages used in this study are downstream of the reregulating dams, however, in the few cases where the gages were upstream of diversion points, it was assumed that the water diversions had minimal influence on the magnitude of bedload transport events downstream (Figure 5). The R statistical software was used for the Kolmogorov-Smirnov tests using a discontinuous sample and bootstrapped techniques.

Field methods

On each of the seven tributaries identified as lacking geomorphic data, one to three study sites were established (Figure 6). Each study site was located as close as possible to a gauging station. Locations were avoided that could possibly be affected by gravel augmentation (determined by a dataset partially collected during this study) as well as gravel mining. Preferable sites were located far from typical river access points and with difficult access to minimize the potential for human interference, particularly for the gravel tracer studies. Most of the sites are on public land and as such, are accessible by the public, making them otherwise difficult to protect. Each study site was chosen carefully to be representative of the respective reach of river, while also having steady, uniform hydraulics. Several of the study sites were vandalized or did not adequately represent steady, uniform flow, and their results will not be considered here. Sites were chosen with care for the application of the bedload transport formulas.

At each study site, one to three cross sections were established that covered the channel and each floodplain (Figure 7). The location of the cross sections was chosen to be the transition from pool tail to riffle at low flow, typically over the upper portion of a bar. This location was chosen for two reasons: it is a location preferred by salmon for spawning habitat and in the absence of other controls it is also the local control on the longitudinal profile. Benchmarks were installed in four locations along each cross section: two bracketing the active channel and two well above the estimated Q5 flow to keep them from moving during the highest floods. Benchmarks were primarily 1.9 cm by 1 meter rebar pins driven at least two-thirds of their length into the ground to keep them immobile. A horizontal tape was stretched between the lowest or highest rebar pairs to provide sufficient control for the cross section survey. At two of the sites (American and Yuba), it was judged too hazardous to boaters to stretch a tape across the full width of the river. Instead, the tape was lined up by sighting along the rebar pins on the near shore with the far bank pins and using a compass bearing. Two instruments were used in the course of the study to measure the vertical dimension in conjunction with a leveling survey staff: a Topcon AT-G2 auto-level (two-person operation) and a Topcon RL-H3C construction-grade laser level (one-person operation).

To characterize each study site, a sketch map and one to three Wolman pebble counts were performed (Wolman 1954). One of the pebble counts was performed approximately two meters downstream of the established cross section to characterize the cross section bed material and was kept to the same patch area as the gravel tracers. This pebble count was located downstream to minimize disturbance to the bed in the immediate vicinity of the cross section, and un-necessary disturbance to the cross section was kept to a minimum (i.e. walking on it). Other pebble counts were performed on nearby bars if they were present.

At the initiation of the study, a longitudinal profile at each site was measured at low flows with the same methods as the cross sections. The initial longitudinal profile extended upstream and downstream of the cross sections for a total length of between ten and thirty channel widths, with width being estimated at the line of perennial vegetation at the cross section. To measure the longitudinal distance away from the cross sections, a tape was stretched along the channel or, for longer straight distances, the distance measurement abilities of the auto-level and survey staff were employed. The low water line, thalweg and high water marks were surveyed along the longitudinal profile. Dates of high water marks were later estimated based on flow records and the estimated age of the deposits, utilizing deposits only less than one year old.

During the course of the study, stage for a variety of flows was recorded at each site. The measurements of stage for low flows coincided with most in-channel work (i.e. gravel tracer placement). For higher flows, direct measurements of stage tied into the cross section benchmarks were made when possible, both at the cross section and in longitudinal profile. Water stage measurements during floods were not possible for all of the sites since flood flows on separate rivers occurred at the same time and were far apart. High water marks, such as debris lines and flattened grass were used to document peak stage of recent floods, with observations made within a week of flood peaks for the

WY2006 flows. Slope was estimated by regression from the measurements of the high water marks or measured high water stage along the longitudinal profile. Slope was not calculated from the bed longitudinal profiles. Larger scale slope estimates were made using published results of hydraulic models, such as HEC-RAS and UNET (e.g. USACE 2002).

Gravel tracers were utilized to estimate initial motion and the width of transport along the bed (Figure 8). A large supply of pure white quartz river rock was collected from the American and Yuba River floodplains. The white quartz river rock was chosen as a tracer because it is foreign in most watersheds, and with the exception of the Yuba, is relatively rare on the beds of the rivers where it is found. The white quartz tracer was chosen over painted rocks because painted rocks were more obvious and hence susceptible to human interference. The line of quartz tracers was not easy to discern until looking directly in line with the cross section. For preparation, the quartz tracer was soaked in a chlorine-bleach solution for several days then scrubbed with wire brushes to eliminate potential biological contamination between the rivers. Each gravel tracer was then measured along the b-axis and marked with the b-axis measurement along at least three sides using a sharpee pen. At the end of the two-years of gravel tracer placement, the sharpee marks were still clearly visible on immobile grains, however, at some sites there was sufficient macrophyte growth to obscure the whole upper surface of the grain (the sharpee marks were still clearly visible on the bottom of the grain). This problem also likely would have occurred if the grain were painted.

In this study, the purpose of the tracer gravel experiments was only to document whether the tracer particles were mobilized (i.e. presence or absence along the cross section line). In other types of tracer gravel studies, the recovery of the tracer particles is important to measure the distance tracers are transported. Many of these studies have tagged tracers with magnetic or radio-frequency tags (Hassan and Egenzinger 2003). However, for the purposes of this study, distance transported was not critical, so I performed only a coarse search for mobilized particles a distance of two channel widths downstream. For this study, the tracer gravel was considered mobilized if its distance away from the cross section line was at least 0.5m. In practice, for the field sites during WY2006, if the particle moved from the cross section line, it was not found again, hence the 0.5 m transport distance rule did not come into effect.

Gravel tracers were placed at the cross section using a modified version of the minimum disturbance technique (see review by Hassan and Ergenzinger 2003). The cross section tape was strung taught across the lower of the two sets of rebar benchmarks, with the tape as close as possible to the water surface, typically within 0.3 m. The tape stretched close to the water surface allowed the researcher to be able to stand above the tape and look down to accurately locate tracer locations along with the use of a stadia rod and bubble level. To minimize disturbance to the natural bed, the researcher approached the cross section from downstream and as far from the cross section as possible. A natural rock along the profile was first selected and its location noted before it was carefully removed to preserve the shape and structure of the gravel pocket. The natural rock was then measured along the b-axis, and a similar-sized and shaped gravel tracer was then chosen and carefully placed back into the pocket. To minimize the amount of time the pocket was exposed, a large supply of tracer gravel, as well as all the measurement instruments, was carried by the researcher in the stream. In this way, it required approximately 30 seconds to locate, remove, measure, and replace a natural rock with a tracer. The water velocities at most underwater sites were below approximately 0.3 m per second and thus had little opportunity to remove fine-grained interstitial material while the main rock was being removed. If the pocket collapsed, as occurred in approximately 20 percent of the cases, the pocket was lightly re-excavated by hand and the gravel tracer was placed as close to the original elevation and orientation of its predecessor as possible. To minimize the disturbance to the bed, the material from the pocket was allowed to fall back onto the tracer but the material was not packed around the tracer, nor was the tracer pushed into the bed. Gravel tracers were located at approximately 10cm to 25cm intervals, with small intervals for smaller rocks, large intervals for larger rocks, to minimize the interactions caused by the tracer placement disturbance. 50 to 120 gravel tracers were placed at each cross section. The distribution of gravel tracers placed was not the same as the Wolman pebble count. The gravel tracer was weighted towards the D90, D84, and D50 estimates from the Wolman pebble count data, though some smaller grain sizes were also included, down to approximately 16mm. Below 16mm, it was difficult to mark the grains or to see them in the bed. Once the gravel tracers were in place, they were surveyed into the cross section using a level and stadia rod.

Each cross section was revisited after major flows. In the case of WY 2006 there were no intermediate flows at most of the sites, with the first flood approaching the 20 year return interval in some cases (see Table 1). Flows did not return to base flow until the next spring. For each successive resurvey of the gravel tracers, the cross section was surveyed with the tape, level and stadia rod. These measurements were then compared against the elevations of the cross section during the emplacement of the gravel tracer. The gravel tracer was assumed to have been moved out of the site if no gravel tracer was present and the cross section elevation at the position of the emplaced gravel tracer was equal to or lower by an amount equal to the b-axis of the placed tracer. If the measured cross section elevation was higher than the elevation at the time of tracer emplacement, the extent of the deposition was determined. Within the deposition area, the largest 3-5 placed gravel tracers were identified from previous records and at each of their positions along the cross section, the deposit was excavated to a depth of the original emplacement minus the b-axis of the tracer particle. To account for potential errors in locating the tracer gravels, an area of approximately 0.25m x 0.25m was excavated at each tracer. If located, the gravel tracer was left in place and was assumed to have been immobile. If the gravel tracer was not located, it was assumed to have been mobile. In addition, a Wolman pebble count was performed on the rocks deposited on top of the tracer to determine grain size.

Desktop methods

On some of the study site cross sections it was not possible to survey the uppermost portion of the cross section due to cliffs or inaccessible banks. The upper-portions of these cross sections were determined by fitting them to floodplain cross sections cut from aerial lidar or photogrammetric surfaces generated from previous studies (see Table 3). The software ESRI ArcGIS 9.1 was used to compile, generate and cut these data. 10-20 other cross sections from each reach were created from the digital elevation model and were used to determine the representativeness of the chosen study cross sections.

Topographic locations with varying geographic coordinates were converted into Universal Transverse Mercator, Zone 10N, NAVD88, Geoid03 using the U.S.A.C.E. CorpsCon Software, version 6.0. The U.S.A.C.E. software HEC-DSS was used to view the water surface slopes from the UNET model by the U.S.A.C.E. (2002). Digitization of data from other reports was completed with the Engauge Digitizer distributed from the Source Forge.

Bedload calculations

A number of bedload transport equations and bedload transport software were reviewed and tested by the author for this study. After review, the surface-based bedload equations of Parker (1990a) and Wilcock and Crowe (2003) were selected as viable options, given the available inputs and their development in similar conditions to the field sites. The Parker (1990a) bedload equation previously has been applied to rivers below dams for determination of effective discharge and management applications (Andrews and Nankervis 1995). These equations were developed for mixed-grain size, gravel-bedded rivers with low- to moderate- bedload transport rates and have been relatively successful at estimating bedload transport when compared to measured rates in similar field conditions (Gaeuman et al. 2009). The software applications, ACRONYM (Parker 1990b), the draft version of EASI (Enhanced ACRONYM Series 1 and 2, Stillwater Sciences 2000), and the recent BAGS (Pitlick et al. 2009), which all implement the bedload equations of Parker (1990a) were tested to calculate sediment transport for a variety of flows. The BAGS model was selected for use in this study since it also implements the Wilcock and Crowe (2003) bedload transport equation, which was useful to compare with some of the sites that had bulk grain size data.

Roughness at the field sites was calculated using the Gauckler-Manning equation from known parameters at the sites near USGS gaging stations:

$$U = \frac{S^{1/2} R^{2/3}}{n} \tag{1}$$

Where U is mean channel velocity, S is slope, R is hydraulic radius, and n is roughness. The calculated n for three of the sites had close total roughness values (mean n = 0.0365, range 0.0359 to 0.037). To determine the roughness associated only with the bed, Horton's method for variable roughness was calculated (Chow 1959):

$$n_c = \left(\frac{\sum_{i=1}^{N} P_i n_i^{3/2}}{P} \right)^{2/3} \tag{2}$$

Where n_c is the composite channel Manning's n, P_i is the wetted perimeter and n_i is the roughness for a given segment i of the cross section, P is the wetted perimeter of the total cross section, and N is the total number of sections used (Chow 1959).

Horton's variable roughness method did not produce appreciable differences in the n values, likely because the floodplains were relatively small at these three sites. At a fourth site, on the Bear River at Wheatland (USGS gage 11424000), the calculated n (0.0245) value was much lower than the other sites, for both a 90.6cms and 1031cms flow, with excellent slope data (400m long). This result might be explained by the location of the gage just downstream of a bridge constriction or a widening of the upper part of the cross section in the downstream direction (i.e. flow is not uniform at higher discharges). The Bear River U.S.G.S. gage site at Wheatland has also had a complex history of adjustment following the excavation of hydraulic mining, including cutting into underlying weakly-consolidated sedimentary layers (James 1991).

The BAGS model uses the Keulegian resistance equation to determine the velocity profile:

$$\frac{U}{u_*} = 2.5 \ln\left(11 \frac{R}{k_s}\right) \tag{3}$$

Where $u*$ is the shear velocity $(g\ R_c\ S_f)^{0.5}$, R and R_c are the hydraulic radius of the main channel, g is gravity, and S_f is the friction slope, and k_s is the roughness, where k_s is determined for the Parker (1990a) and Wilcock and Crowe (2003) equations from the original approximations ($k_s = 2D_{90}$ for Parker (1990a), and $k_s = 2D_{65}$ for Wilcock and Crowe (2003)).

The Parker (1990a) surface-based bedload equation was developed using empirical bedload measurements from Oak Creek, Oregon (Milhous 1973), a supply-limited gravel-bedded stream with a developed armor layer (Shih and Komar 1990). Particles smaller than 2mm were excluded from calculation in the Parker model since original formulation of the equations were formulated only for grain sizes larger than 2mm (Parker 1990a).

The Parker (1990a) surface-based bedload equations are calculated from the transport intensity relationships (W_i^* in equations 4 and 5 below) from three nested equations: the hiding function (equation 6), the strain function (equation 7), and the transport stage (equation 8). Different transport intensities are matched with the following relationship (Parker 1990a, using Wilcock et al. 2009 notation and modification):

$$W_i^* = \begin{cases} 11.9\left(1 - \dfrac{0.853}{\phi}\right)^{4.5} & \phi_{50} > 1.59 \\ 0.00218\exp\left[14.2(\phi - 1) - 9.28(\phi - 1)^2\right] & 1.0 \leq \phi_{50} \leq 1.59 \\ 0.00218\phi^{14.2} & \phi_{50} < 1.0 \end{cases} \qquad (4)$$

where ϕ is a dimensionless parameter relating the amount of force available to move a grain against the resistance due to weight and other forces (ϕ_{50} is this dimensionless parameter for D_{50} grain), and W_i^* is a dimensionless parameter representing the amount of power required to transport bedload scaled by the amount of power available (Parker et al. 1982).

W_i^* is calculated as:

$$W_i^* = \frac{(s - 1)gq_{bi}}{u_*^3 F_i} \qquad (5)$$

where s is the relative submerged density of rock in water (ρ_s/ρ, density of rock / density of water), g is gravity, q_{bi} is the width-normalized bedload transport rate for size fraction i, $u*$ is the shear velocity (calculated using equation 3, with $k_s = 2D_{90}$), and F_i is the fraction of surface grain size fraction i.

The hiding function (taking into account the effect of large particles "hiding" small particles) is calculated as:

$$\phi = \omega \phi_{sg} \left(\frac{D_i}{D_{sg}}\right)^{-0.0951} \tag{6}$$

Where ω is the strain function (calculated from equation 7 below) that accounts for the sorting of the bed surface as stresses increase, ϕ_{sg} is the ϕ dimensionless parameter calculated for the surface geometric mean grain size (equation 8 below), and D_i and D_{sg} are the grain size of the *i*-th fraction and the geometric mean grain size respectively.

The strain function is calculated from:

$$\omega = 1 + \frac{\sigma_\phi}{\sigma_{\phi_o}}(\omega_o - 1) \tag{7}$$

Where $\sigma_{\phi o}$ and ω_o are functions of ϕ_{sg} determined from a strain plot (see Parker 1990a) and σ_ϕ is the standard deviation of the ϕ parameter.

The third equation determines the relative amount of force available to move a grain against the resistance due to weight and other forces:

$$\phi_{sg} = \frac{\tau^*_{sg}}{\tau^*_{r_{sg}}} \tag{8}$$

Where τ^*_{sg} is calculated in equation 9, and τ^*_{rsg} is the reference Shields stress, assumed to be 0.0386 (Parker 1990a).

$$\tau^*_{sg} = \frac{u_*^2}{(s - 1)gD_{sg}} \tag{9}$$

Finally, Q_{bi}, the total bedload transport rate for size fraction *i*, is given as:

$$Q_{b_i} = \frac{W_i^* F_i B u_*^3 \rho_s}{(s - 1)g} \tag{10}$$

where B is the channel width and u^* is calculated in BAGS from the Keulegan resistance equation (equation 3 above) for the parameters from the main channel (Parker 1990a, notation from Wilcock et al. 2009). The Q_{bi} for each size fraction is then summed to determine the total bedload transport rate.

The Wilcock and Crowe (2003) surface-based bedload equation has a form similar to the Parker (1990a) surface-based bedload equation, the main difference being that Wilcock and Crowe (2003) incorporates an equation for increased transport observed when the sand fraction constitutes a portion of the bed.

The W_i^* function of Wilcock and Crowe (2003), takes the function:

$$W_i^* = \begin{cases} 0.002\phi^{7.5} & \text{for } \phi < 1.35 \\ 14\left(1 - \frac{0.894}{\phi^{0.5}}\right)^{4.5} & \text{for } \phi \geqslant 1.35 \end{cases} \tag{11}$$

where:

$$\phi = \frac{\tau}{\tau_{r_i}} \tag{12}$$

where τ is the shear stress ($\rho g R S_f$), and τ_{ri} is the reference shear stress for size fraction i:

$$\frac{\tau_{ri}}{\tau_{rs50}} = \left(\frac{D_i}{D_{s50}}\right)^{b} \tag{13}$$

Where τ_{rs50} is the reference shear stress for the surface median particle size (D_{s50}), D_i is the diameter of size fraction i. The exponent b in equation 13, is calculated from:

$$b = \frac{0.67}{1 + \exp\left(1.5 - \frac{D_i}{D_m}\right)} \tag{14}$$

where D_m is the mean surface grain size.

The reference dimensionless shear stress for the mean surface grain size is found from the Shields stress:

$$\tau^*_{r_m} = \frac{\tau_{r_m}}{(s\text{-}1)gD_m} \qquad (15)$$

where τ_{rm} is the reference shear stress, and where τ^*_{rm} is found from:

$$\tau^*_{rm} = 0.021 + 0.015^{(-20F_s)} \qquad (16)$$

where F_s is the amount of sand on the bed surface expressed as a percent. Lastly, the Q_{bi} for each size fraction is found from equation 10 above (same as the Parker 1990a solution) and summed for the total bedload transport rate.

As a test, the Wilcock and Crowe (2003) and Parker (1990a) bedload transport equations were used to calculate bedload transport at the Bend Bridge gage (U.S.G.S. gage #11377100), where bedload measurement data were available for the years 1977-1980. Slope and grain size data (average of four bed material samples in 1977) were available, but no cross section was available, so the BAGS functions were applied using width only. The results (Figure 9) show a relatively good fit, though the three years for which there were bedload data were relatively low flow years.

The BAGS model was used to calculate bedload transport for approximately fifteen equal-spaced bins spanning the full range of flows. Fifteen bins were chosen after a review of the literature (see Table 4), though guidance on this issue is relatively sparse for bedload transport flux calculations (see Discussion). The guidelines of Crowder and Knapp (2005), developed for suspended sediment, were adhered to where possible for most of the sites (i.e. less than 10% of total load in the first bin). Pre- and post-dam flow frequencies were grouped into these fifteen bins and used to calculate the magnitude-frequency curves, with the mid-point of the bins used for plotting and calculation.

Results

Flood frequencies and flow duration

The results of the flood frequency analysis show a wide range in the dam-induced alteration of the flow regime in the Sacramento-San Joaquin river system, with an average reduction in the 2-year flow event by 65% (Table 5). The maximum reduction was on Putah Creek, with a 95% reduction in the 2-year flow event, from 790cms pre-dam to 43cms post-dam. The Feather River and San Joaquin Rivers were close behind with a 93% and 89% reduction in 2-year flows. These are some of the highest reported rates of dam-induced flow reduction in the United States (Magilligan et al. 2003). With increasing return interval, the effects of the dams diverged, with some rivers, like the Bear River, having larger 25-year return interval events post-dam than pre-dam (Table 5). Additionally, a Kolmogorov-Smirnov test using daily flow frequency curves showed that all dams had significantly different distributions of flows in the post-dam period compared to the pre-dam period (Table 6).

Field sites and tracer gravels

The results of the tracer gravel and field evidence of bedload transport during WY2006 are presented in Table 7. The different sites were exposed to a range of flows, experiencing flow events with post-dam return intervals from 7- to 15- years (<1 to ~30 year pre-dam events), with particularly large flows occurring in the Sacramento basin tributaries (Table 1). As a result, all sites had tracer gravel movement, with complete transport occurring at six of the eight sites and partial transport occurring at Stony Creek and the San Joaquin (WY2006 return interval flows of 10 and 10+ years respectively for the post-dam period). At all sites, the tracer gravels were mobilized across the full width of the cross section where they were placed, so it is assumed that the full cross section was transporting sediment. All of the site cross sections exhibited topographic change within the order of decimeters, supporting the results of the gravel tracer (Table 7).

The calculated normalized Shields stress (the shear stress of the flow divided by the reference Shields stress of the D50) for the WY2006 flows experienced at the study sites, varied from near 1 at most sites to over 2.3 at the Bear River BR2 site. These values of normalized Shields stress correlate well with the results of the tracer gravel observations, indicating that the D50 of most sites were in the range of partial to complete bedload transport.

Bedload calculations

On average, the amount of total post-dam bedload transport was reduced by 45% of pre-dam rates (Table 8). Since total bedload rates can be dominated by finer particles, bedload was also broken into size fractions of greater and less than 8mm. Using only 8mm grains, post-dam bedload transport rates were reduced to 42% of pre-dam rates.

Some of the dams greatly increased bedload transport (Table 8, Figures 10a-n) due to higher post-dam flow releases (e.g. Stony Creek). Of particular importance were medium-frequency medium-magnitude events that were not apparent in the flood frequency analyses, but which dominated the bedload transport (Figure 10a). Stony Creek, for example, had a 2-year return interval flow decreased by 32% from pre-dam conditions, yet had a 180% increase in bedload transport due to medium frequency, medium magnitude events (Figure 10a). This finding is contrary to the assumption that dam-induced alteration of floods, such as the 2-year return interval, is directly related to the magnitude of geomorphic change (e.g. Magilligan et al. 2003, Schmidt and Wilcock 2008).

In general, the magnitude-frequency plots (after Wolman and Miller 1960), show some average changes in the relative effectiveness of the post-dam discharges but the results do not trend in a single direction (Figure 10a-n). While it might be expected that all of the rivers would be dominated in the post-dam period by larger flows due to the increase in the transport threshold as grain size increases (Wolman and Miller 1960), a number of the rivers in the Sacramento-San Joaquin river system still have large percentages of their bedload transported at relatively low discharges (e.g Yuba River, Figure 10b). In general, the sites with larger sediment sources (Yuba), or with greatly reduced flows (San Joaquin) had a stronger dominance of the high-frequency, low-magnitude events. Sites with smaller sediment source areas (Feather) or without reduced flows (Bear) had more dominance by larger flows. This effect was likely primarily realized through the post-dam grain size which was used in the calculations. Other factors that might be influencing the changes and could be explored at a later date include the time since closure, and the distance downstream of the dam.

Discussion

One significant confounding factor for the hydrologic analyses that was not expected at the outset of this study was the large capacity of other dams in the watersheds upstream of the foothill dams (Table 9). In several of the rivers, the foothill dam contributed only 50-70% of the total reservoir storage capacity of the watershed. In addition, in some watersheds there were very large dams built upstream of the foothill dam, which lessened the effect of the foothill dam (e.g. New Bullards Bar upstream of Englebright Dam). In most cases, these effects were partially controlled by sub-dividing the temporal hydrologic record into three categories instead of two to account for the construction of major upstream dams (e.g. New Bullards Bar on the Yuba River) (Table 2). The sheer number of reservoirs constructed in the upstream watersheds, some of which transfer water out of the respective basins, makes an accurate evaluation of the hydrologic changes a daunting task (see Curtis et al. 2005). Much of the restoration responsibility falls on the lowermost dams, however, it is clear that downstream effects are partially caused by reservoirs farther upstream. One potentially viable solution would be to model the downstream changes using all the dams in the system, similar to water-supply models, particularly since many of the dams already coordinate transfers between dams.

Given the bedload transport rates calculated in this study, a major question for the reaches below the foothill dams, is why haven't they incised more? Incision rates for the rivers that have been studied are approximately 1-4m (Cain 1997, James 1991, 1997, Kondolf and Swanson 1993, Fairman 2007), yet there are still significant amounts of sediment being transported. One possible explanation is that there has been extensive uncovering of claypan deposits on the beds of the streams (Figure 11). The claypan bedrock outcrops are a weakly cemented sedimentary layer of mudstone, and are mentioned in passing by numerous authors on the beds of several of the rivers (Kondolf and Swanson 1993, Cain 1997, McBain and Trush 2001). Some of this outcropping may be due to historical human activities, particularly on the rivers affected and rerouted by hydraulic mining waste (James 1991), and by rivers affected by instream mining (Cain 1997). The result may be that much of the riverbeds are held up by these claypan layers instead of being incised. During field work for this study, extensive claypan outcrops were found on Putah Creek, American River, San Joaquin River, Bear River and Stony Creek (Figure 11).

Gravel-bedded rivers, like those studied here, exhibit much more complex adjustments in response to reductions in sediment supply than just the adjustment in gross sediment flux studied here. Primary responses of gravel-bedded rivers to cessation of sediment supply include incision into the bed and a concurrent decrease in slope (Gilbert 1917, Dietrich et al. 1989), coarsening in grain size (Dietrich et al. 1989, Lisle et al. 1993, Vendittti et al., in prep), development and persistence of armor layers (Kinerson 1990, Whiting and King 2003), shrinking sediment transport zones (Dietrich et al. 1989, Lisle et al. 1993) and changes in patch dynamics (Nelson et al. 2009). Alternate bar sequences (Venditti et al. in prep.) and vegetation interactions also add another layer of complexity. The results found here using surface-based bedload equations are directly tied to the use of the post-dam grain size, which might reflect some of the processes listed above, but does not incorporate the more complex interactions.

The post-dam grain size distributions used here reflect some of the best historical data available, however, they come with some important limitations. First, the use of the pebble count method for determining grain size distributions of the bed was chosen by this study because of the relative abundance of historical data and its direct relation to the Parker (1990a) bedload equation. There are more sophisticated methods of determining the characteristic grain size of a reach of river combining facies mapping and grain size estimation (e.g. Bunte and Abt, 2001, Buffington and Montgomery 1999), but these methods were not employed here in order for the data from the various rivers to be compared. Secondly, the Parker (1990a) surface-based bedload equation was chosen for this study because of the relative lack of fines and sand on the surface of the riverbed. While the historical photographs found for most of the major tributaries suggest they were gravel-bedded before the dams were constructed, there is some evidence that suggests that this was not historically the case for at least the San Joaquin River. Cain (1997) quotes from Grunsky, a Lieutenant visiting the San Joaquin River in 1878 near the present day Friant dam site, "River fordable – water flows over sand and fine gravel and very flat – low sandbars sub divided into a number of streams." The post-dam grain size for this site is now well into the gravel range (D50 of 60mm). It is likely that the pre-dam grain size is smaller than the value used in the bedload calculations here and hence pre-dam bedload transport would be underestimated.

One unintended product of this study is that while there has been much discussion in the literature about determining appropriate bedload transport equations, there has been relatively little written about applying these equations to flux through time, particularly with the use of flow-duration curves. A review of several bedload studies that have computed total flux and effective discharge (Table 4) shows a variety of methods used. The use of the flow-duration curve method originally began with suspended sediment studies and has been imported for use in bedload studies without significant investigation into the potential effects of the size of bins used or the distribution of the bins through time. Some of the critical papers relating bankfull flow to magnitude and frequency of low return interval events (i.e. 1.5 year or 2 year flow) have used the flow-duration method (Table 4). In particular, the strongly heteroschedastic streams draining the Coast Ranges were very sensitive to the class size of the bin chosen because the flattening of the curve of flow frequencies coincided with the steepening of the bedload transport curve. Small discrepancies in the approximation of either of the curves resulted in order of magnitude differences in sediment transport.

The effects of small tributary inputs of water and sediment (particularly sand) have not been well studied in the Sacramento-San Joaquin river system, particularly compared to other large river systems (e.g. Grand Canyon, Trinity River). The decrease of sediment supply from the upper watershed has increased the relative contribution and importance of these lower tributaries. Some of these tributary watersheds below the dams are substantial, and many are urbanized, leading to higher peak flows and potentially increased sediment supply. The timing of the small tributary peak flows is often mis-matched with the mainstem river, particularly for those rivers with flow peaks that are suppressed for flood control and for those rivers in the rainfall dominated watersheds, such as the west-side tributaries to the Sacramento River and the lower-elevation watersheds on the east-side. On Putah Creek for example, at least three of the tributaries that enter Putah Creek below Monticello Dam have downcut extensively, contributing large volumes of fine sediment and sand to lower Putah Creek, resulting in the aggradation of floodplains by 60cm or more (Rich Marovich, personal communication, 1/26/2006). During field work for this study in WY2006, 30cm of sand deposition was measured on the floodplain at site PC1, immediately downstream of the Putah Diversion Dam. One possible explanation for the downcutting of the tributaries downstream of the dam is that the stage of Putah Creek is kept artificially low for flood control purposes, hence, in the post-dam period, the tributaries have a lower base elevation and have downcut in response (note in USACE 1995 reconnaissance report).

It is surprising that there has been so little monitoring of sediment conditions or transport given the ecological importance and expense put into restoration on the

Sacramento-San Joaquin river system. One important use of these monitoring data would be to establish rates of gravel augmentation to minimize bed degradation downstream of the dam or for spawning gravel. The San Joaquin River Restoration Program, which started operating in WY2010, provides an example of how these rivers could be monitored, with the initiation of bedload and suspended sediment monitoring at five new stations (Scott Wright, USGS, personal communication). While the monitoring of site-scale gravel augmentation and restoration projects has greatly improved in the last decade (Kondolf et al. 1996, CDWR 2004b), there is a lack of reporting of baseline data (i.e. pre-project conditions) for a number of the restoration projects. A wider monitoring network, combined with better reporting of current conditions would greatly improve restoration effectiveness and science.

Implications for river restoration

While other studies have been able to show distinct dam-related changes in geomorphically important flows related to dam operation (Schmidt and Rubin 1995), the Sacramento-San Joaquin river system does not exhibit effects nearly as distinct. The long history of human activity, such as hydraulic mining, gold dredging and instream mining, as well as the large number of dams constructed at varying times, makes the signal of dam-caused degradation difficult to see. While the exact effects of the dams might not ever be clearly shown in light of the various other human-caused disturbances in the watersheds, it is clear that the dams have greatly altered the downstream geomorphic processes and continue to alter the downstream rivers. In particular, halting downstream sediment supply and altering flows have greatly modified the functioning of downstream geomorphic processes.

Rather than attempting to reconstruct a past condition, it might be more productive to try to recreate a semblance of alluvial processes in the rivers downstream of the foothill dams using general geomorphic guidelines (e.g. Trush et al. 2000). The Trinity River Restoration Program and the Lower Clear Creek restoration program are good examples of river-scale restoration programs that provide templates for future programs in the Sacramento-San Joaquin system. Establishing flood pulses, supplying a variety of coarse sediment (not just spawning gravel) (e.g. McBain and Trush 2000), and enabling upstream-to-downstream sediment connectivity would be a good start to re-creating geomorphic processes.

Conclusions

Using empirical field data and bedload transport equations, this study found that the lowermost “foothill” dams of the major tributaries to the Sacramento-San Joaquin river system had quite diverse effects on bedload transport in the downstream gravel-bedded rivers. Field data on six tributaries for the WY2006 year showed widespread bedload transport, indicating that the channels were continuing to adjust to post-dam conditions. While the 2-year return interval flow was reduced by all the dams (average reduction of 65%), the calculated post-dam bedload transport varied greatly, with some dams increasing the bedload transport downstream due to higher medium magnitude, medium frequency flow events. Other dams greatly decreased bedload sediment transport, primarily through reductions in flow magnitudes. Further studies into the effects of reduced sediment supply on the downstream bed condition (particularly bar topography and grain size) would be warranted given the direct influence of sediment transport and bed condition on endangered salmonid habitat downstream of the foothill dams. Future restoration programs in the Sacramento-San Joaquin river system could gain important understanding of the system, by using a large-scale comparative approach, such as that used in this study, instead of only river-specific approaches as is currently practiced.

References

Andrews, E.D., 1980. Effective and bankfull discharges of streams in the Yampa river basin, Colorado and Wyoming. Journal of Hydrology 46, 311-330.

Andrews, E.D., 1984. Downstream effects of Flaming Gorge Reservoir on the Green River, Colorado and Utah. Geological Society of America Bulletin 97, 1012-1023.

Andrews, E.D., and J.M. Nankervis, 1995. Effective discharge and the design of channel maintenance flows for gravel-bed rivers. In Costa, J.E., Miller, A.J., Potter, K.W., and P.R. Wilcock (eds.), *Natural and Anthropogenic Influences in Fluvial Geomorphology: The Wolman Volume*. American Geophysical Union, Geophysical Monograph 89, 151-164.

Blodgett, J.C., and G.L. Bertoldi, 1968. Determination of channel capacity of the Merced River downstream from Merced Falls Dam, Merced County, California. United States Geological Survey, Open-File Report. 26p. plus appendices, figures and plates.

Blodgett, J.C., and H.T. Mitten, 1970. Determination of channel capacity of the Tuolumne River downstream from La Grange, Stanislaus County, California. United States Geological Survey, Open-File Report. 27p. plus appendices, figures and plates.

Brandt, S.A., 2000. Classification of geomorphological effects downstream of dams. Catena 40(4), 375-401.

Brice, J., 1977. Lateral migration of the Middle Sacramento River, California: U.S. Geological Survey Water-Resources Investigations Report 77-43. 51p.

Brune, G.M., 1953. Trap Efficiencies of Reservoirs. Trans. Am. Geoph. Union 34(3), 407-418.

Buffington, J.M., and D.R. Montgomery, 1999. Effects of sediment supply on surface textures of gravel-bed rivers. Water Resources Research 35(11), 3523-3530.

Bunte, K. and S.R. Abt, 2001. Sampling surface and subsurface particle-size distributions in wadable gravel- and cobble-bed streams for analysis in sediment transport, hydraulics and streambed monitoring. United States Forest Service, General Technical Report, RMRS-GTR-74. 450p.

Cain J, 1997. Hydrologic and geomorphic changes to the San Joaquin River between Friant Dam and Gravely Ford and implications for restoration of Chinook salmon (*Oncorhynchus tshawytscha*). Unpublished Masters thesis, University of California, Berkeley.

CalFed Bay-Delta Program, 2000a. Ecosystem Restoration Program Plan, Volume I: Ecological Attributes of the San Francisco Bay-Delta Watershed. CalFed Bay-Delta Program, Final Programmatic EIS/EIR Technical Appendix.

CalFed Bay-Delta Program, 2000b. Ecosystem Restoration Program Plan, Volume II: Ecological Management Zone Visions. CalFed Bay-Delta Program, Final Programmatic EIS/EIR Technical Appendix.

California Department of Water Resources, 1981. Upper Sacramento River baseline study: Hydrology, geology and gravel resources. Prepared by CDWR, Northern District. 87p.

California Department of Water Resources, 1994. San Joaquin River tributaries spawning gravel assessment Stanislaus, Tuolumne, Merced Rivers. Report by Department of Water Resources, Northern District. 178p.

California Department of Water Resources, 2004a. SP-G2: Effects of project operations on geomorphic processes downstream of Oroville Dam. Oroville Facilities Relicensing, FERC project no. 2100.

California Department of Water Resources, 2004b. Tuolumne River La Grange gravel addition project, Phase II: Geomorphic monitoring report. Prepared by San Joaquin District, River Management Section. 42p.

California Division of Safety of Dams (CDSD), 2005. Electronic database of dams and reservoirs in California, damsafety.water.ca.gov, accessed April 2005.

Carl Mesick Consultants, 1998. Studies of spawning habitat for Fall-run Chinook salmon in the Stanislaus River between Goodwin Dam and Riverbank from 1994-1997.

Childs, J.R., N.P. Snyder, N.P., and M.A. Hampton, 2003. Bathymetric and geophysical surveys of Englebright Lake, Yuba-Nevada Counties, California, United States Geological Survey, Open-file Report 03-383, 20 pp.

Childs, J.R., Snyder, N.P. and M.A. Hampton, 2003. Bathymetric and geophysical surveys of Englebright Lake, Yuba-Nevada Counties, California. Open-File Report 03-383. 20 p.

Chow, V.T., 1959. Open-Channel Hydraulics. McGraw-Hill, New York.

Clark, W.B., 1969. Gold Districts of California. California Department of Conservation, Division of Mines and Geology, Bulletin 193. 199p.

Collier M, Webb RH, and JC Schmidt, 1996. A Primer on the Downstream Effects of Dams. U.S.G.S. Circular 1126. Menlo Park, CA. 94p.

Crowder, D.W., H.V. Knapp, 2005. Effective discharge recurrence intervals of Illinois streams. Geomorphology 64, 167-184.

Curtis, J.A., Flint, L.E., Alpers, C.N., and S.M. Yarnell, 2005. Conceptual model of sediment processes in the upper Yuba River watershed, Sierra Nevada, CA. Geomorphology 68, 149-166.

Dietrich, W.E., Kirchner, J.W., Ikeda, H., and F. Iseya, 1989. Sediment supply and the development of the coarse surface layer in gravel-bedded rivers. Nature 340(6230), 215-217.

Emmett, W.W. and M.G. Wolman, 2001. Effective discharge and gravel-bed rivers. Earth Surface Processes and Landforms 26,1369-1380.

Everitt, B.L., 1995. Hydrologic factors in regeneration of Fremont Cottonwood along the Fremont River, Utah. in J.E. Costa et al. (eds.), Natural and Anthropogenic Influences in Fluvial Geomorphology (the Wolman Volume). American Geophysical Union, Geophysical Monograph 89. Washington, D.C. pp. 197-208.

Fairman, D., 2007. A gravel budget for the Lower American River. Masters thesis, Department of Geology, California State University, Sacramento. 158p.

Gaeuman, D., Andrews, E.D., Krause, A., and W. Smith, 2009. Predicting fractional bed load transport rates: Application of the Wilock-Crowe equations to a regulated gravel bed river. Water Resources Research 45, W06409, doi:10.1029/2008WR007320. 15p.

Gasith, A., and V.H. Resh, 1999. Streams in Mediterranean Climate Regions: Abiotic influences and biotic responses to predictable seasonal events. Annual Review of Ecology and Systematics 30, 51-81.

Gilbert, G.K., 1917. Hydraulic-mining Debris in the Sierra Nevada. United States Geological Survey, Professional Paper 105. 107p.

Gilvear, D.J., 2004. Patterns of channel adjustment to impoundment of the Upper River Spey, Scotland (1942-2000). River Research and Applications 20, 151-165.

Grams, P.E., and J.C. Schmidt, 2005. Equilibrium or indeterminate? Where sediment budgets fail: Sediment mass balance and adjustment of channel form, Green River downstream from Flaming Gorge Dam, Utah and Colorado. Geomorphology 71, 156-181.

Grant, G.E., Schmidt, J.C. and S.L. Lewis, 2003. A Geological Framework for Interpreting Downstream Effects of Dams on Rivers. In Grant, G.E. and J.E. O'Connor (eds), *A Peculiar River*. Water Science and Application 7. American Geophysical Union, San Francisco. Pp. 209-226.

Gregory, S.V., Swanson, F.J., McKee, W.A., and K.W. Cummins, 1991. An ecosystem perspective of riparian zones. Bioscience 41(8): 540-551.

H.T. Harvey and Associates, 2007a. Stony Creek Watershed Assessment, Volume 1: Lower Stony Creek watershed analysis. Prepared in collaboration with G.M. Kondolf and Graham Matthews and Associates. Prepared for Glenn County Resource Conservation District, Project no. 2610-01. 159p.

H.T. Harvey and Associates, 2007b. Stony Creek Watershed Assessment, Volume 2: Existing conditions report. Prepared in collaboration with G.M. Kondolf and Graham Matthews and Associates. Prepared for Glenn County Resource Conservation District, Project no. 2610-01. 311p.

Hassan, M.A. and P. Ergenzinger, 2003. Use of tracers in fluvial geomorphology. In Kondolf, G.M. and H. Piegay (eds.), *Tools in Fluvial Geomorphology*. Wiley, San Francisco. Pp. 397-423.

Hazel, J.E., Topping, D.J., Schmidt, J.C., and M. Kaplinski, 2006. Influence of a dam on fine-sediment storage in a canyon river. Journal of Geophysical Research 111, F01025, doi:10.1029/2004JF000193.

James, A., 1997. Channel incision on the lower American River, California, from streamflow gage records. Water Resources Research 33(3), 485-490.

James, A., 1999. Time and the persistence of alluvium: River engineering, fluvial geomorphology and mining sediment in California. Geomorphology 31, 265-290.

James, L.A., 1991. Incision and morphologic evolution of an alluvial channel recovering from hydraulic mining sediment. Geological Society of America Bulletin 103, 723-746.

James, L.A., 2005. Sediment from hydraulic mining detained by Englebright and small dams in the Yuba basin, Geomorphology 71, 202-226.

Johnson, W.C., 2002. Riparian vegetation diversity along regulated rivers: contribution of novel and relict habitats. Freshwater Biology 47: 749-759.

Jones, B.L., Hawley, N.L., and J.R. Crippen, 1972. Sediment transport in the western tributaries of the Sacramento River, California. United States Geological Survey, Water-Supply Paper 1798-J. 27p.

Kinerson, D., 1990. Bed surface response to sediment supply. Masters thesis, Department of Geology, University of California, Berkeley. 420p.

Kondolf, G.M. and W.V.G. Matthews, 1993. Management of Coarse Sediment on Regulated Rivers. California Water Resources Center, University of California, Report no. 80. 128p.

Kondolf, G.M., 1993. Geomorphological observations on spawning gravel, channel change, and riparian vegetation on the lower Mokelumne River, California. Report submitted to Environmental Sciences Division, Oak Ridge National Laboratory, Oak Ridge, TN 37831. 28pp.

Kondolf, G.M., 1997. Hungry water: effects of dams and gravel mining on river channels. *Environmental Management*. 21(4), 533-551.

Kondolf, G.M., and M.L. Swanson, 1993. Channel adjustments to reservoir construction and instream gravel mining, Stony Creek, California. Environmental Geology and Water Science 21, 256-269.

Kondolf, G.M., and W.V.G. Matthews, 1991. Unmeasured residuals in sediment budgets: a cautionary note. Water Resources Research 27(9), 2483-2486.

Kondolf, G.M., Falzone, A., and K.S. Schneider, 2001. Reconnaissance-level assessment of channel change and spawning habitat on the Stanislaus River below Goodwin Dam. Report submitted to U.S. Fish and Wildlife Service, Sacramento, CA. 233p.

Kondolf, G.M., Vick, J.C., and T.M. Ramirez, 1996. Salmon spawning habitat rehabilitation in the Merced, Tuolumne, and Stanislaus Rivers, California: An evaluation of project planning and performance. University of California, Water Resources Center Report No. 90. 147p.

Lee, K.W., 1968. Determination of channel capacity of Stony Creek downstream from Black Butte Dam, Glenn and Tehama Counties, California. United States Geological Survey, Open-File Report. 15p. plus appendices, figures and plates.

Levin, P.S. and N. Tolimieri, 2001. Differences in the impacts of dams on the dynamics of salmon populations. Animal Conservation 4, 291-299.

Ligon, F.K., Dietrich, W.E., and W.J. Trush, 1995. Downstream ecological effects of dams. Bioscience 45(3), 183-192.

Lisle, T.E., Iseya, F., and H. Ikeda, 1993. Response of a channel with alternative bars to a decrease in supply of mixed-size bed load: a flume experiment. Water Resources Research, 29, 3623-3629.

Lowe, R.L., 1979. Phytobenthic ecology and regulated streams. In Ward, J.V., and J.A. Stanford (eds.), *The Ecology of Regulated Streams*. Plenum Press, New York. Pp. 25-34.

Magilligan, F.J., Nislow, K.H., and B.E. Graber, 2003. Scale-independent assessment of discharge reduction and riparian disconnectivity following flow regulation by dams. Geology 31(7), 569-572.

Mahoney, J.M., and S.B. Rood, 1998. Streamflow requirements for Cottonwood seedling recruitment – an integrative model. Wetlands 18(4), 634-645

Major, J.J., 2004. Posteruption suspended sediment transport at Mount St. Helens: Decadal-scale relationships with landscape adjustments and river discharges. Journal of Geophysical Research 109. 22p.

McBain and Trush and Graham Matthews and Associates, 1999. Lower Clear Creek bedload transport measurements – Technical memorandum for WY1998. Report prepared for Lower Clear Creek Technical Workgroup, November 1999. 17p.

McBain and Trush, 2000. Habitat restoration plan for the Lower Tuolumne River corridor. Prepared for The Tuolumne River Technical Advisory Committee. Prepared by McBain and Trush, Arcata, CA. 217p.

McBain and Trush, 2001. Final report: Geomorphic evaluation of Lower Clear Creek downstream of Whiskeytown Dam, California. Prepared by McBain and Trush, Graham Matthews and Associates, North State Resources, and Stillwater Sciences. 190p.

McKee, L., Ganju, N., Schollhamer, D., Davis, J., Yee, D., Leatherbarrow, J., and R. Hoenicke, 2002. Estimates of suspended sediment flux entering San Francisco Bay from the Sacramento and San Joaquin Delta. Report prepared for San Francisco Bay Regional Monitoring Program for Trace Substances. San Francisco Estuary Institute contribution 65. 28p.

Michelli, E.R., Kirchner, J.W., and E.W. Larsen, 2004. Quantifying the effect of riparian forest versus agricultural vegetation on river meander migration rates, Central Sacramento River, California, USA. River Research and Applications 20, 537-548.

Milhous, R.T., 1973. Sediment transport in a gravel-bottomed stream. Ph.D. thesis, Oregon State University, Corvallis, Oregon. 232p.

Milhous, R.T., 1997. Reservoir construction, river sedimentation and tributary sediment size. In. Human Impact on Erosion and Sedimentation, Proceedings of Rabat Symposium S6, April 1997, IAHS publication no. 245, 275-282.

Naiman, R.J. and H. Decamps, 1997. The ecology of interfaces: riparian zones. Annual Review of Ecology and Systematics 28, 621-658.

Naiman, R.J. and R.E. Bilby (eds.), *River Ecology and Management*. Springer, New York. 705p.

Naiman, R.J., Fetherston, K.L., McKay, S.J., and J. Chen, 1998. Chapter 12: Riparian Forests. In Naiman RJ and RE Bilby (eds.), *River Ecology and Management*. Springer, New York. 705p.

Nakamura, F. and N. Shin, 2001. The downstream effects of dams on the regeneration of tree species in Northern Japan. In Dorava, Montgomery, Palcsak and Fitzpatrick (eds.) *Geomorphic Processes and Riverine Habitat*. American Geophysical Union, Water Science and Application 4. pp 173-183.

Nash, D.B., 1994. Effective sediment-transporting discharge from magnitude-frequency analysis. Journal of Geology 102, 79-95.

Nelson, P.A., Venditti, J.G., Dietrich, W.E., Kirchner, J.W., Ikeda, H., Iseya, F., and L.S. Sklar, 2009. Response of bed surface patchiness to reductions in sediment supply. Journal of Geophysical Research 144. F02005, doi:10.1029/2008JK001144.

Nilsson, C. and K. Berggren, 2000. Alterations of riparian ecosystems caused by river regulation. Bioscience 50(9), 783-792.

Ogden Beeman and Associates, 1992. Sediment budget study for San Francisco Bay. Report prepared for the San Francisco District, Corps of Engineers. 25p.

Parker, G., 1990a. Surface-based bedload transport relation for gravel rivers. Journal of Hydraulic Research, 28(4), 417-436.

Parker, G., 1990b. The "ACRONYM" series of Pascal programs for computing bedload transport in gravel rivers. External Memorandum M-220, St. Anthony Falls Hydraulic Laboratory, University of Minnesota. 123p.

Parker, G., Klingeman, P.C., and D.L. McLean, 1982. Bedload and size distribution in paved gravel bed streams. Journal of Hydraulics Division 108, 544-571.

Petts, G.E., 1979. Complex response of river channel morphology subsequent to reservoir construction. Progress in Physical Geography 3(3), 329-362.

Petts, G.E., 1984. *Impounded Rivers: Perspectives for Ecological Management*. John Wiley and Sons, New York. 326 p.

Petts, G.E., 1987. Time-scales for ecological change in regulated rivers. In Craig, J.F. and J.B. Kemper (eds.). Regulated Streams: Advances in Ecology. Plenum Press, NY. 431p.

Pickup, G. and R.F. Warner, 1976. Effects of hydrologic regime on magnitude and frequency of dominant discharge. Journal of Hydrology 29(1-2), 51-57.

Pitlick, J., 1988. Variability of bed load measurement. Water Resources Research 24(1), 173-177.

Pitlick, J., Cui, Y., and P. Wilcock, 2009. Manual for Computing Bed Load Transport Using BAGS (Bedload Assessment for Gravel-bed Streams) Software. United States Forest Service General Technical Report RMRS-GTR-223. 45p.

Poff, N.L., Allan, J.D., Bain, M.B., Karr, J.R., Prestegaard, K.L., Richter, B.D., Sparks, R.E., and J.C. Stromberg, 1997. The natural flow regime: a paradigm for river conservation and restoration. Bioscience 47(100), 769-784.

Poff, N.L., and J.D. Allan, 1995. Functional organization of stream fish assemblages in relation to hydrological variability. Ecology 76(2), 606-627.

Poff, N.L., and J.V. Ward, 1989. Implications of streamflow variability and predictability for lotic community structure: a regional analysis of streamflow patterns. Canadian Journal of Fisheries and Aquatic Sciences 46, 1805-1818.

Porterfield, G., 1980. Sediment transport of streams tributary to San Francisco, San Pablo, and Suisun Bays, California, 1909-1966. United States Geological Survey, Water-Resources Investigations 80-64. 92p.

Porterfield, G., Busch, R.D., and A.O. Waananen, 1978. Sediment transport in the Feather River, Lake Oroville to Yuba City, California. United States Geological Survey, Water-Resources Investigations 78-20. 73p.

Power, M.E., W.E. Dietrich, and J.C. Finlay. 1996. Dams and downstream aquatic biodiversity: Potential food web consequences of hydrologic and geomorphic change. Environmental Management 20, 887-895.

Resh, V.H., Brown, A.V., Covich, A.P., Gurtz, M.E., Li, H.W., Minshall, G.W., Reice, S.R., Sheldon, A.L., Wallace, J.B., and R.C. Wissmar, 1988. The role of disturbance in stream ecology. Journal of the North American Benthological Society 7(4), 433-455.

Richter, B.D., Baumgartner, J.V., Powell, J., and D.P. Braun, 1996. A method for assessing hydrologic alteration within ecosystems. Conservation Biology 10, 1163-1174.

Salant, N.L., Renshaw, C.I., and F.J. Magilligan, 2006. Short and long-term changes to bed mobility and bed composition under altered sediment regimes. Geomorphology 76, 43-53.

Schmidt, J.C., and D.M. Rubin, 1995. Regulated streamflow, fine-grained deposits, and effective discharge in canyons with abundant debris fans. In J.E. Costa et al. (eds.), *Natural and Anthropogenic Influences in Fluvial Geomorphology (the Wolman Volume).* American Geophysical Union, Geophysical Monograph 89. Washington, D.C. pp. 177-195.

Schmidt, J.C., and P.R. Wilcock, 2008. Metrics for assessing the downstream effects of dams. Water Resources Research 44. doi:10.1029/2006WR005092.

Shih, S.M., and P.D. Komar, 1990. Differential bedload transport rates in a gravel-bed stream: A grain-size distribution approach. Earth Surface Processes and Landforms, 15, 539-552.

Simpson, R.G., 1972. Determination of channel capacity of the Mokelumne River downstream from Camanche Dam, San Joaquin and Sacramento Counties, California. United States Geological Survey, Open-File Report. 14p, plus appendices, figures and plates.

Singer, M.B., 2008. Downstream patterns of bed material grain size in a large, lowland alluvial river subject to low sediment supply. Water Resources Research 44, 7p.

Singer, M.B., and T. Dunne, 2004. Modeling decadal bed material sediment flux based on stochastic hydrology. Water Resources Research 40, W03302, doi:10.1029/2003WR002723.

Sommer, T., McEwan, D., and R. Brown, 2001. Factors affecting Chinook Salmon spawning in the Lower Feather River. In Brown, R.L. (ed.), Contributions to the Biology of Central Valley Salmonids, Vol. 1 and 2. State of California, Department of Fish and Game, Fish Bulletin 179, 269-297.

Stillwater Sciences, 2001. Merced River corridor restoration plan baseline studies. Volume II: Geomorphic and riparian vegetation investigations report. Prepared by Stillwater Sciences, Berkeley, California for CALFED Bay-Delta Program, Sacramento, California.

Surian, N., 1999. Channel changes due to river regulation: The case of the Piave River, Italy. Earth Surface Processes and Landforms 24, 1135-1151.

Swanson, M.L., and G.M. Kondolf, 1991. Geomorphic study of bed degradation in Stony Creek, Glenn County, California. Report submitted to California Department of Transportation, Division of Structures, Sacramento, CA. 80p. plus appendices.

Trush, W.J., McBain, S.M., and L.B. Leopold, 2000. Attributes of an alluvial river and their relation to water policy and management. Proceedings of the National Academy of Sciences 97(22), 11858-11863.

United States Army Corps of Engineers (USACE), 2002. Sacramento and San Joaquin River Basins, California, Comprehensive Study, Interim Report.

United States Army Corps of Engineers, 1995. Winters and vicinity reconnaissance report, Appendix A.

United States Department of Agriculture, Soil Conservation Service, 1976. Flood Hazard Analyses, City of Winters, including portions of Putah Creek, Dry Creek, and Moody (Dry) Slough, Yolo County, California. Prepared in Cooperation with: City of Winters, Western Yolo Resource Conservation District, California Department of Water Resources.

United States Geological Survey (USGS), 1982. Guidelines for determining flood flow frequency. Interagency Advisory Committee on Water Data, Hydrology Subcommittee, Bulletin 17B.

Vericat, D., and R.J. Batalla, 2006. Sediment transport in a large impounded river: The lower Ebro, NE Iberian Peninsula. Geomorphology 79, 72-92.

Vick, J.C., 1995. Habitat rehabilitation in the Lower Merced River: A geomorphological perspective. Unpublished Masters thesis, University of California, Berkeley.

Ward, J.V. and J.A. Stanford, 1983. The intermediate-disturbance hypothesis: an explanation for biotic diversity patterns in lotic ecosystems. In Fontaine, T.D. and S.M. Bartell (eds.), Dynamics of Lotic Ecosystems. Ann Arbor Science Publishers, Ann Arbor, Michigan. Pp. 355-395.

Ward, J.V., and J.A. Stanford (eds.), 1979. *The Ecology of Regulated Streams*. Plenum Press, New York. 398p.

Whiting, P.J. and J.G. King, 2003. Surface particle sizes on armoured gravel streambeds: Effects of supply and hydraulics. Earth Surface Processes and Landforms 28, 1459-1471.

Wilcock, P., Pitlick, J., and Y. Cui, 2009. Sediment Transport Primer Estimating Bed-Material Transport in Gravel-bed Rivers. United States Forest Service, General Technical Report, RMRS-GTR-226. 78p.

Wilcock, P.R. and J.C. Crowe, 2003. Surface-based transport model for mixed-size sediment. Journal of Hydraulic Engineering 129(2), 120-128.

Wilcock, P.R., Kondolf, G.M., Matthews, W.V.G., and A.F. Barta, 1996. Specification of sediment maintenance flows for a large gravel-bed river. Water Resources Research 32(9), 2911 – 2921.

Williams, G.P. and M.G. Wolman, 1984. Downstream Effects of Dams on Alluvial Rivers. U.S. Geological Survey Professional Paper 1286. U.S. Government Printing Office, Washington. 83 p.

Williams, J.G., 2001. Chinook Salmon in the Lower American River, California's largest urban stream. In Brown, R.L. (ed.), Contributions to the Biology of Central Valley Salmonids, Vol. 1 and 2. State of California, Department of Fish and Game, Fish Bulletin 179. 38p.

Wolman, G.M., 1954. A method of sampling coarse riverbed material. Transactions of the American Geophysical Union, 35(6).

Wolman, M.G., and J.P. Miller, 1960. Magnitude and frequency of forces in geomorphic processes, Geology 68(1), 54-74.

Wolman, M.G., and R Gerson, 1978. Relative scales of time and effectiveness of climate in watershed geomorphology. Earth Surface Processes 3, 189-208.

Wright, S.A., and D.H. Schoellhamer, 2004. Trends in the sediment yield of the Sacramento River, California, 1957-2001. San Francisco Estuary and Watershed Science, 2(2), article 2.

Yoshiyama, R.M., Gerstung, E.R., Fisher, F.W., and P.B. Moyle, 1996. Historical and present distribution of Chinook salmon in the Central Valley drainage of California. In Sierra Nevada Ecosystem Project final report to Congress. Centers for Water and Wildland Resources, University of California, Davis. Volume 3, p 309-361.

Zar, J.H., 1999. Biostatistical Analysis, 4th edition. Prentice-Hall Inc, Upper Saddle River, New Jersey. 663p.

Figures

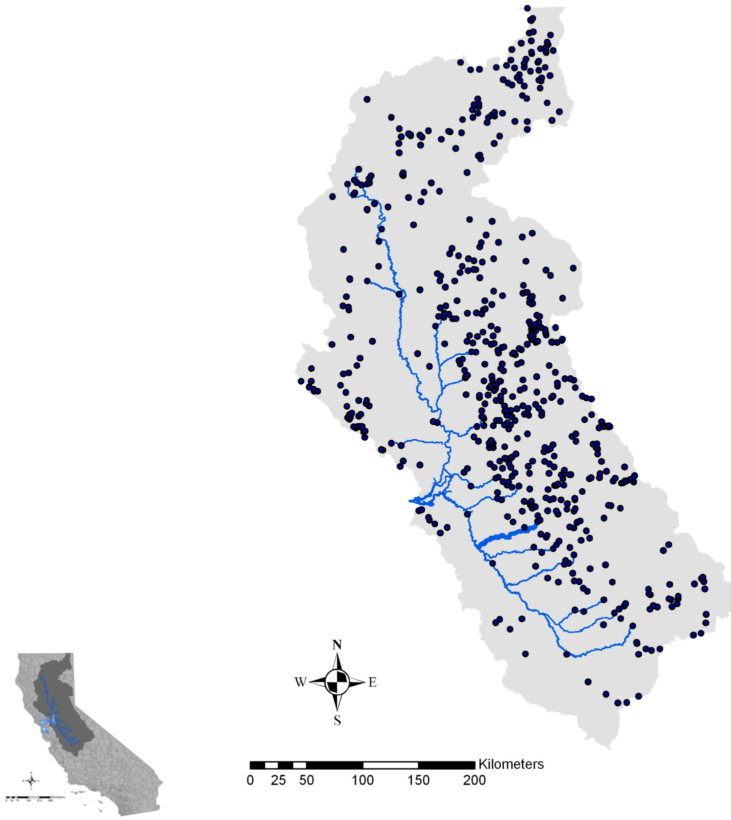

Figure 1. Map of the Sacramento-San Joaquin river system, showing dams in the watershed regulated by CDSD (CDSD 2005).

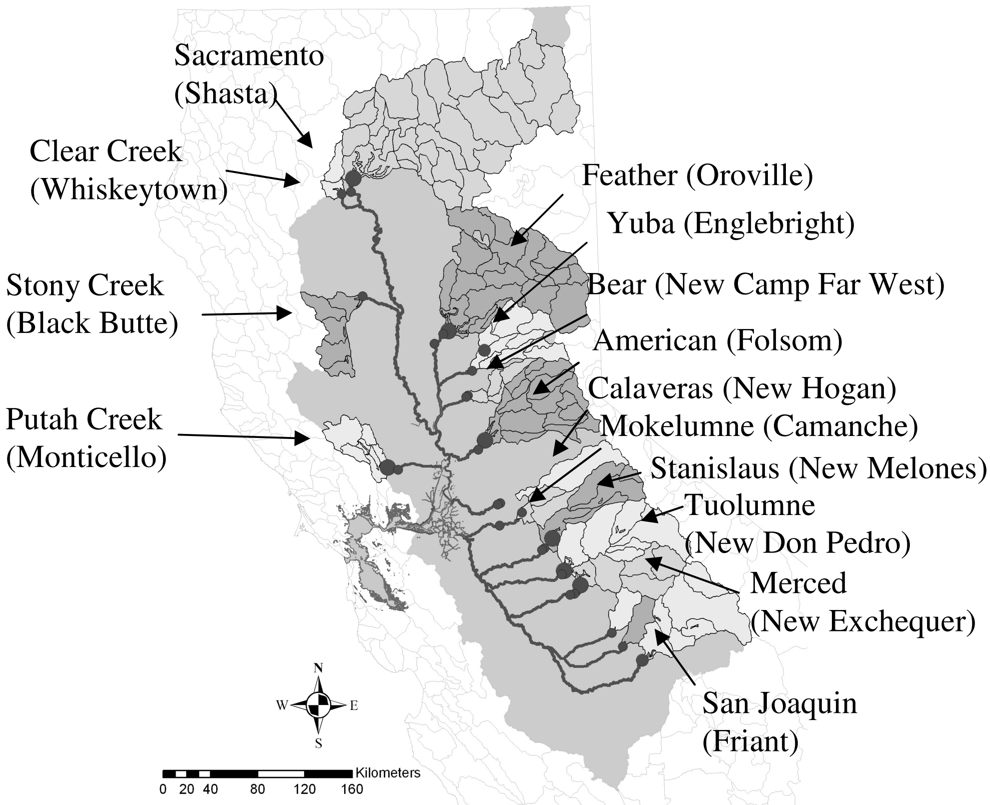

Figure 2. Map of the major watersheds of the Sacramento-San Joaquin river system dammed by the foothill dams. Watersheds are labeled with river name with foothill dams in parentheses.

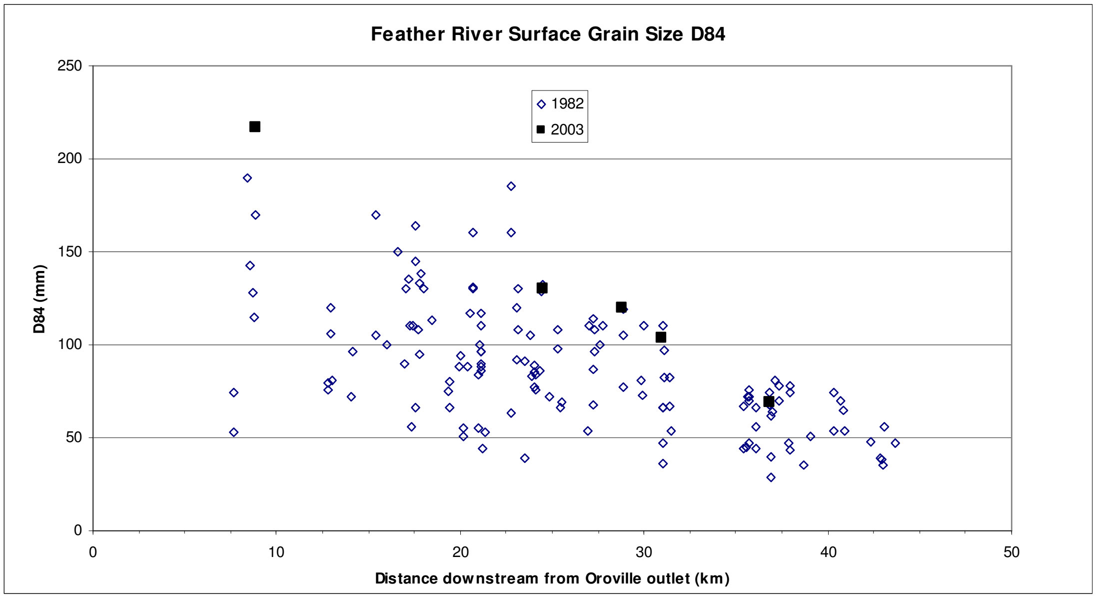

Figure 3. Downstream trends of D84 grain size downstream of Oroville Dam on the Feather River, suggesting coarsening from 1982 to 2003 (from CDWR 2004a).

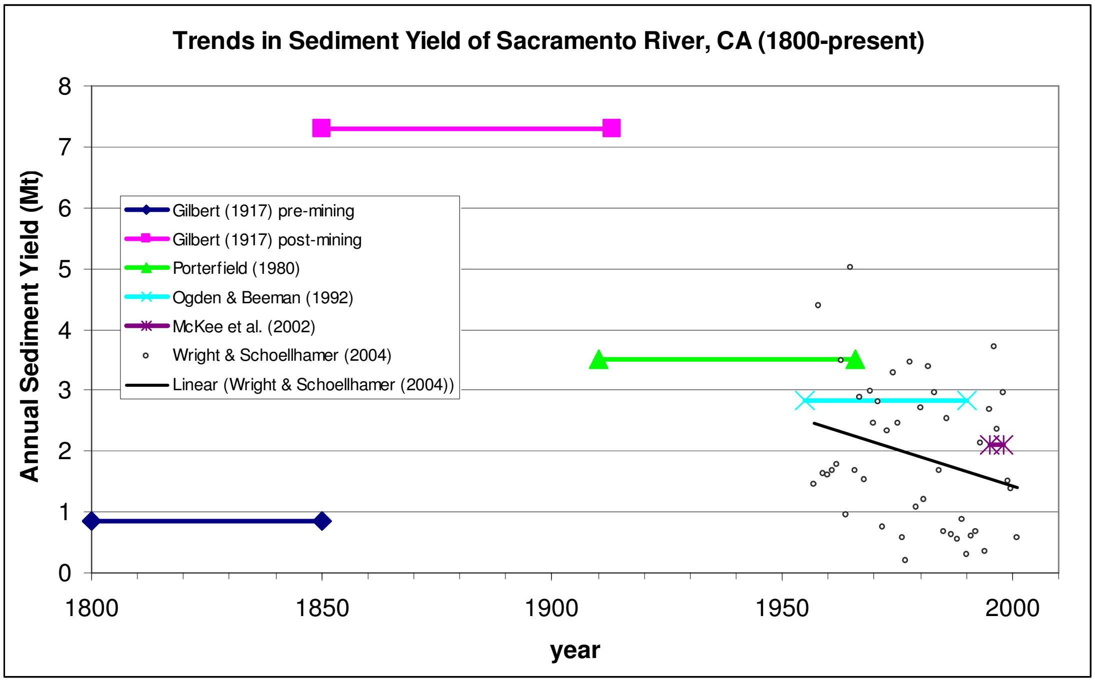

Figure 4. Trends in the sediment yield of the Lower Sacramento River, 1800 to present, showing the large peak in yield from hydraulic mining in the late 1800s, and the gradual declining trends to the present (modified from Wright and Schoellhamer 2004).

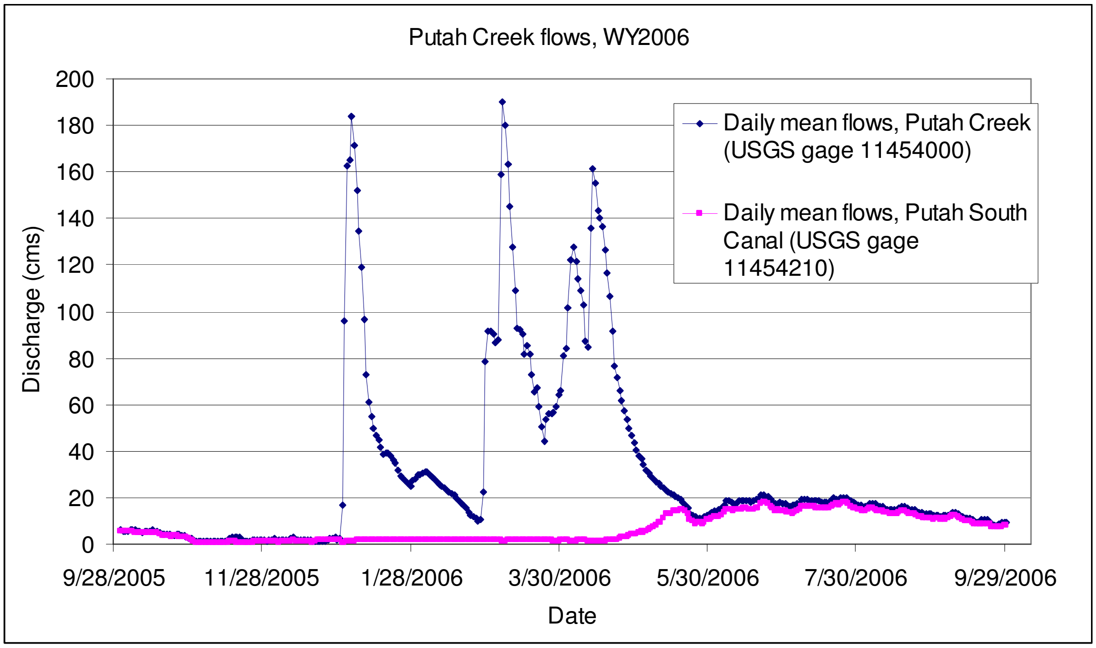

Figure 5. Graph showing WY2006 flows on Putah Creek at Winters (USGS gage 11454000), and the reduction in baseflows from the Putah South Canal just downstream (USGS gage 11454210). The majority of stream gages used in this study were downstream of the reregulating dams, however, in the few cases where the gages were upstream of diversion points, it was assumed that the water diversions had minimal influence on the magnitude of bedload transport events downstream. In this case, the diversion of the Canal occurs at the Putah Diversion Dam, just upstream of study sites PC1 and PC2.

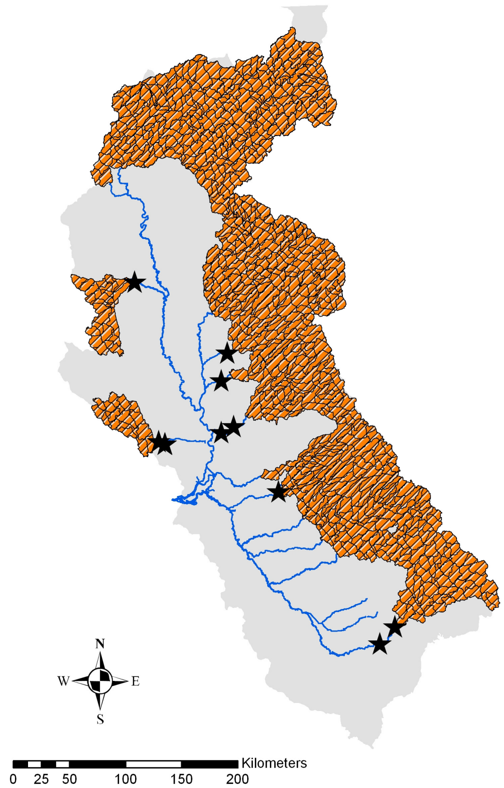

Figure 6. Map of study sites established in this study. Stars show location of study sites, shaded area is the watershed upstream of the major foothill dams.

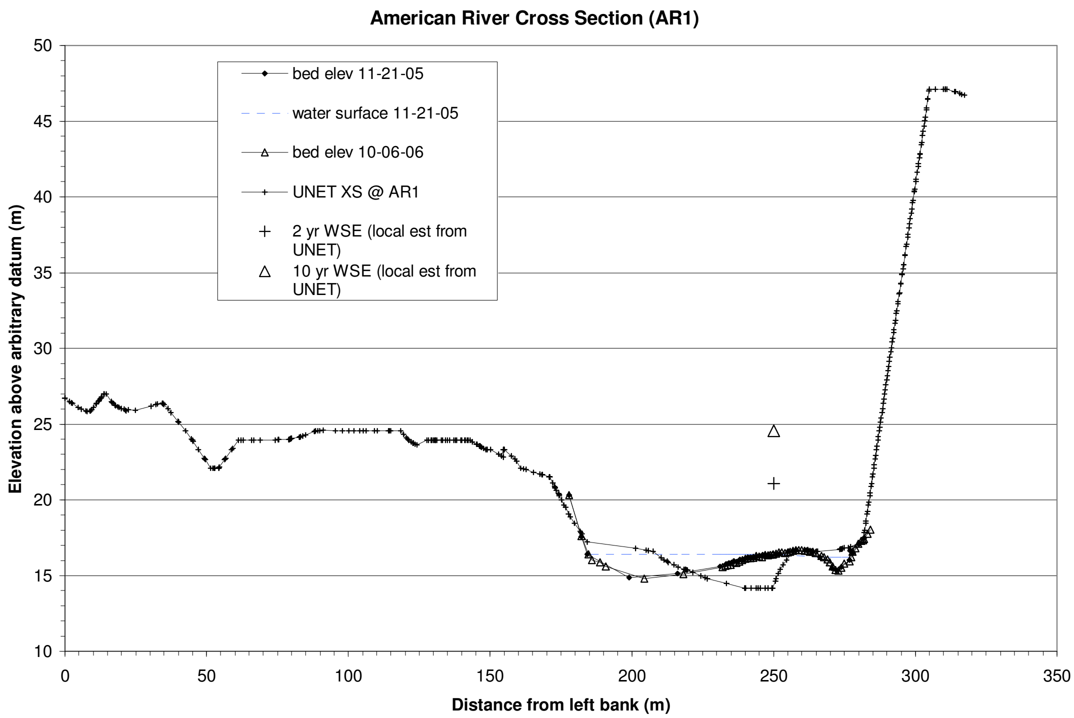

Figure 7. American River site, AR1, showing measured bed elevations and water stage elevations (from USACE 2002).

Figure 8. Placement of 1st set of tracer gravel lines at Bear River site, BR2. A second set of stone was placed approximately 0.5m upstream soon after the photo was taken. Note the relatively undisturbed bed and low-elevation of the stationing tape, which allowed for precise relocation in the event of aggradation.

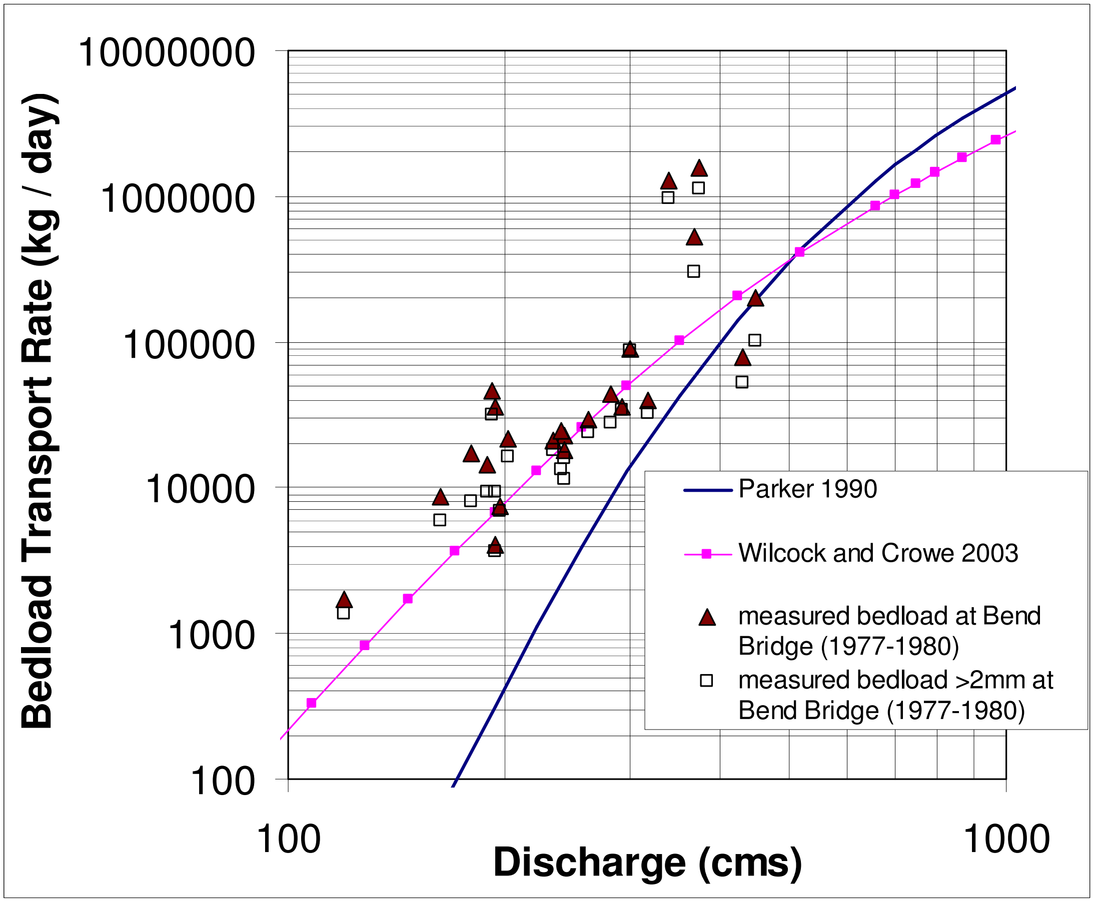

Figure 9. Graph of measured bedload at the USGS gage on the Sacramento River at Bend Bridge above Red Bluff (#11377100) for the WY 1977-1980, plotted with the bedload transport equations from Parker (1990a) and Wilcock and Crowe (2003) calculated using bed material collected at the same site on 1/5/1977 (average of four samples). Note: this station is the only station with records of bedload measurements in the Sacramento-San Joaquin river system other than the Lower Sacramento and Lower Clear Creek. The discharges during which these bedload measurements were taken are high-frequency, low-magnitude events. The maximum flow of 447cms during which bedload was sampled, is exceeded a large portion of the time at this site (14% for post-dam period) and likely reflects transport only at lower discharges.

Following pages, Figures 10a-n. Graphs of magnitude-frequency of bedload transport for pre- and post-dam periods on the major tributaries to the Sacramento-San Joaquin river system. “GSD” in the graph title is “grain size distribution”.

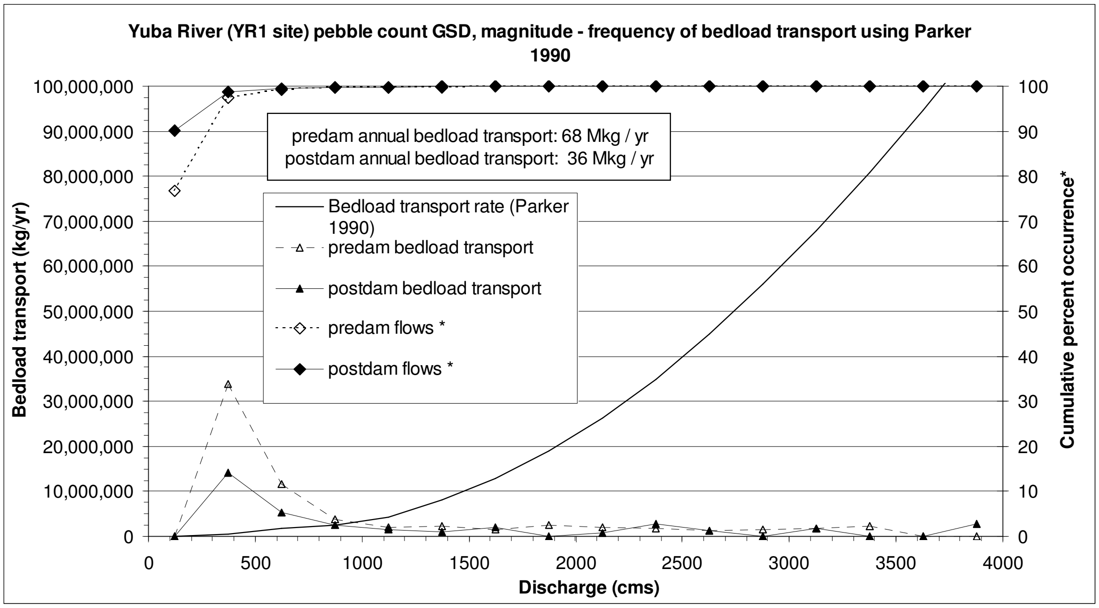

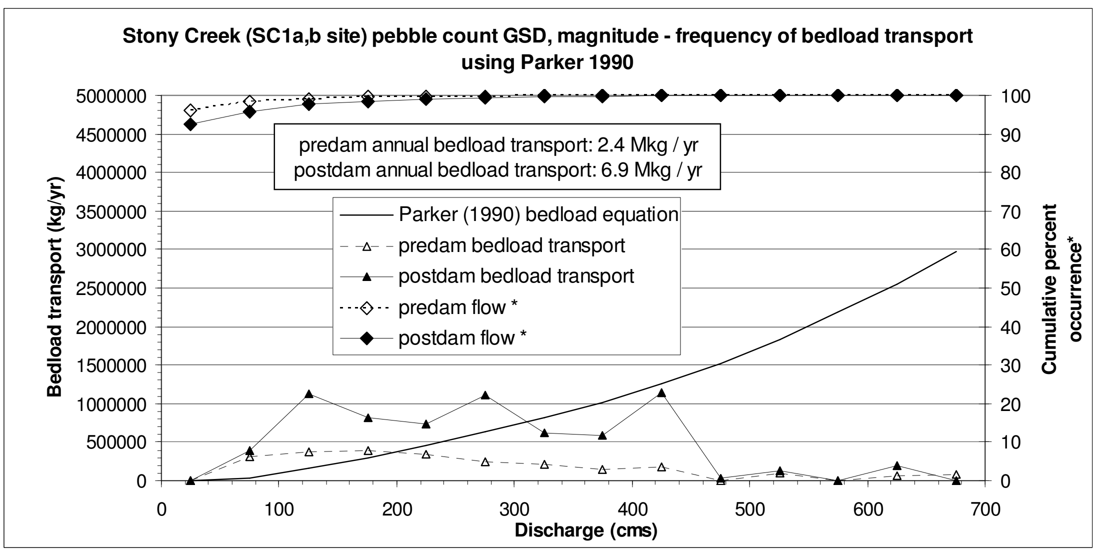

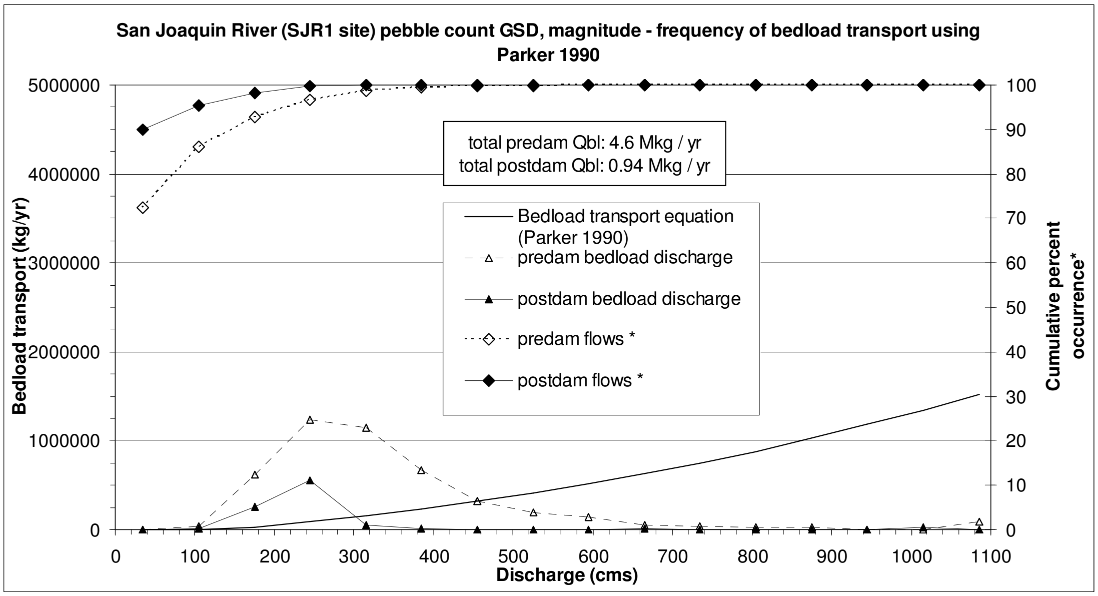

San Joaquin River (SJR1 site) pebble count GSD, magnitude - frequency of bedload transport using Parker 1990
total predam Qbl: 4.6 Mkg / yr
total postdam Qbl: 0.94 Mkg / yr
Bedload transport equation (Parker 1990)
predam bedload discharge
postdam bedload discharge
predam flows *
postdam flows *
Bedload transport (kg/yr)
Cumulative percent occurrence*
Discharge (cms)
0
1000000
2000000
3000000
4000000
5000000
0
100
200
300
400
500
600
700
800
900
1000
1100
0
10
20
30
40
50
60
70
80
90
100

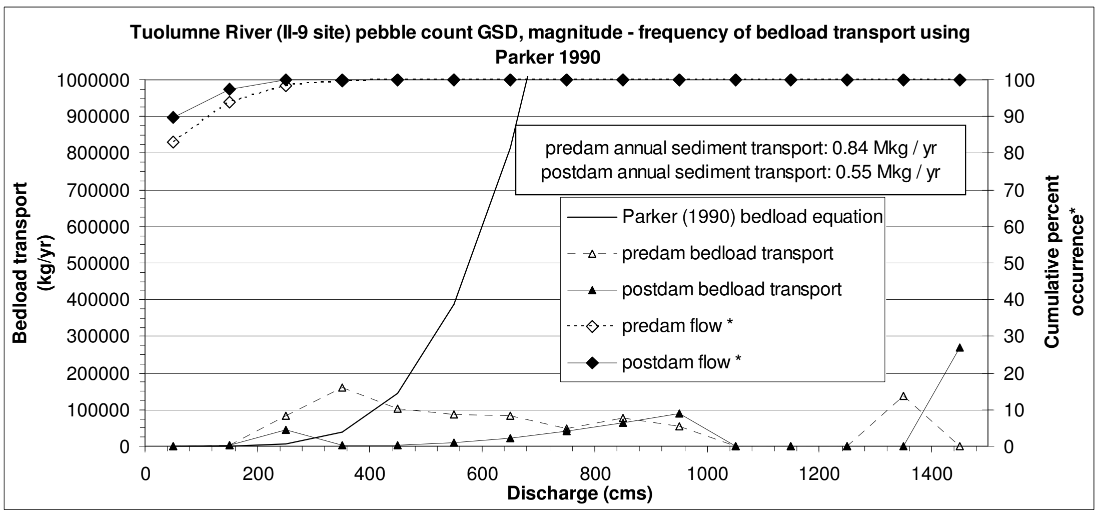

Tuolumne River (II-9 site) pebble count GSD, magnitude - frequency of bedload transport using Parker 1990
predam annual sediment transport: 0.84 Mkg / yr
postdam annual sediment transport: 0.55 Mkg / yr
Parker (1990) bedload equation
predam bedload transport
postdam bedload transport
predam flow *
postdam flow *
Bedload transport (kg/yr)
Cumulative percent occurrence*
Discharge (cms)
0
100000
200000
300000
400000
500000
600000
700000
800000
900000
1000000
0
200
400
600
800
1000
1200
1400
0
10
20
30
40
50
60
70
80
90
100

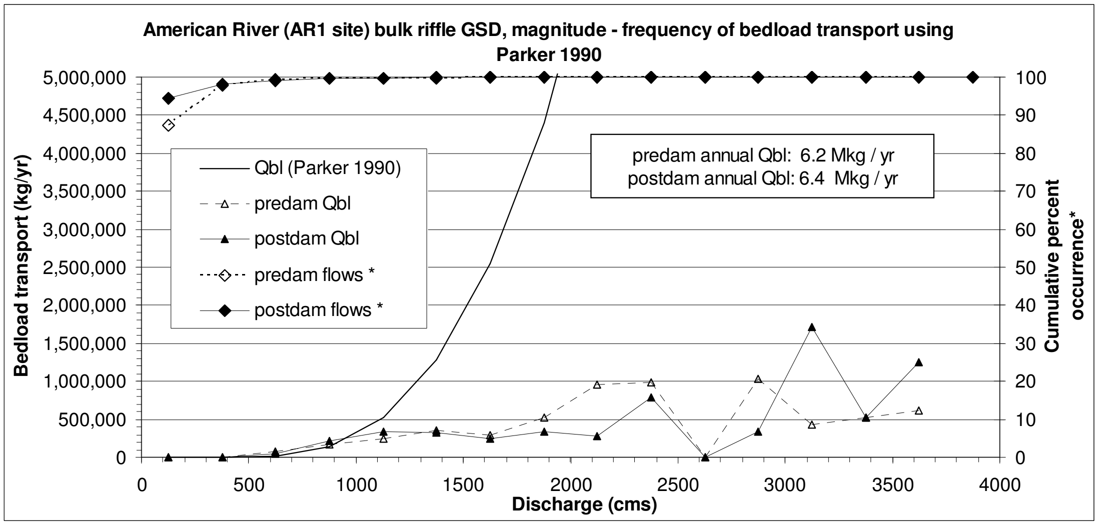
American River (AR1 site) bulk riffle GSD, magnitude - frequency of bedload transport using Parker 1990
Bedload transport (kg/yr)
Cumulative percent occurrence*
Discharge (cms)
Qbl (Parker 1990)
predam Qbl
postdam Qbl
predam flows *
postdam flows *
predam annual Qbl: 6.2 Mkg / yr
postdam annual Qbl: 6.4 Mkg / yr

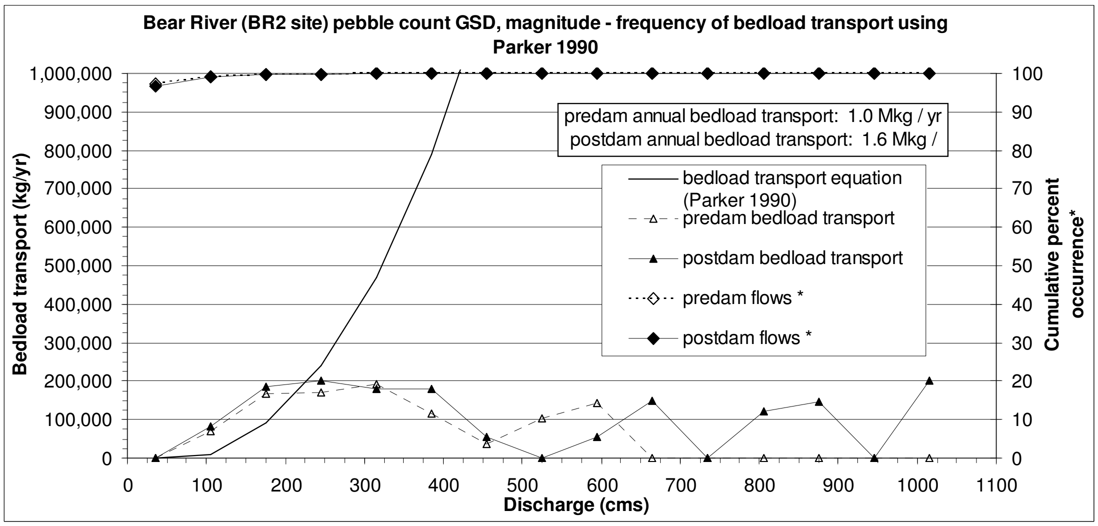
Bear River (BR2 site) pebble count GSD, magnitude - frequency of bedload transport using Parker 1990
Bedload transport (kg/yr)
Cumulative percent occurrence*
Discharge (cms)
predam annual bedload transport: 1.0 Mkg / yr
postdam annual bedload transport: 1.6 Mkg /
bedload transport equation (Parker 1990)
predam bedload transport
postdam bedload transport
predam flows *
postdam flows *

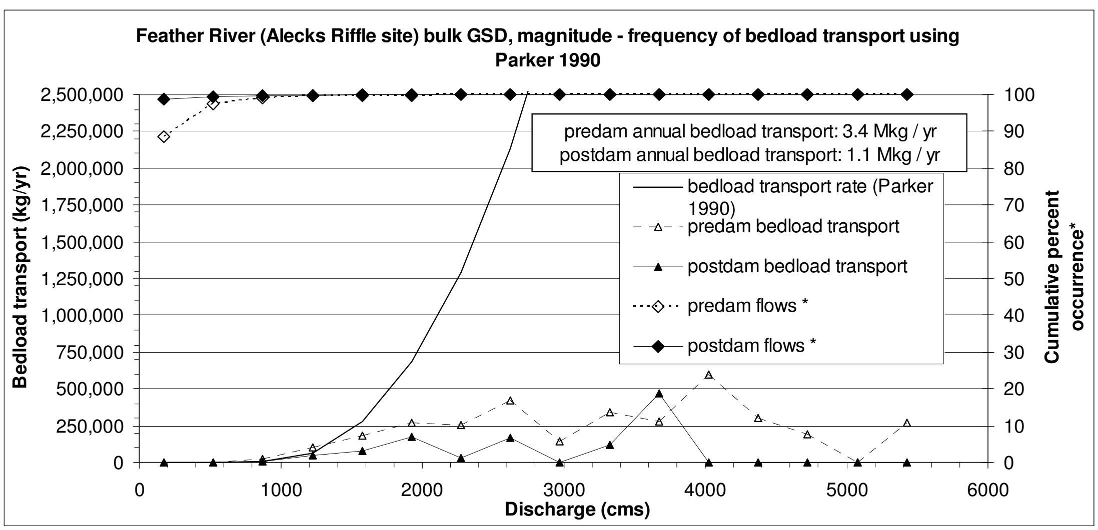
Feather River (Alecks Riffle site) bulk GSD, magnitude - frequency of bedload transport using Parker 1990
Bedload transport (kg/yr)
Cumulative percent occurrence*
Discharge (cms)
predam annual bedload transport: 3.4 Mkg / yr
postdam annual bedload transport: 1.1 Mkg / yr
bedload transport rate (Parker 1990)
predam bedload transport
postdam bedload transport
predam flows *
postdam flows *

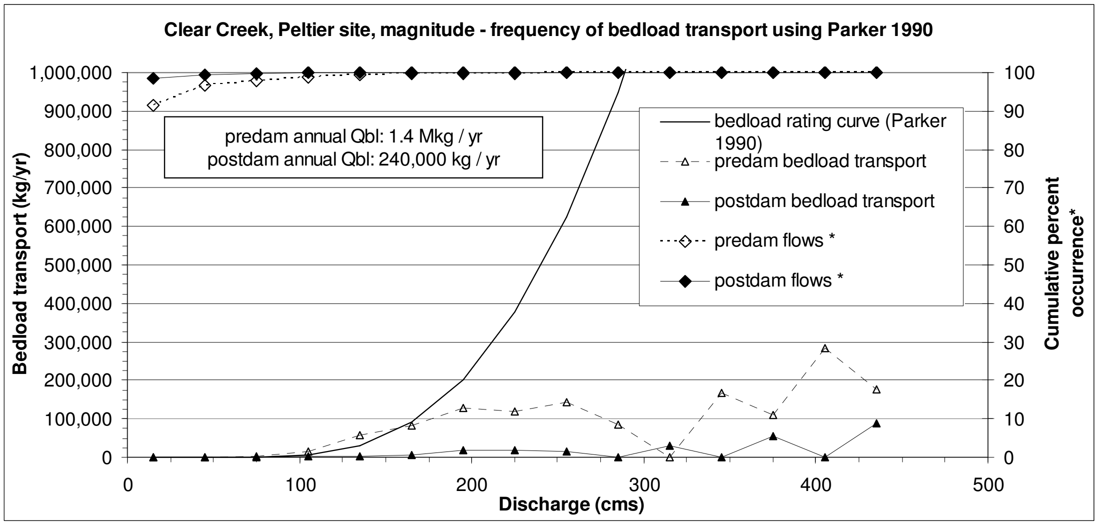
Clear Creek, Peltier site, magnitude - frequency of bedload transport using Parker 1990
predam annual Qbl: 1.4 Mkg / yr
postdam annual Qbl: 240,000 kg / yr
bedload rating curve (Parker 1990)
predam bedload transport
postdam bedload transport
predam flows *
postdam flows *
Bedload transport (kg/yr)
Cumulative percent occurrence*
Discharge (cms)

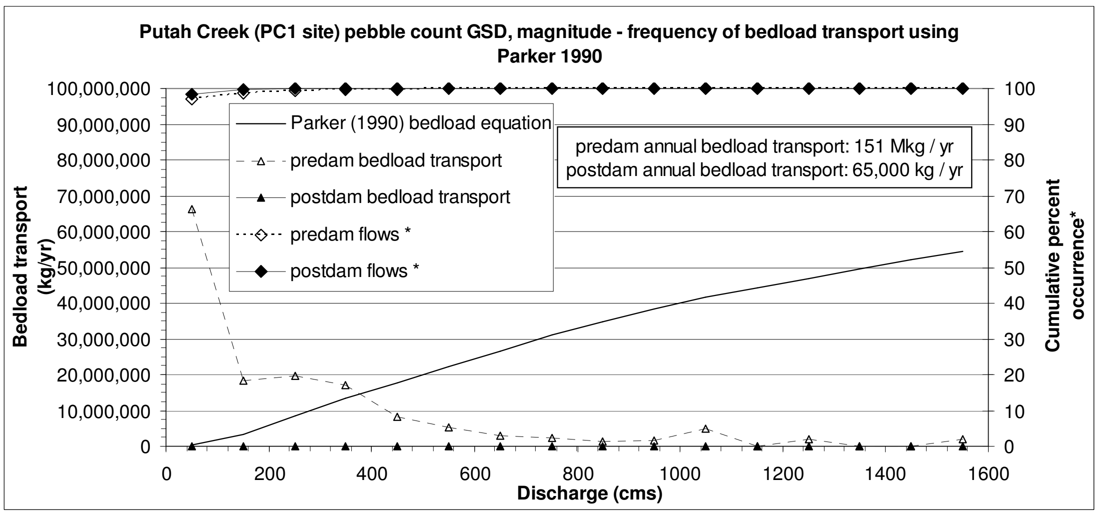
Putah Creek (PC1 site) pebble count GSD, magnitude - frequency of bedload transport using Parker 1990
Parker (1990) bedload equation
predam bedload transport
postdam bedload transport
predam flows *
postdam flows *
predam annual bedload transport: 151 Mkg / yr
postdam annual bedload transport: 65,000 kg / yr
Bedload transport (kg/yr)
Cumulative percent occurrence*
Discharge (cms)

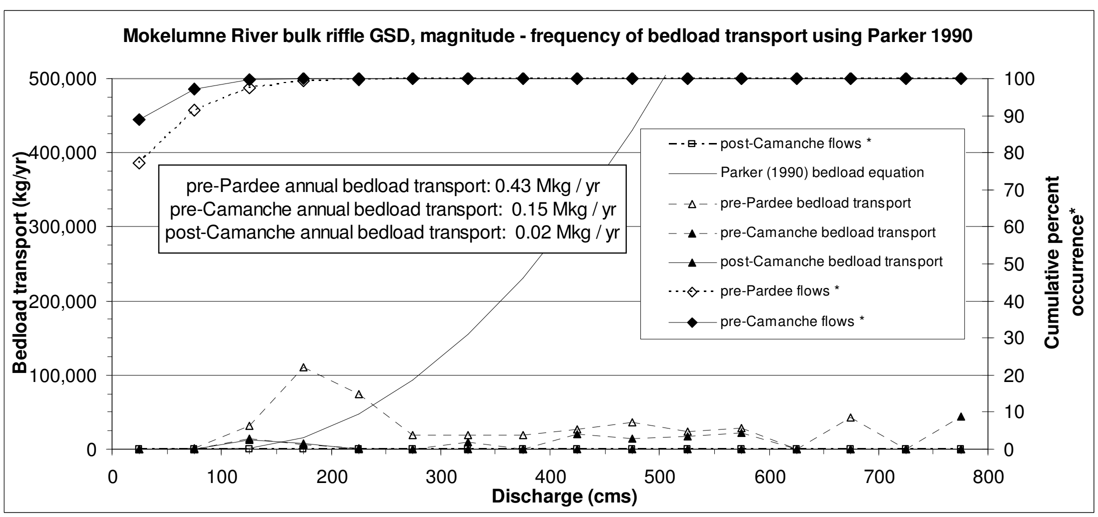
Mokelumne River bulk riffle GSD, magnitude - frequency of bedload transport using Parker 1990
pre-Pardee annual bedload transport: 0.43 Mkg / yr
pre-Camanche annual bedload transport: 0.15 Mkg / yr
post-Camanche annual bedload transport: 0.02 Mkg / yr
post-Camanche flows *
Parker (1990) bedload equation
pre-Pardee bedload transport
pre-Camanche bedload transport
post-Camanche bedload transport
pre-Pardee flows *
pre-Camanche flows *
Bedload transport (kg/yr)
Cumulative percent occurrence*
Discharge (cms)

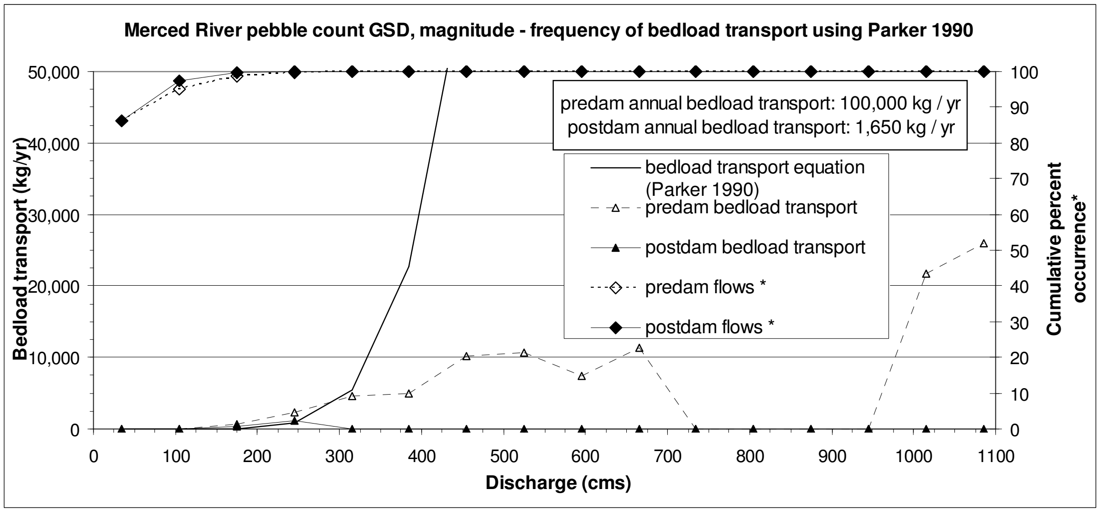

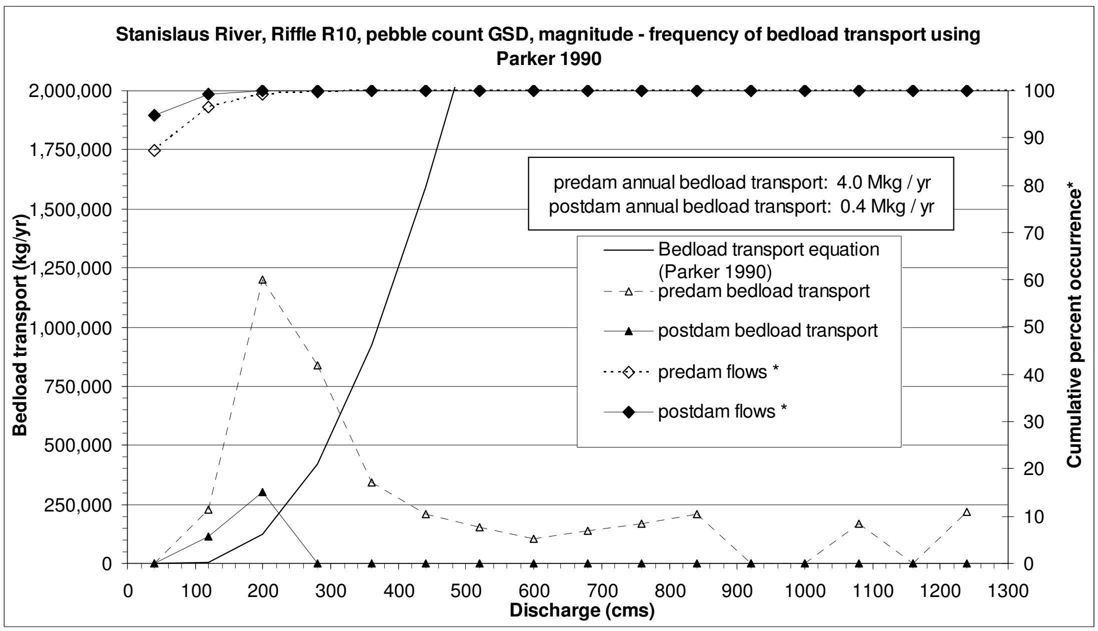

Figures 10a-n (preceding pages). Graphs of magnitude-frequency of bedload transport for pre- and post-dam periods on the major tributaries to the Sacramento-San Joaquin river system.

Figure 11. Claypan outcrop on Stony Creek, extending approximately 2/3 width of river. Outcropping of claypan is common in many of the Sacramento-San Joaquin streams and was observed in this study at numerous locations on Stony Creek, Bear River, American River, Putah Creek, and San Joaquin River.

Tables

Table 1. Maximum flows during WY 2006. See Table 2 for a list of the gages used.					
River	**Site**	**WY 2006 max. flow (cms)**	**Date**	**Return Interval of maximum WY 2006 flow (years)****	
				Pre-dam	**Post-dam**
Yuba	YR1	2707	12/31/05	~15	~15
Bear	BR2	1031	12/31/05	~30	~15
American	AR1	1056	12/31/05	~1.9	~7
Stony Creek	SC1a,b	426.6*	1/02/06	~8	~10
Putah Creek	PC1	203.9	3/7/06	<1	~10
Putah Creek	PC2	203.9	3/7/06	<1	~10
San Joaquin	SJR1	291.6	4/5/06	~1.3	~10+
San Joaquin	SJR2	291.6	4/5/06	~1.3	~10+

* obtained from CDEC event data.

** - see Appendix A for additional hydrologic analyses.

Table 2. Stream gages used for flood frequency and flow-duration studies.

River	Dam	Year built	Gage Location	Gage Name	Gage Period (WY)	pre-dam	mid-dam	post-dam
Clear Creek	Whiskeytown	1963	Igo	USGS 11-372000	1941-2008	1941-1962		1965-2008
Stony Creek	Black Butte	1963	Nr Orland Hamilton City* blw Black Butte blw Black Butte	USGS 11-387500 USGS 11-388500 USGS 11-388000 CDEC BLB	1921-1934 1942-1955 1956-1990 1993-2008	1921-1934, 1942-1962		1965-2008
Putah Creek	Monticello	1957	Winters	USGS 11-454000	1931-2008	1931-1956		1959-2008
Sacramento	Shasta	1945	Keswick Kennet	USGS 11-370500 USGS 11-369500	1939-2008 1926-1938	1926-1944	1947-1962	1965-2008
Feather	Oroville	1968	Oroville	USGS 11-407000	1902-2008	1902-1967		1970-2008
Yuba	Englebright	1941	nr Smartville blw Englebright	USGS 11-419000 USGS 11-418000	1904-1941 1942-2008	1904-1940	1943-1967	1970-2008
Bear	New Camp Far West	1963	Wheatland	USGS 11-424000	1929-2008	1929-1962		1965-2008
American	Folsom	1956	Fair Oaks	USGS 11-446500	1905-2008	1905-1955		1958-2008
Mokelumne	Camanche	1963	blw Camanche	USGS 11-323500	1905-2008	1905-1962		1965-2008
Calaveras	New Hogan	1963	blw New Hogan blw New Hogan	USGS 11-308900 CDEC NHG	1961-1991 1993-2008	na		1965-2008
Stanislaus	New Melones	1979	nr Knight's Ferry blw Goodwin	USGS 11-300000 USGS 11-302000	1915-1932 1957-2008	1915-1978		1981-2008
Tuolumne	New Don Pedro	1971	abv La Grange blw La Grange	USGS 11-288000 USGS 11-289650	1912-1970 1970-2008	1912-1970		1973-2008
Merced	New Exchequer	1967	blw Merced Falls	USGS 11-270000	1901-2008	1901-1966		1969-2008
San Joaquin	Friant	1942	blw Friant	USGS 11-251000	1908-2008	1908-1941		1944-2008

*- flood flows at this gage (despite being ~20km downstream) are nearly 1:1 with the overlapping flows at Black Butte, so the Hamilton City gage was used to fill in the time period from WY1942-1955.

Table 3. Summary of data used in calculations of sediment transport.* See Table 2 for a list of the dams and construction year.

River	Drainage Area (km^2)***	Cross section *					Slope*		Grain Size Distribution*		
		Name	Distance from dam (km)	Width at top of bank (m)	Source	post-dam Q2 max. depth (m)		Source	D50 (mm)	D84 (mm)	Source
Putah Creek	1,492	PC1	10.5	29	a, g	1.9	0.00186	a, i	19	64	a
Stony Creek	1,919	XS 61	3.87	48	j	2.4	0.00246	a, k	47	107	a
Clear Creek	521	XS 891+80	1.67	22	m	2.0	0.0036	n	124	250	o
Sacramento River	23,051	USGS gage at Bend Bridge**	102.7	110	**	3.5	0.0012	b	22	41	s
Feather River	9,342	Alecks Riffle	14.05	44	e	2.4	0.001282	f	105	182	f
Yuba River	2,849	YR1	10.4	75	a	3.5	0.00164	a, h	36	77	a
Bear River	738	BR1	10.7	32	a, e	2.9	0.001143	c	33	64	a
American River	4,882	AR1	8.34	110	a	4.0	0.00121	c	55	81	a
Calaveras River	940	na	na	na			na		na	na	
Mokelumne River	1,603	XS 121	2.25	27	p	1.4	0.000947	p	24	70	
Stanislaus River	2,331	R10	8.76	32	x	1.9	0.0016	v	46	80	w
Tuolumne River	3,994	II-10	3.1	46	u	2.2	0.0016	t	66	102	u
Merced River	2,694	XS 144	13.8	37	q	2.1	0.00208	q	133	204	r
San Joaquin River	4,338	SJR1	1.51	28	a, e	1.7	0.001254	c	56	146	a

Notes for Table 3:
*- see Appendix B for the full set of data used in the bedload calculations.
**- no cross section was available for the reach downstream of Keswick, though CDWR has a HEC model of the area. The Bend Bridge site was chosen to compare to bedload samples taken there from 1977 to 1980.
***- Drainage area taken at dam. See Chapter 4 for assessment of drainage areas downstream of the dam.
a- field data collected by this study
b- CDWR, 1981
c- 10yr water surface slope calculated with UNET, from Comp Study USACE, 2002
d- 2yr water surface slope calculated with UNET, from Comp Study USACE, 2002
e- derived from topographic data collected during Comp Study USACE, 2002
f- CDWR, 2004a
g- field data collected in channel and lower floodplains, upper part of cross section from aerial lidar (obtained from Rich Marovich, Putah Creek Streamkeeper, Feb. 2006)
h – a 1.7km longitudinal water surface profile was collected on January 14, 2006 by the author, immediately following the December 31, 2005 major flood (2,707cms peak). Trash lines were excellent and extensive.
i- a 140m longitudinal water surface profile was collected by the author on April 16, 2006 during a 142cms event
j- survey by Graham Matthews and Associates in 2006 (reported in Harvey, 2007).
k- a 700m longitudinal survey on 1-14-06 by the author. Survey was immediately after the December 31, 2005 flood (425cms).
m- survey of Peltier geomorphic monitoring site cross section 891+80 (McBain and Trush, 2001).
n- survey of 1997 High water marks (McBain and Trush 2001). McBain and Trush (2001) found a slope of 0.0036 from the 1997 high water marks.
o- pebble count performed just downstream of cross section 891+80 (Figure 35, McBain and Trush, 2001).
p- from Simpson (1972).
q- from Blodgett and Bertoldi (1968).
r- Kondolf et al. (1996). Grain size from section 0+16 (upstream of gravel augmentation project). This grain size distribution is one of the only pre-gravel augmentation GSDs available from the upper reaches of the Merced. The gravel mobility and bedload transport grain size used in Stillwater 2001 is located just downstream of a gravel augmentation site that had been used for augmentation for at least 15-years before the Stillwater study. It is more likely that the "fossilized bar" deposits mapped by Stillwater (2001) were more indicative of the pre-augmentation state, which is similar to the Kondolf et al. (1996) grain size.
s- from USGS NWIS database for USGS gage at Bend Bridge (average of four bed material samples taken on 1/5/1977). Used to compare to bedload measurements at Bend Bridge.
t- slope data for this reach is not in published documents, though CDWR has a short HEC model of the reach upstream of Old La Grange Bridge. In lieu of a measured or calculated water surface slope, several sources were used to best estimate slope at this site, including

back calculating slope from critical shear estimates made by Kondolf et al. 1996 and CDWR 2004b. Final slope was close to the slope of the profile downstream of Old La Grange Bridge in McBain and Trush (2000).
u- pebble count and cross section II-10 from CDWR (2004b). The area around La Grange has had extensive gravel augmentation and modification, and much attention was given to try to find a representative control reach, however, none was located. Cross section II-10 was located well downstream of the berms built to retain gravel at Riffle 1B during a 1994 DFG gravel augmentation project (Kondolf et al. 1996) and well upstream of the berms built at Riffle 3A. Large amounts of gravel were added to this reach during the 1999 and 2000 gravel injections (DFG 2004).
v-from Kondolf et al. (1996).
w- from CDWR (1994).
x-CMC (1998).

Table 4. Attributes of previous studies using binning methods for magnitude-frequency analysis				
Author	**Type of sediment transport**	**Size / # of bins**	**Distribution of bins**	**Plotting position of bin**
Major, 2004	Suspended	15-20	Equal	Center
Andrews, 1980	Total load	20	Equal	Unclear
Salant et al. 2006	Bedload	5cms increments	Equal	Maximum
Porterfield, 1980	Suspended and total load	Varying	Unequal – chosen to fit probability curve	Center
Emmett and Wolman, 2001	Bedload	18	Equal	Determined for each daily value using slope between bins, unclear location of end points
Schmidt and Rubin, 1995	Suspended	Summed over 25cms bins (~100 total)	Equal	Unclear
Pickup and Warner 1976	Bedload	~60	Unequal, unclear distribution	Unclear

Table 5. Flood frequency analysis summary for Q2, Q5 and Q10 flows (all flows in cms)*

River	Dam	Q2 pre-dam	Q2 post-dam	Q2 %change	Q5 pre-dam	Q5 post-dam	Q5 %change	Q10 pre-dam	Q10 post-dam	Q10 %change
Clear Creek	Whiskeytown	213	85	-60%	368	176	-52%	493	255	-48%
Stony Creek	Black Butte	235	155	-34%	547	445	-19%	841	674	-20%
Putah Creek	Monticello	790	43	-95%	1,464	120	-92%	1,917	226	-88%
Sacramento	Shasta	1,665	864	-48%	2,860	1,538	-46%	3,738	2,056	-45%
Feather	Oroville	1,523	112	-93%	3,030	634	-79%	4,248	1,764	-58%
Yuba	Englebright	759	365	-52%	1,552	1,133	-27%	2,251	2,044	-9%
Bear	New Camp Far West	294	160	-46%	532	538	1%	714	909	27%
American	Folsom	1,107	382	-65%	2,186	1,102	-50%	3,171	2,027	-36%
Mokelumne	Camanche	154	54	-65%	328	104	-68%	467	143	-69%
Calaveras	New Hogan	168	46	-73%	428	146	-66%	694	268	-61%
Stanislaus	New Melones	260	68	-74%	609	117	-81%	906	162	-82%
Tuolumne	New Don Pedro	343	106	-69%	702	242	-66%	1,019	379	-63%
Merced	New Exchequer	202	110	-46%	430	170	-61%	640	213	-67%
San Joaquin	Friant	394	43	-89%	756	166	-78%	1,087	337	-69%
Average:	**Sacramento basin:**			**-69%**			**-71%**			**-70%**
	San Joaquin basin:			**-62%**			**-45%**			**-35%**
	Sacramento- San Joaquin:			**-65%**			**-56%**			**-49%**

* - Results for additional flood frequency return intervals and other hydrologic analyses can be found in Appendix A.

Table 6. Inputs and results of Kolmogorov-Smirnov test using daily mean flows for pre- and post-dam conditions.

River	Dam	pre-dam	mid-dam	post-dam	n for K-S test*	Dcrit**	Results of K-S test			
		n	n	n			D value	p value	# of bootstraps	Result***
Clear Creek	Whiskeytown	8035		16070	5357	0.01852486	0.23516	2.2 E-16	500	accept H(a)
Stony Creek	Black Butte	12783		14606	6817	0.01642447	0.25361	2.2 E-16	500	accept H(a)
Putah Creek	Monticello	9497		18263	6248	0.01715485	0.44548	2.2 E-16	500	accept H(a)
Sacramento	Shasta	6940		22646	5312	0.01860231	0.40469	2.2 E-16	500	accept H(a)
Feather	Oroville	24106		14245	8954	0.01433383	0.94167	2.2 E-16	500	accept H(a)
Yuba	Englebright	13515	10227	12784	6570	0.01673021	0.33795	2.2 E-16	500	accept H(a)
Bear	New Camp Far West	12396		16071	6998	0.01621072	0.20598	2.2 E-16	500	accept H(a)
American	Folsom	18627		18628	9314	0.01405453	0.3468	2.2 E-16	500	accept H(a)
Mokelumne	Camanche	21184		16071	9138	0.01418863	0.66902	2.2 E-16	500	accept H(a)
Calaveras	New Hogan			14669		na	na	na	na	na
Stanislaus	New Melones	22543		10227	7035	0.0161679	0.17584	2.2 E-16	500	accept H(a)
Tuolumne	New Don Pedro	21550		13149	8166	0.01500823	0.55637	2.2 E-16	500	accept H(a)
Merced	New Exchequer	23194		14610	8964	0.01432597	0.27912	2.2 E-16	500	accept H(a)
San Joaquin	Friant	12023		23742	7981	0.01518093	0.69604	2.2 E-16	500	accept H(a)

* - n calculated for the K-S test using (n1*n2)/(n1+n2) (see Zar 1999 for details); ** - critical D calculated using the Miller 1956 approximation (see Zar 1999, Appendix B.9);*** - where H(o): distributions come from the same population, and H(a): distributions come from separate populations

Table 7. Results of gravel tracer studies for WY 2006.

River	Site	Norm. Shield Stress *	Bed D50 (mm)	Gravel tracers					
				D50 of placed gravel tracer (mm)	Partial or complete mobilization	Maximum size grain moved (mm)	Range of grains moved (mm)	Width of sediment transport **	Aggradation or degradation?
Yuba	YR1	3.1	37	54	Complete	180	29-180	Full width	-40cm to +50cm depending on location
Bear	BR2	3.61	32	52	Complete	106	23-106	Full width	15cm degradation
American	AR1	1.24	80	105	Complete	180	28-180	Full width	20cm degradation
Stony Creek	SC1a,b	2.58	47	49	Partial	120	25-120	Full width	10-20cm degradation
Putah Creek	PC1	4.5	21	43	Complete	95	27-95	Full width	10cm aggradation (sand)
Putah Creek	PC2	4.5	23	45	Complete	65	32-65	Full width	10-15cm degradation
San Joaquin	SJR1	1.35	53	54	Partial (some 55-88mm tracers still in place)	115	27-115	Full width	-6cm to +15cm, depending on location
San Joaquin	SJR2	~1.35	30	47	Complete	157 ***	26-157 ***	Full width	20-30cm aggradation

*- calculated at the maximum flow during WY 2006.

**- if all gravel tracers moved, it was assumed that the full width of the stream was transporting sediment.

*** - the gravels deposited on top of the gravel tracers were larger than the largest gravel tracer. Largest gravel tracer was 112mm.

Table 8. Results of bedload transport calculations.

River	Dam	Pre-dam annual bedload transport (10^6 kg / yr)	Post-dam annual bedload transport (10^6 kg / yr)		Percent change in bedload transport	Pre-dam annual >8mm bedload transport (10^6 kg / yr)	Post-dam annual >8mm bedload transport (10^6 kg / yr)	Percent change in >8mm bedload transport
Clear Creek	Whiskeytown	1.4	0.24		-83%	1.4	0.24	-83%
Stony Creek	Black Butte	2.4	6.9		+188%	0.086	0.3	+248%
Putah Creek	Monticello	96	31	*	-68%	70	21.7	-69%
Sacramento	Shasta	510	350	*	-31%	500	340	-32%
Feather	Oroville	8.3	2.8		-66%	0.27	0.22	-19%
Yuba	Englebright	68.3	61.7		-10%	15.4	5.8	-62%
Bear	New Camp Far West	1.0	1.6		+60%	0.073	0.092	+26%
American	Folsom	6.2	6.4		0%	0.64	0.87	+36%
Mokelumne	Camanche	0.43	0.02		-95%	0.021	0.003	-86%
Calaveras	New Hogan	na	na		na	na	na	na
Stanislaus	New Melones	4.0	0.42		-89%	4.0	0.42	-90%
Tuolumne	New Don Pedro	0.84	0.55		-35%	0.84	0.55	-35%
Merced	New Exchequer	0.100	0.0017		-98%	0.014	0.00007	-95%
San Joaquin	Friant	4.6	0.93		-80%	0.53	0.25	-53%

* - estimates of bedload made using the BAGS distribution.

Table 9. Impounded Runoff for major dammed Sacramento-San Joaquin rivers.

River	Dam	Year built	# dams upstream		Average Annual Runoff *	Impounded Runoff			
						foothill dam		Total watershed impounded runoff **	
			year built	2008	($M\ m^3$)	capacity ($M\ m^3$)	IR	year foothill dam built	2008
Clear Creek	Whiskeytown	1963	0	0	232.5	297.4	128%	128%	128%
Stony Creek	Black Butte	1963	7	9	447.3	177.3	40%	68%	68%
Putah Creek	Monticello	1957	9	27	410.5	1,976.0	481%	484%	494%
Sacramento	Shasta	1945	42	73	7,993.0	5,614.8	70%	74%	77%
Feather	Oroville	1968	35	37	3,588.2	4,363.5	122%	186%	186%
Yuba	Englebright	1941	34	46	2,358.5	86.3	4%	17%	69%
Bear	New Camp Far West	1963	4	9	364.4	127.0	35%	37%	61%
American	Folsom	1956	31	57	3,319.4	1,245.8	38%	40%	68%
Mokelumne	Camanche	1963	14	17	764.9	532.2	70%	140%	140%
Calaveras	New Hogan	1963	7	9	199.5	391.0	196%	198%	199%
Stanislaus	New Melones	1979	21	28	805.1	2,960.4	368%	396%	425%
Tuolumne	New Don Pedro	1971	23	27	1,628.2	2,504.0	154%	178%	179%
Merced	New Exchequer	1967	4	4	1,191.4	1,273.0	107%	107%	107%
San Joaquin	Friant	1942	14	21	1,221.3	642.0	53%	87%	116%

Note: * - Average annual runoff as measured at the gages below the foothill dams. No attempt was made to calculate the losses from evaporation or diversion. Impounded runoff was calculated as the storage capacity of the dams divided by the average annual runoff. **- Total watershed impounded runoff takes into account the capacity of all the dams in the watershed upstream of the main foothill dam, including the foothill dam.

Chapter 4: Sediment Budgets for the Major Dammed Rivers in the Sacramento-San Joaquin River System

Abstract

There has been much attention given to estimating rates of sediment yield into the Sacramento-San Joaquin Delta and San Francisco Bay, however, little attention has been given to the upper watersheds to estimate sediment trapping by dams or the amount of sediment contributed by the watersheds immediately downstream of the dams. In this paper, sediment budgets are constructed for both coarse and total sediment for each of the fourteen major rivers to the Sacramento-San Joaquin system downstream of the major "foothill" dams. The methods used to construct the sediment budget include a reservoir sedimentation model to estimate pre-dam sediment inputs and trapping by upstream dams, sediment yield models for the watersheds downstream of the dams, and bedload transport equations, suspended and bedload measurements from gaging stations to estimate sediment transport for the gravel-bed reaches below the dams. The results of the sediment budget indicate a sediment volume of approximately 244 million m^3 is trapped behind the dams, with 4.0 million m^3 currently trapped by the dams each year, which would otherwise be supplied to downstream rivers. With the exception of the Sacramento River, very little bedload material is supplied by tributaries to the gravel-bed reaches downstream of the foothill dams. Ten of the fourteen rivers do not have enough coarse sediment supply from small tributaries to meet the average annual post-dam bedload transport. Several of the rivers (Putah Creek, the Mokelumne River, and the San Joaquin River) may be strongly affected by small tributaries downstream of the dams, since they have relatively large watersheds downstream of the dams and highly reduced post-dam transport ability. From a compilation of historical reports, approximately 267,000 m^3 of gravel has been augmented from 1978 to 2004 into rivers of the Sacramento-San Joaquin system downstream of the foothill dams. While gravel augmentation projects have been extensive on six of the rivers, they are minimal or absent on the other eight rivers. On average, gravel is augmented at only 3.7% of the post-dam bedload transport capacity, however, some rivers with highly reduced flows have added significant amounts of gravel that exceed the annual post-dam gravel transport rate. In an idealized model scenario wherein the bed grain size of all the gravel-bed rivers downstream of the foothill dams was set equal to that of an ideal gravel augmentation grain size, the calculated amount of gravel transport would be 214,000 m^3 / year. This rate would be the required average annual volume of gravel augmentation necessary to meet transport conditions for post-dam flows. Hence, the total volume of gravel that has been augmented historically over the last thirty years would only meet the transport capacity of the post-dam flows for one single year. Under this idealized scenario, only the gravel augmentation programs on rivers with significantly reduced flows and nearly zero bedload transport, such as the Mokelumne, have added gravel at rates that would match post-dam transport rates.

Introduction

The large foothill dams constructed in the Sacramento-San Joaquin river system have greatly reduced sediment supply to the downstream rivers (see Porterfield et al. 1978, Porterfield 1980). Due to the large sizes of the dams relative to the water inflow, even fine sediment rarely escapes to the downstream river reaches and coarse sediment is completely trapped (Brune 1953, Porterfield, 1980, Porterfield et al. 1978). Rivers downstream of dams regain sediment supply as downstream watersheds contribute sediment (Grant et al. 2003, Schmidt et al. 1995), but the effects on the mainstem river depend on the transport ability of the river and the amount and type of sediment supplied by the tributary (Petts 1984). On gravel-bedded rivers with dams that have greatly reduced sediment transport ability, such as the Trinity River, excess tributary sediment supply can create aggrading deltas, which disrupts bedload continuity on the mainstem river (Wilcock et al. 1996). In addition, excessive fine sediment inputs from the tributaries can cause the riverbed to become much finer, consisting of a large percentage of sand (Wilcock et al. 1996, Milhous 1997). For the Sacramento-San Joaquin river system, sediment supply from the tributaries and their potential effects on the gravel-bedded river reaches immediately downstream of the dams have not been investigated.

One of the main concerns of tributary sediment contribution downstream of the foothill dams is the adverse effect on salmonids (CalFed 2000a,b). The blocking of access to upstream habitat by the foothill dams and their reregulation dams has reduced available salmonid habitat to 28% of the pre-dam value (Yoshiyama et al. 1996). The habitat downstream of the dams, already unsuitable for some runs of Central Valley salmon, has since been degraded by the continued operation of the foothill dams (CalFed 2000a,b). Many of the rivers in the Sacramento-San Joaquin river system have fine sediment problems, primarily associated with the reduction in spawning gravel mobility and the infiltration of fine sediment into the spawning gravel (Vyverberg et al. 1997, Horner et al. 2004, CDWR 2004, Kondolf et al. 2001). The source of the fine sediment has rarely been investigated.

The effects of fine sediment supply on salmonids depend primarily on the size of the sediment and the timing of its addition to the channel (Chapman 1988, Kondolf 2000). While coarse sediment between the range of 10mm to 55mm is needed for spawning by adults (Chapman 1988, Kondolf and Wolman 1993) and for cover by juveniles (review in Kondolf 2000), fine sediment and sand can have a detrimental effect, both on emergence and juvenile rearing quality (Chapman 1988, Kondolf 2000, Suttle et al. 2004). Fine sediment filters down through the framework gravels to plug pore spaces, decreasing permeability and potentially inhibiting the flow of adequate water to eggs or alevins located in the redd (Kondolf 2000). In particular, the timing of sediment supply is important, since the eggs must incubate for several months before emergence (Chapman 1988). Percentages of fine sediment from 10% to 30% significantly decrease incubation and emergence rates, with greater percentages (30-100%) being more lethal (Chapman, 1988). The size of fine sediment that significantly decreases survival of incubating eggs varies, but is generally considered to be less than 1mm (Kondolf, 2000), with sizes up to 9.5mm that have also been found to decrease survival rates (Chapman, 1988). For the purposes of this discussion, fine sediment here will be defined as that finer than 0.063mm, sand from 0.063 to 2mm and coarse sediment from 2mm and larger.

Objectives

The objectives of this chapter are two-fold: to determine how much sediment is trapped behind dams in the Sacramento-San Joaquin river system and to establish a sediment budget for fine and coarse sediment for the river reaches downstream of the major foothill dams. The research questions for this chapter are: How much sediment is trapped behind dams in the Sacramento-San Joaquin river system that otherwise would have been contributed to downstream rivers? Are the rivers downstream of the foothill dams able to offset the losses from trapping in upstream reservoirs by inputs from tributaries? Which of the rivers might be affected by tributary inputs?

Site Description

The Sacramento-San Joaquin River System

The Sacramento-San Joaquin river system is located approximately 150 kilometers inland of the Pacific Ocean and connects to the coast via the San Francisco Delta and San Francisco Bay, eventually exiting through the Golden Gate (Figure 1). The Sacramento River drains the northern part of the valley, and the San Joaquin River drains from the south. Both the Sacramento and San Joaquin receive waters from the Sierra Nevada Mountains, as well as the Coast Ranges. Runoff from the Coast Ranges is primarily dominated by winter-storm events (Jones et al. 1972), while runoff from the Sierra Nevada Mountains is dominated by a combination of snowmelt and winter-storm events. Summer months in California's Mediterranean climate have little precipitation, with the majority of precipitation occurring between November and April.

There are fourteen major foothill dams in the Sacramento-San Joaquin river system, but there are 619 dams in the watersheds and many dams are located upstream of the foothill dams (Figure 1, Table 1). Many of the foothill dams in the Sacramento-San Joaquin river system have smaller reregulation dams downstream, which serve several purposes, including rerouting water from the larger dams into canals, providing stable downstream flows, or are connected to hydroelectric operations. Several of the foothill dams are second generation dams, as they have replaced older structures located near the same site, often with a significant increase in capacity. For example, New Don Pedro dam with a capacity of 2.5 billion m^3 was built in 1971 to replace the original Don Pedro dam built in 1926 with a capacity of 358 million m^3.

Methods

A sediment budget approach was selected to best inventory sediment processes downstream of the foothill dams in the Sacramento-San Joaquin river system (Reid and Dunne 1996, Reid and Dunne 2001). While the use of sediment budgets has an extensive history in geomorphology (e.g. Gilbert, 1917, Porterfield 1980, Dietrich and Dunne 1978, Lehre 1982, Trimble 1999), some important caveats apply. First, one or more unmeasured terms may necessarily be obtained from subtraction, resulting in large "unmeasured residuals", which can result in significant error (Kondolf and Matthews 1991). Kondolf and Matthews (1991) recommend measuring as many of the terms as possible to reduce this error, and that it is approach attempted here. The change in storage of coarse sediment in the bed, however, is poorly known and often significantly dwarfs annual sediment transport in gravel-bed rivers (Reid and Dunne 1996). Second, terms computed from sediment transport relations can produce relatively large errors (Singer and Dunne 2004, bedload in particular, Ferguson 2003) and should be applied with caution to sediment budget calculations (Grams and Schmidt 2005).

Key steps in developing a sediment budget include identifying and quantifying relevant geomorphic processes and delineating storage components (Reid and Dunne 1996, 2001). Figure 2 shows a conceptual diagram of the sediment budget used in this study, which is described in the next few paragraphs. For this study, coarse sediment (>2mm) was assumed to be transported only by fluvial processes in the main channels and tributaries. Landslides and debris flows are important sediment generation mechanisms in steeper source areas (Lehre 1982, Reid and Dunne 1996), however, for this sediment budget, landslides and debris flows were assumed to contribute negligible amounts due to the primarily lower slope of the watersheds downstream of the dams. There have been large landslides documented in regions similar to the lower source areas, including large land-slide dams caused by earthquakes on Cache Creek (Manson 1989, Manson 1990), but these are not considered here.

In this study, the storage component was estimated as all sediment within the valley walls of the gravel-bedded reaches, including streambanks, downstream of the foothill dams (Figure 2). The reduction in flood flows and subsequent vegetation encroachment has meant that on many of the rivers in the Sacramento-San Joaquin river system, previous streambed areas have become relatively immobile terraces (e.g. Kondolf and Matthews 1993, Stillwater 2001). Hence, in this study, streambeds and banks were kept together in the sediment budget, and defined as a single storage term between the valley walls (Figure 2). The length of the storage component is defined as the length of reach over which the bedload transport equations were considered valid (Table 2). While some sediment budget studies separate out the terms for streambank erosion in sediment budgets (i.e. delineating the storage term at the edge of the channel), in this study, it was not possible to evaluate streambank erosion on all the major rivers. There is some evidence in the Sacramento-San Joaquin river system that streambank erosion plays a relatively minor role in the post-dam response for the gravel-bedded rivers immediately downstream of the foothill dams (Ghoshal et al. 2010, Fairman

2007). Fairman (2007) found that in a morphologically-based gravel budget for the Lower American River, streambank and terrace contributions were approximately 20% of the total gravel exported over a 36-year period (1962-1998), with the majority of sediment coming from the bed. Ghoshal et al. (2010), used a morphologically-based sediment budget for the years 1906-1999 for two short sections of the Lower Yuba River just upstream of the confluence with the Feather River, and found that the majority of sediment contribution came from the bed, with only 5-25% of the net erosion from terraces. Figure 3 qualitatively shows the incision that has occurred in these areas (up to 10m in some locations, Ghoshal et al. 2010).

The connectivity of tributaries to the main channel is a primary factor limiting the contribution of sand and coarser material from hillslope areas to larger stream channels (Reid and Dunne 1996, Reid and Dunne 2001). In this study, it was assumed that only tributary streams downstream of the dam that were larger than 10 km^2 contributed significant amounts of sand or bedload directly to the main channel (Figure 2). In reality, there are a number of different factors that influence both sediment supply rates and sediment size, including stream size, slope, geology, landuse and land history among others (Reid and Dunne 1996). The watershed immediately bounding the river channel downstream of the dam was assumed to be a continuous linear sediment contributor unless there was a tributary exceeding the 10 km^2 rule. Bedload was assumed not to be contributed from the contiguous linear watersheds (i.e. the watershed area without a tributary), because it was unlikely that this area would be able to transport bedload into the valley storage component (Figure 2). Fine sediment was assumed to be contributed equally by all areas of the watershed. Other key assumptions were that during the post-dam era, no sediment from upstream of the foothill dams was contributed to the downstream areas. The two smallest of the foothill dams, Friant and Englebright have trap efficiencies of 97% and 86% respectively. Hence, only very small particles would make it through the dams and would be unlikely to deposit in the turbulent river reaches below the dams.

In this study, the sediment budget was evaluated for two different scenarios in the river reaches downstream of the foothill dams: a post-dam condition (current), and a "restored" condition, which assumes coarse sediment is added at the rate that it is transported. The volume of sediment trapped by upstream dams also was calculated as a reference for the two sediment budgets. The general form of the sediment budget is (Reid and Dunne 1996):

$$dS = I - O \quad (1)$$

where dS is the change in storage, I is inputs, and O is outputs, and all units are in mass. It should be noted, however, that while only mass is conserved, volume can also be used in sediment budgets so long as the densities of the terms are equal. In this study, volume estimates are used because a consistent density is used for each of the budgets, they are conventionally reported for gravel augmentation, and because they are easily visualized. Mass estimates have been converted using a constant density of 1,600 kg / m^3 for gravel and sand mixtures (e.g. for the bedload and >2mm sediment budget), and a density of 960 kg / m^3 for the reservoir sediment and total sediment loads (total sediment budget).

For the post-dam sediment budget of sediment greater than 2mm, yield from the drainage area downstream of the dam and gravel augmentation are considered to be the only inputs because the supply from upstream is assumed to be zero. For the gravel augmentation estimates, the augmentation rate was calculated over the period of time over which the gravel augmentation was applied, not over the full period since dam closure. Total sediment load, bedload, and greater than 2mm bedload are supplied according to the rules given previously. The post-dam sediment budget takes the form:

$$dS = I_{trib} + I_{ws} + I_{ga} - Q_{bl} \quad (2)$$

where dS is the change in storage, I_{trib} is the input from tributaries, I_{ws} is the input from the watershed downstream of the dam but not from a tributary (only for the total sediment budget, not bedload or >2mm sediment budgets), I_{ga} is the input from gravel augmentation (only used in the >2mm budgets), and Q_{bl} is the current post-dam sediment transport rate calculated in Chapter 3 (only used in the >2mm sediment budget). All units here are in m^3 since all terms for each of the sediment budgets have been expressed with the same density.

The second sediment budget considered is of full gravel augmentation conditions, such that gravel augmentation is added at a rate to equal downstream export (i.e. no change in storage), taking into account the gravel additions by downstream tributaries (only for >2mm grain sizes):

$$0 = dS = I_{trib} + I_{ga} - Q_{blga} \quad (3)$$

where dS is the change in storage (zero here), I_{trib} is the contribution of >2mm from tributaries downstream of the dam, I_{ga} is the input of gravel augmentation, and Q_{blga} is the post-dam bedload sediment transport (>2mm) calculated using the bedload sites in Chapter 3, but utilizing separate bedload transport curves based on the grain size of an idealized, simulated gravel augmentation. The grain size chosen for the simulated gravel augmentation is shown in Figure 4, and represents a grain size typically utilized in gravel augmentation projects (Vyverberg et al. 1997). For the estimates of gravel augmentation volumes, the cross sections and slope of the bedload calculation sites established in Chapter 3 are held constant, as is the post-dam flow duration curve. One consequence of fining the bed material as in a gravel augmentation is that the bedload rating curve shifts as the bed particles become easier to transport (Figure 5). It is for this reason that the estimates of post-dam bedload transport and bedload rating curves should not be held constant when there are large volumes of gravel being added to the channel.

Previous reports and studies were reviewed to compile sediment yields, bedload measurements, and bedload transport calculations and to estimate total sediment production and the percentage of fine, sand and coarse material (Table 2). What sparse suspended and bedload measurements exists, were collected from gaging stations within the United States Geological Survey (USGS) National Water Information System database (Table 3). A handful of previous studies have calculated or measured bedload in the gravel-bed rivers downstream of the foothill dams in the Sacramento-San Joaquin system (Table 2), a few of which are highlighted here in the text. Singer and Dunne (2004) and Singer (2008), calculate total sediment and bedload passing the Bend Bridge USGS gage. The restoration program at Clear Creek has collected a number of years of bedload samples (McBain and Trush and Graham Matthews and Associates (GMA) 1999, GMA 2003), some taken as part of monitoring for a restoration project, but the sampling site at Igo has proven unreliable at high flows and likely does not reflect uniform flow conditions (McBain and Trush and GMA 1999). Bedload also has been sampled on Lower Clear Creek at Renshaw Riffle and at the restoration site, Phase 3A, but they are far downstream of the dam and are influenced by gravel augmentation projects upstream (GMA 2003). The recent restoration program on the San Joaquin has installed bedload sampling stations on the San Joaquin River for WY 2010, but the restoration flows were relatively low with little bedload transport and the data has not yet been approved for publication (Scott Wright, USGS, personal communication). The table of gravel augmentation projects was collected from the previous studies and from a previously unpublished database collected by G.M. Kondolf (personal communication).

From the review of the previous studies, USGS gaging data, and sediment yield rates calculated in Chapter 2, sediment yield rates were assigned to the various regions (Figure 6, Table 4). The majority of studies reviewed here used a computational approach for bedload instead of measuring it directly, hence, the proportion of bedload to total load is poorly known. Most of the reviewed studies calculated bedload as 8-15% of the total load, but it was unclear how most of the studies treated sand since it can travel as either bedload or suspended depending on the discharge. One of the few sites in the gravel-bedded rivers downstream of the dams with adequate paired bedload and suspended sediment is at the USGS gage (USGS #11377100) on the Sacramento at Bend Bridge for the period, 1977-1980 (Figure 7), which has approximately 10% of total load during this period passing as bedload. It is unlikely, however, that the paired bedload and suspended measurements taken at this gage are representative of the other gravel-bedded rivers downstream of the foothill dams because the data were collected following an abnormally long and severe drought (WY1976-1977), the bedload measurements span a relatively low-range of flows and the gage is far downstream of the dam (103km) with a large number of tributary inputs upstream.

Immediately following dam closure on the Mokelumne and Feather Rivers, the regions downstream of the foothill dams had a two- to three-fold increase in sediment yield, while the overall sediment load was greatly reduced (Porterfield 1980, Porterfield et al. 1978) (Figure 8). Porterfield (1980) and Porterfield et al. (1978) speculated that the increases might be due to downcutting of the riverbed as the bed adjusted to reduced supply. These effects were not accounted for in the present study. In this study, the approximate percentage of bedload to total sediment yield was assumed to be 10%, and 50% of the bedload was assumed to be greater than 2mm. Estimates of pre-dam sediment supply were estimated with the 3W model developed in Chapter 2, with a variable trap efficiency for total sediment loads, and 100% trap efficiency for bedload and >2mm bedload estimates. The estimates of bed sediment transport out of the main channel were calculated using the flow-duration curves and methods described in Chapter 3, using the Parker (1990) surface-based bedload equation.

The ability for fine sand (0.063mm) and coarse sand (2mm) to travel as suspended load was investigated using a Stokes solution for the settling velocity of the fine sand and an Engelund-Hansen (1967) solution for the coarse sand (Sturm 2005). The results of the evaluation show that fine sand has a settling velocity (w_f) of around 0.003 m/s, while the coarse sand has a settling velocity of approximately 0.17 m/s. In the gravel-bedded reaches downstream of the foothill dams, with slopes of between 0.001 and 0.003, and depths ranging from 1 to 4m, the fine sand would travel predominantly as suspended load for all flows ($u^*/w_f < 0.4$), where u^* is the shear velocity ($(ghS)^{1/2}$, where g is gravitational acceleration (m / s^2), h is flow depth (m), and S is slope). The coarse sand would travel predominantly as bedload / transitional loads ($0.4 < u^*/w_f < 2.5$) for the same conditions.

The drainage areas upstream and downstream of the dams were estimated using ESRI ArcGIS 9.1 software, with a state-wide watershed coverage (Watershed Boundary Dataset, WBD, 2009) obtained from the California Spatial Information Library. The National Hydrography Dataset (obtained 2/2009) for California was overlain on top of the watershed coverages to aid in delineation of smaller stream tributaries. Dam location was obtained from the National Inventory of Dams dataset (obtained 3/2007).

Results

The sediment trapping by foothill dams in the Sacramento-San Joaquin river system is approximately 2.67 million m^3 per year (Table 5). Table 5 shows the results for each of the individual rivers. If all the dams in the watersheds upstream are taken into account, the total annual sediment trapped is 4.0 million m^3, with the foothill dams trapping 60% on average of the total sediment yield coming off the upstream watersheds. The amount of total sediment supply deficit to downstream reaches (the amount trapped by the foothill dams) over the life of the foothill dams is estimated at 159 million m^3, and if all dams are taken into account, the total sediment supply deficit is 244 million m^3 (Table 5).

The amount of bedload trapped by the foothill dams is approximately 149,000 m^3 per year, with 74,600 m^3 per year of >2mm particles (Tables 6, 7). If all dams upstream are taken into account, the amount of bedload trapped each year is 408,000 m^3, with 204,000 m^3 of >2mm particles. The total bedload deficit since the foothill dams have been constructed is 9.1 million m^3 for just the foothill dams, and 24.8 million m^3 if all dams upstream are taken into account.

Overall, the major rivers in the Sacramento-San Joaquin river system have relatively small watersheds downstream of the foothill dams (Figures 9, 10, 11). Of the thirteen rivers studied here, nine regain less than 10% of their upstream drainage areas within 50km downstream of the dam (Figure 10). Several of the downstream gravel-bedded streams, Putah Creek, Mokelumne River, Merced River and San Joaquin River, could have significant tributary inputs of bedload sediment, particularly in light of the reduction in downstream transport capacity (Tables 8, 9).

The total amount of gravel augmented (added by people) in the Sacramento-San Joaquin river system from 1978 through 2004 is approximately 267,000 m^3, with the majority of gravel augmentation occurring on the Sacramento River (Table 10). The amount of gravel augmented is on average 3.7% of post-dam bedload sediment transport (for >2mm particles) (Table 8). While most rivers have much less gravel augmented than is transported, some rivers have large amounts of gravel added relative to the sediment deficit, namely Clear Creek, Mokelumne River, Stanislaus River, Tuolumne River, and Merced River.

Using a scenario wherein the grain size of the bed equaled the idealized gravel augmentation mixture (Figure 4), 214,000 m^3 of sediment would need to be added each year under current post-dam flow conditions (i.e. assuming no alteration of post-dam flow regime) (Table 11). Under this scenario, of the rivers with current gravel augmentation programs, only the rates of gravel augmentation occurring at rivers with significantly reduced flows and currently nearly zero downstream gravel transport, such as the Mokelumne River, would meet the required rates of gravel augmentation. This finding suggests that flow reduction in some of the rivers is enough to stop nearly all sediment transport downstream even if the bed were to approach idealized gravel augmentation mixtures. Excluding the Merced and Mokelumne Rivers, on average, only 22% of post-dam gravel augmentation needs would be met, including the supply from tributary sources.

Discussion

The foothill dams in the Sacramento-San Joaquin river system greatly reduce total sediment supply and bedload to the downstream reaches. Previous studies of sediment supply to the Sacramento-San Joaquin Delta and the San Francisco Bay (Figure 12), have noted a large decrease in sediment supply but have not fully evaluated the upstream causes of the reduction. For the Sacramento River basin, annual trapping by dams is 3.1 million m^3 in the foothill dam watersheds (i.e. including only dams located in the foothill dam watersheds). Average annual sediment transport from the Sacramento River into the Delta is currently 680,000 m^3 / year (Wright and Schoelhamer 2004), down from a peak of 5.6 million m^3 / year in the 1909-1966 period (Porterfield 1980). From the results of this study, it appears that the scale of the sediment trapped by upstream dams is slightly more than the reduction seen in the downstream sediment supply to the Delta, and certainly would be a good explanation if causal mechanisms could be explained and downstream deposition and erosion controls could be discounted.

A superior method to estimate bedload transport on these rivers would be to establish sediment gaging stations on the major rivers, similar to the restoration programs on Clear Creek, the Trinity River or the recently started program on the San Joaquin River. Given the ecological importance of these major rivers, it is particularly surprising that there are essentially no established bedload sediment sampling stations with the exception of the Sacramento River downstream of Red Bluff or at altered restoration sites. The already sparse suspended sediment sampling data are additionally twenty to thirty years out of date. The bedload transport calculations utilized here, while being the best available estimates at these sites, are not the ideal method to estimate bedload transport. In particular, the dependence of the formulas on the grain size distribution, the fact that only post-dam grain size information were available and the uncertainty inherent in the bedload formulas, should cause the results to be regarded tentatively. In addition, the cross section geometry at many of these sites has likely changed in response to dam closure and vegetation encroachment. A superior method would be to combine bedload measurements with bedload calculations to estimate bed movement on these major rivers, as well as morphometric estimates of riverine sediment export relative to instream mining. On several of these rivers, instream mining is an order of magnitude more than post-dam sediment transport (Table 12).

While the majority of the gravel-bedded reaches downstream of the foothill dams do not have significant sediment contribution areas downstream of the dam, there are several that could be significantly affected, including Putah Creek, the Mokelumne River and the San Joaquin River. In particular, the reduced transport capacity downstream of these dams suggests that the tributaries likely play a more significant role in both sediment supply and flow dynamics in the lower reaches. Even if there are large volumes of bedload material greater than 2mm available, the large particles might be buried by the supply of sand and smaller particles. A key component of the downstream response of the main channel will likely depend on the amount of sand in the sediment supplied by the tributary (e.g. Wilock et al. 1996), particularly since for these channels, sand is mobile over the full range of flows as suspended, transitional and bedload. Porterfield (1980) found that on the undammed Cosumnes River, sand was approximately 25-50% of total load. The excess sand could lead to large tributary deltas, like the one seen on Putah Creek at the Dry Creek confluence, or lead to problems like those on the Trinity River (Wilcock et al. 1996). The uneven timing of tributary sediment inputs could result in non-linear feedback dynamics more complex than those modeled here. For example, the tributary deltas could decrease upstream slope, initiate bedload disconnectivity, and encourage vegetation encroachment. Further field investigations for these three rivers would be well warranted.

Restoration recommendations

Given the high ecological importance of the gravel-bed reaches downstream of the major foothill dams in the Sacramento-San Joaquin river system (Calfed 2000a,b), better science should be used to coordinate the sediment management of these rivers. Incorporating the results of this study with further studies comparing the effects of the foothill dams would be an excellent start, and it is surprising this has not been attempted earlier. Good examples of restoration programs that are incorporating science into sediment management include Clear Creek, the Trinity River, and the San Joaquin River. On most rivers to date in the Sacramento-San Joaquin river system, nearly all gravel augmentation projects have been planned without reference to the bedload transport rate, and only recently have they been planned with critical shear stress in mind (Kondolf et al. 2001), though many projects still consider mobility to be a negative result. Coordinating gravel augmentation with flood pulse flows, and moving towards the concept of alluvial functioning (Trush et al. 2000), with regular additions and movement of gravel, like the restoration approach used by the Clear Creek restoration program, would be an excellent idea (McBain and Trush 2001).

Unfortunately, a number of the Federal Energy Regulatory Commission hydroelectric permits and the state and federal water service contracts reviewed by the author have been approved with substandard environmental review (e.g. USBoR 2005). Many of the accepted permits propose only minimal improvements, if at all, to the sediment and ecological management of these systems. Private, state and federal dam operators, should be held accountable for the continued degradation of the downstream river systems (i.e. continued downstream transport) and adequate scientific review of the permits should be performed by the reviewing agencies. Many of these dams have had cumulative long-term effects on the downstream rivers, including sediment starvation, cessation of flood flows, and alteration of flow magnitude frequencies. Incentives to improve the management of the major rivers could be imagined, however, increased enforcement of existing standards most likely would produce results.

Every effort should be made to preserve and improve those rivers that are closer to full alluvial functioning. In particular, the Middle Sacramento River is a real gem, with relatively high sediment resupply from tributaries downstream of the dam and relatively little flow alteration from Shasta Dam. Every effort should be made to maintain conditions on the Sacramento River below Red Bluff, however, the large number of salmonids using the reach upstream of Red Bluff suggest that restoration efforts would be successful if they were attempted upstream. The Upper Sacramento River remains one of the rivers with the largest additions of gravel for augmentation in California and possibly the United States (total of 200,000 m^3 added between 1978 and 2004), particularly following the addition of 76,000 m^3 in Phase I of the Sacramento River Spawning Gravel Restoration project in the mid-1990s. Phase II of that project, for which all the planning was completed, proposed adding over 800,000 m^3 of sediment, but was abandoned for some reason in the late-1990s.

Conclusions

This study compiled sediment data to estimate the pre-dam sediment supply, sediment trapping effects, and sediment budgets for the gravel-bed reaches of the rivers downstream of major “foothill” dams of the Sacramento-San Joaquin river system. Large amounts of sediment are trapped behind the dams in the watershed, significantly reducing sediment supply to downstream rivers and the Sacramento-San Joaquin Delta. For most of the rivers, there is insufficient bedload supplied downstream of the dams to offset bed degradation as the rivers continue to adjust to the post-dam imposition of greatly reduced sediment supply. Due to flow reductions caused by the foothill dams, and the relative size and contribution of small tributaries downstream of the dams, however, several of the streams may be adversely affected by tributary sediment. Future restoration efforts are recommended to focus on better science, a comparative approach, and adequate review of environmental permitting.

References

Brune, G. M., 1953. Trap efficiencies of reservoirs. Eos Trans. AGU, 34(3), 407.

Cain J, 1997. Hydrologic and geomorphic changes to the San Joaquin River between Friant Dam and Gravely Ford and implications for restoration of Chinook salmon (*Oncorhynchus tshawytscha*). Unpublished Masters thesis, University of California, Berkeley.

CalFed Bay-Delta Program, 2000a. Ecosystem Restoration Program Plan, Volume I: Ecological Attributes of the San Francisco Bay-Delta Watershed. CalFed Bay-Delta Program, Final Programmatic EIS/EIR Technical Appendix.

CalFed Bay-Delta Program, 2000b. Ecosystem Restoration Program Plan, Volume II: Ecological Management Zone Visions. CalFed Bay-Delta Program, Final Programmatic EIS/EIR Technical Appendix.

California Department of Water Resources, 1982. Feather River spawning gravel baseline study. California Department of Water Resources publication, Sacramento, CA.

California Department of Water Resources, 2004a. SP-G2: Effects of project operations on geomorphic processes downstream of Oroville Dam. Oroville Facilities Relicensing, FERC project no. 2100.

California Department of Water Resources, 2004b. Tuolumne River La Grange gravel addition project, Phase II: Geomorphic monitoring report. Prepared by San Joaquin District, River Management Section. 42p.

California Division of Safety of Dams (CDSD), 2007. Electronic database of dams and reservoirs in California, damsafety.water.ca.gov, accessed April 2007.

Chapman, D.W., 1988. Critical review of variables used to define effects of fines in redds of large salmonids. Transactions of the American Fisheries Society, 117(1), 1-21.

Dietrich, W.E., and T. Dunne, 1978. Sediment budget for a small catchment in mountainous terrain. Zeitschrift fur Geomorphologie Suppl. Bd. 29, 191-206.

Engelund, F., and E. Hansen, 1967. A Monograph on Sediment Transport to Alluvial Streams. Copenhagen, Teknik Vorlag. 78p.

Fairman, D., 2007. A gravel budget for the Lower American River. Masters thesis, Department of Geology, California State University, Sacramento. 158p.

Ferguson, R.I., 2003. The missing dimension: Effects of lateral variation on 1-D calculations of fluvial bedload transport. Geomorphology 56(1-2), 1-14.

Ghoshal, S., James, L.A., Singer, M., and R. Aalto, 2010. Channel and floodplain change analysis over a 100-year period: Lower Yuba River, California. Remote Sensing 2, 1797-1825.

Gilbert, G.K., 1917. Hydraulic-mining Debris in the Sierra Nevada. United States Geological Survey, Professional Paper 105. 107p.

Graham Matthews and Associates, 2003. Clear Creek floodplain rehabilitation project, Shasta County, California: WY2003 Geomorphic monitoring report. Prepared for Western Shasta Resource Conservation District, Anderson, CA. 90p.

Grams, P.E., and J.C. Schmidt, 2005. Equilibrium or indeterminate? Where sediment budgets fail: Sediment mass balance and adjustment of channel form, Green River downstream from Flaming Gorge Dam, Utah and Colorado. Geomorphology 71, 156-181.

Grant, G.E., Schmidt, J.C. and S.L. Lewis, 2003. A Geological Framework for Interpreting Downstream Effects of Dams on Rivers. In Grant, G.E. and J.E. O'Connor (eds), *A Peculiar River*. Water Science and Application 7. American Geophysical Union, San Francisco. Pp. 209-226.

Horner, T., Titus, R., and M. Brown, 2003. American River gravel studies 2004: Phase 3 gravel assessment on the Lower American River. 93p.

James, A., 1999. Time and the persistence of alluvium: River engineering, fluvial geomorphology and mining sediment in California. Geomorphology 31, 265-290.

Jones, B.L., Hawley, N.L., and J.R. Crippen, 1972. Sediment transport in the western tributaries of the Sacramento River, California. United States Geological Survey, Water-Supply Paper 1798-J. 27p.

Kondolf, G.M. and W.V.G. Matthews, 1993. Management of Coarse Sediment on Regulated Rivers. California Water Resources Center, University of California, Report no. 80. 128p.

Kondolf, G.M., 2000. Assessing salmonid spawning gravel quality. Transactions of the American Fisheries Society, 129, 262-281.

Kondolf, G.M., and M.G. Wolman, 1993. The sizes of salmonid spawning gravels. Water Resources Research, 29(7), 2275-2285.

Kondolf, G.M., and M.L. Swanson, 1993. Channel adjustments to reservoir construction and instream gravel mining, Stony Creek, California. Environmental Geology and Water Science 21, 256-269.

Kondolf, G.M., and W.V.G. Matthews, 1991. Unmeasured residuals in sediment budgets: a cautionary note. Water Resources Research 27(9), 2483-2486.

Kondolf, G.M., Falzone, A., and K.S. Schneider, 2001. Reconnaissance-level assessment of channel change and spawning habitat on the Stanislaus River below Goodwin Dam. Report submitted to U.S. Fish and Wildlife Service, Sacramento, CA. 233p.

Kondolf, G.M., Vick, J.C., and T.M. Ramirez, 1996. Salmon spawning habitat rehabilitation in the Merced, Tuolumne, and Stanislaus Rivers, California: An evaluation of project planning and performance. University of California, Water Resources Center Report No. 90. 147p.

Lehre, A.K., 1982. Sediment budget of a small Coast Range drainage basin in north-central California. in Swanson, F.J., Janda, R.J., Dunne, T. and D.N. Swanson (eds.), Sediment Budgets and Routing in Forested Drainage Basins: U.S. Forest Service Pacific Northwest Forest and Range Experiment Station General Technical Report PNW-141, 67-77.

Major, J.J., 2004. Posteruption suspended sediment transport at Mount St. Helens: Decadal-scale relationships with landscape adjustments and river discharges. Journal of Geophysical Research 109. 22p.

Manson, M.W., 1989. Landslides and geology along Cache Creek between Clear Lake and Capay Valley, Lake, Colusa, and Yolo Counties, California: Landslide hazards identification map no. 19. California Division of Mines and Geology, Open-File Report 89-30. 16p.

Manson, M.W., 1990. Landslide and flood potential along Cache Creek. California Geology, May, 1990, California Department of Conservation, Division of Mines and Geology, 99-106.

McBain and Trush and Graham Matthews and Associates, 1999. Lower Clear Creek bedload transport measurements – Technical memorandum for WY1998. Report prepared for Lower Clear Creek Technical Workgroup, November 1999. 17p.

McBain and Trush, 2001. Final report: Geomorphic evaluation of Lower Clear Creek downstream of Whiskeytown Dam, California. Prepared by McBain and Trush, Graham Matthews and Associates, North State Resources, and Stillwater Sciences. 190p.

McKee, L., Ganju, N., Schollhamer, D., Davis, J., Yee, D., Leatherbarrow, J., and R. Hoenicke, 2002. Estimates of suspended sediment flux entering San Francisco Bay from the Sacramento and San Joaquin Delta. Report prepared for San Francisco Bay Regional

Monitoring Program for Trace Substances. San Francisco Estuary Institute contribution 65. 28p.

Milhous, R.T., 1997. Reservoir construction, river sedimentation and tributary sediment size. In. Human Impact on Erosion and Sedimentation, Proceedings of Rabat Symposium S6, April 1997, IAHS publication no. 245, 275-282.

Ogden Beeman and Associates, 1992. Sediment budget study for San Francisco Bay. Report prepared for the San Francisco District, Corps of Engineers. 25p.

Parker, G., 1990. Surface-based bedload transport relation for gravel rivers. Journal of Hydraulic Research, 28(4), 417-436.

Petts, G.E., 1984. *Impounded Rivers: Perspectives for Ecological Management*. John Wiley and Sons, New York. 326 p.

Porterfield, G., 1980. Sediment transport of streams tributary to San Francisco, San Pablo, and Suisun Bays, California, 1909-1966. United States Geological Survey, Water-Resources Investigations 80-64. 92p.

Porterfield, G., Busch, R.D., and A.O. Waananen, 1978. Sediment transport in the Feather River, Lake Oroville to Yuba City, California. United States Geological Survey, Water-Resources Investigations 78-20. 73p.

Reid, L.M., and T. Dunne, 1996. Rapid evaluation of sediment budgets. Catena Verlag, GeoEcology paperback, GMBH, Reiskirchen, Germany. 164p.

Reid, L.M., and T. Dunne, 2001. Sediment budgets as an organizing framework in fluvial geomorphology. in Kondolf, G.M. and H. Piegay (eds.), *Tools in Fluvial Geomorphology*. Wiley, San Francisco. Pp. 463-500.

Schmidt, J.C., and D.M. Rubin, 1995. Regulated streamflow, fine-grained deposits, and effective discharge in canyons with abundant debris fans. In J.E. Costa et al. (eds.), *Natural and Anthropogenic Influences in Fluvial Geomorphology (the Wolman Volume).* American Geophysical Union, Geophysical Monograph 89. Washington, D.C. pp. 177-195.

Schmidt, J.C., Grams, P.E., and R.H. Webb, 1995. Comparison of the magnitude of erosion along two large regulated rivers. Water Resources Research 31(4), 617-631.

Singer, M.B., 2008. Downstream patterns of bed material grain size in a large, lowland alluvial river subject to low sediment supply. Water Resources Research 44, 7p.

Singer, M.B., and T. Dunne, 2004. Modeling decadal bed material sediment flux based on stochastic hydrology. Water Resources Research 40, W03302, doi:10.1029/2003WR002723.

Stillwater Sciences, 2001. Merced River corridor restoration plan baseline studies. Volume II: Geomorphic and riparian vegetation investigations report. Prepared by Stillwater Sciences, Berkeley, California for CALFED Bay-Delta Program, Sacramento, California.

Sturm, T.W., 2005. Open Channel Hydraulics. McGraw-Hill, New York. 493p.

Suttle, K.B., Power, M.E., Levine, J.M., and C. McNeely, 2004. How fine sediment in riverbeds impairs growth and survival of juvenile salmonids. Ecological Applications, 14(4), 969-974.

Swanson, M.L., and G.M. Kondolf, 1991. Geomorphic study of bed degradation in Stony Creek, Glenn County, California. Report submitted to California Department of Transportation, Division of Structures, Sacramento, CA. 80p. plus appendices.

Trimble, S. W., 1999. Decreased rates of alluvial sediment storage in the Coon Creek basin, Wisconsin, 1975– 1993. Science, 285(5431), 1244–1246, doi:10.1126/science.285.5431.1244.

United States Army Corps of Engineers (USACE), 2002. Sacramento and San Joaquin River Basins, California, Comprehensive Study, Interim Report.

United States Bureau of Reclamation, 2005. Final Environmental Assessment: Long-term renewal of water service contracts in the Black Butte Unit, Corning Canal Unit, and Tehama-Colusa Canal Unit of the Sacramento River Division, Central Valley Project, California. Report prepared by United States Bureau of Reclamation, Mid-Pacific Region, Sacramento, CA.

Vyverberg, K., Snider, B., and R.G. Titus, 1997. Lower American River Chinook Salmon Spawning Habitat Evaluation, October 1994. California Department of Fish and Game, Environmental Services Division. 44p.

Western Shasta Resource Conservation District, 1999. Lower Clear Creek sediment budget report. United States Department of Agriculture, Department of Conservation. 15p.

Wilcock, P.R., Kondolf, G.M., Matthews, W.V.G., and A.F. Barta, 1996. Specification of sediment maintenance flows for a large gravel-bed river. Water Resources Research 32(9), 2911 – 2921.

Williams, G.P. and M.G. Wolman, 1984. Downstream Effects of Dams on Alluvial Rivers. U.S. Geological Survey Professional Paper 1286. U.S. Government Printing Office, Washington. 83 p.

Wright, S.A., and D.H. Schoellhamer, 2004. Trends in the sediment yield of the Sacramento River, California, 1957-2001. San Francisco Estuary and Watershed Science, 2(2), article 2.

Yoshiyama, R.M., Gerstung, E.R., Fisher, F.W., and P.B. Moyle, 1996. Historical and present distribution of Chinook salmon in the Central Valley drainage of California. In Sierra Nevada Ecosystem Project final report to Congress. Centers for Water and Wildland Resources, University of California, Davis. Volume 3, p 309-361.

Figures

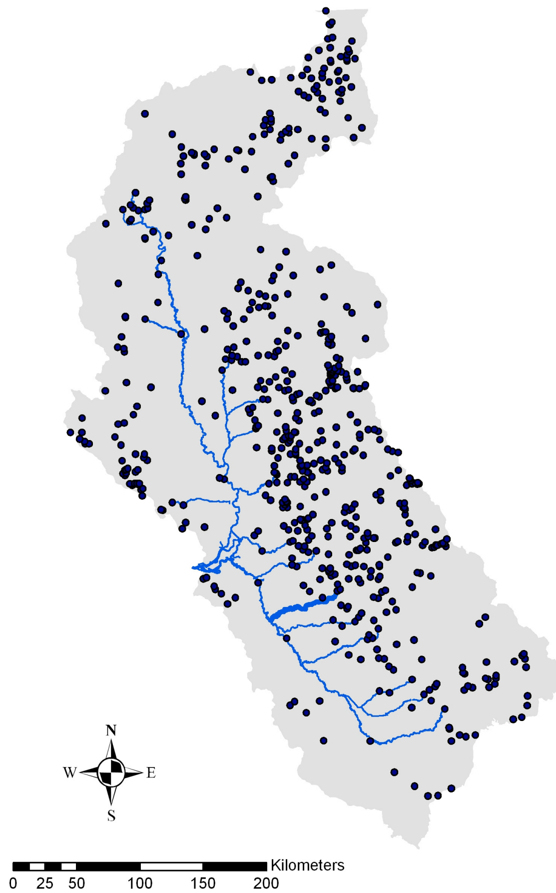

Figure 1. Map of the Sacramento-San Joaquin river system with the 619 upstream dams marked (dam information from CDSD 2007).

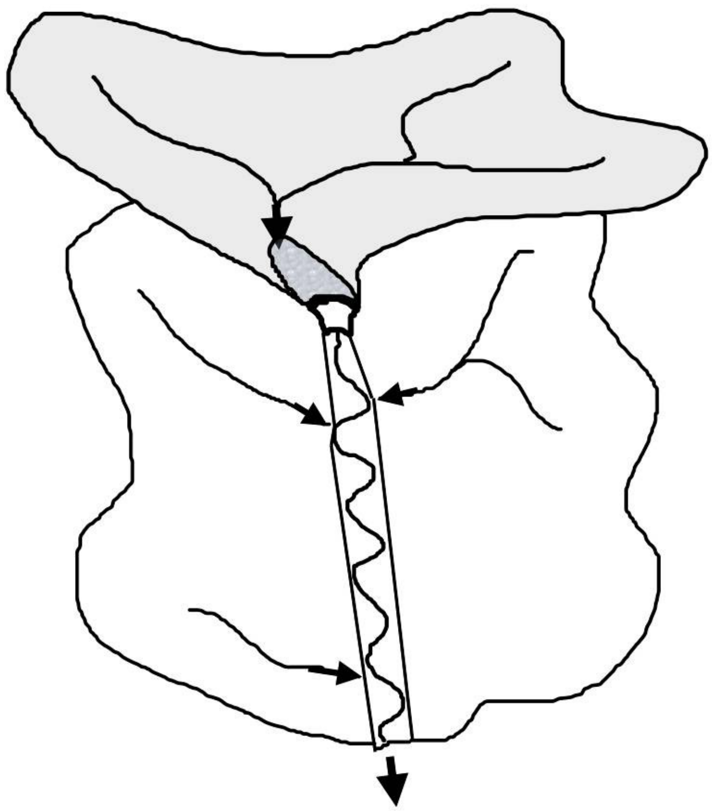

Figure 2. Schematic diagram of the sediment budget used in this study. The shaded area is the drainage area upstream of the dam, the unshaded area is the drainage area downstream of the dam. In this study, the assumption was that no sediment from the area upstream of the dam was contributed to the downstream area. The straight lines bounding the river downstream of the dam are the limits of the storage component, which is defined as extending from valley-wall to valley-wall (i.e. including channel bed, streambanks and terraces). The length of the storage component is the river reach over which the bedload equations were considered valid (see Table 2). For the area downstream of the dam, bedload was assumed to be supplied only by tributaries with drainage areas greater than 10 km^2.

Figure 3. Lower Yuba River. Top– historical photo of Barrier No. 1 on the Lower Yuba River taken in September 1906 by Gilbert, just after completion and the season before it failed (Gilbert 1917). The debris dam was built by the California Debris Commission in 1904-1906 and was breached by floods on the Yuba River in 1907 (Gilbert 1917). Middle - historical photograph of Barrier No. 1 by Lippincott in 1913, six years after the dam failed (in University of California, Water Resources Center Archives, Lippincott collection). Bottom – the remains of the same dam in 2006 (photo by J.T.Minear). The bed of the river is approximately 7 meters lower than the base of the dam.

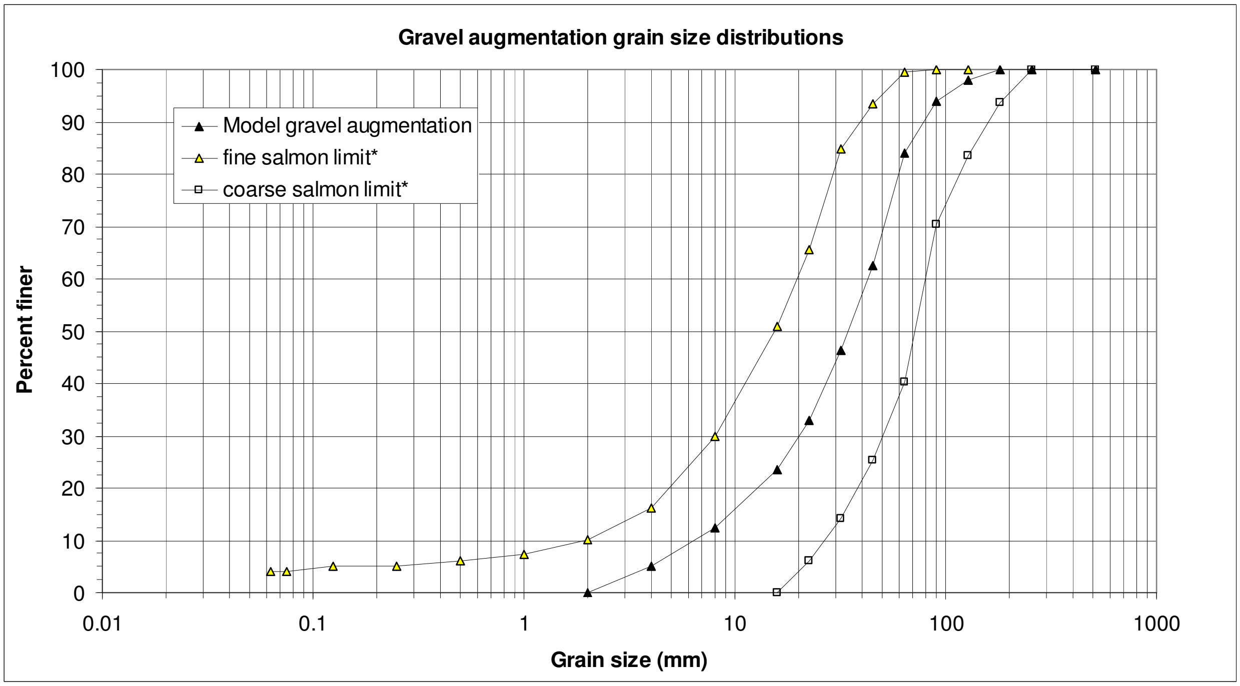

Figure 4. Model gravel augmentation grain size, shown within an ideal grain size distribution (*) for salmonids (from Vyverberg et al. 1997).

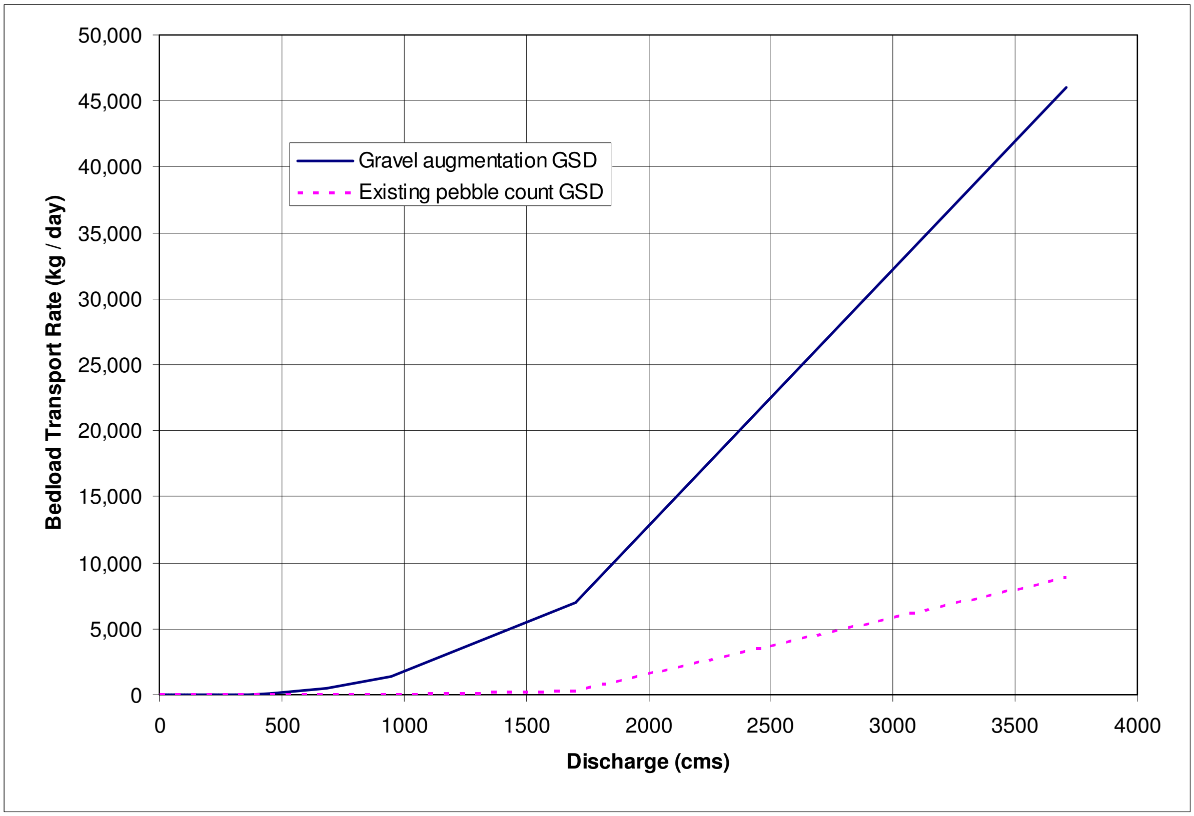

Figure 5. Change in bedload transport rates observed with a fining of the bed from gravel augmentation, the result of which is an increase in bedload transport and mobilization at lower flows. Site shown is for American River AR1 site, grain size for gravel augmentation is shown in Figure 3.

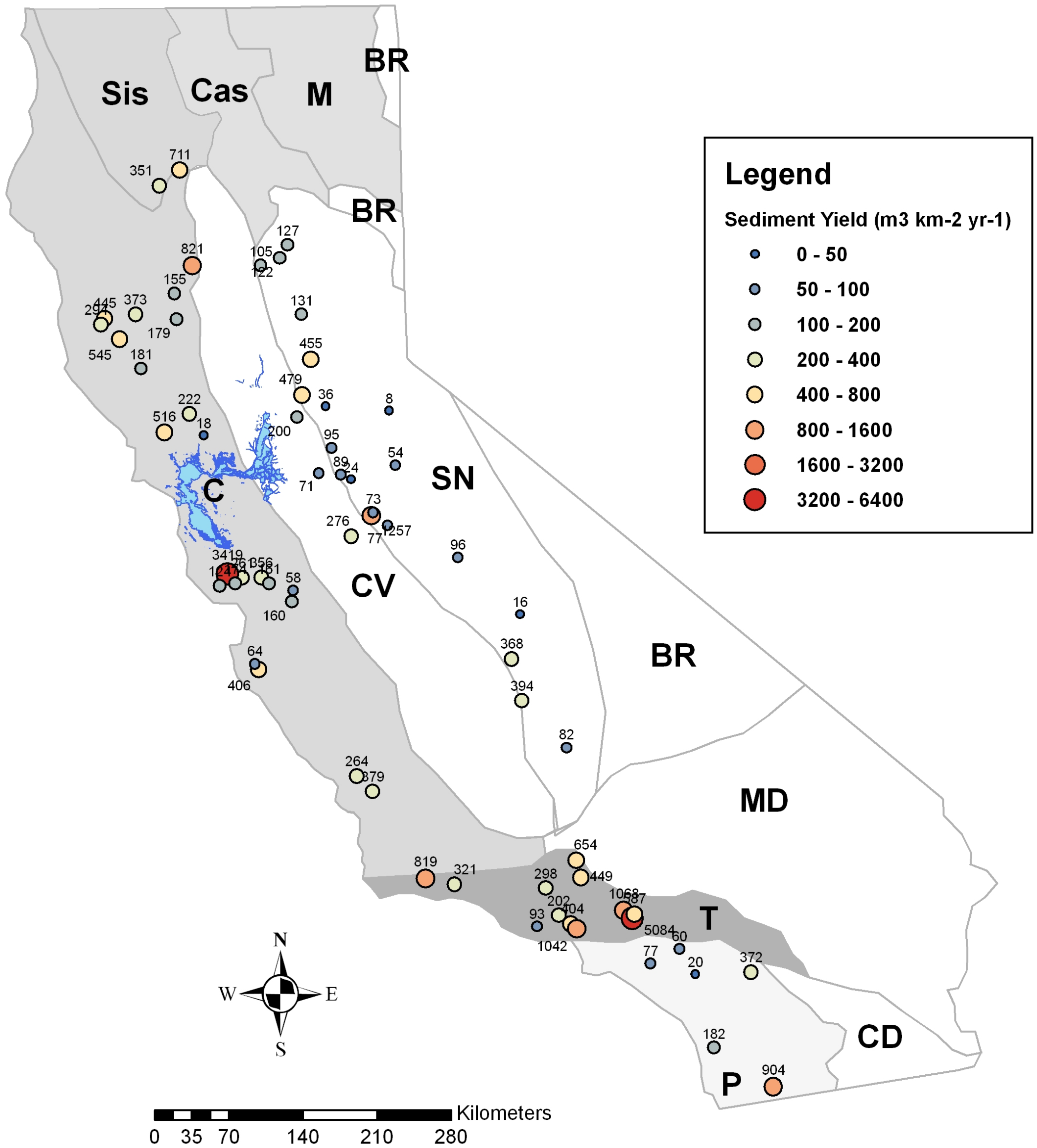

Figure 6. Individual sediment yield rates from reservoir sedimentation surveys calculated in Chapter 2. Note the relatively low rates of sediment yield for the majority of the Sierra Nevada, with the exception of some of the northern rivers affected by hydraulic mining waste.

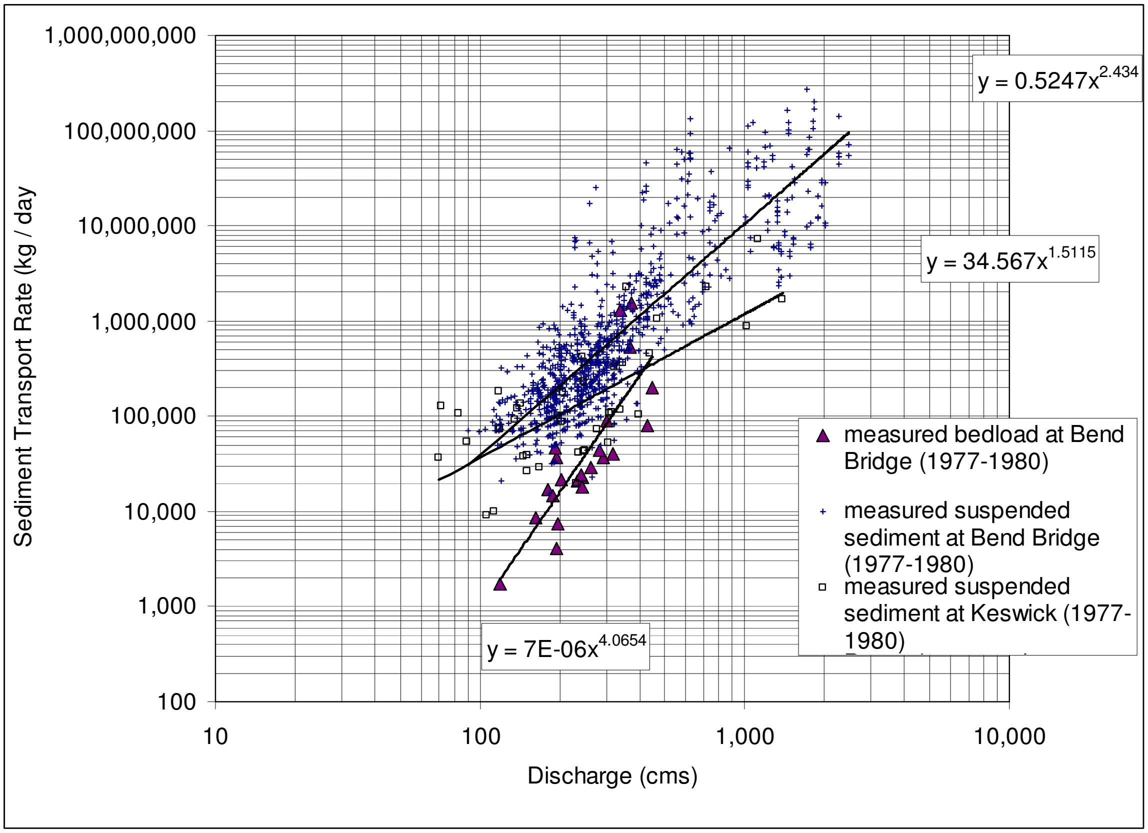

Figure 7. Graph of measured bedload and suspended load discharges at USGS Sacramento River gages at Bend Bridge (#11371000) and below Keswick (#11370500). Note the relative values of bedload to suspended load at Bend Bridge, and the smaller exponent for the suspended discharge at Keswick (just downstream of Shasta Dam) compared to the suspended sediment concentration for Bend Bridge (103km downstream of Shasta Dam).

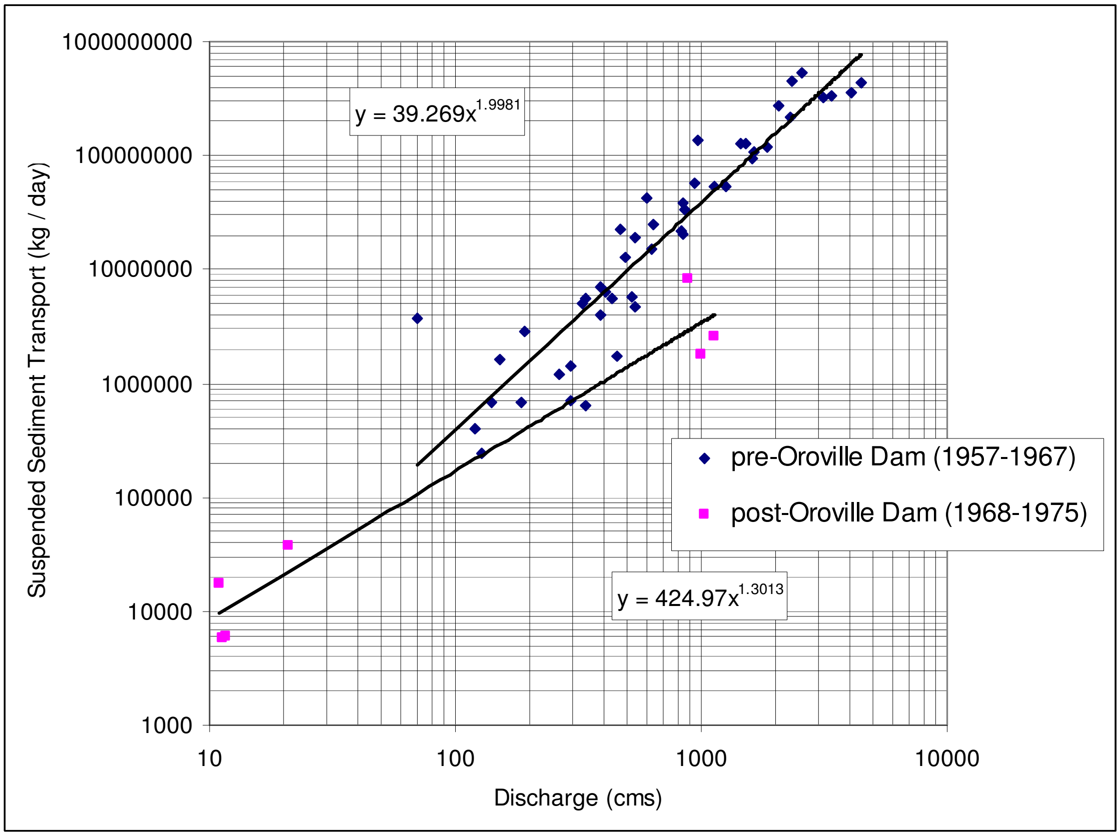

Figure 8. Pre- and post-Oroville Dam suspended sediment measurements on the Feather River below Oroville (USGS Gage #11407000). Note that not only do the dams decrease sediment transport by decreasing the sediment concentration of the flows downstream, they also tend to shift the flow-duration curves towards lower flows.

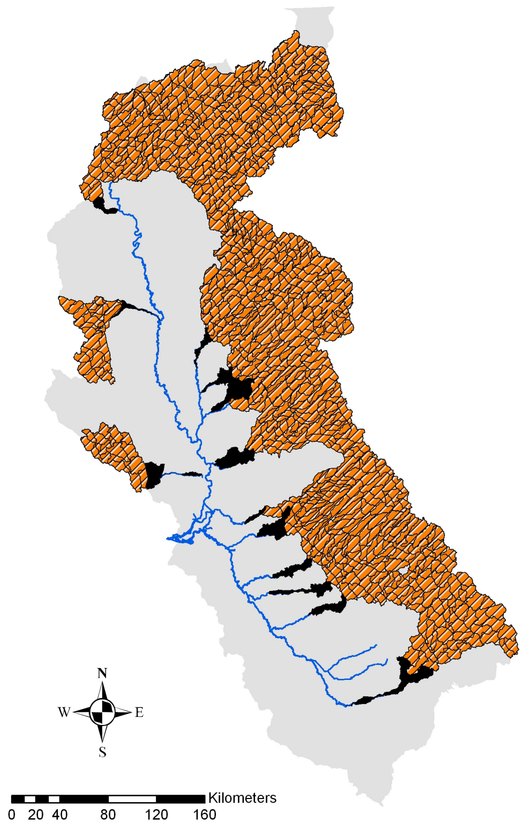

Figure 9. Map of the Sacramento-San Joaquin river system with watersheds upstream of the foothill dams marked in orange stripe, areas draining into the gravel-bed reaches downstream of the dams are marked in black. The watershed of the Sacramento River downstream of Shasta Dam is excluded here for clarity but if included would take up much of the northern Sacramento valley.

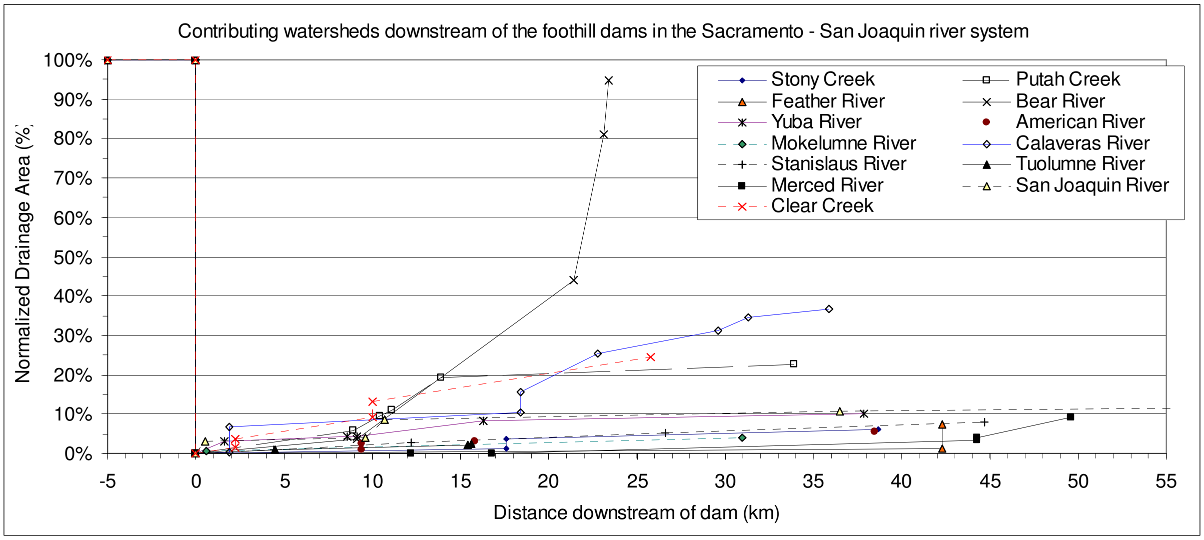

Figure 10. Results of the analysis of drainage areas downstream of the foothill dams in the Sacramento-San Joaquin river system (Sacramento River not shown). Of the thirteen river reaches shown here, nine of the rivers regain less than 10% of the watershed upstream of the dam within 50km of the dam (i.e. the gravel-bedded reaches). The four that regain more than 10% of their upstream watershed area are Clear Creek, Bear River, Calaveras River, and Putah Creek.

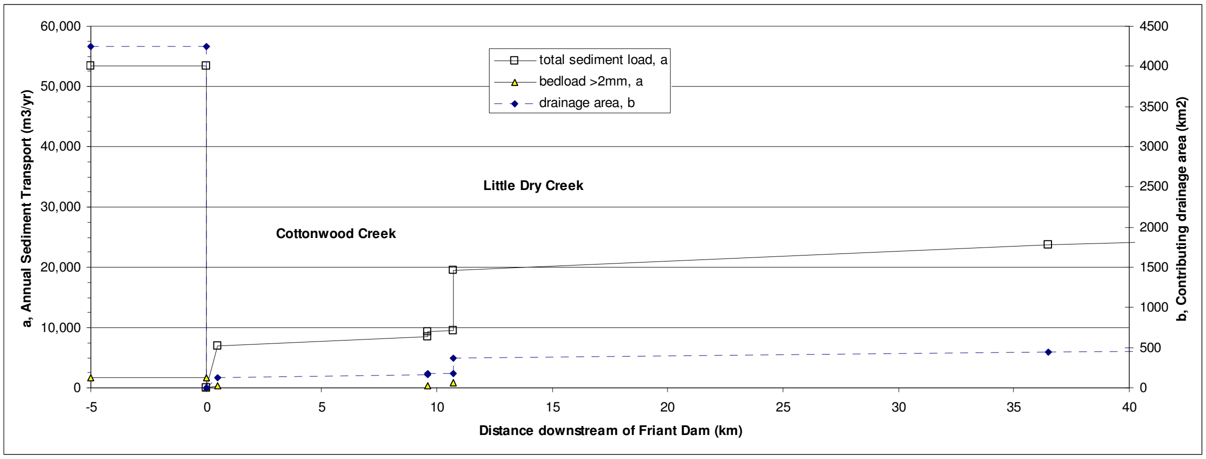

Figure 11. Example of the river-specific sediment budget for the gravel-bedded reach of the San Joaquin River downstream of Friant Dam. For the San Joaquin, the bedload contributions from two major tributaries at 0.5km and 10.7km greatly increase the bedload supplied to the reach. The connectivity of these tributaries is doubtful given the highly disturbed floodplain of the San Joaquin, but they are assumed to be connected here.

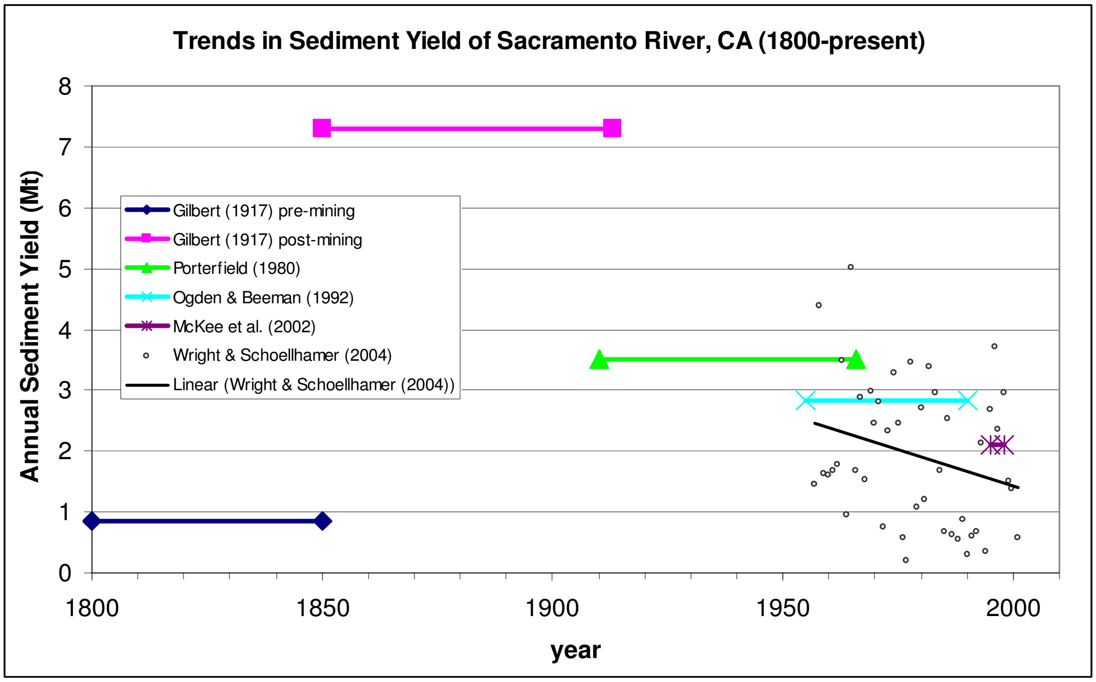

Figure 12. Trends in sediment yield of the Lower Sacramento River, 1800-present (after Wright and Schoelhamer, 2004).

Tables

Table 1. Impounded Runoff for major dammed Sacramento-San Joaquin rivers.									
River	**Dam**	**Year built**	**# dams upstream**		**Average Annual Runoff ***	**Impounded Runoff**			
						foothill dam		**Total watershed impounded runoff ****	
			year built	**2008**	**(M m^3)**	**capacity (M m^3)**	**IR**	**year foothill dam built**	**2008**
Clear Creek	Whiskeytown	1963	0	0	232.5	297.4	128%	128%	128%
Stony Creek	Black Butte	1963	7	9	447.3	177.3	40%	68%	68%
Putah Creek	Monticello	1957	9	27	410.5	1,976.0	481%	484%	494%
Sacramento	Shasta	1945	42	73	7,993.0	5,614.8	70%	74%	77%
Feather	Oroville	1968	35	37	3,588.2	4,363.5	122%	186%	186%
Yuba	Englebright	1941	34	46	2,358.5	86.3	4%	17%	69%
Bear	New Camp Far West	1963	4	9	364.4	127.0	35%	37%	61%
American	Folsom	1956	31	57	3,319.4	1,245.8	38%	40%	68%
Mokelumne	Camanche	1963	14	17	764.9	532.2	70%	140%	140%
Calaveras	New Hogan (Old Hogan)	1963 (1910)	7	9	199.5	391.0	196%	198%	199%
Stanislaus	New Melones (Old Melones)	1979 (1926)	21	28	805.1	2,960.4	368%	396%	425%
Tuolumne	New Don Pedro (Old Don Pedro)	1971 (1923)	23	27	1,628.2	2,504.0	154%	178%	179%
Merced	New Exchequer (Old Exchequer)	1967 (1926)	4	4	1,191.4	1,273.0	107%	107%	107%
San Joaquin	Friant	1942	14	21	1,221.3	642.0	53%	87%	116%

Note: * - Average annual runoff as measured at the gages below the foothill dams. The effects of evaporation or diversion were not taken into account. Impounded runoff was calculated as the storage capacity of the dams divided by the average annual runoff. **- Total watershed impounded runoff takes into account the capacity of all the dams in the watershed upstream of the main foothill dam, including the foothill dam. Years in parentheses are the dates of construction for the 1st generation of foothill dams (previous to the current dams in place).

Table 2. Previous studies estimating sediment yields in areas near the gravel-bedded reaches of major rivers of the Sacramento-San Joaquin area. *				
Author	**Date of estimate**	**Region**	**Sediment Yield**	**Comments**
Gilbert 1917	WY1906	Lower Yuba River	1,700 m^3 / km^2 / yr	c
	1849-1906	Lower Yuba River	1,400 m^3 / km^2 / yr	Piedmont deposits, d
	1849-1880	Lower American River	307 m^3 / km^2 / yr	Piedmont deposits, e
	1849-1880	Lower Bear River	1,200 m^3 / km^2 / yr	Piedmont deposits, f
	1849-1913	Lower Feather River	68 m^3 / km^2 / yr	Piedmont deposits, g
Porterfield 1980	1957-1966	Mokelumne R. downstream of Camanche Dam	206** m^3 / km^2 / yr	
	1957-1959	Cosumnes R. at Michigan Bar	39 m^3 / km^2 / yr	Sand 35% of total load, i
		Sacramento R. at Red Bluff	933,900 m^3 / yr***	
		Feather River at Oroville	633,700 m^3 / yr, unclear size watershed***	
	1957-1966	Calaveras R.	72 m^3 / km^2 / yr	
Porterfield et al. 1978	1902-1962	Feather River, pre-Oroville Dam	87 m^3 / km^2 / yr	I
	1957-1962	Feather River, pre-Oroville Dam	30 m^3 / km^2 / yr	I
	1965-1967	Feather River, pre-Oroville Dam	97 m^3 / km^2 / yr	I
	1968-1975	Feather River, post-Oroville Dam	200 m^3 / km^2 / yr	I, k
	1974-1975	Feather River, post-Oroville Dam	111 m^3 / km^2 / yr	I, k
CDWR 1982	1902-1962	Feather River, pre-Oroville Dam	11 m^3 / km^2 / yr (1), 1 m^3 / km^2 / yr (2)	Bedload (1), and spawning gravel (2), h
Kondolf et al. 2001	1949 to 1999	Stanislaus River upstream of dams	5.8 m^3 / km^2 / yr	Only sand and gravel
	1949 to 1999	Stanislaus River, Tulloch Dam to Oakdale (downstream of dams)	1,296 m^3 / yr, unclear size watershed	Only sand and gravel
	1949 to 1999	Stanislaus River downstream of Oakdale	9,670 m^3 / yr, no size watershed mentioned	Only sand and gravel

Jones et al. 1972	1957-1968	Tributaries draining into Sacramento River from Coast Range	Qss: 36 – 762 m^3 / km^2 /yr; Qbl: 3 – 46 m^3 / km^2 / yr	a
	1962-1968	Upper Putah Creek, upstream of Monticello Dam	Qss: 252 m^3 / km^2 / yr	
WSRCD, 1999	1998	Lower Clear Creek	164 m^3 / km^2 / yr	
USACE, 1990 (in Kondolf et al. 2001)	1990	Area upstream New Melones Dam, Stanislaus	711 m^3 / km^2 / yr	

*- Weight yields were converted to volume yields using 1,600 kg / m^3 density conversion.
** Porterfield (1980) found high sediment yield rates immediately after construction of Camanche Dam (Pardee Dam was already in place). He speculated that the high yields might be from the downcutting of the riverbed below Camanche.
*** Porterfield only reported suspended sediment for these sites but he assumed 10% bedload for all the other sites so that rate was applied here for a total load.
a –the authors attributed the wide range of rates to the geologic type, with Coast Range geologies, such as the Franciscan formation creating the highest sediment yield rates. Bedload calculated using modified Meyer-Peter, Mueller bedload equation.
c – Gilbert (1917) calculated the amount of sediment that was deposited in WY1906 behind Barrier No. 1 as 1.29 M m^3 (see Figure 2), and used measurements of suspended and calculated bedload transport to come up with an estimate of total load. Gilbert's estimates are converted here using the drainage area at the USGS Smartville gage (3108 km^2) where Gilbert estimated suspended sediment. Gilbert's estimates were conducted during the period when the discharge of mining waste was still extremely high. His measurements were extremely impressive given the general lack of knowledge at the time. It is possible that Gilbert's estimates from the deposit behind Barrier No. 1 included some of the sediment he measured as suspended sediment, however, no correction was made to his original estimates, which are presented here.
d – Volume estimated for Yuba mining-waste piedmont deposit by Gilbert (1917) citing Hart (1906), converted here using the drainage area at Smartsville (3108 km^2) for the estimated period of record (1849-1906).
e – Volume estimated for American mining-waste piedmont deposit by Gilbert (1917) citing Manson (1882), converted here using the drainage area at USGS gage below Folsom Dam (4823 km^2) for the period of record (1849-1880).
f – Volume estimated for Bear mining-waste piedmont deposit by Gilbert (1917), citing Mendell (1882), converted here using the drainage area at New Camp Far West Dam (738 km^2) over the implied period of record (1849-1880).
g- Volume estimated for Feather mining-waste piedmont deposit by Gilbert (1917), citing Hall (1880), converted here using the drainage area at the USGS gage below Oroville Dam (9386 km^2).

h- CDWR (1982) estimated spawning gravel size from unpublished data on Sacramento River, which suggested that 10% of bedload is spawning gravel size (12.5mm or larger).
i- Porterfield (1980) also mentioned that much of the sand was being transported even at relatively low flows (1200cfs).
j- Cain's (1997) estimates of sediment contributions were evaluated for this study, but were found to be at least an order of magnitude too large for most reasonable sites (e.g. 12,850 m^3 / km^2 / yr – on the order of the maximum sediment yields following the eruption of Mount St. Helens (Major 2004)).
k- adjusted by Porterfield et al. (1978) to include only the drainage area downstream of Oroville Dam. Porterfield et al. (1978) reported higher sediment yields per drainage area for the area downstream of the dam immediately following dam closure, and attributed it to adjustment of the channel to the reduction in sediment supply.
l- Porterfield et al. (1978) used an adjusted drainage area of 7806 km^2 for their calculations of pre-Oroville dam sediment yield (drainage area at Oroville is 9386 km^2). If all dams upstream are taken into account, only 3538 km^2 of the upstream watershed is not dammed. It is likely that Porterfield et al. did not locate all the dams upstream of Oroville, since there were at least 37 large dams upstream when Oroville Dam was built in 1968 (CDSD 2007).

Table 3. Bedload and suspended sediment gages in the gravel-bedded reaches of the Sacramento-San Joaquin river system, excluding the Sacramento River gages downstream of Red Bluff.				
River	**Gage**	**Location**	**Dates of sediment sampling**	**Number of samples for Qss or Qbl ***
Sacramento	USGS 11370500	blw Keswick	1977-1994	146 Qss
Sacramento	USGS 11377100	Bend Bridge	1977-1980	23 Qbl
Sacramento	USGS 11377100	Bend Bridge	1977-2000	1018 Qss
Stony Creek	USGS 11388000	blw Black Butte	1958-1965	53 Qss
Feather	USGS 1140700	blw Oroville	1957-1975	43 Qss
Yuba	USGS 11421000	Marysville	1996	8 Qss
Yuba	USGS 11421500	Marysville	1996-1998	17 Qss
Bear	USGS 1142400	Wheatland	1999-2000	18 Qss
American	USGS 11447000	Sacramento	1996	24 Qss
Mokelumne	USGS 11323500	blw Camanche	1966-1970	52 Qss

* - Qss = suspended sediment discharge, Qbl = bedload discharge.

Table 4. Sediment yield used to estimate sediment trapping by upstream dams.						
River	Dam	Gravel-bed study reach length (km)*	Sediment yield used for upstream watersheds (m^3 / km^2 / yr) **	Source / Justification	Sediment yield used for downstream watersheds (m^3 / km^2 / yr) ***	Source / Justification
Clear Creek	Whiskeytown	15.3	157	a	53	e
Stony Creek, f	Black Butte	27.7	157	a	53	e
Putah Creek	Monticello	20.1	157	a	53	e
Sacramento	Shasta	103	150	b	53	e
Feather	Oroville	12.6	58	c	53	e
Yuba	Englebright	37.9	58	c	53	e
Bear	New Camp Far West	23	58	c	53	e
American	Folsom	17	58	c	53	e
Mokelumne	Camanche	15.9	58	d	53	e
Calaveras	New Hogan	35.9	58	d	53	e
Stanislaus	New Melones	26.6	58	h	53	e
Tuolumne	New Don Pedro	25.8	58	I	53	e
Merced	New Exchequer	32.8	58	j	53	e
San Joaquin	Friant	36.5	58	k	53	e

*- length of the gravel-bedded reach modeled here is chosen to reflect the length of river most likely represented by the bedload transport sites used in Chapter 3. Measured downstream from the lowermost dam (either foothill dam or reregulating dam).
**- Upstream of the foothill dams.
***- Downstream of the foothill dams.
a- median rate for Coast Ranges (Chapter 2).
b- approximate sediment yield, since there is little data for the regions upstream of Shasta Reservoir (325 m^3 / km^2 / yr for the Siskiyou region, 58 m^3 / km^2 / yr for Sierra Nevadas).
c- median sediment yield rate for Sierra Nevada (Chapter 2), not accounting for elevated sediment supply from hydraulic mining. The lower elevation foothills (<2,000m elevation) are where the majority of hydraulic mining took place. Sediment yield from the hydraulically mined areas has been decreasing since the late 1800s (Gilbert 1917, James 1999) (Figure 11), more recent rates measured at Combie Reservoir (Bear River, 1928-1935) and Folsom Reservoir (American River, 1956-1991) have rates of 273 and 287 m^3 / km^2 / yr respectively.
d- median sediment yield rate for Sierra Nevada (Chapter 2).
e- median sediment yield rate for Central Valley (Chapter 2).

f- it was discovered late in this study that Stony Gorge, one of the major dams upstream of Black Butte Dam, had an incorrect drainage area in the CDSD database (1903 km^2 instead of 768 km^2). The drainage area was measured at 768 km^2 and corrected for this part of the study, though it had been used in Chapter 2 to estimate sediment yields in the Coast Ranges.
k- median rate for Sierra Nevada (estimated in Chapter 2), similar to reservoir sedimentation rate of Crane Valley Reservoir on North Fork San Joaquin from 1901-1946 (58 m^3 / km^2 / yr) – see Chapter 2.
j- median rate for Sierra Nevada (estimated in Chapter 2), similar to reservoir sedimentation rate of Old Exchequer Dam on Merced River from 1926-1946 (46 m^3 / km^2 / yr) – see Chapter 2.
i- median rate for Sierra Nevada (estimated in Chapter 2), similar to reservoir sedimentation rate of Old Don Pedro Dam on Tuolumne River from 1923-1945 (44 m^3 / km^2 / yr) – see Chapter 2.
h- median rate for Sierra Nevada (estimated in Chapter 2), similar to reservoir sedimentation rate of Lyons Reservoir on South Fork Stanislaus River from 1930-1946 (33 m^3 / km^2 / yr) – see Chapter 2.

Table 5. Estimated rates of total sediment load trapped by foothill and upstream dams, annually for the year 2008, and as a deficit (since foothill dam construction date).							
River	**Year foothill dam completed ***	**sediment trapped per year (2008)**			**sediment deficit (through 2008)**		
		individual dam (m^3)	**including all dams (m^3) ****	**%*****	**individual dam (m^3)**	**including all dams (m^3)****	**%*****
Clear Creek	1963	46,474	46,473	100.00%	2,138,184	2,138,167	100.00%
Stony Creek	1963	52,617	286,445	18.37%	2,066,130	13,183,052	15.67%
Putah Creek	1957	220,191	233,517	94.29%	11,556,494	12,143,106	95.17%
Sacramento	1945	1,298,048	1,529,975	84.84%	73,597,401	97,977,801	75.12%
Feather	1968	347,616	536,754	64.76%	13,925,912	22,007,515	63.28%
Yuba	1941	52,149	141,469	36.86%	3,668,673	9,668,646	37.94%
Bear	1963 (1928)	22,918	41,676	54.99%	1,062,379	3,376,667	31.46%
American	1956	123,261	278,139	44.32%	7,306,861	14,742,539	49.56%
Mokelumne	1963	7,537	84,247	8.95%	347,009	3,875,367	8.95%
Calaveras	1963 (1910)	47,103	49,541	95.08%	2,173,237	4,904,974	44.31%
Stanislaus	1979 (1926)	59,736	134,793	44.32%	7,250,696	11,187,920	64.81%
Tuolumne	1971 (1923)	192,207	230,048	83.55%	17,171,615	19,784,969	86.79%
Merced	1967 (1926)	152,718	154,777	98.67%	12,735,794	12,847,544	99.13%
San Joaquin	1942	53,383	243,867	21.89%	4,678,496	16,341,573	28.63%
	Totals	**2,668,465**	**3,991,721**	**60.14%**	**159,334,168**	**244,179,840**	**56.57%**

*- dates in parentheses are the dates the original foothill dam was constructed (i.e. 1st generation dam). For the calculation of the deficit, the construction date of the original foothill dam was used, assuming that the original dam was not emptied of sediment before the 2nd generation dam was built. **- includes all dams present in the upstream watershed.***- percent of total watershed sediment trapping due to foothill dams.

Table 6. Estimated rates of bedload trapping by foothill and upstream dams, annually for the year 2008, and as a total bedload deficit (since foothill dam construction date).

River	Year foothill dam completed*	Bedload trapped per year (2008)			Bedload deficit (through 2008)		
		individual dam (m^3)	including all dams (m^3) **	%***	individual dam (m^3)	including all dams (m^3)**	%***
Clear Creek	1963	4,688	4,688	100.00%	215,637	215,637	100.00%
Stony Creek	1963	17,868	30,150	59.26%	822,101	1,386,903	59.28%
Putah Creek	1957	22,064	23,436	94.14%	1,158,366	1,218,698	95.05%
Sacramento	1945	23,047	155,421	14.83%	1,855,666	9,946,975	18.66%
Feather	1968	20,535	54,226	37.87%	841,922	2,223,249	37.87%
Yuba	1941	4,101	16,537	24.80%	333,527	1,124,501	29.66%
Bear	1963 (1928)	2,266	4,285	52.88%	104,448	347,047	30.10%
American	1956	7,387	28,338	26.07%	509,462	1,501,915	33.92%
Mokelumne	1963	651	8,546	7.62%	30,112	393,096	7.66%
Calaveras	1963 (1910)	4,677	5,011	93.33%	216,559	415,944	52.06%
Stanislaus	1979 (1926)	5,054	13,530	37.36%	696,789	1,122,997	62.05%
Tuolumne	1971 (1923)	18,365	23,182	79.22%	1,653,680	1,993,613	82.95%
Merced	1967 (1926)	15,339	15,636	98.10%	1,282,324	1,297,811	98.81%
San Joaquin	1942	3,232	25,181	12.84%	216,557	1,687,127	12.84%
	Totals	**149,273**	**408,167**	**52.74%**	**9,937,151**	**24,875,512**	**51.49%**

*- dates in parentheses are the dates the original foothill dam was constructed (i.e. 1st generation dam). For the calculation of the deficit, the construction date of the original foothill dam was used, assuming that the original dam was not emptied of sediment before the 2nd generation dam was built. **- includes all dams present in the upstream watershed. ***- percent of total watershed sediment trapping due to foothill dams.

Table 7. Estimated rates of bedload greater than 2mm trapped by foothill and upstream dams, annually for the year 2008, and as a total deficit (since foothill dam construction date).							
River	Year foothill dam completed *	>2mm trapped per year (2008)			>2mm deficit (through 2008)		
		individual dam (m^3)	including all dams (m^3) **	%***	individual dam (m^3)	including all dams (m^3)**	%***
Clear Creek	1963	2,344	2,344	100.00%	107,819	107,819	100.00%
Stony Creek	1963	8,934	15,075	59.26%	411,051	693,452	59.28%
Putah Creek	1957	11,032	11,718	94.14%	579,183	609,349	95.05%
Sacramento	1945	11,524	77,711	14.83%	927,833	4,973,487	18.66%
Feather	1968	10,267	27,113	37.87%	420,961	1,111,624	37.87%
Yuba	1941	2,051	8,268	24.80%	166,763	562,250	29.66%
Bear	1963 (1928)	1,133	2,142	52.88%	52,224	173,523	30.10%
American	1956	3,693	14,169	26.07%	254,731	750,957	33.92%
Mokelumne	1963	325	4,273	7.62%	15,056	196,548	7.66%
Calaveras	1963 (1910)	2,338	2,506	93.33%	108,279	207,972	52.06%
Stanislaus	1979 (1926)	2,527	6,765	37.36%	348,394	561,499	62.05%
Tuolumne	1971 (1923)	9,182	11,591	79.22%	826,840	996,807	82.95%
Merced	1967 (1926)	7,669	7,818	98.10%	641,162	648,905	98.81%
San Joaquin	1942	1,616	12,590	12.84%	108,278	843,563	12.84%
	Totals	**74,637**	**204,083**	**52.74%**	**4,968,575**	**12,437,756**	**51.49%**

*- dates in parentheses are the dates the original foothill dam was constructed (i.e. 1st generation dam). For the calculation of the deficit, the construction date of the original foothill dam was used, assuming that the original dam was not emptied of sediment before the 2nd generation dam was built. **- includes all dams present in the upstream watershed. ***- percent of total watershed sediment trapping due to foothill dams.

Table 8. Post-dam annual sediment budget, >2mm particles.					
River	Length of study reach (km)*	Post-dam annual sediment budget, >2mm particles			
		tributary supply, a (m^3)	gravel augmentation, b (m^3)	transport, c, ** (m^3)	supply / transport
Clear Creek	15.3	84	5,039	148	34.66
Stony Creek	27.7	125	0	4,303	0.03
Putah Creek	20.1	476	8	41	11.79
Sacramento	103		7,420	218,818	0.03
Feather	12.6	0	168	1,739	0.10
Yuba	37.9	500	0	22,414	0.02
Bear	23	785	0	975	0.81
American	17	190	512	4,022	0.17
Mokelumne	15.9	32	730	13	60.24
Calaveras	35.9	418	0	na	na
Stanislaus	26.6	188	2,000	260	8.41
Tuolumne	25.8	111	2,376	343	7.26
Merced ***	32.8	271	137	1	408
San Joaquin	36.5	889	0	584	1.52

*- measured downstream of the lowermost dam (either foothill dam or reregulating dam). The study reach was defined as the area over which the bedload equations developed in Chapter 3, would be applicable. Only qualitative means were available to estimate this – the factors that went in the assessment were cross section, slope, grain size, tributaries.
**-bedload transport estimates were made using post-dam grain sizes.
***- bedload transport estimates for the Merced River were made using a coarse grain size distribution that represented pre-gravel augmentation conditions. No bedload transport was predicted for this site for either pre- or post-dam conditions.
a- tributary supply estimated for >2mm bedload.
b- gravel augmentation estimates were made by dividing the total volume of augmentation by the period over which the gravel had been added, up to the year 2004 (since this was the latest data available). As such, this estimate does not take into account the many years before gravel augmentation started and it assumes that gravel augmentation will continue to be added at the same rate as the recent past.
c- estimates of bedload transport from Chapter 3.

Table 9. Post-dam sediment deficit, >2mm particles					
River	period since closure (years)*	Post-dam sediment deficit, >2mm particles			
		tributary supply, a (m^3)	gravel augmentation, b (m^3)	transport, c, ** (m^3)	supply / transport
Clear Creek	45	3,794	45,350	6,652	7.39
Stony Creek	45	5,645	0	193,627	0.03
Putah Creek	51	24,284	85	2,093	11.64
Sacramento	63		200,344	13,785,541	0.01
Feather	40	0	3,857	69,574	0.06
Yuba	67	33,492	0	1,501,724	0.02
Bear	45	35,307	0	43,855	0.81
American	52	9,860	7,163	209,147	0.08
Mokelumne	45	1,431	10,945	569	21.76
Calaveras	45	18,788	0	na	na
Stanislaus	29	5,439	21,999	7,541	3.64
Tuolumne	37	4,110	26,135	12,680	2.39
Merced ***	41	11,122	2,595	41	332.10
San Joaquin	66	58,701	0	38,572	1.52

*- period since closure of most recent foothill dam. Several of the 1st generation foothill dams have been replaced by 2nd generation dams (Table 6). Only the 2nd generation construction date was used here to estimate sediment deficit.
**-bedload transport estimates were made using post-dam grain sizes.
***- bedload transport estimates for the Merced River were made using a coarse grain size distribution that represented pre-gravel augmentation conditions. No bedload transport was predicted for this site for either pre- or post-dam conditions.
a- tributary supply estimated for >2mm bedload.
b- includes all gravel added as augmentation projects over the life of the dam.
c- estimates of bedload transport from Chapter 3.

Table 10. Gravel enhancement projects below foothill dams, Sacramento-San Joaquin river system.

#	River (Regulating Dam)	Years	Number of projects	Agencies	Type	Volume (m3)	Cost
1	Clear Creek (Whiskeytown)	1996-2004	22	Western Shasta RCD	injection, riffle construction	45,350	$823,998
2	Sacramento (Keswick)	1978-2004	20	USBR, CDFG, DWR	injection, riffle construction and maintenance	200,344	$4,135,000
3	Putah Creek	1994	1	LPCCC	riffle construction	85	na
4	Feather (Oroville Res.)	1982-1987	2	CDFG	riffle construction and maintenance, ripping	3,857	na
5	American (Nimbus)	1991-1999	2	Sacramento Co, CDFG, USFWS, USBR	injection, ripping, gravel cleaning	4,163	$280,000
6	Mokelumne (Camanche)	1990-2003	12	EBMUD	injection, ripping	10,945	$299,575
7	Stanislaus (Goodwin)	1994-2004	10	CDFG, DWR, Carl Mesick Consultants	riffle construction and maintenance, injection and ripping	21,999	$1,500,240
8	Tuolumne (La Grange)	1994-2004	5	CDFG, DWR	riffle construction and maintenance, injection, ripping	26,135	$765,425
9	Merced (Crocker-Huffman)	1986-2004	11	Merced Irr. District, CDFG, DWR	riffle construction and maintenance, injection	2,595	$460,000
	Total	**1978-2004**	**80**			**267,339**	**$8,264,238**

Table 11. Post-dam annual sediment budget, assuming the riverbed is composed entirely of gravel augmentation grains, >2mm particles.					
River	**Length of study reach (km)***	**Post-dam annual sediment budget, >2mm particles**			
		tributary supply, a (m^3)	**gravel augmentation, b (m^3)**	**bedload transport, c (m^3)**	**supply / transport**
Clear Creek	15.3	84	5,039	7,021	0.73
Stony Creek	27.7	125	0	11,917	0.01
Putah Creek	20.1	476	8	9,418	0.05
Sacramento	103		7,420	85,955	0.09
Feather	12.6	0	168	18,073	0.01
Yuba	37.9	500	0	22,246	0.02
Bear	23	785	0	27,590	0.03
American	17	190	512	17,171	0.04
Mokelumne	15.9	32	730	1	1348.33
Calaveras	35.9	418	0	na	na
Stanislaus	26.6	188	2,000	2,426	0.90
Tuolumne	25.8	111	2,376	9,688	0.26
Merced	32.8	271	137	6,300	0.07
San Joaquin	36.5	889	0	2,982	0.30

*- measured downstream of the lowermost dam (either foothill dam or reregulating dam).
a- tributary supply estimated for >2mm bedload.
b- gravel augmentation estimates were made by dividing the total volume of augmentation by the period over which the gravel had been added, up to the year 2004 (since this was the latest data available). As such, this estimate does not take into account the many years before gravel augmentation started and it assumes that gravel augmentation will continue to be added at the same rate as the recent past.
c- estimates of bedload transport using the bedload transport sites developed in Chapter 3, but using the idealized gravel augmentation grain size (Figure 3).

Table 12. Partial list of gravel mining in rivers downstream of dams in the Sacramento-San Joaquin river system.

River	Reach (km)	Amounts mined (M m^3)	Years	Source	comments
San Joaquin	0 to 6.4	387.4*		Cain (1997)	likely an error*
	6.4 to 14.2	1,303*		Cain (1997)	likely an error*
	18.3 to 33.4	1,875*		Cain (1997)	likely an error*
Stony Creek	Dam to I-5	0.02		Kondolf and Swanson 1993	
	I-5 to Sacto confl.	0.02 to 0.11		Kondolf and Swanson 1993	
Stanislaus	0 (Goodwin) to 40.62 (Riverbank)	0.79	1949-1999	Kondolf et al. 2001	Instream mining
	0 (Goodwin) to 40.62 (Riverbank)	4.05	1949-1999	Kondolf et al. 2001	Floodplain mining

*- the volumes reported in Cain (1997) are very high and may be due to a similar calculation error in Cain (1997) as the estimate of sediment yield rates.

Appendix A: Additional Hydrologic Analyses Results

See Chapter 3 for description of the methods.

Table A.1. Percent of total watershed impounded runoff due to main foothill dam.

River	Dam	Year built	# dams upstream		Percent of total watershed IR due to main foothill dam*	w/ res sed	w/o res sed**
			year built	2008	year built	2008	2008
Clear Creek	Whiskeytown	1963	1	1	100%	100%	100%
Stony Creek	Black Butte	1963	7	9	58%	58%	66%
Putah Creek	Monticello	1957	9	27	100%	98%	98%
Sacramento	Shasta	1945	42	73	95%	92%	94%
Feather	Oroville	1968	35	37	66%	66%	66%
Yuba	Englebright	1941	34	46	6%	5%	5%
Bear	New Camp Far West	1963	4	9	95%	57%	57%
American	Folsom	1956	31	57	94%	56%	56%
Mokelumne	Camanche	1963	14	17	50%	50%	50%
Calaveras	New Hogan	1963	7	9	99%	99%	99%
Stanislaus	New Melones	1979	21	28	93%	86%	87%
Tuolumne	New Don Pedro	1971	23	27	86%	86%	86%
Merced	New Exchequer	1967	4	4	100%	100%	100%
San Joaquin	Friant	1942	14	21	61%	45%	46%

Note: * - Total watershed impounded runoff takes into account the capacity of all the dams in the watershed upstream of the main foothill dam, as well as the foothill dam. ** - takes into account the reduction in reservoir capacity due to reservoir sedimentation, which is calculated in Chapter 4.

Table A.2. Percent of watershed upstream of main foothill dams impounded by other dams.						
River	**Dam**	**Year built**	**Number of dams upstream**		**percent upstream area impounded by foothill dam**	
			At time of completion	2008	At time of completion	2008
Clear Creek	Whiskeytown	1963	1	1	100%	100%
Stony Creek	Black Butte	1963	7	9	62%	62%
Putah Creek	Monticello	1957	9	27	97%	94%
Sacramento	Shasta	1945	42	73	27%	15%
Feather	Oroville	1968	35	37	38%	38%
Yuba	Englebright	1941	34	46	37%	25%
Bear	New Camp Far West	1963	4	9	54%	53%
American	Folsom	1956	31	57	78%	26%
Mokelumne	Camanche	1963	14	17	7%	7%
Calaveras	New Hogan	1963	7	9	98%	94%
Stanislaus	New Melones	1979	21	28	53%	37%
Tuolumne	New Don Pedro	1971	23	27	80%	80%
Merced	New Exchequer	1967	4	4	98%	98%
San Joaquin	Friant	1942	14	21	13%	13%

Table A.3. Flood frequency analysis summary for Q1 and Q1.5 flows (all flows in cms)								
			Q1			Q1.5		
River	**Dam**	**Year built**	**pre-dam**	**post-dam**	**% change**	**pre-dam**	**post-dam**	**% change**
Clear Creek	Whiskeytown	1963	39	8	-78%	161	57	-64%
Stony Creek	Black Butte	1963	15	1	-96%	150	76	-49%
Putah Creek	Monticello	1957	48	7	-85%	538	28	-95%
Sacramento	Shasta	1945	244	142	-42%	1,240	637	-49%
Feather	Oroville	1968	157	3	-98%	1,048	51	-95%
Yuba	Englebright	1941	88	12	-86%	524	202	-61%
Bear	New Camp Far West	1963	35	1	-98%	210	76	-64%
American	Folsom	1956	179	35	-80%	790	233	-70%
Mokelumne	Camanche	1963	9	5	-44%	100	37	-63%
Calaveras	New Hogan	1963	10	1	-87%	104	25	-76%
Stanislaus	New Melones	1979	11	21	84%	159	53	-67%
Tuolumne	New Don Pedro	1971	40	11	-72%	234	70	-70%
Merced	New Exchequer	1967	24	30	24%	137	87	-36%
San Joaquin	Friant	1942	74	1	-99%	286	22	-92%

Table A.4. Flood frequency analysis summary for Q20 and Q50 flows.										
River	**Dam**	Q20			Q50					
		pre-dam	**post-dam**	**%change**	**pre-dam**		**post-dam**		**%change**
Clear Creek	Whiskeytown	629	345	-45%	748	*	484		-35%
Stony Creek	Black Butte	1,206	898	-26%	1,555	*	1,070	*	-31%
Putah Creek	Monticello	2,342	405	-83%	2,682	*	838		-69%
Sacramento	Shasta	4,701	2,605	-45%	5,380	*	3,398		-37%
Feather	Oroville	5,578	4,417	-21%	7,504		10,449	*	39%
Yuba	Englebright	3,058	3,341	9%	4,021	*	5,154	*	28%
Bear	New Camp Far West	898	1,334	49%	1,085	*	1,937		79%
American	Folsom	4,304	3,455	-20%	6,201		6,626		7%
Mokelumne	Camanche	614	183	-70%	818		240		-71%
Calaveras	New Hogan	1,034	447	-57%	1,620		660	*	-59%
Stanislaus	New Melones	1,235	216	-82%	1,705		278	*	-84%
Tuolumne	New Don Pedro	1,385	558	-60%	1,954		784	*	-60%
Merced	New Exchequer	892	257	-71%	1,308		317		-76%
San Joaquin	Friant	1,489	609	-59%	1,954	*	1,201		-39%

*- flow record approaching maximum return interval.

Table A.5. Flood frequency analysis summary for Q100 flows.						
River	**Dam**	**Q100**				
		pre-dam		**post-dam**		**% change**
Clear Creek	Whiskeytown	878	*	555	*	-37%
Stony Creek	Black Butte	1,957	*	1,218	*	-38%
Putah Creek	Monticello	2,973	*	1,181	*	-60%
Sacramento	Shasta	6,173	*	3,851	*	-38%
Feather	Oroville	8,665	*	21,294	*	146%
Yuba	Englebright	4,955	*	7,192	*	45%
Bear	New Camp Far West	1,254	*	2,234	*	78%
American	Folsom	7,334	*	8,948	*	22%
Mokelumne	Camanche	932	*	269	*	-71%
Calaveras	New Hogan	1,994	*	929	*	-53%
Stanislaus	New Melones	1,996	*	343	*	-83%
Tuolumne	New Don Pedro	2,330	*	1,034	*	-56%
Merced	New Exchequer	1,574	*	345	*	-78%
San Joaquin	Friant	2,458	*	1,676	*	-32%

*- flow record approaching maximum return interval.

Figures A.1a-g. (following 4 pages) Changes in hydrologic timing of rivers downstream of the foothill dams in the Sacramento-San Joaquin river system.

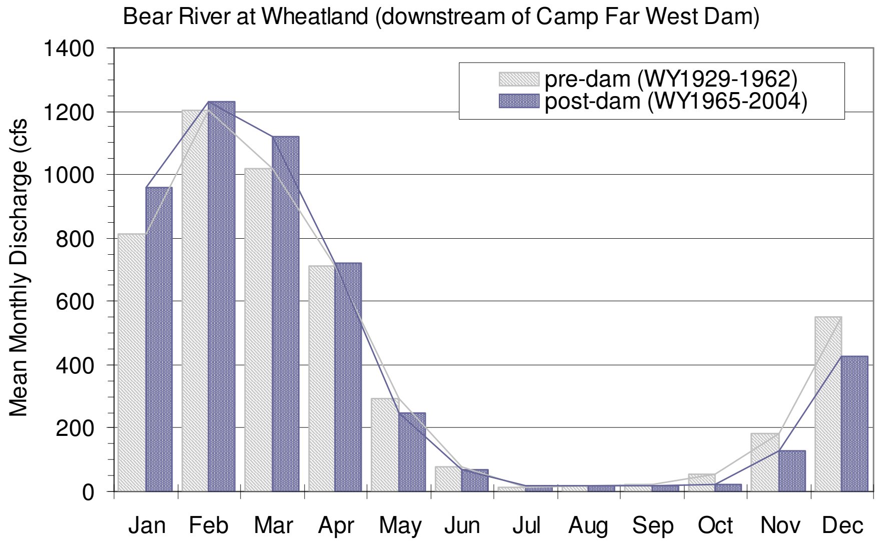

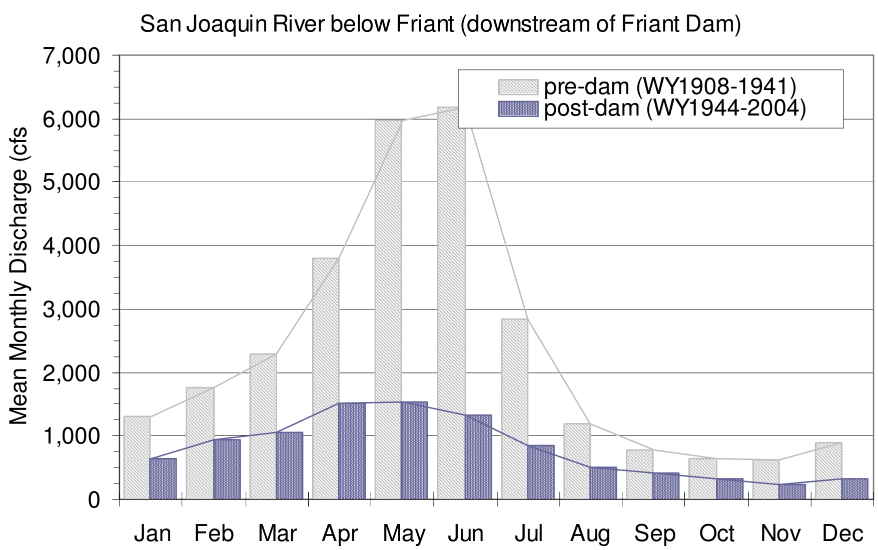

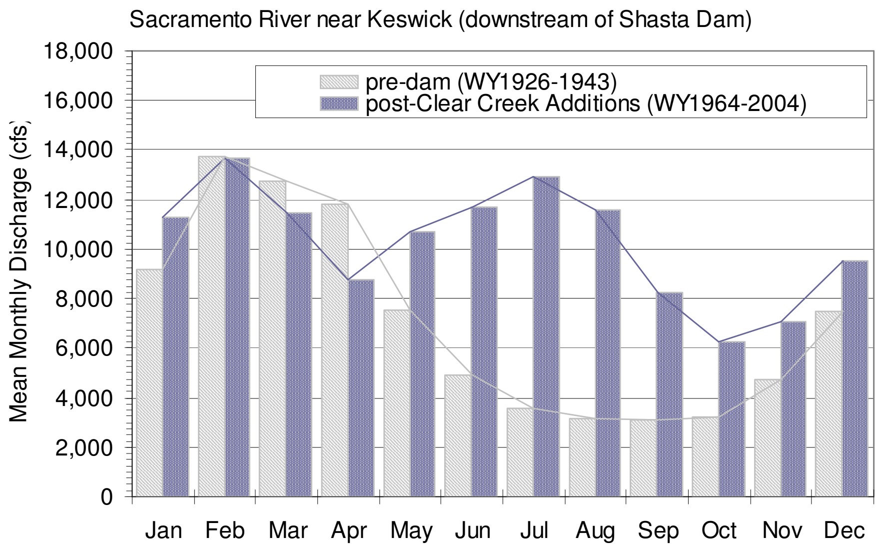
Sacramento River near Keswick (downstream of Shasta Dam)
Mean Monthly Discharge (cfs)
pre-dam (WY1926-1943)
post-Clear Creek Additions (WY1964-2004)
18,000
16,000
14,000
12,000
10,000
8,000
6,000
4,000
2,000
0
Jan Feb Mar Apr May Jun Jul Aug Sep Oct Nov Dec

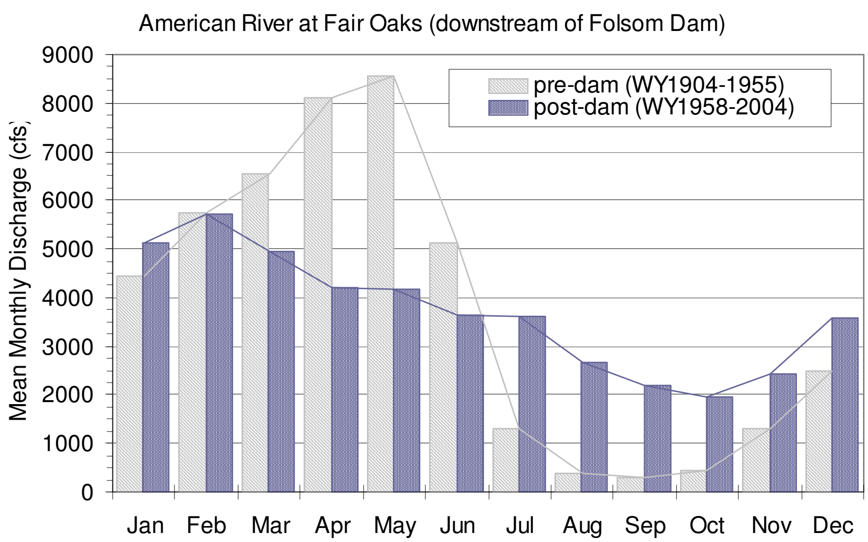
American River at Fair Oaks (downstream of Folsom Dam)
Mean Monthly Discharge (cfs)
pre-dam (WY1904-1955)
post-dam (WY1958-2004)
9000
8000
7000
6000
5000
4000
3000
2000
1000
0
Jan Feb Mar Apr May Jun Jul Aug Sep Oct Nov Dec

Clear Creek at Igo (downstream of Whiskeytown Dam)

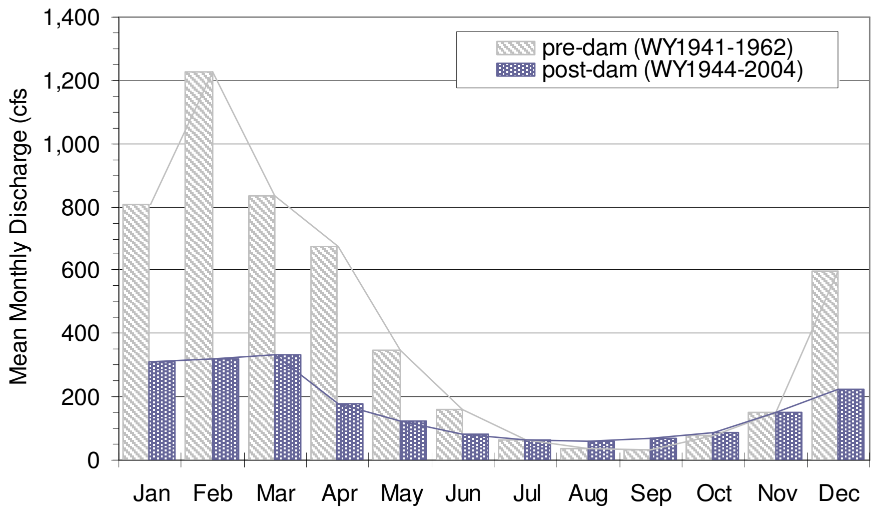

Feather River at Oroville (downstream of Oroville Dam)

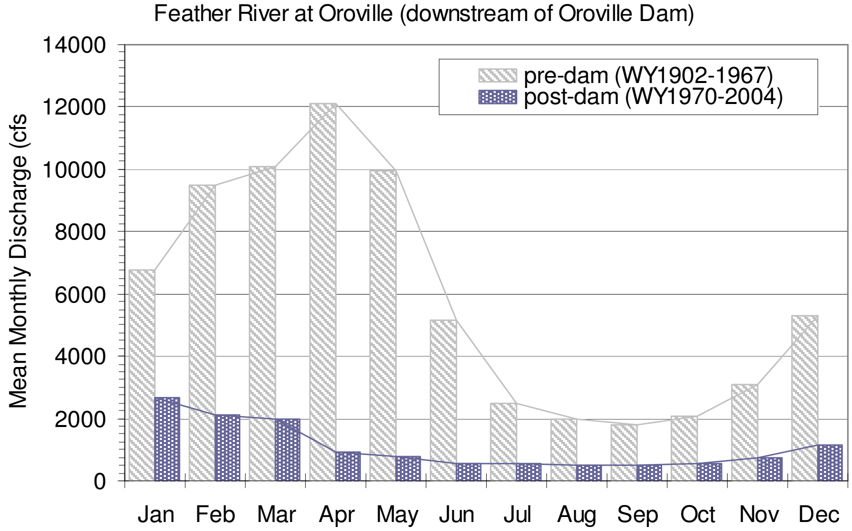

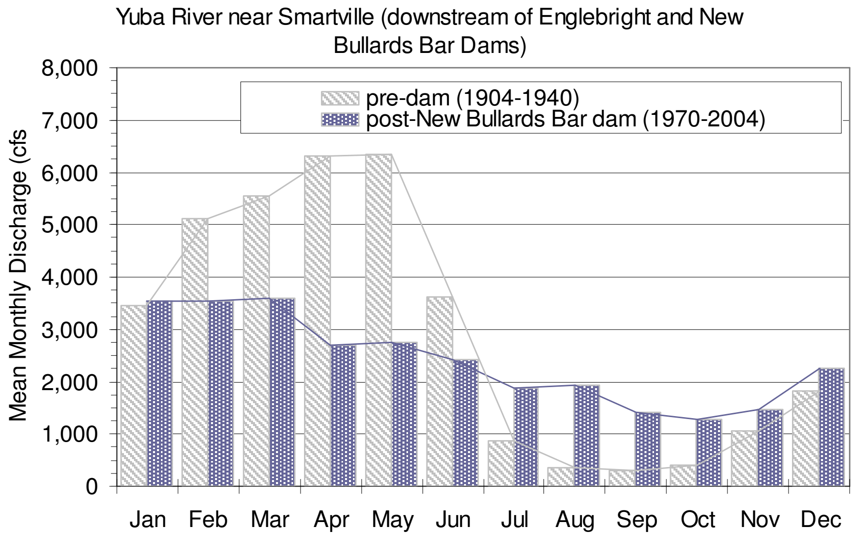

Figures A.1a-g. (preceding 4 pages) Changes in hydrologic timing of rivers downstream of the foothill dams in the Sacramento-San Joaquin river system.

Figures A.2a-ac. (following pages) Flood Frequency diagrams of Central Valley Rivers downstream of dams. Plots produced by U.S. Army Corps of Engineers software HEC-SSP.

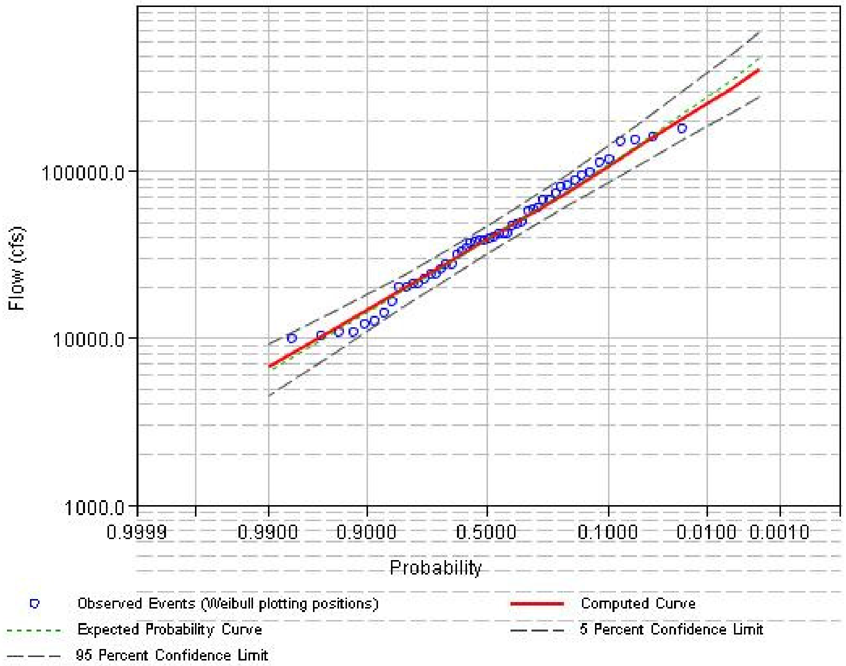

Figure A.2a. American River at Fairoaks, pre-dam conditions, USGS Gage 11-446500 (WY1905-1955)

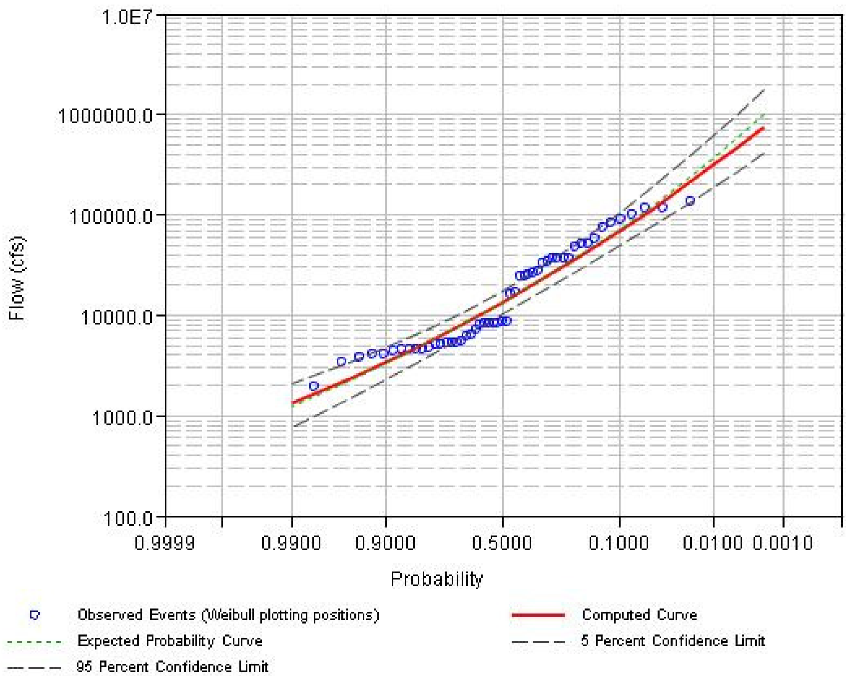

Figure A.2b. American River at Fairoaks, post-dam conditions, USGS Gage 11-446500 (WY1958-2008).

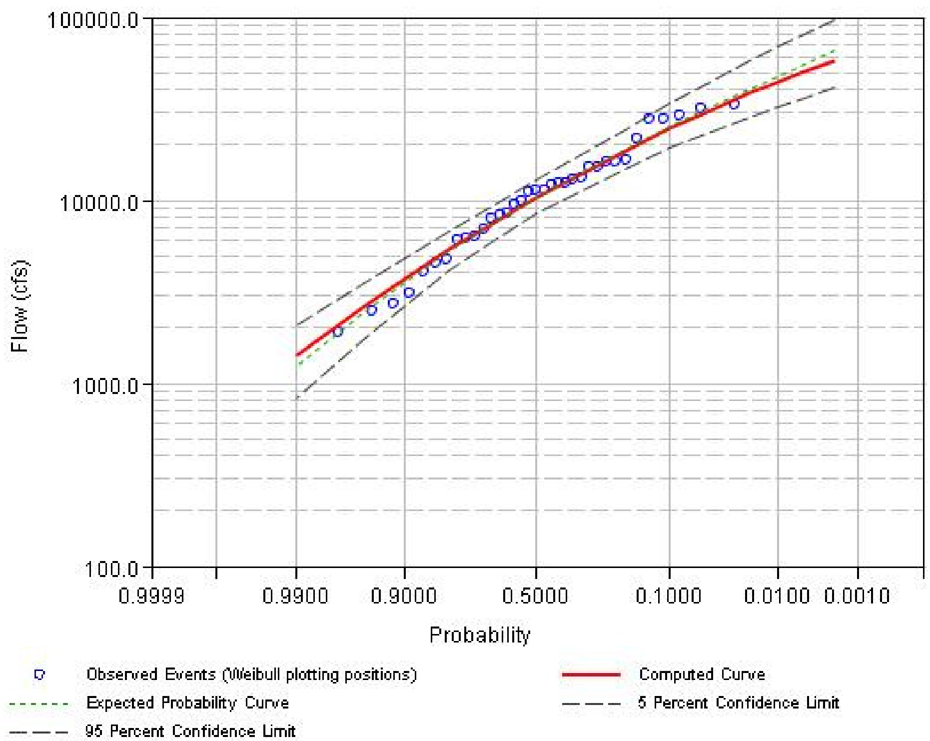

Figure A.2c. Bear River at Wheatland, pre-dam conditions, USGS Gage 11-424000 (WY1929-1962)

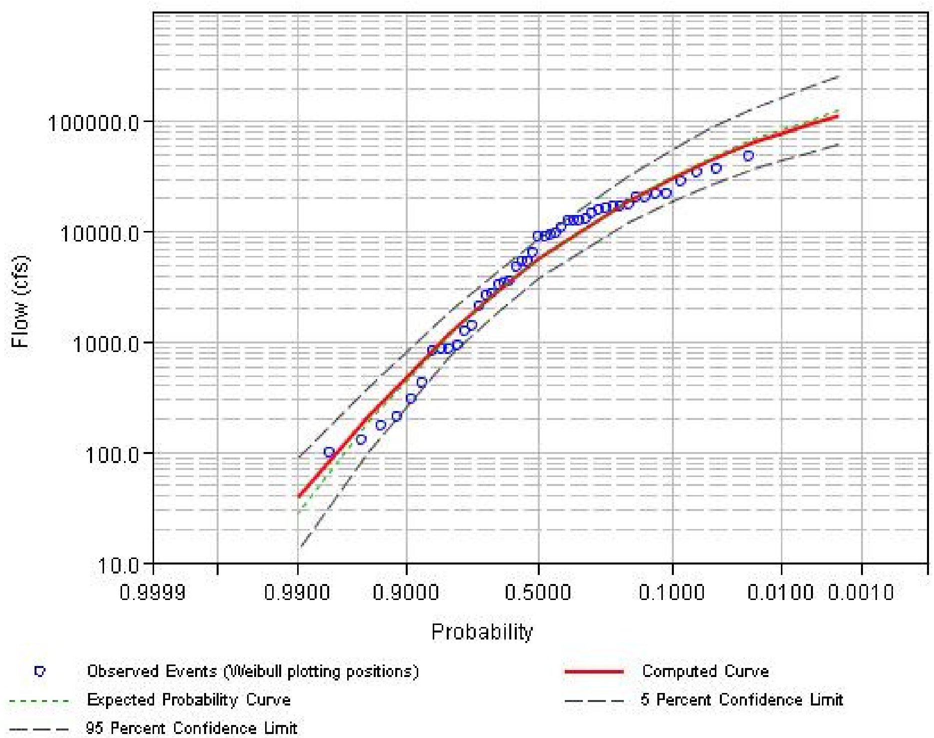

Figure A.2d. Bear River at Wheatland, post-dam conditions, USGS Gage 11-424000 (WY1965-2008)

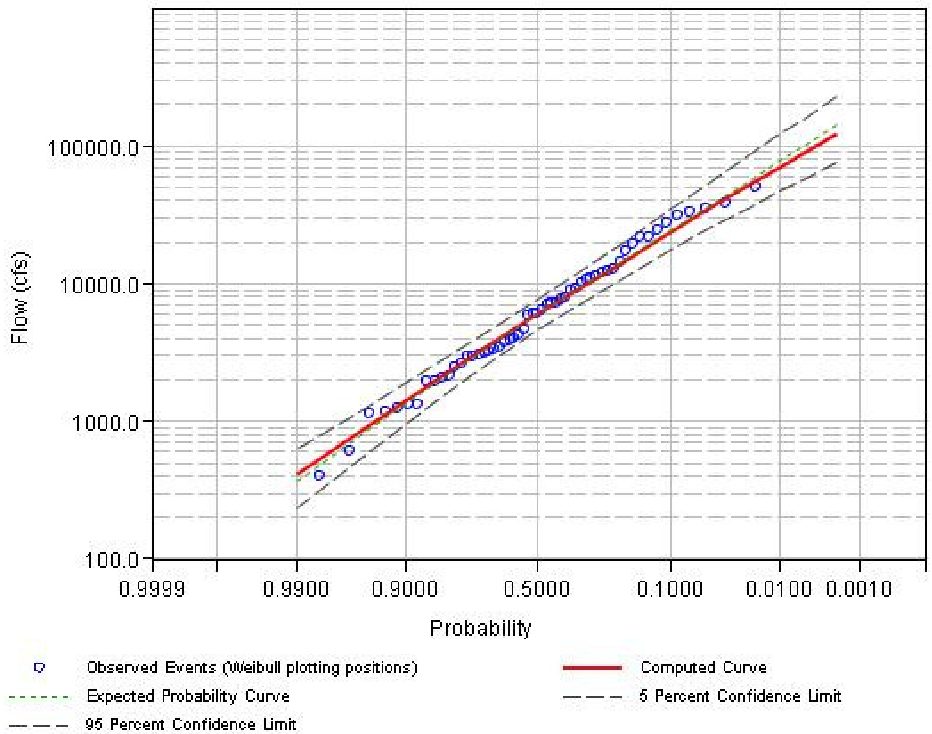

Figure A.2e. Calaveras River at Jenny Lind and below New Hogan Dam, pre-dam conditions, USGS Gages 11-309500 and 11-308900 (WY1907-1962)

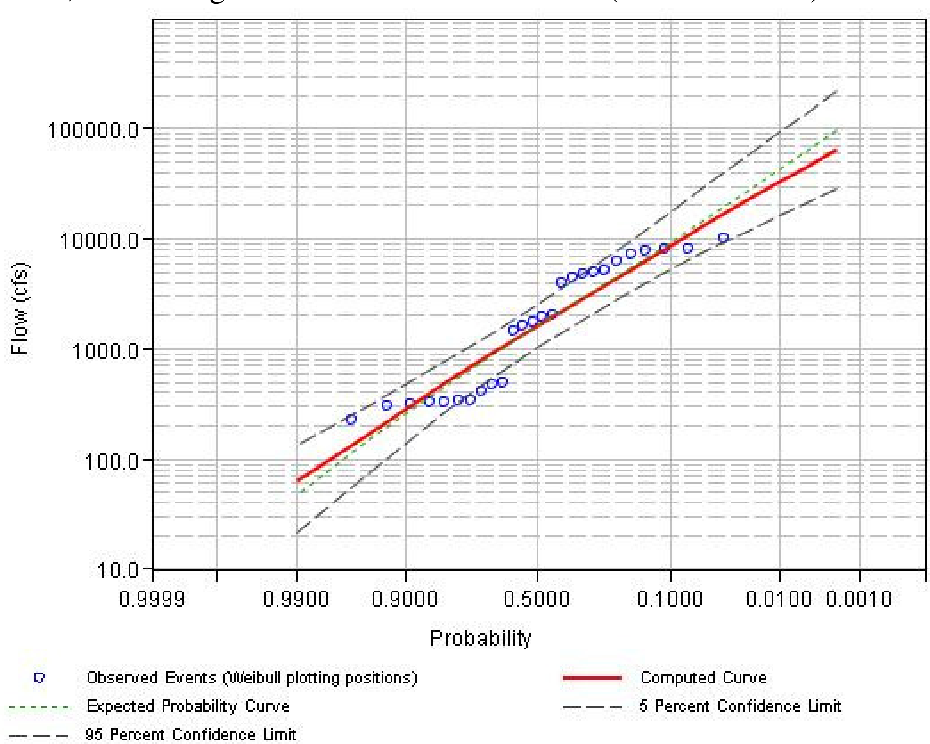

Figure A.2f. Calaveras River below New Hogan Dam, post-dam conditions, USGS Gage 11-308900 (WY1965-2008)

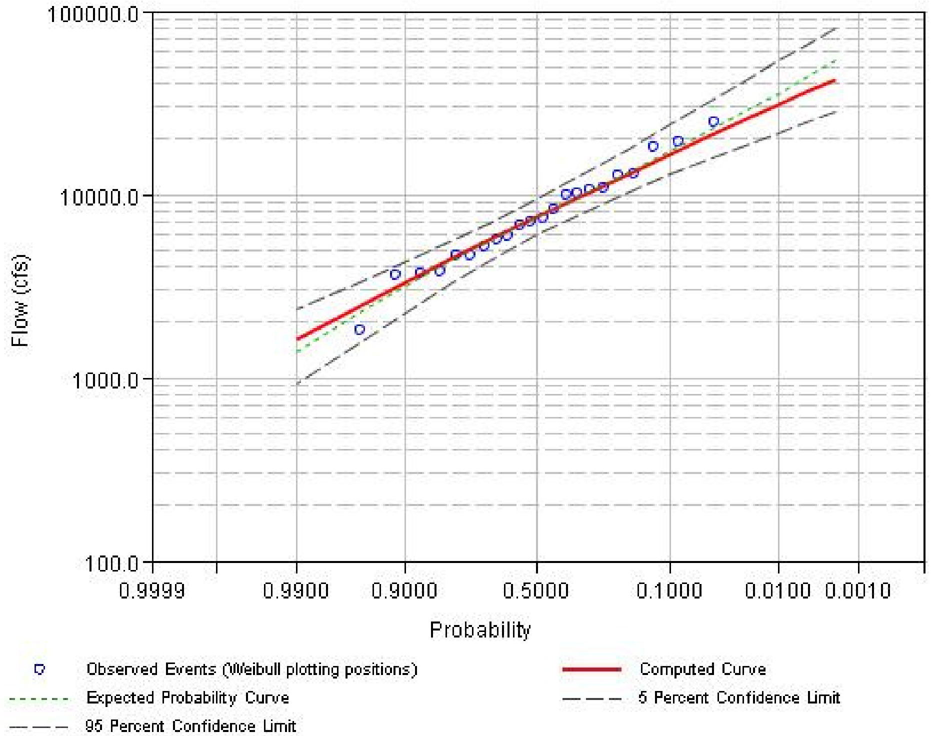

Figure A.2g. Clear Creek at Igo, pre-dam conditions, USGS Gage 11-372000 (WY1941-1962)

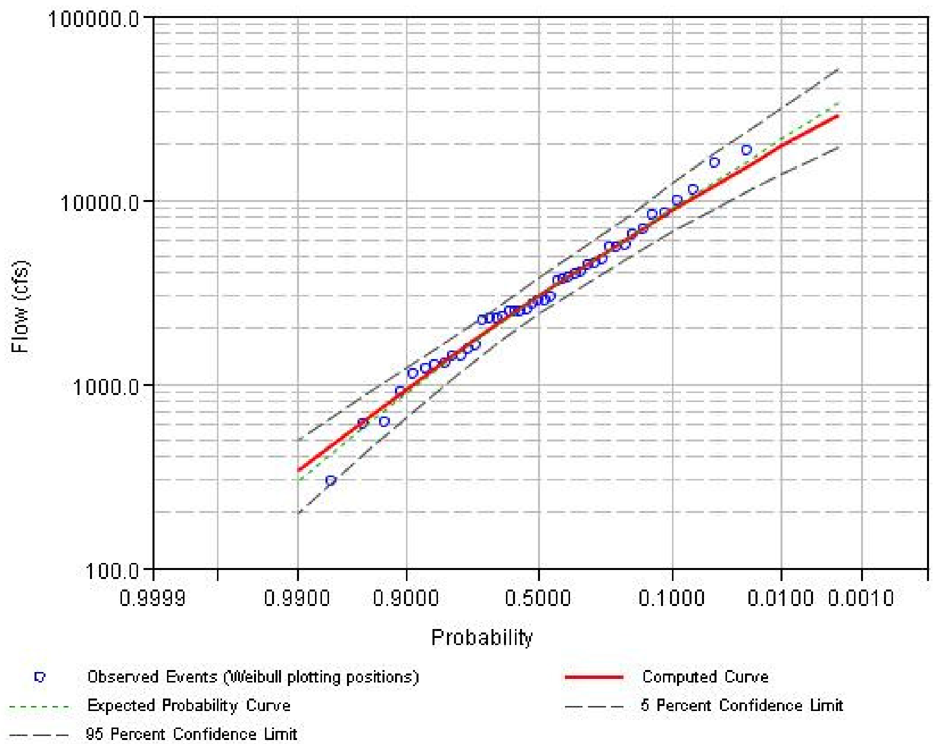

Figure A.2h. Clear Creek at Igo, post-dam conditions, USGS Gage 11-372000 (WY1965-2008)

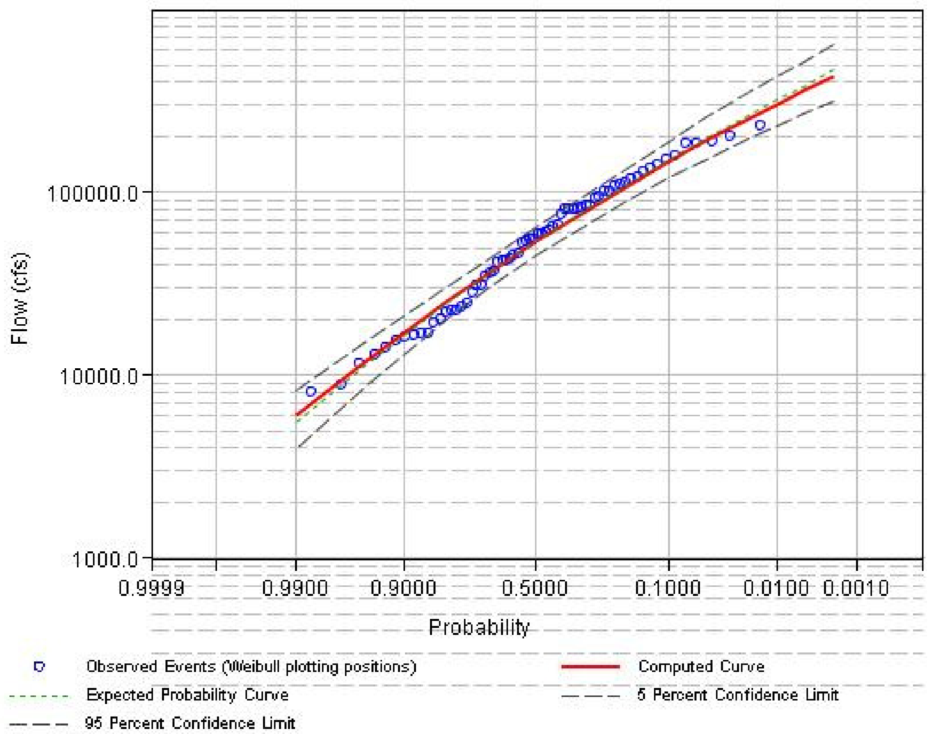

Figure A.2i. Feather River at Oroville, pre-dam conditions, USGS Gage 11-407000 (WY1902-1967)

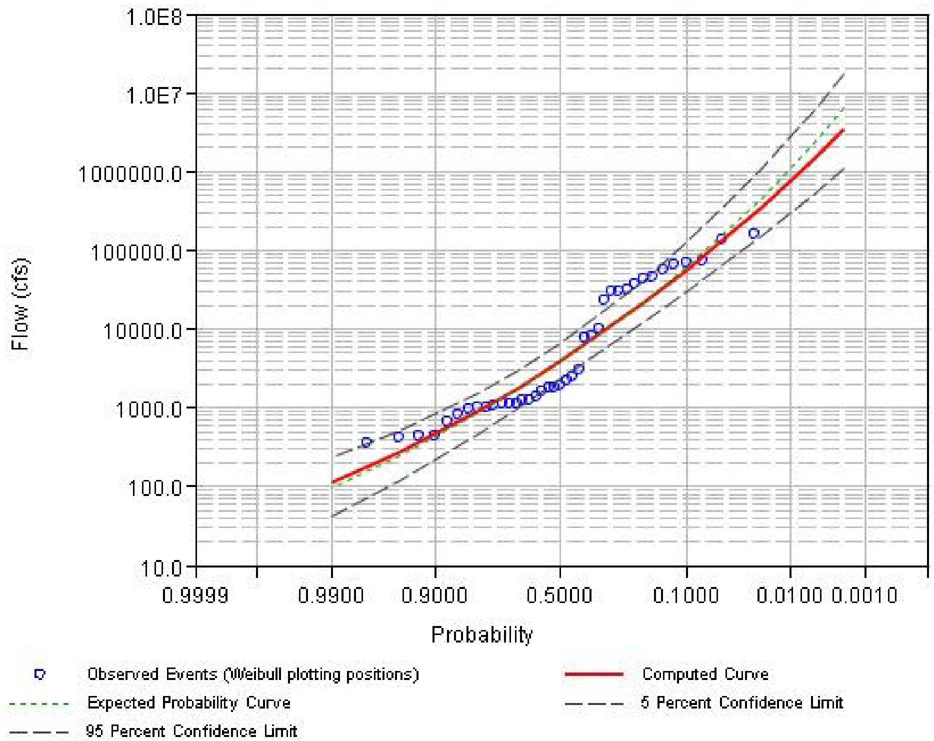

Figure A.2j. Feather River at Oroville, post-dam conditions, USGS Gage 11-407000 (WY1970-2008)

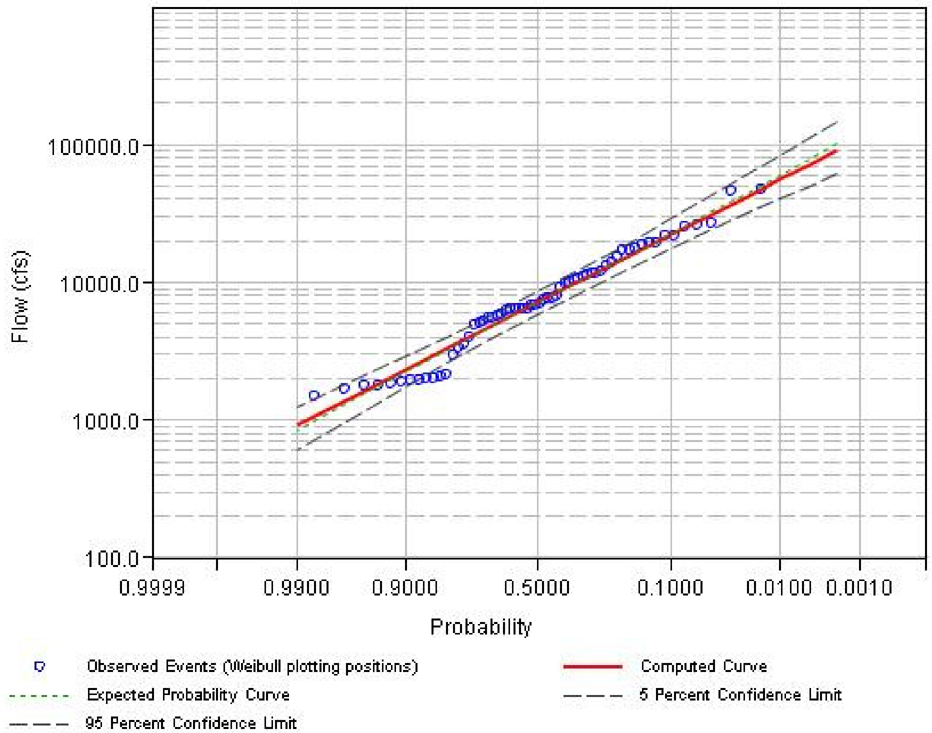

Figure A.2k. Merced River at Exchequer and below Merced Falls (combined), pre-dam conditions, USGS Gages 11-270000 and 11-270900 (WY1901-1966)

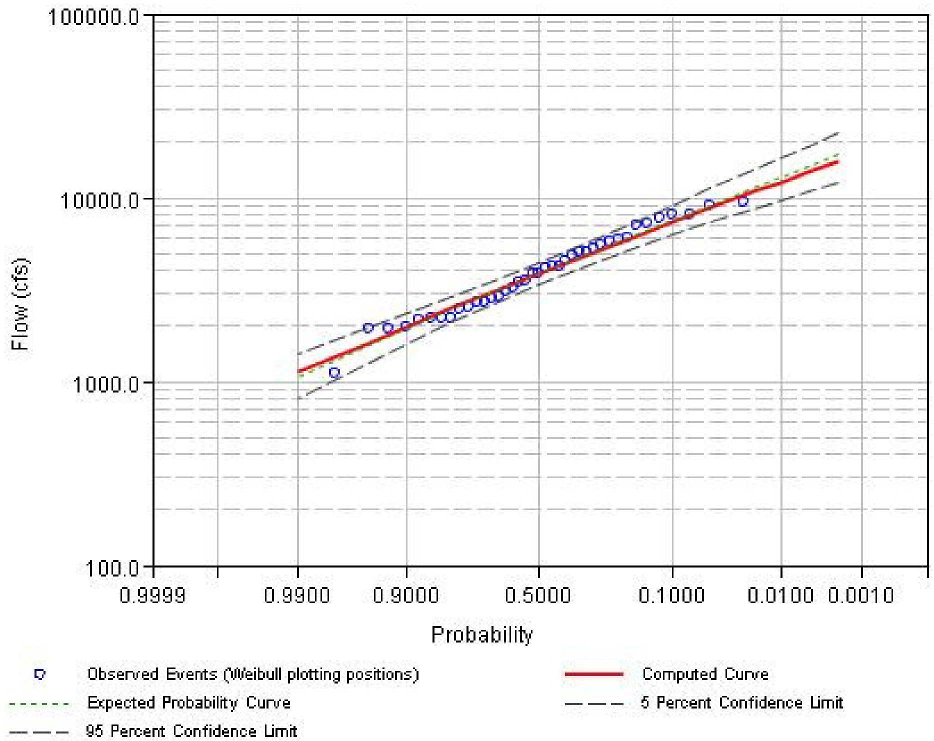

Figure A.2l. Merced River below Merced Falls, post-dam conditions, USGS Gage 11-270900 (WY1969-2008)

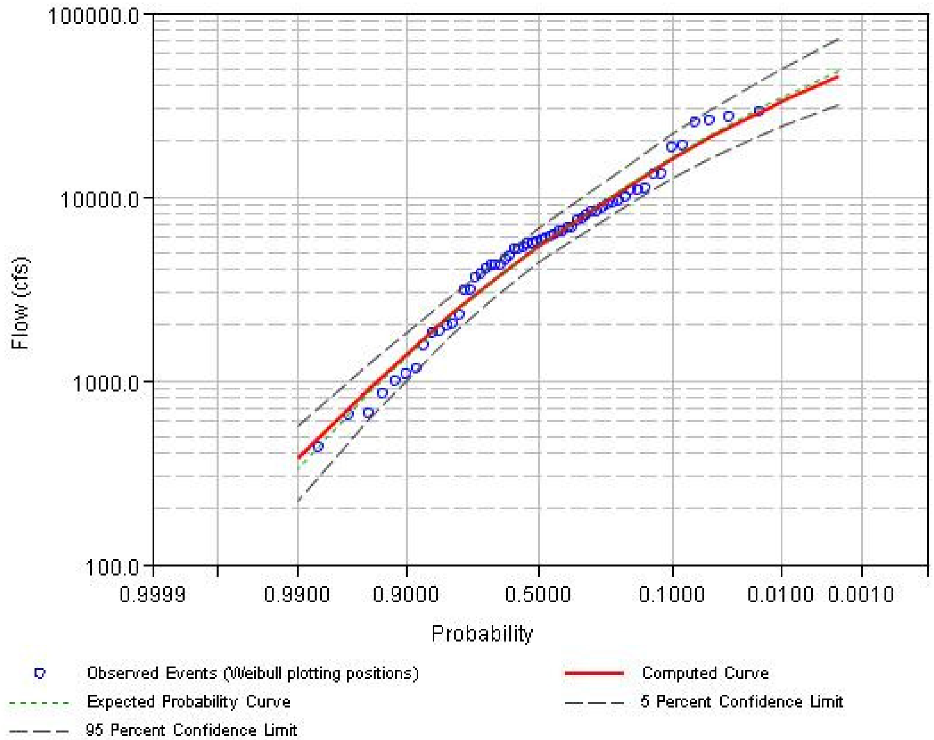

Figure A.2m. Mokelumne River below Camanche Dam, pre-dam conditions, USGS Gage 11-323500 (WY1905-1962)

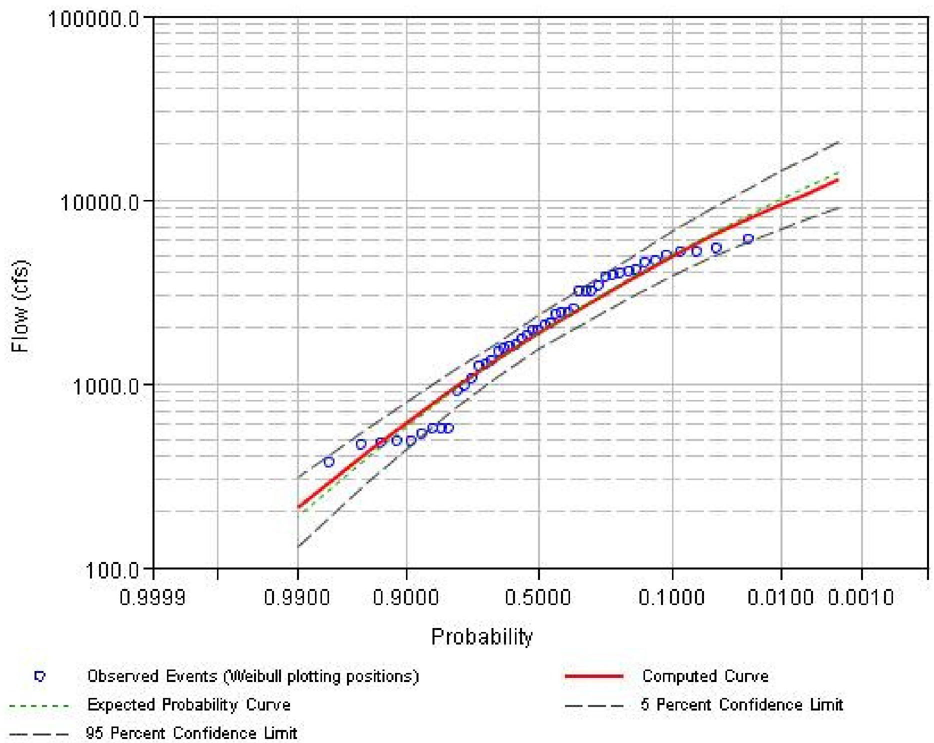

Figure A.2n. Mokelumne River below Camanche Dam, post-dam conditions, USGS Gage 11-323500 (WY1965-2008)

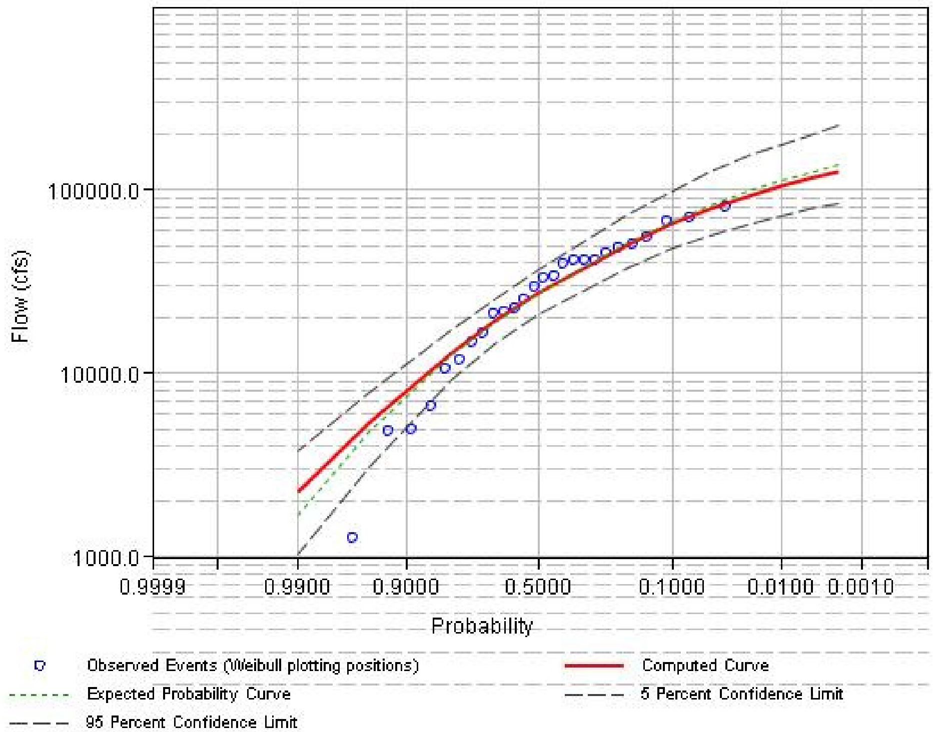

Figure A.2o. Putah Creek at Winters, pre-dam conditions, USGS Gage 11-454000 (WY1931-1956).

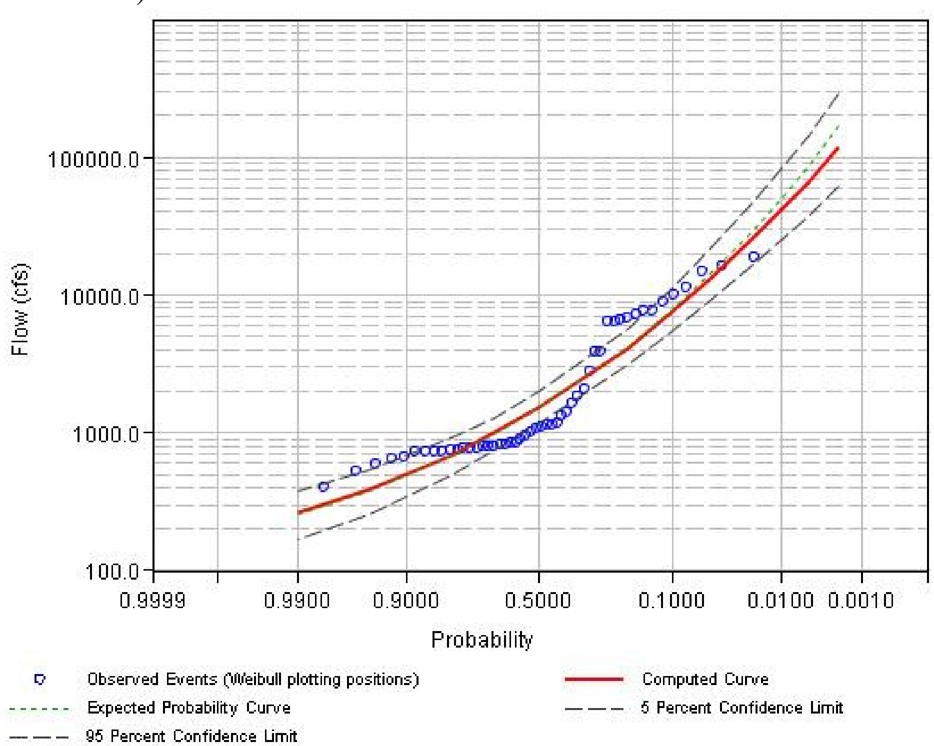

Figure A.2p. Putah Creek at Winters, post-dam conditions, USGS Gage 11-454000 (WY1959-2008)

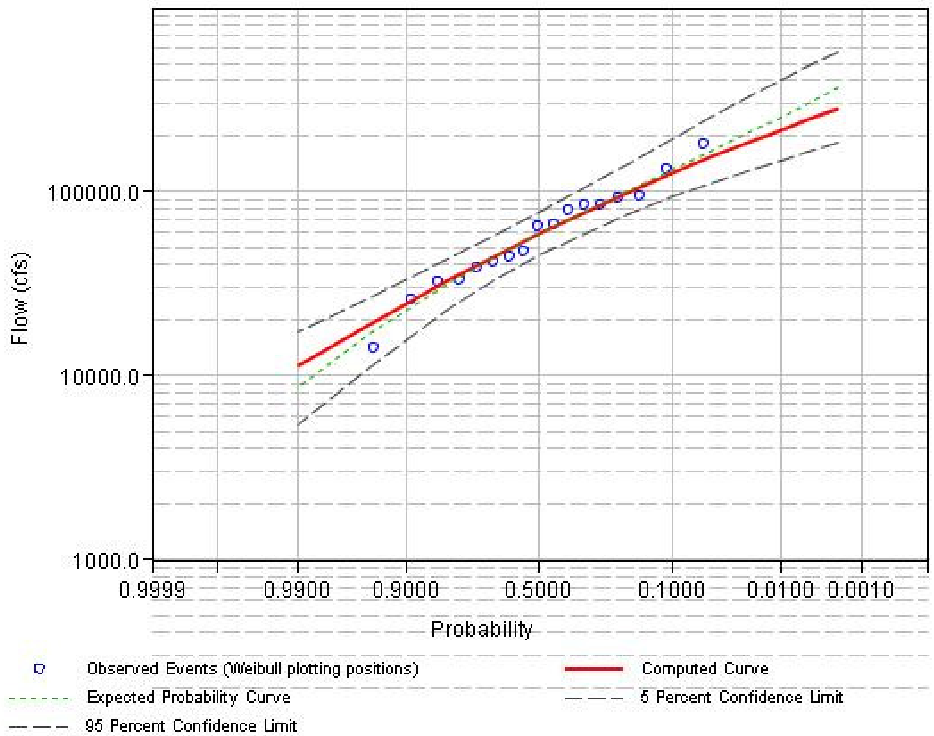

Figure A.2q. Sacramento River at Kennet and at Keswick, pre-dam conditions, USGS Gages 11-369500 and 11-370500 (WY1926-1944)

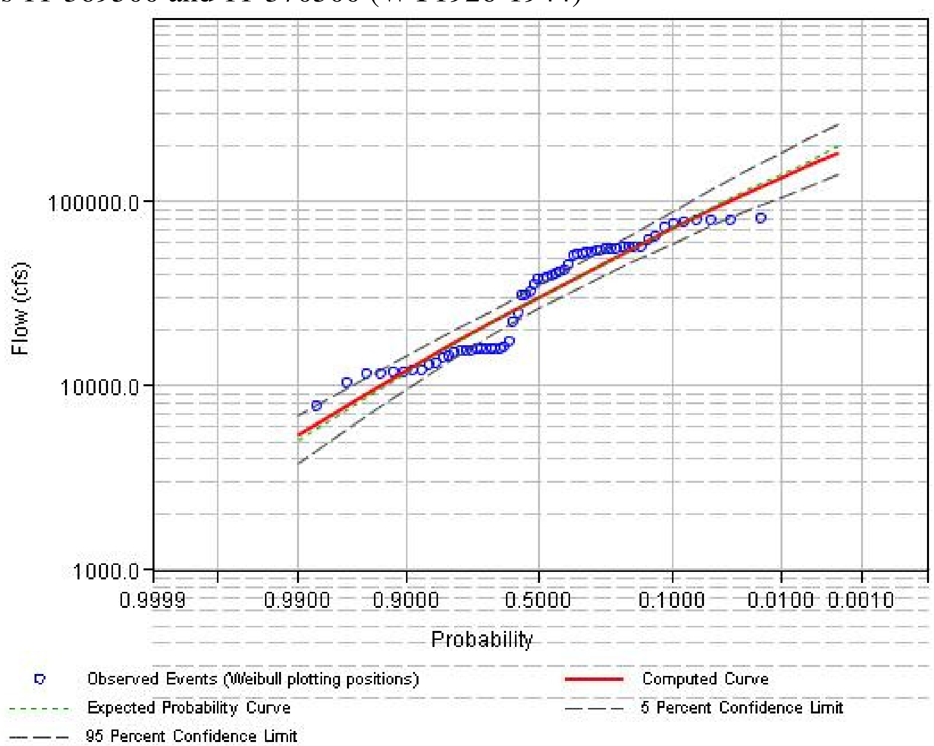

Figure A.2r. Sacramento River at Keswick, post-dam conditions, USGS Gage 11-370500 (WY1947-2008)

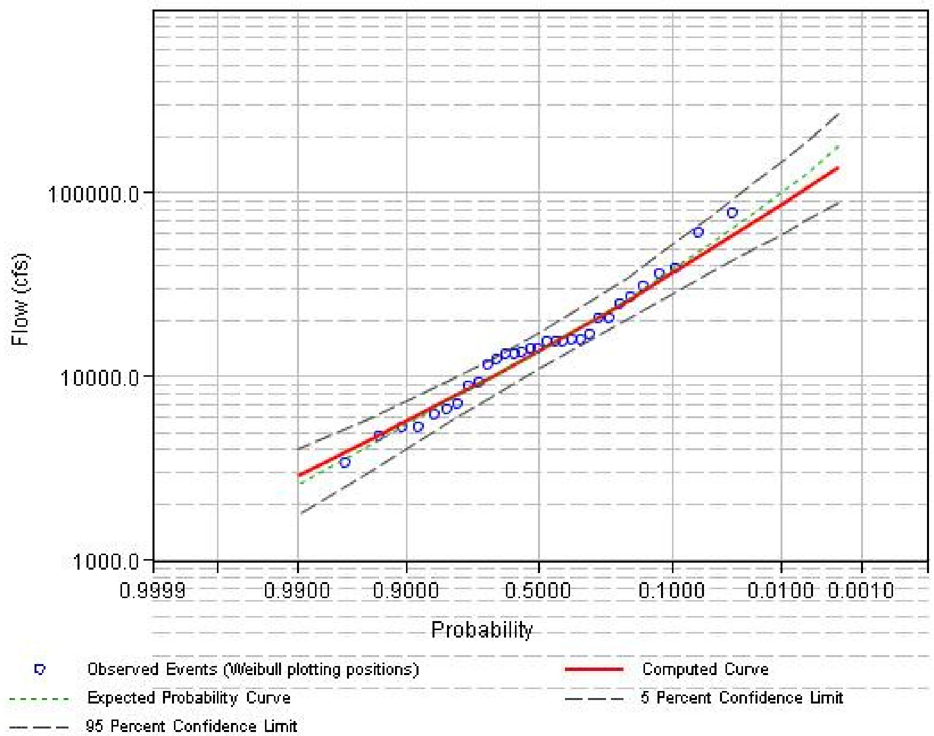

Figure A.2s. San Joaquin River below Friant, pre-dam conditions, USGS Gage 11-251000 (WY1908-1941)

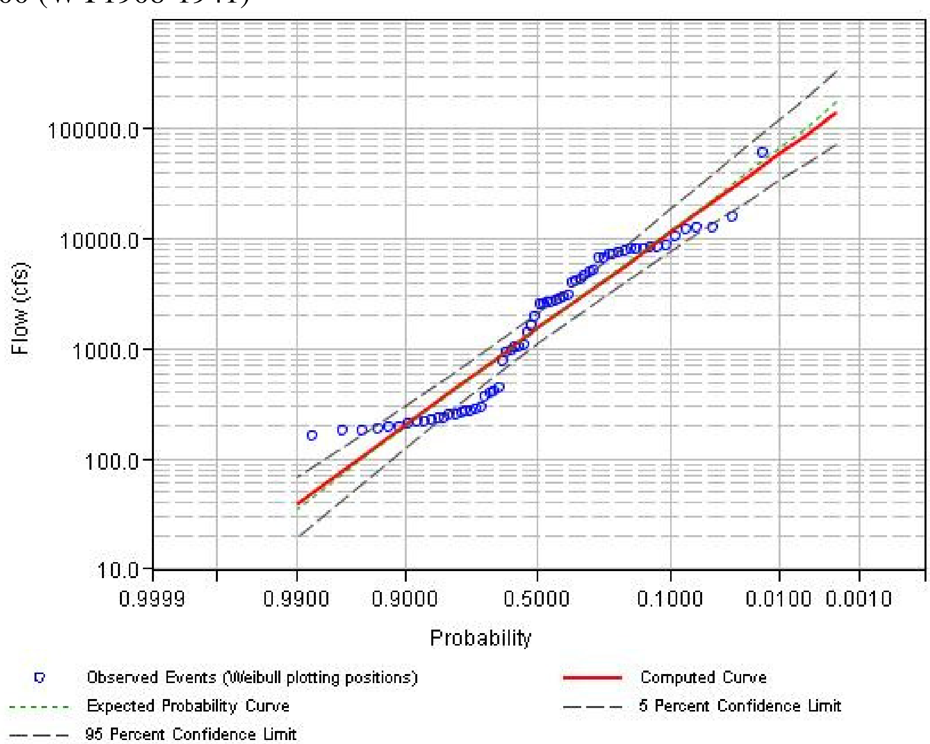

Figure A.2t. San Joaquin River below Friant, post-dam conditions, USGS Gage 11-251000 (WY1944-2008)

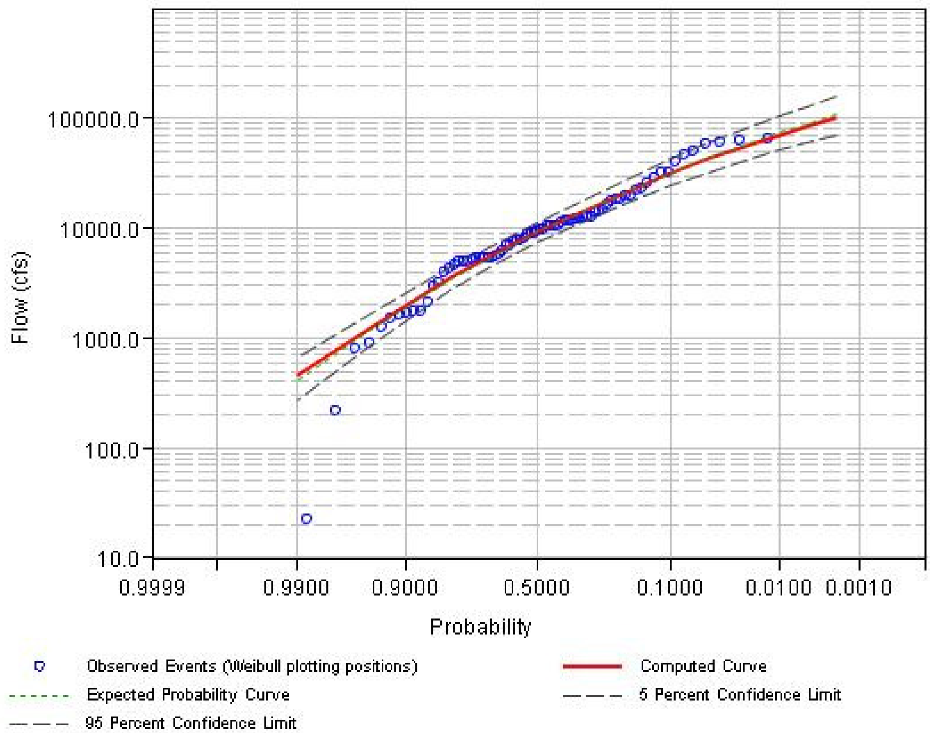

Figure A.2u. Stanislaus River near Knight's Ferry and below Goodwin, pre-dam conditions, USGS Gages 11-300000 and 11-302000 (WY1915-1978)

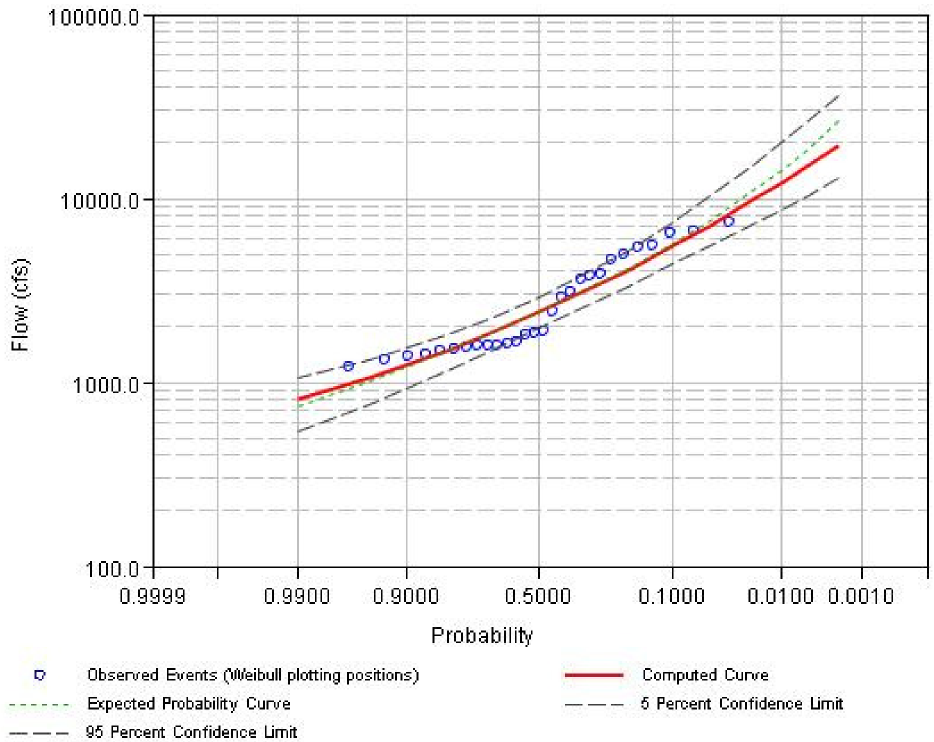

Figure A.2v. Stanislaus River below Goodwin, post-dam conditions, USGS Gage 11-302000 (WY1981-2008)

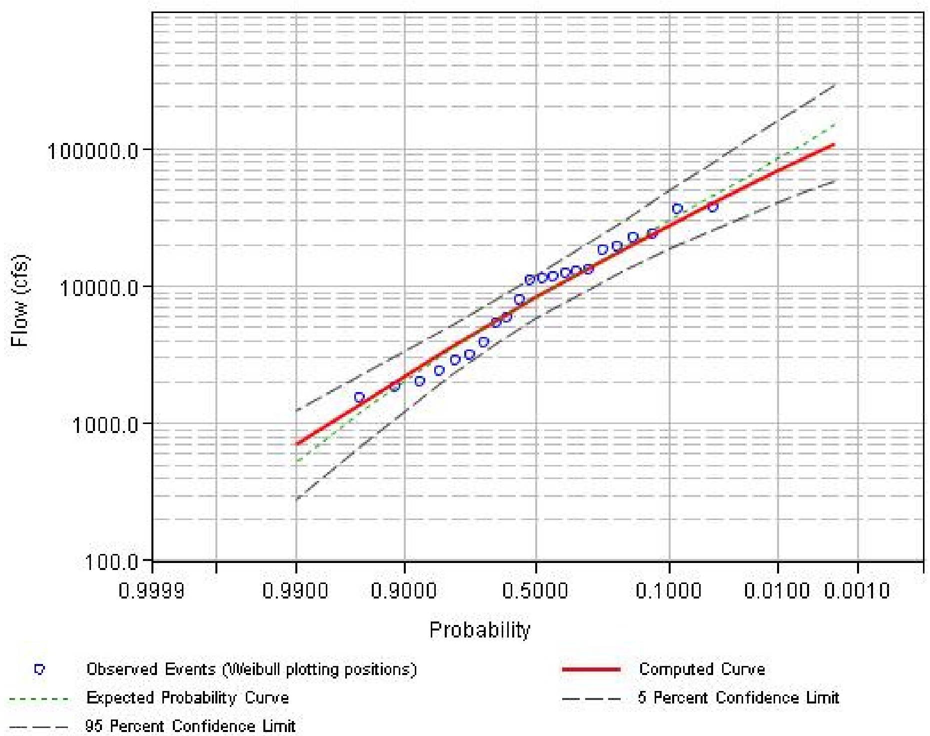

Figure A.2w. Stony Creek near Hamilton City and below Black Butte Dam, pre-dam conditions, USGS Gages 11-388500 and 11-388000 (WY1941-1962)

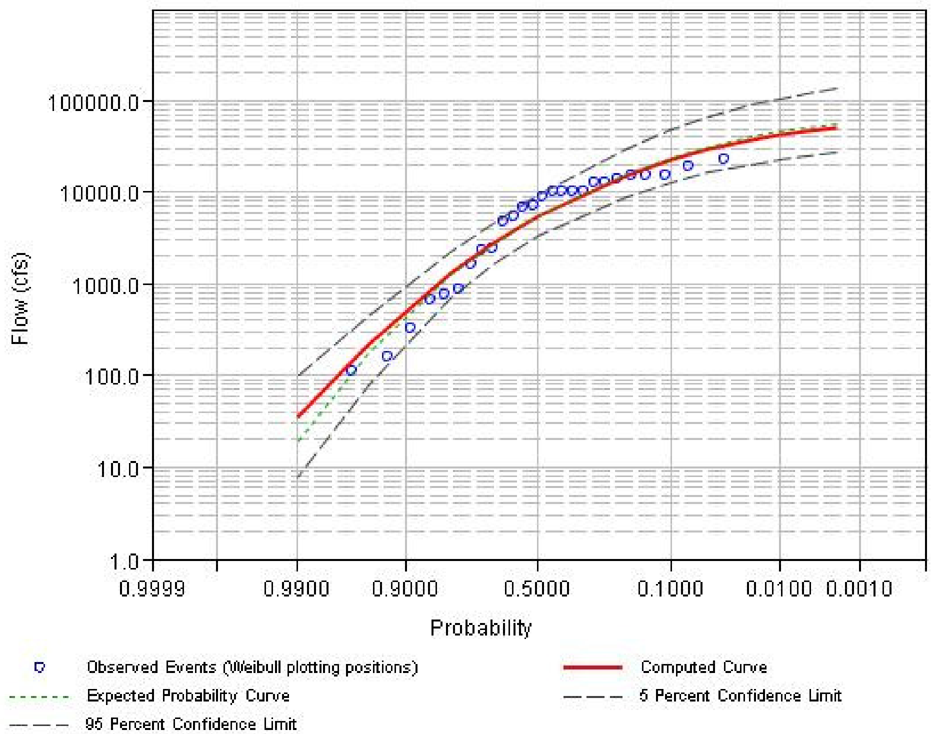

Figure A.2x. Stony Creek below Black Butte Dam, post-dam conditions, USGS Gage and 11-388000 (WY1965-2008)

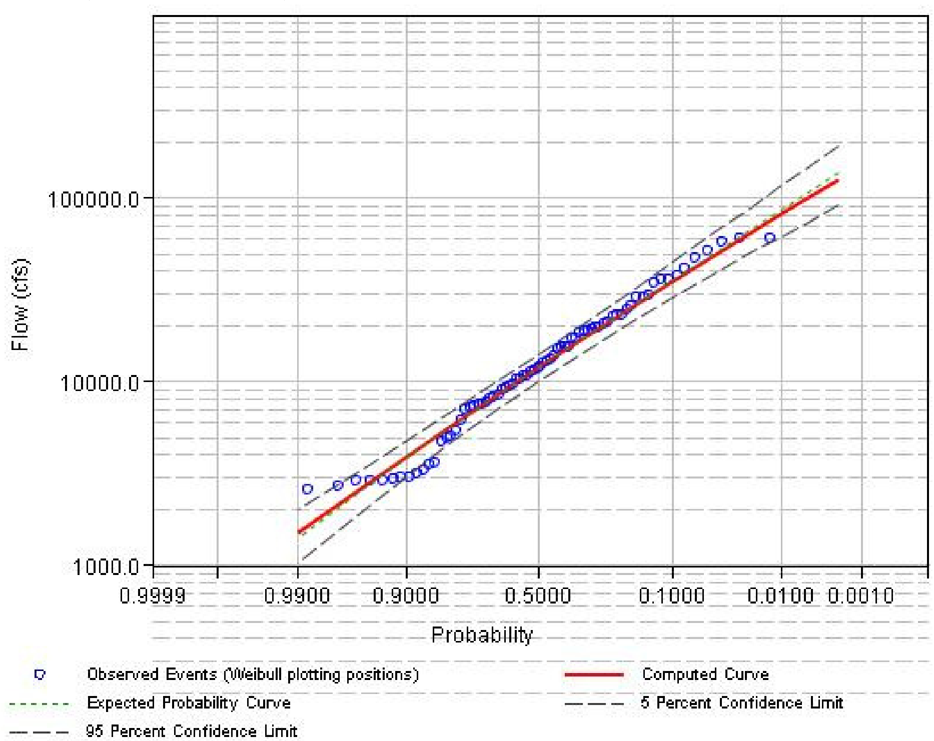

Figure A.2y. Tuolumne River above La Grange, pre-dam conditions, USGS Gage 11-288000 (WY1912-1970)

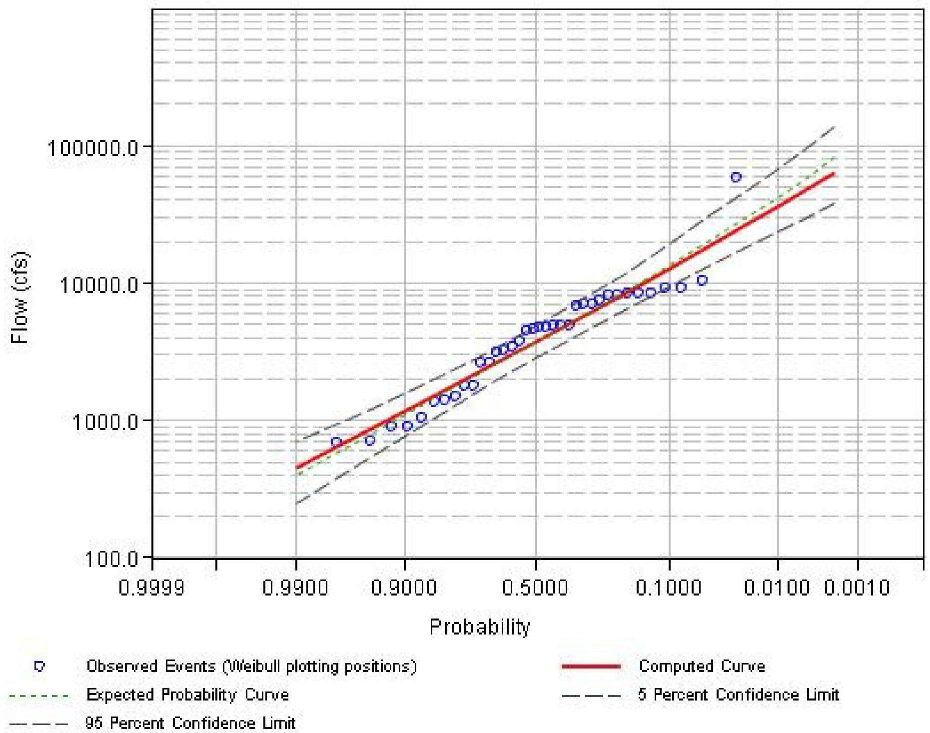

Figure A.2z. Tuolumne River below La Grange, post-dam conditions, USGS Gage 11-289650 (WY1973-2008)

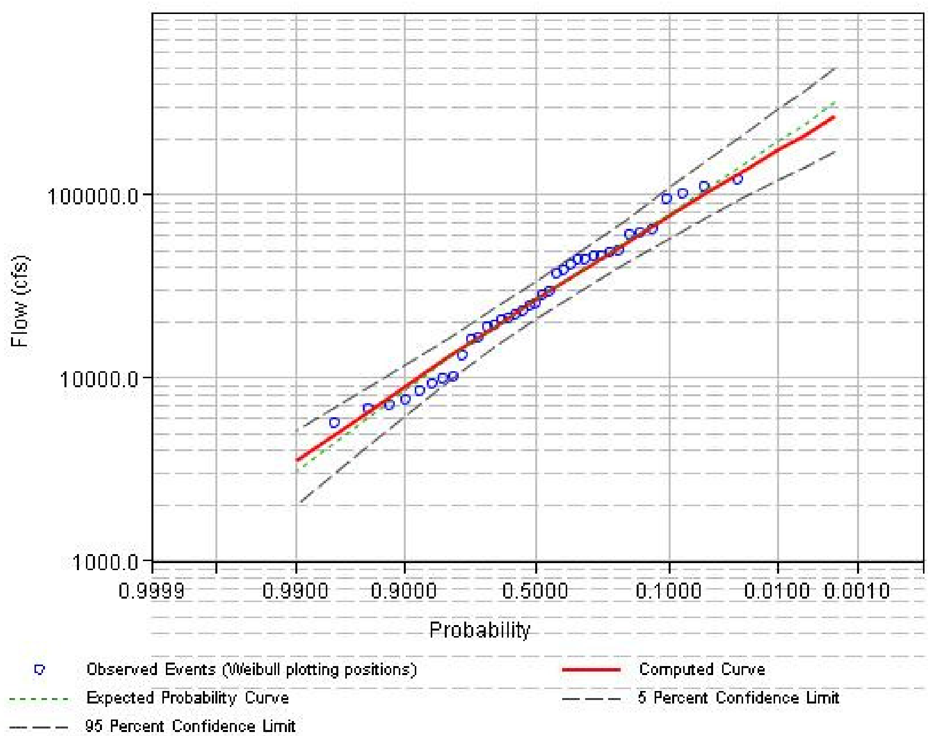

Figure A.2aa. Yuba River near Smartville, pre-dams conditions, USGS Gage 11-419000 (WY1904-1940)

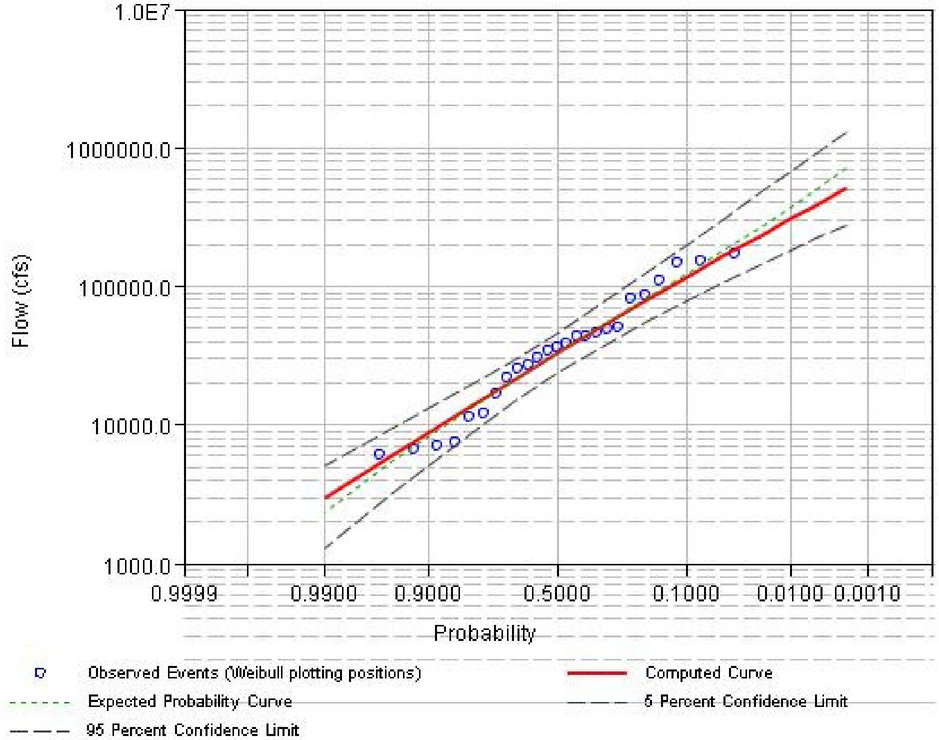

Figure A.2ab. Yuba River below Englebright, between-dams conditions, USGS Gage 11-418000 (WY1943-1967)

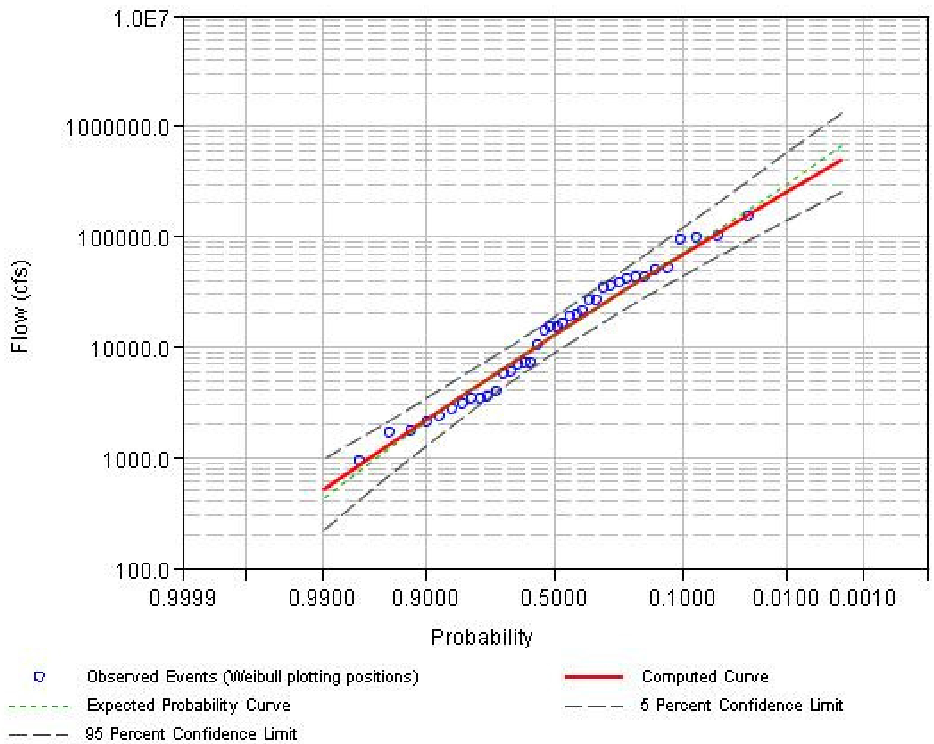

Figure A.2ac. Yuba River below Englebright, post-dams conditions, USGS Gage 11-418000 (WY1970-2008).

Appendix B: Bedload Transport Calculation Sites

See Chapter 3, Table 3 for source and reference information. The combination of the information from Chapter 3, Table 3 and this appendix will allow for a complete calculation of bedload transport if combined with flow from the gages listed in Chapter 3, Table 2.

Table B.1. Background data for Putah Creek bedload transport calculation site, PC1	
Site Name	PC1
Location	10.5 km downstream of Monticello Dam, 0.3 km downstream of Putah Diversion Dam
Gravel tracer?	yes, WY2006
Roughness, n	0.0365 (Manning-Gauckler n)
Floodplain, n	0.1
Floodplain extent (using cross section stationing)	<96 m, >109 m

Table B.2. Grain Size Distribution. See Chapter 3, Table 3 for the data source. Excluding 2mm grains.				
Size (mm)	**% Finer**		**Grain Size Statistics**	
180	100		**Geometric mean (mm)**	18.93
128	99		**Geometric standard deviation**	2.88
90	94		**D10 (mm)**	3.56
64	84		**D16 (mm)**	6.39
45	77		**D25 (mm)**	9.51
32	67		**D50 (mm)**	19.32
22.6	55		**D65 (mm)**	30.2
16	44		**D75 (mm)**	42.03
11.3	30		**D84 (mm)**	64
8	20		**D90 (mm)**	78.53
5.1	12			
4	12			
2	0			

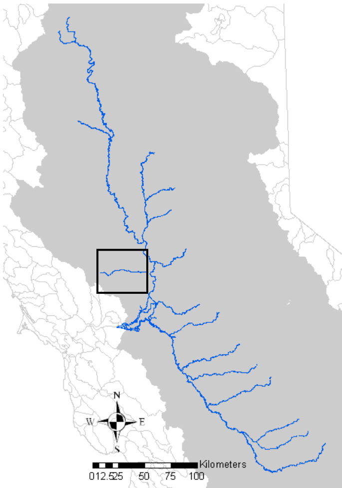

a

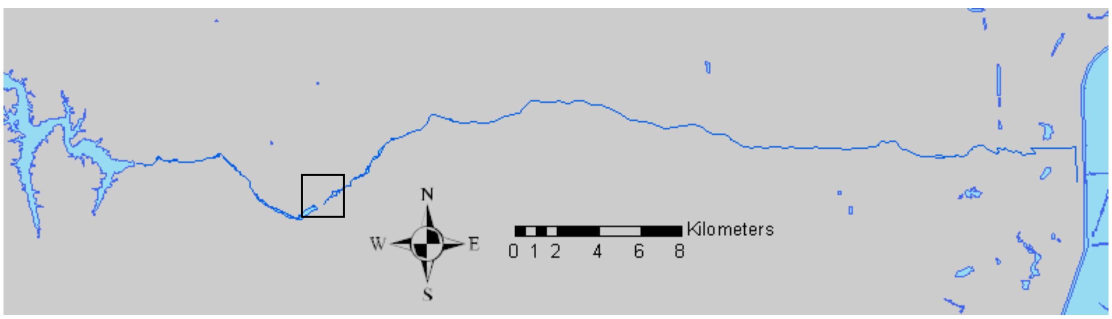

b

c

Figure B.1a-c. Location of Putah Creek site PC1. Figure B.1a is the location of the site in the Sacramento-San Joaquin river system, with the box showing the location of Figure B.1b. Figure B.1b is a reach-scale map from Monitcello Dam down to the confluence with the Yolo Bypass, flow is left to right, with a box showing the location of figure B.1c. Figure B.1c is a recent aerial photograph, with the cross section line overlaid in white and Putah Diversion Dam on the lower left..

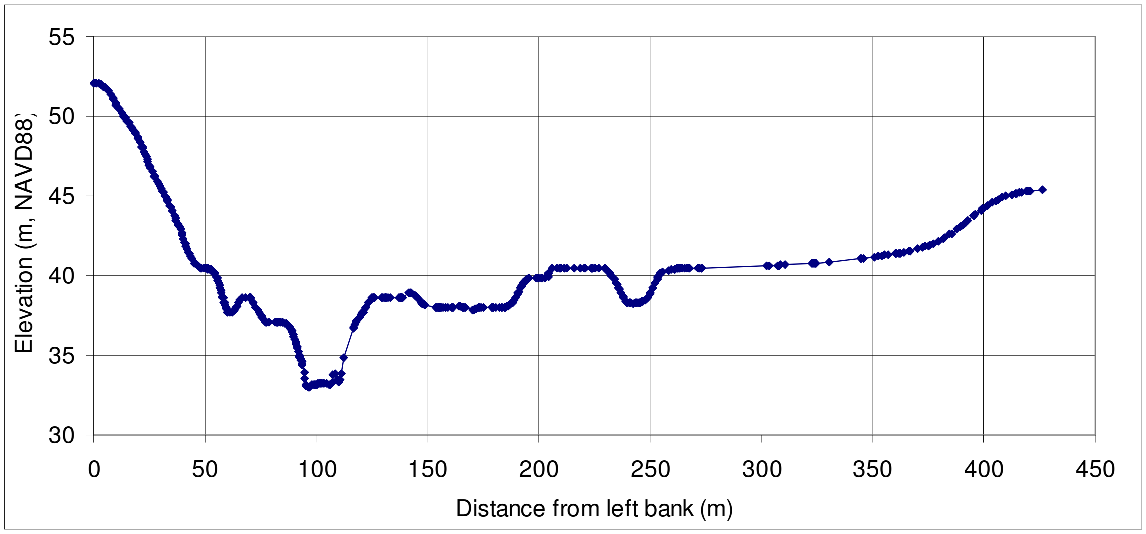

Figure B.2. Putah Creek PC1 cross section.

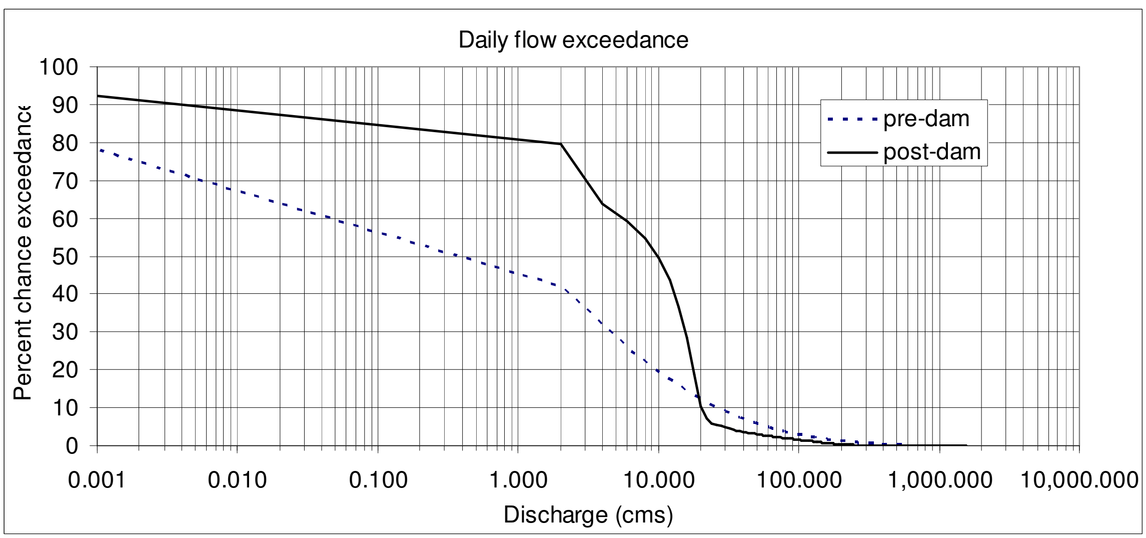

Figure B.3. Putah Creek flow exceedance, see Chapter 3, Table 2 for a list of the gages used and the dates of the pre- and post-dam periods.

Table B.3. Background data for Stony Creek bedload transport calculation site, SC1a,b	
Site Name	SC1a,b
Location	3.87 km downstream of Black Butte Dam
Gravel tracer?	yes, WY2006
Roughness, n	0.0365 (Manning-Gauckler n)
Floodplain, n	0.1
Floodplain extent (using cross section stationing)	<293 m, >336 m

Table B.4. Grain Size Distribution. See Chapter 3, Table 3 for the data source. Excluding 2mm grains.				
Size (mm)	**% Finer**		**Grain Size Statistics**	
256	100		**Geometric mean (mm)**	32.55
180	97		**Geometric standard deviation**	3.53
128	92		**D10 (mm)**	3.17
90	76		**D16 (mm)**	8
64	65		**D25 (mm)**	17.38
45	48		**D50 (mm)**	46.9
32	41		**D65 (mm)**	64
22.3	31		**D75 (mm)**	87.25
16	23		**D84 (mm)**	107.33
11.6	18		**D90 (mm)**	122.49
8	16			
5.6	15			
4	15			
2	0			

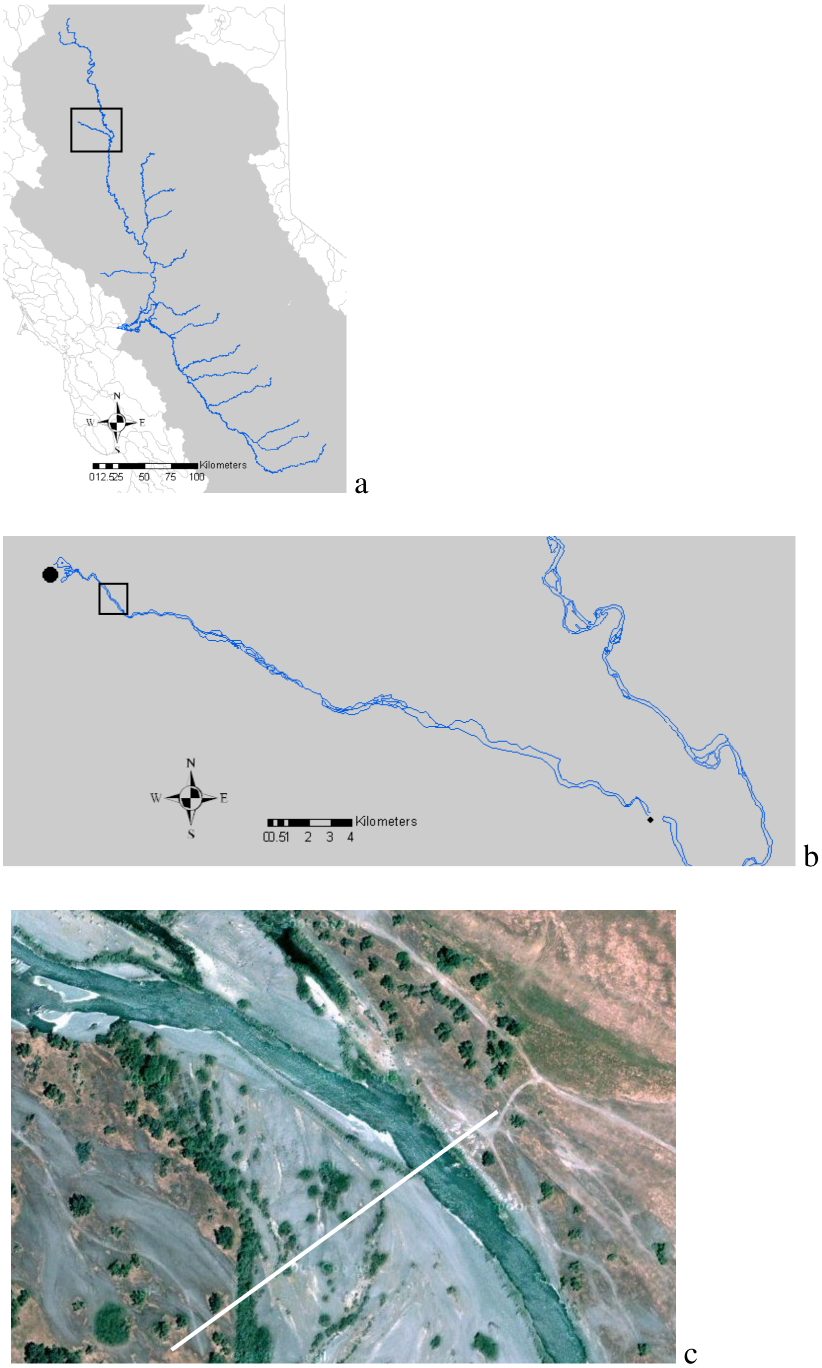

Figure B.4a-c. Location of Stony Creek site SC1a,b. Figure B.1a is the location of the site in the Sacramento-San Joaquin river system, with the box showing the location of Figure B.1b. Figure B.1b is a reach-scale map from Black Butte Dam down to the confluence with the Sacramento River, flow is left to right, with a box showing the location of figure B.1c. Figure B.1c is a recent aerial photograph, with the cross section line overlaid in white, and post-dates the WY2006 flood, hence, the non-vegetated region is larger than used in the floodplain estimations.

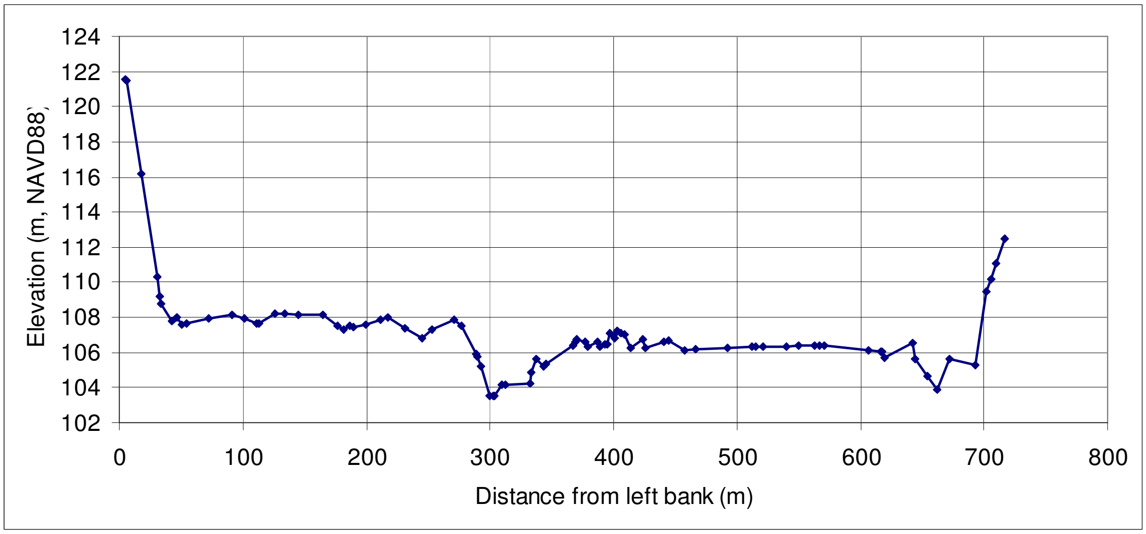

Figure B.5. Stony Creek SC1a cross section.

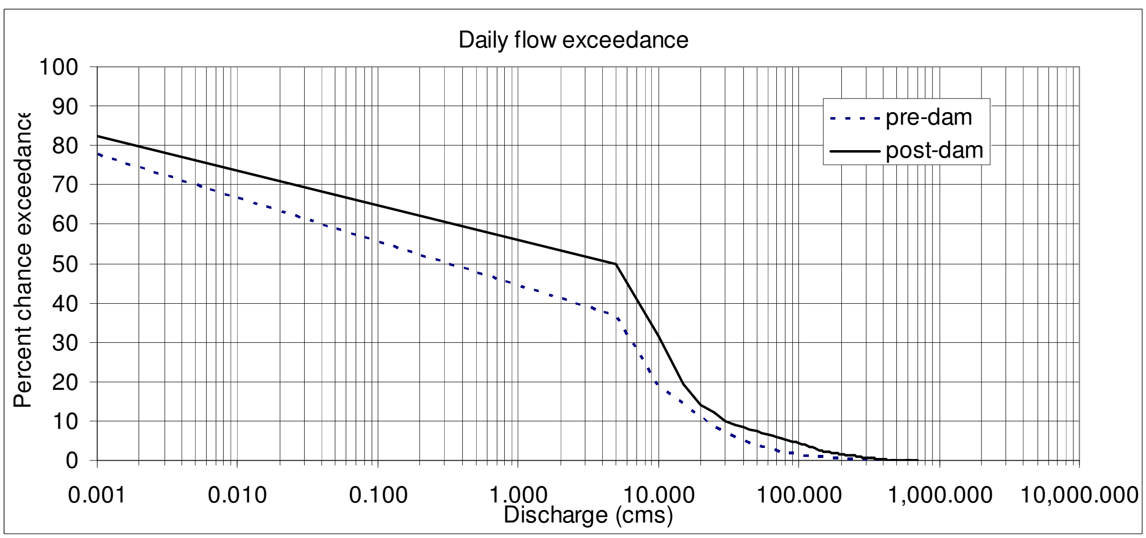

Figure B.6. Stony Creek flow exceedance, see Chapter 3, Table 2 for a list of the gages used and the dates of the pre- and post-dam periods.

Table B.5. Background data for Clear Creek bedload transport calculation site, Peltier XS 891+80	
Site Name	Peltier XS 891+80
Location	1.67 km downstream of Whiskeytown Dam
Gravel tracer?	no
Roughness, n	0.0365 (Manning-Gauckler n)
Floodplain, n	0.1
Floodplain extent (using cross section stationing)	<13 m, >34.5 m

Table B.6. Grain Size Distribution. See Chapter 3, Table 3 for the data source. Excluding 2mm grains.				
Size (mm)	**% Finer**		**Grain Size Statistics**	
512	100		**Geometric mean (mm)**	117.59
360	97.86		**Geometric standard deviation**	2.14
256	84.12		**D10 (mm)**	42.48
180	62.27		**D16 (mm)**	52.43
128	51.47		**D25 (mm)**	67.97
90	35.41		**D50 (mm)**	123.95
64	22.77		**D65 (mm)**	188.1
45	10.81		**D75 (mm)**	221
32	6.03		**D84 (mm)**	255.51
22.6	2.04		**D90 (mm)**	296.23
16	1.02			
11.3	0			
8	0			
5.6	0			

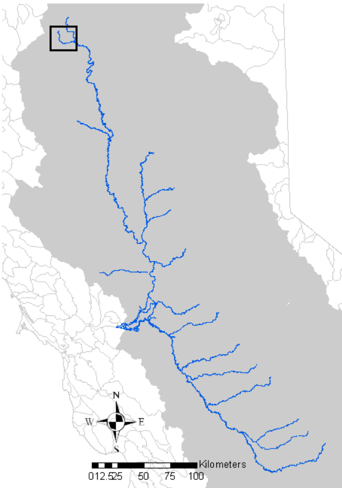

a

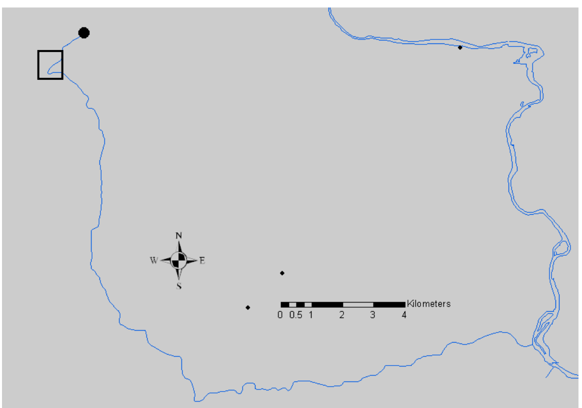

b

c

Figure B.7a-c. Location of Clear Creek Peltier 891+80 site. Figure B.1a is the location of the site in the Sacramento-San Joaquin river system, with the box showing the location of Figure B.1b. Figure B.1b is a reach-scale map from Whiskeytown Dam down to the confluence with the Sacramento, flow is top to bottom, with a box showing the location of figure B.1c. Figure B.1c is a recent aerial photograph, with the cross section line overlaid in white, and the Peltier Bridge downstream.

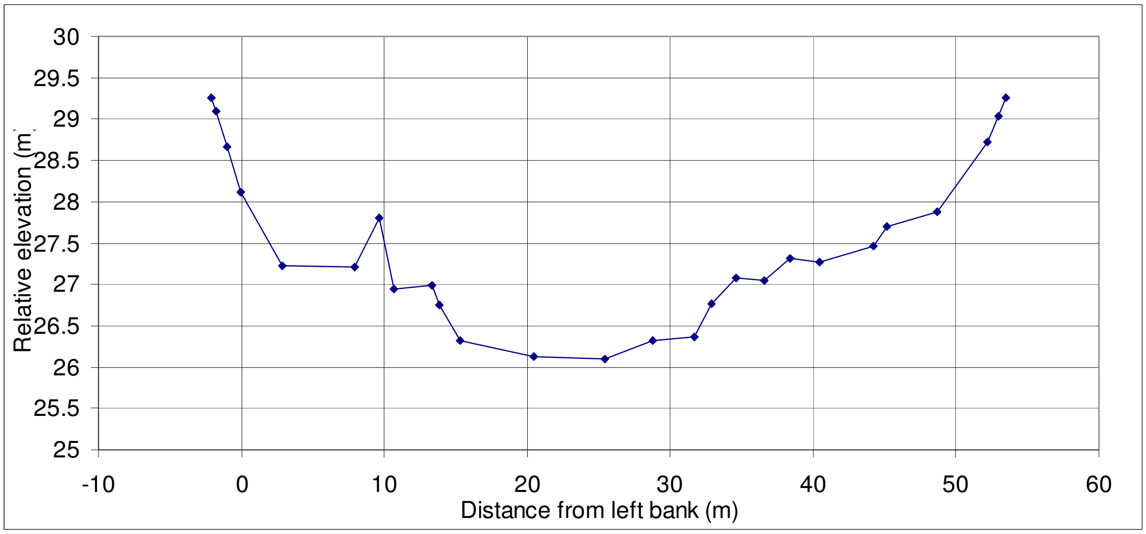

Figure B.8. Clear Creek Peltier 891+80 cross section.

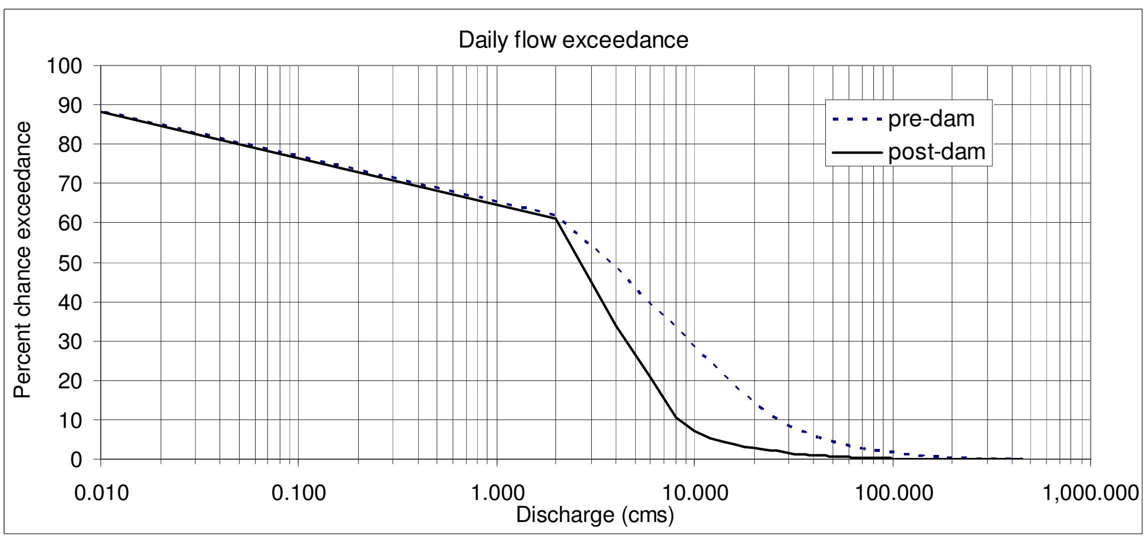

Figure B.9. Clear Creek flow exceedance, see Chapter 3, Table 2 for a list of the gages used and the dates of the pre- and post-dam periods.

Table B.7. Background data for Sacramento River bedload transport calculation site, at Bend Bridge gage	
Site Name	Bend Bridge
Location	102.7 km downstream of Keswick Dam
Gravel tracer?	no
Roughness, n	0.0365 (Manning-Gauckler n)
Floodplain, n	none – constant width of channel
Floodplain extent (using cross section stationing)	na

Table B.8. Grain Size Distribution. See Chapter 3, Table 3 for the data source. Excluding 2mm grains.				
Size (mm)	**% Finer**		**Grain Size Statistics**	
64	100		**Geometric mean (mm)**	21.48
32	75.19		**Geometric standard deviation**	1.72
16	30.13		**D10 (mm)**	9.74
8	2.02		**D16 (mm)**	11.29
4	0.16		**D25 (mm)**	14.1
2	0		**D50 (mm)**	21.72
			D65 (mm)	27.36
			D75 (mm)	31.9
			D84 (mm)	40.93
			D90 (mm)	48.4

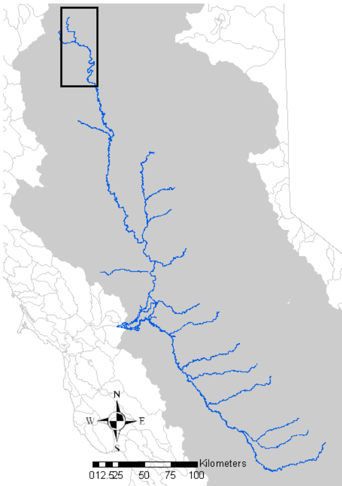

a

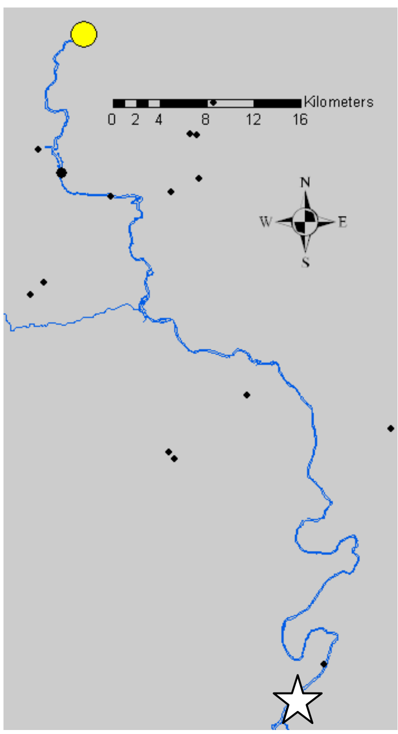

b

Figure B.10a,b. Location of Sacramento River Bend Bridge site. Figure B.1a is the location of the site in the Sacramento-San Joaquin river system, with the box showing the location of Figure B.1b. Figure B.1b is a reach-scale map from Shasta Dam (yellow dot) past the Clear Creek confluence (inflow from the west). Flow is top to bottom, with a star marking the location of the Bend Bridge gage. No cross section was used here to estimate bedload transport, instead, a constant width of 110 m was used.

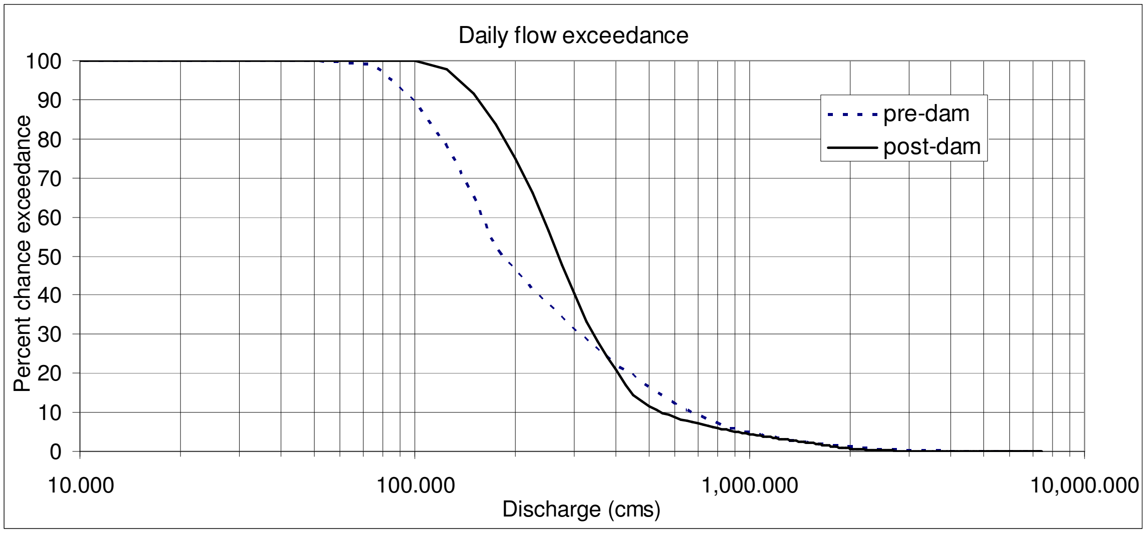

Figure B.11. Sacramento River daily flow exceedance, see Chapter 3, Table 2 for a list of the gages used and the dates of the pre- and post-dam periods. Here, only the pre-Shasta Dam and post-Whiskeytown Dam periods are shown.

Table B.9. Background data for Feather River bedload transport calculation site, Alecks Riffle (in Low Flow Channel)	
Site Name	Alecks Riffle
Location	14.05 km downstream of Oroville Dam
Gravel tracer?	no
Roughness, n	0.0365 (Manning-Gauckler n)
Floodplain, n	0.1
Floodplain extent (using cross section stationing)	<535 m, >639 m

Table B.10. Grain Size Distribution. See Chapter 3, Table 3 for the data source. Excluding 2mm grains.				
Size (mm)	**% Finer**		**Grain Size Statistics**	
256	100		**Geometric mean (mm)**	83.83
180	83.51		**Geometric standard deviation**	2.46
128	60.82		**D10 (mm)**	24.28
90	41.24		**D16 (mm)**	38.69
64	26.8		**D25 (mm)**	59.25
45	18.56		**D50 (mm)**	105.36
32	12.78		**D65 (mm)**	136.29
22.6	9.28		**D75 (mm)**	158.4
16	6.8		**D84 (mm)**	181.91
11.5	4.74		**D90 (mm)**	206.78
8	3.3			
5.6	2.06			
4	1.03			
2	0			

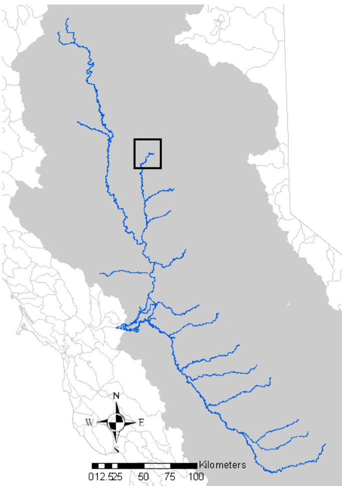

a

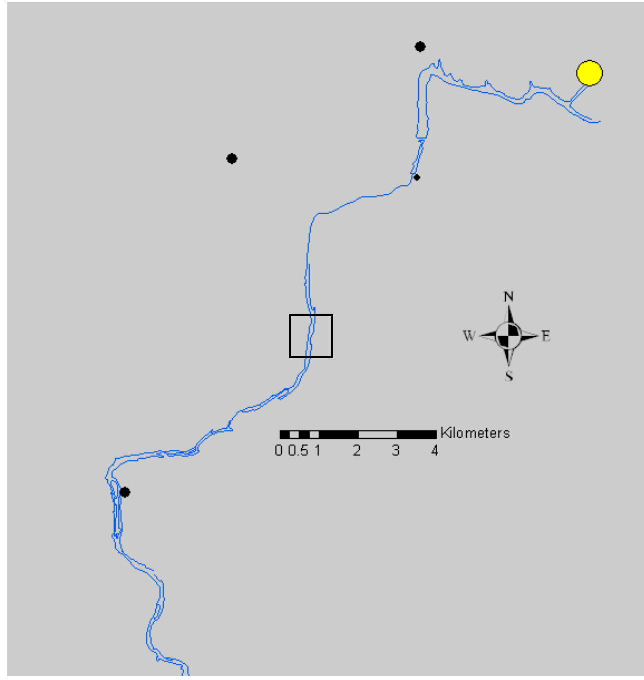

b

c

Figure B.12a-c. Location of Feather River site at Alecks Riffle (in Low Flow Channel). Figure B.1a is the location of the site in the Sacramento-San Joaquin river system, with the box showing the location of Figure B.1b. Figure B.1b is a reach-scale map from Oroville Dam (yellow dot), flow is top-right to bottom-left, with a box showing the location of figure B.1c. The diversion through the Thermalito complex re-enters the Feather River near the black dot in the lower left (Thermalito Outlet Dam, though it is plotted on the wrong side of the river). Figure B.1c is a recent aerial photograph, with the cross section line overlaid in white.

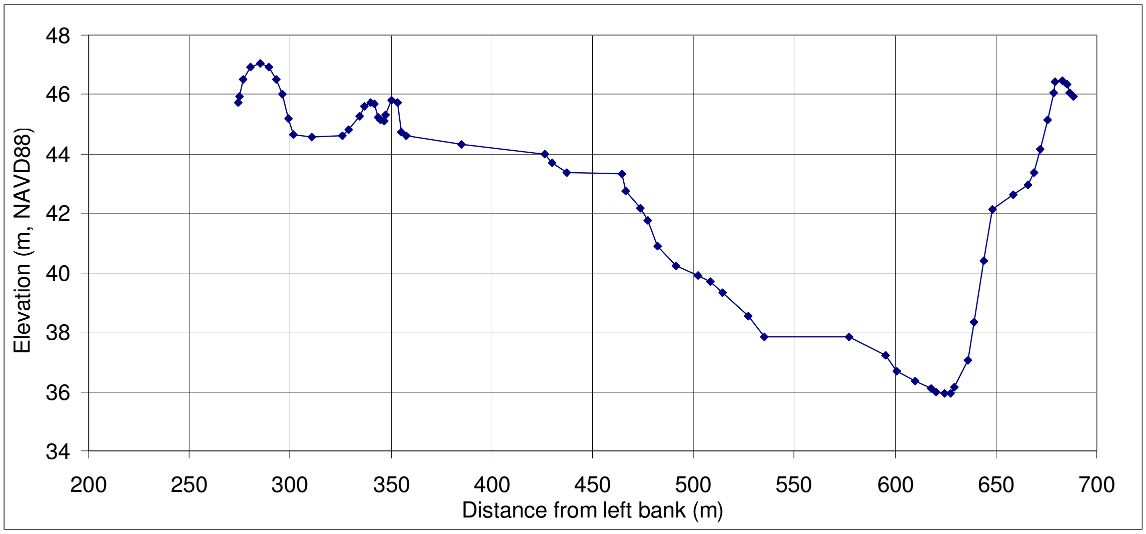

Figure B.13. Feather River Alecks Riffle cross section.

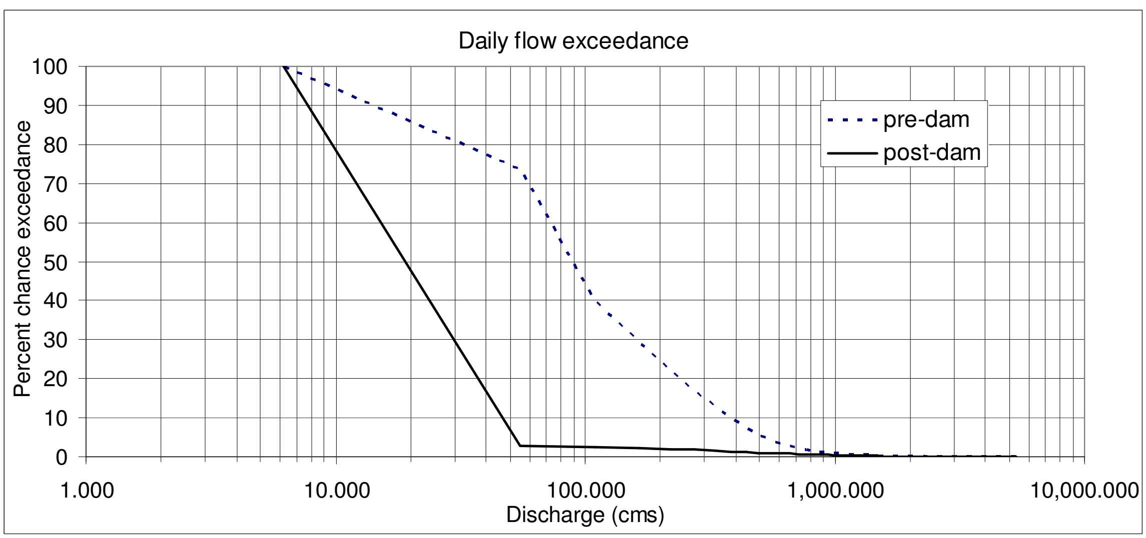

Figure B.14. Feather River flow exceedance, see Chapter 3, Table 2 for a list of the gages used and the dates of the pre- and post-dam periods.

Table B.11. Background data for Yuba River bedload transport calculation site, YR1	
Site Name	YR1
Location	10.4 km downstream of Englebright Dam
Gravel tracer?	yes, WY2006
Roughness, n	0.0365 (Manning-Gauckler n)
Floodplain, n	0.1
Floodplain extent (using cross section stationing)	<2.7 m, >148 m

Table B.12. Grain Size Distribution. See Chapter 3, Table 3 for the data source. Excluding 2mm grains.				
Size (mm)	**% Finer**		**Grain Size Statistics**	
180	100		**Geometric mean (mm)**	33.64
128	97		**Geometric standard deviation**	2.27
90	88		**D10 (mm)**	10.67
64	79		**D16 (mm)**	16
45	63		**D25 (mm)**	20.73
32	43		**D50 (mm)**	36.06
22.6	28		**D65 (mm)**	47.03
16	16		**D75 (mm)**	58.61
11.3	11		**D84 (mm)**	77.35
8	5		**D90 (mm)**	97.33
5.6	2			
4	2			
2	0			

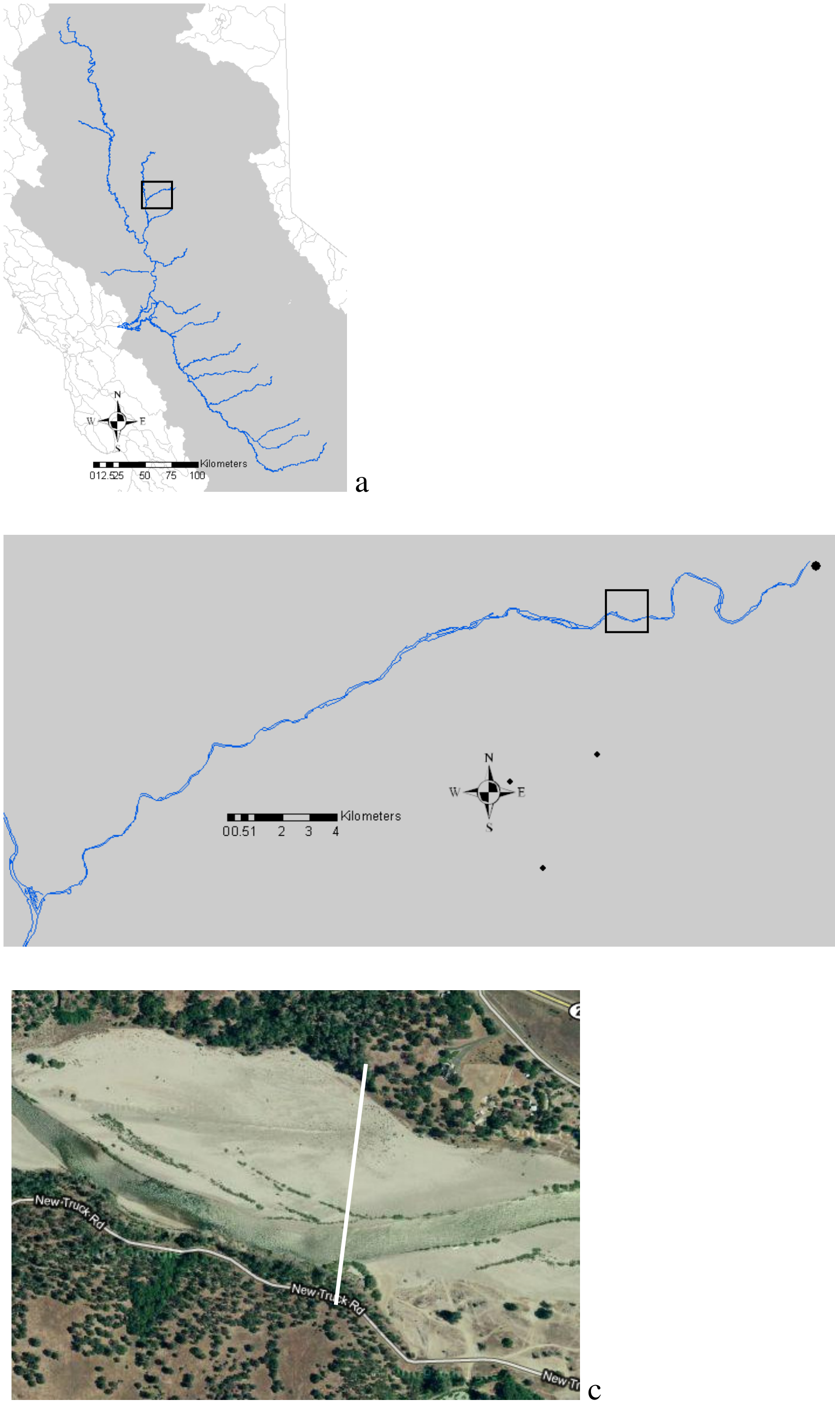

Figure B.15a-c. Location of Yuba River site YR1. Figure B.1a is the location of the site in the Sacramento-San Joaquin river system, with the box showing the location of Figure B.1b. Figure B.1b is a reach-scale map from Englebright Dam (black dot in upper right) down to the confluence with the Feather River, flow is right to left, with a box showing the location of figure B.1c. Figure B.1c is a recent aerial photograph, with the cross section line overlaid in white.

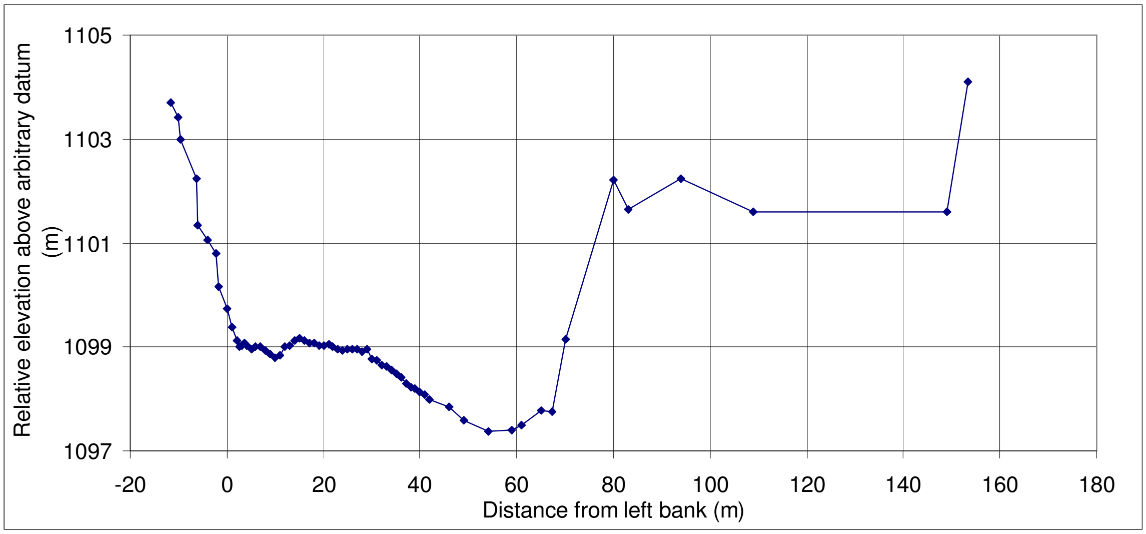

Figure B.16. Yuba River YR1 cross section.

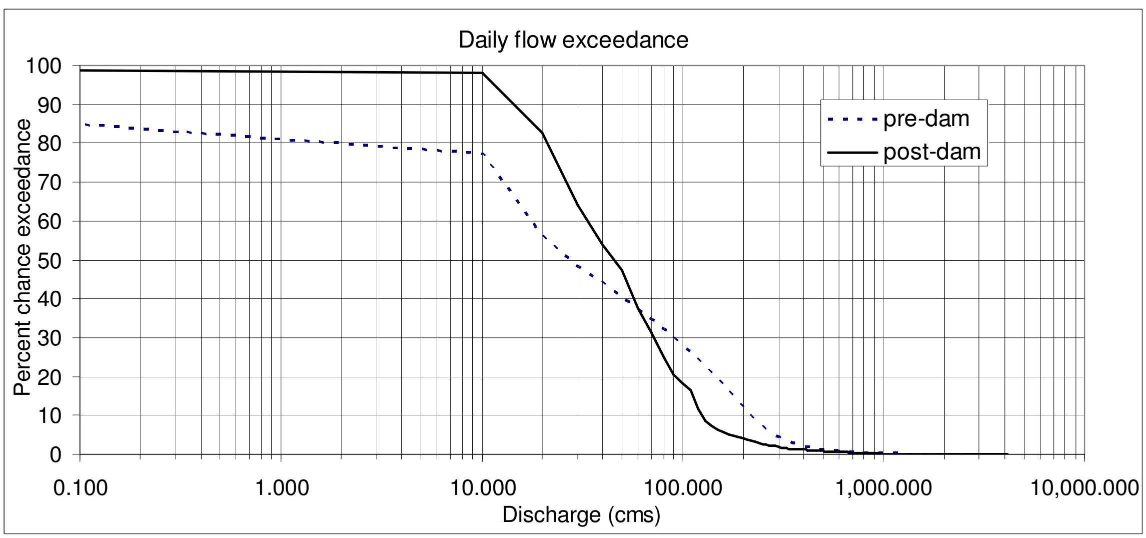

Figure B.17. Yuba River daily flow exceedance, see Chapter 3, Table 2 for a list of the gages used and the dates of the pre- and post-dam periods. Here, only the pre-Englebright Dam and post-New Bullards Bar Dam periods are shown.

Table B.13. Background data for Bear River bedload transport calculation site, BR1	
Site Name	BR1
Location	10.7 km downstream of New Camp Far West Dam
Gravel tracer?	yes, WY2006
Roughness, n	0.0365 (Manning-Gauckler n)
Floodplain, n	0.1
Floodplain extent (using cross section stationing)	<229 m, >267 m

Table B.14. Grain Size Distribution. See Chapter 3, Table 3 for the data source. Excluding 2mm grains.				
Size (mm)	**% Finer**		**Grain Size Statistics**	
180	100		**Geometric mean (mm)**	24.55
128	99		**Geometric standard deviation**	2.89
90	92		**D10 (mm)**	3.56
64	84		**D16 (mm)**	8.31
45	69		**D25 (mm)**	13.45
32	48		**D50 (mm)**	33.06
22.6	39		**D65 (mm)**	42.17
16	26		**D75 (mm)**	51.81
11.3	24		**D84 (mm)**	64
8	15		**D90 (mm)**	82.65
5.6	12			
4	12			
2	0			

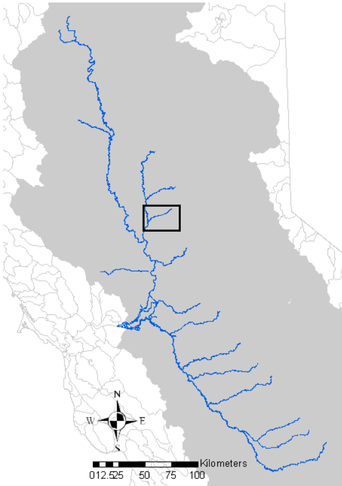

a

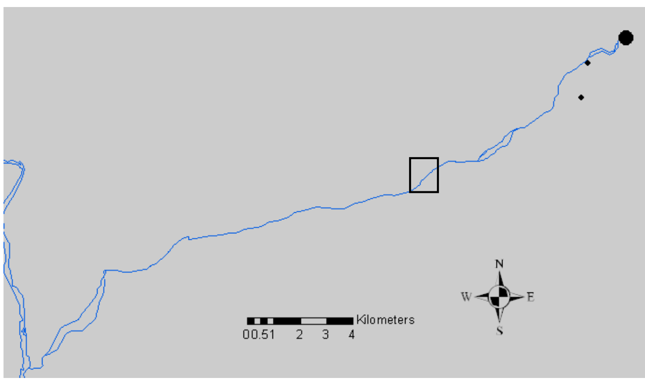

b

c

Figure B.18a-c. Location of Bear River site BR1. Figure B.1a is the location of the site in the Sacramento-San Joaquin river system, with the box showing the location of Figure B.1b. Figure B.1b is a reach-scale map from New Camp Far West Dam (large black dot in upper right) down to the confluence with the Feather River, flow is right to left, with a box showing the location of figure B.1c. Figure B.1c is a recent aerial photograph, with the cross section line overlaid in white and the Highway 65 bridge in the upper right..

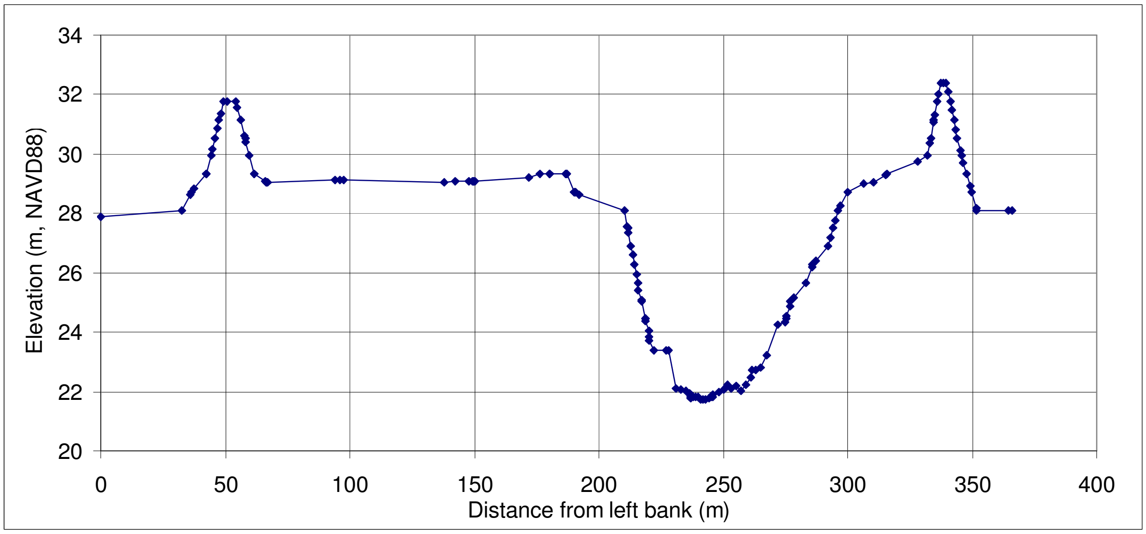

Figure B.19. Bear River BR1 cross section.

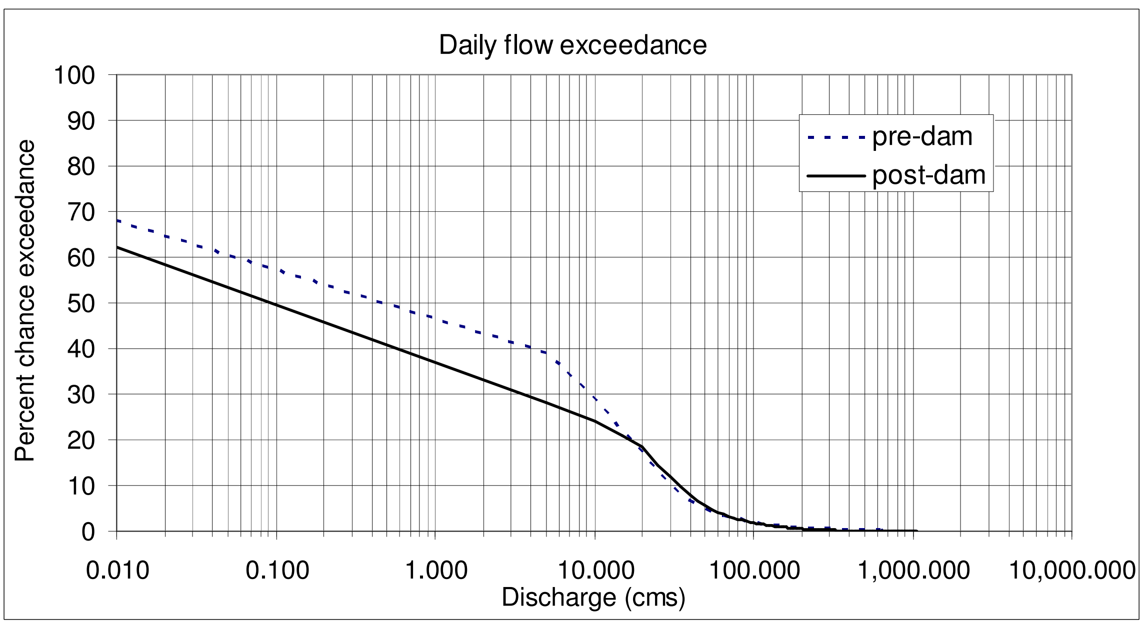

Figure B.20. Bear River flow exceedance, see Chapter 3, Table 2 for a list of the gages used and the dates of the pre- and post-dam periods.

Table B.15. Background data for American River bedload transport calculation site, AR1	
Site Name	AR1
Location	8.3 km downstream of Nimbus Dam
Gravel tracer?	yes, WY2006
Roughness, n	0.0365 (Manning-Gauckler n)
Floodplain, n	0.1
Floodplain extent (using cross section stationing)	<170 m, >280 m

Table B.16. Grain Size Distribution. See Chapter 3, Table 3 for the data source. Excluding 2mm grains.				
Size (mm)	**% Finer**		**Grain Size Statistics**	
256	100		**Geometric mean (mm)**	45.84
180	100		**Geometric standard deviation**	2
128	100		**D10 (mm)**	17.47
90	93.71		**D16 (mm)**	25.4
64	62.05		**D25 (mm)**	35.75
45	33.64		**D50 (mm)**	55.12
32	20.83		**D65 (mm)**	66.07
22.6	13.56		**D75 (mm)**	73.58
16	8.79		**D84 (mm)**	81.06
8	3.18		**D90 (mm)**	86.47
4	1.14			
2	0			

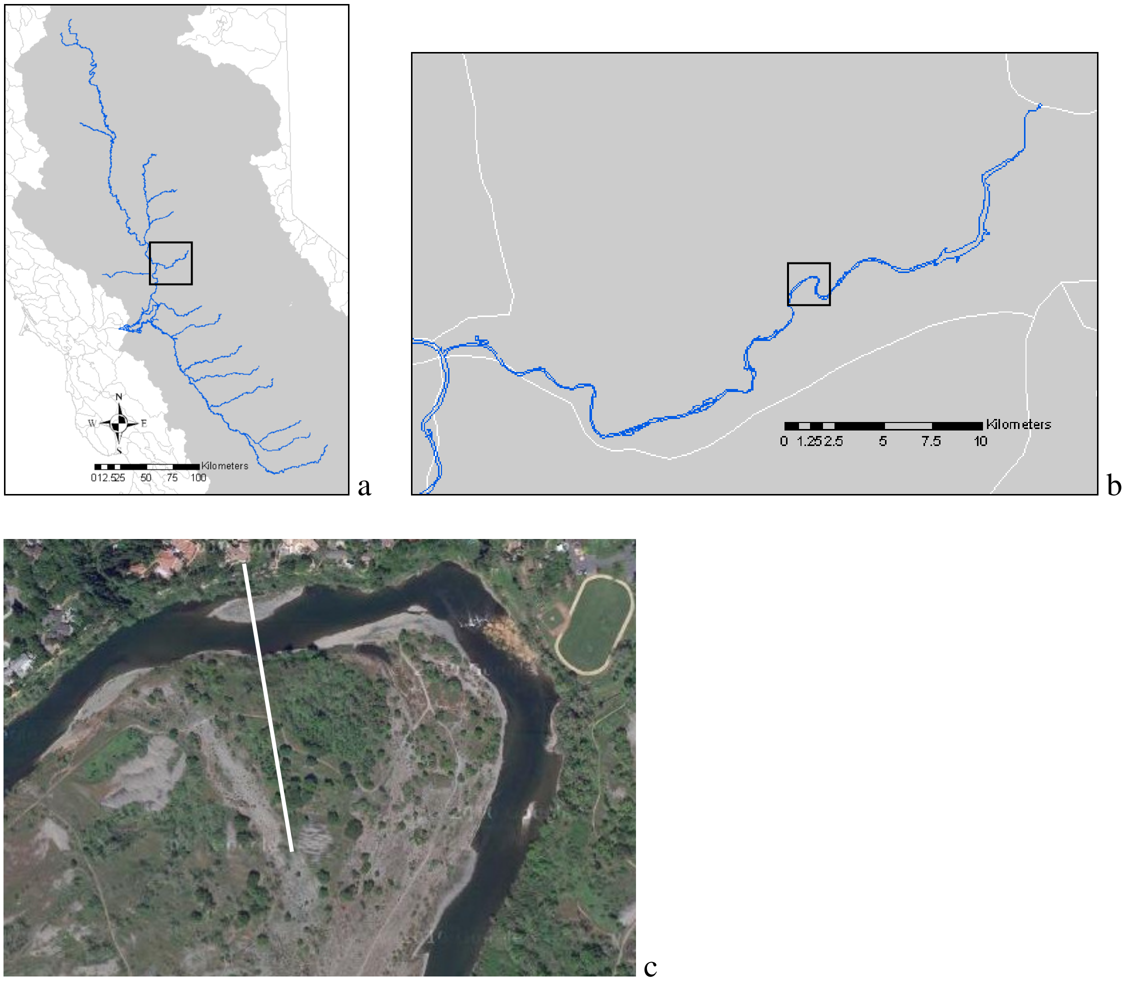

Figure B.21a-c. Location of American River site AR1. Figure B.1a is the location of the site in the Sacramento-San Joaquin river system, with the box showing the location of Figure B.1b. Figure B.1b is a reach-scale map from Folsom Dam down to the confluence with the Sacramento River, flow is right to left, with a box showing the location of figure B.1c. Figure B.1c is a recent aerial photograph, with the cross section line overlaid in white.

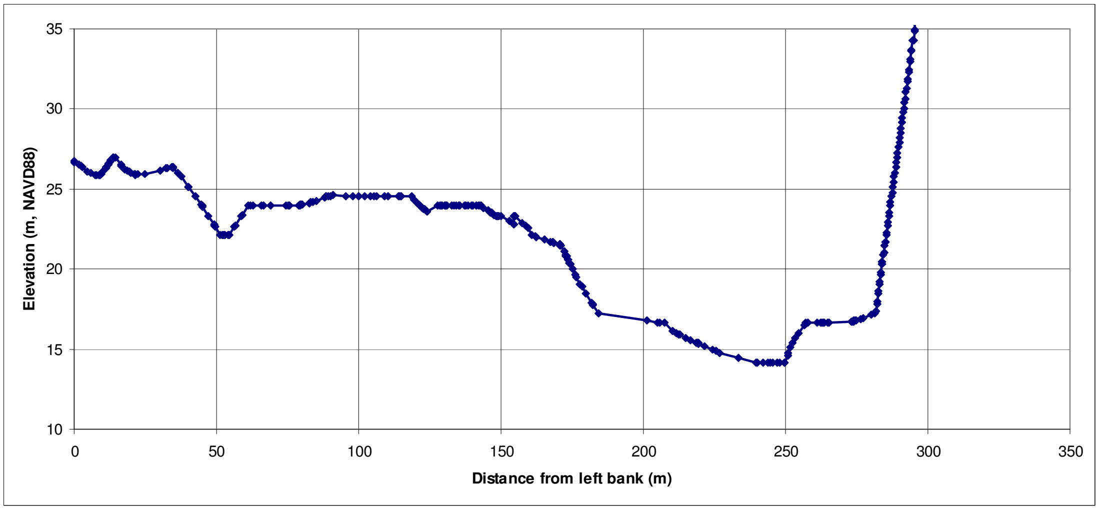

Figure B.22. American River site AR1 cross section.

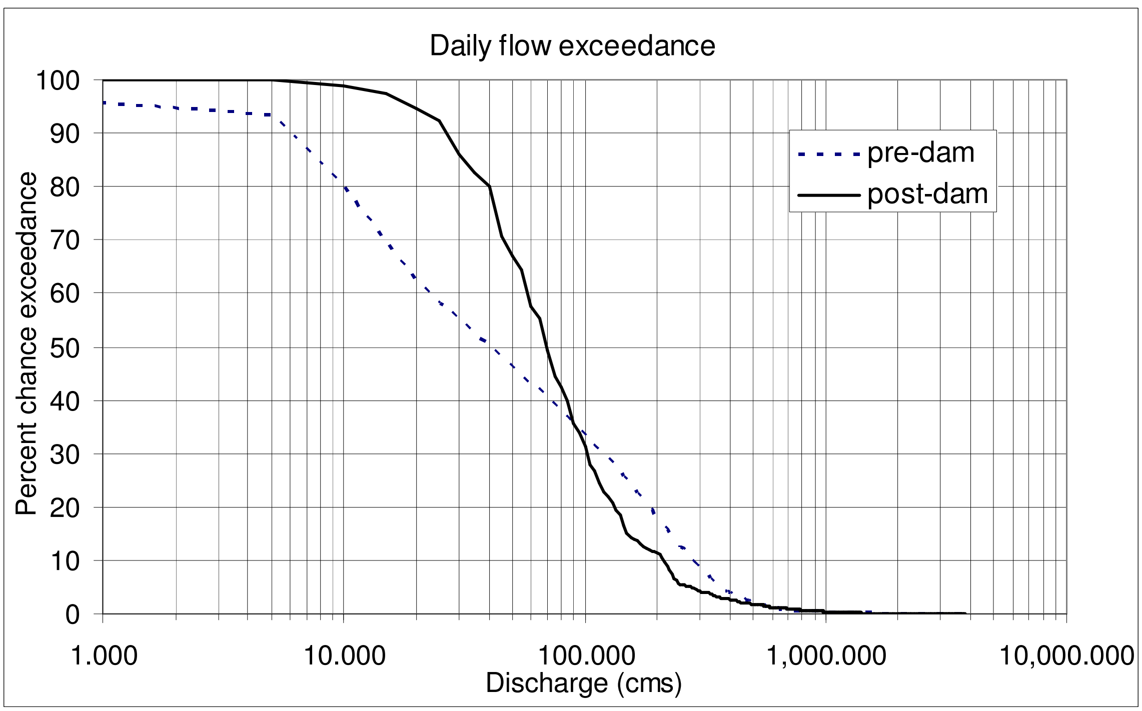

Figure B.23. American River site AR1 flow exceedance, see Chapter 3, Table 2 for a list of the gages used and the dates of the pre- and post-dam periods.

Table B.17. Background data for Mokelumne River bedload transport calculation site, XS 121	
Site Name	XS 121
Location	2.25 km downstream of Camanche Dam
Gravel tracer?	yes, WY2006
Roughness, n	0.0365 (Manning-Gauckler n)
Floodplain, n	0.1
Floodplain extent (using cross section stationing)	<178 m, >228 m

Table B.18. Grain Size Distribution. See Chapter 3, Table 3 for the data source. Excluding 2mm grains.				
Size (mm)	**% Finer**		**Grain Size Statistics**	
305	100		**Geometric mean (mm)**	23.18
152	100		**Geometric standard deviation**	2.7
76	86.81		**D10 (mm)**	5.65
38	64.84		**D16 (mm)**	7.52
19	42.86		**D25 (mm)**	10.97
10	21.98		**D50 (mm)**	23.8
4.8	6.59		**D65 (mm)**	38.2
2.5	0		**D75 (mm)**	52.36
			D84 (mm)	69.55
			D90 (mm)	89.86

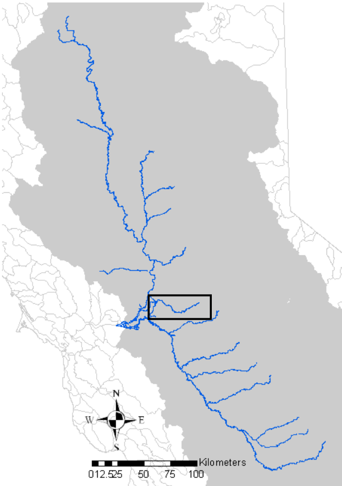

a

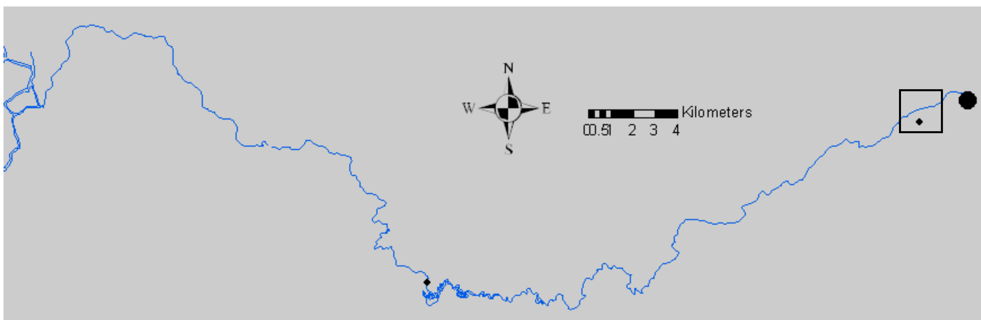

b

c

Figure B.24a-c. Location of Mokelumne River site XS 121. Figure B.1a is the location of the site in the Sacramento-San Joaquin river system, with the box showing the location of Figure B.1b. Figure B.1b is a reach-scale map from Camanche Dam (large black dot on far right) down to the Delta. Flow is right to left, with a box showing the location of figure B.1c. Figure B.1c is a recent aerial photograph, with the cross section line overlaid in white.

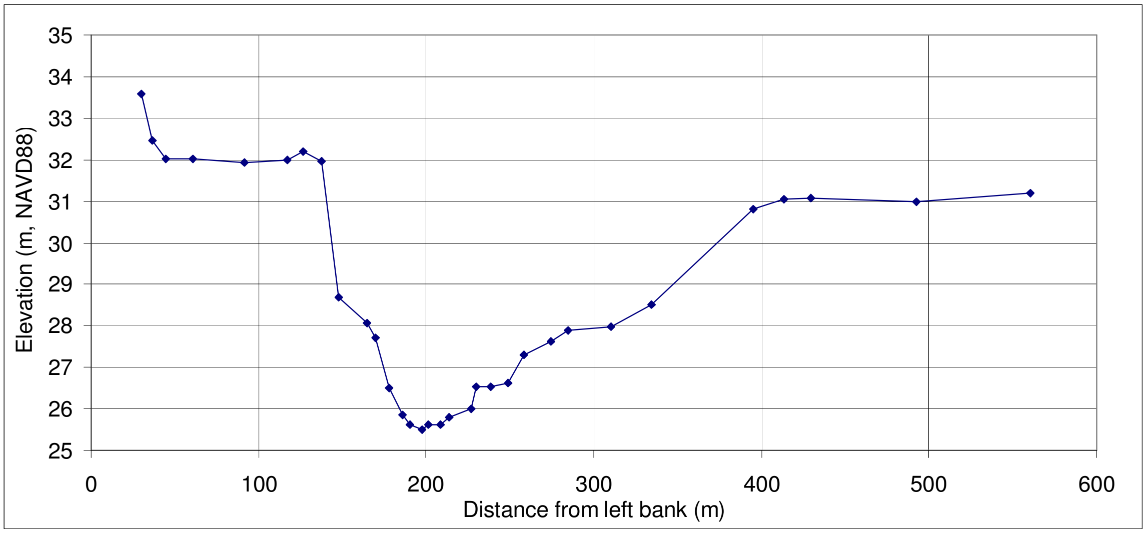

Figure B.25. Mokelumne River XS121 cross section.

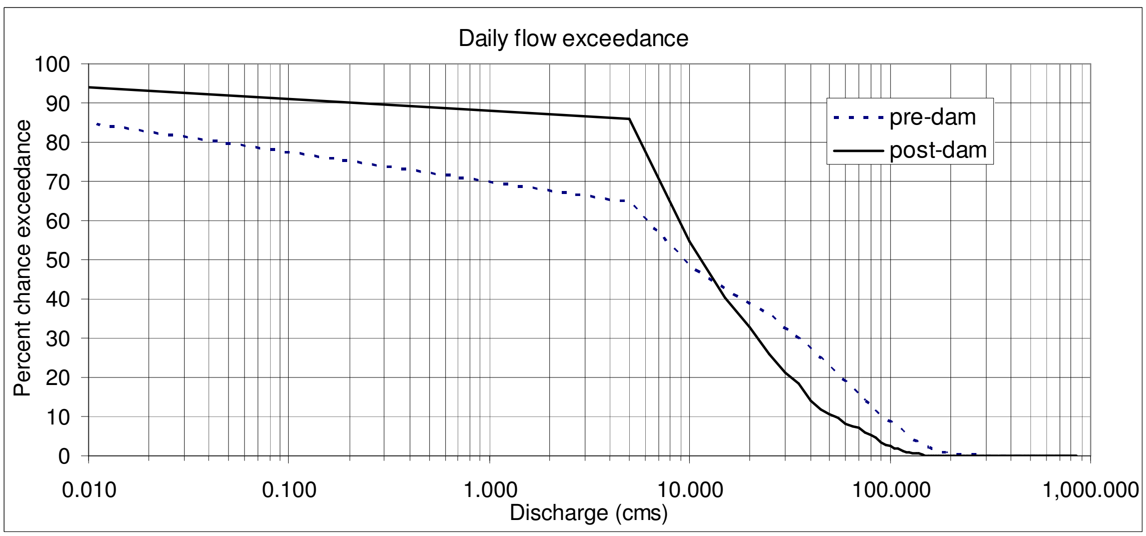

Figure B.26. Mokelumne River daily flow exceedance, see Chapter 3, Table 2 for a list of the gages used and the dates of the pre- and post-dam periods. Pre-dam data is for pre-Pardee Dam, post-dam data is for post-Camanche Dam.

Table B.19. Background data for Stanislaus River bedload transport calculation site, R10	
Site Name	R10
Location	8.8 km downstream of Goodwin Dam
Gravel tracer?	no
Roughness, n	0.0365 (Manning-Gauckler n)
Floodplain, n	0.1
Floodplain extent (using cross section stationing)	<3.7 m, >27.8 m

Table B.20. Grain Size Distribution. See Chapter 3, Table 3 for the data source. Excluding 2mm grains.				
Size (mm)	**% Finer**		**Grain Size Statistics**	
128	100		**Geometric mean (mm)**	44.98
92	90		**Geometric standard deviation**	1.75
80	84		**D10 (mm)**	24.5
69	75		**D16 (mm)**	28
46.5	50		**D25 (mm)**	31
31	25		**D50 (mm)**	46.5
28	16		**D65 (mm)**	58.92
24.5	10		**D75 (mm)**	69
8	0		**D84 (mm)**	80
			D90 (mm)	92

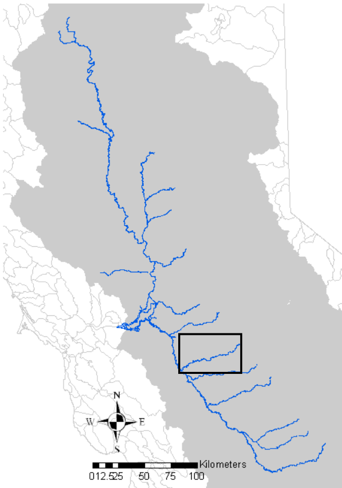

a

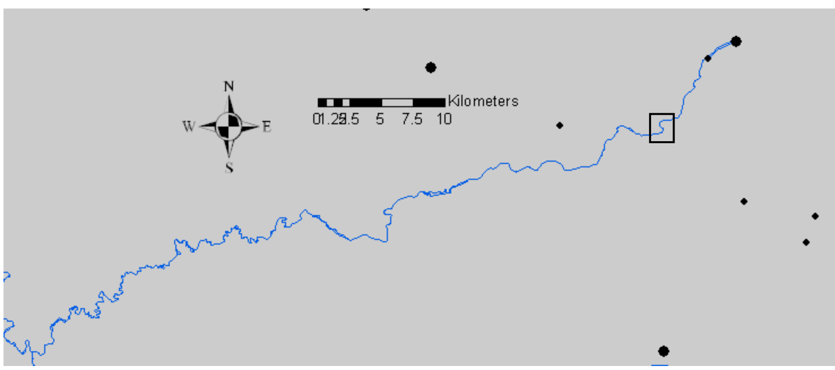

b

c

Figure B.27a-c. Location of Stanislaus River site R10. Figure B.1a is the location of the site in the Sacramento-San Joaquin river system, with the box showing the location of Figure B.1b. Figure B.1b is a reach-scale map from Goodwin Dam down to the confluence with the San Joaquin River (Tulloch Dam is the largest black dot to the right, immediately upstream of Goodwin Dam, the next black dot). Flow is right to left, with a box showing the location of figure B.1c. Figure B.1c is a recent aerial photograph, with the cross section line overlaid in white.

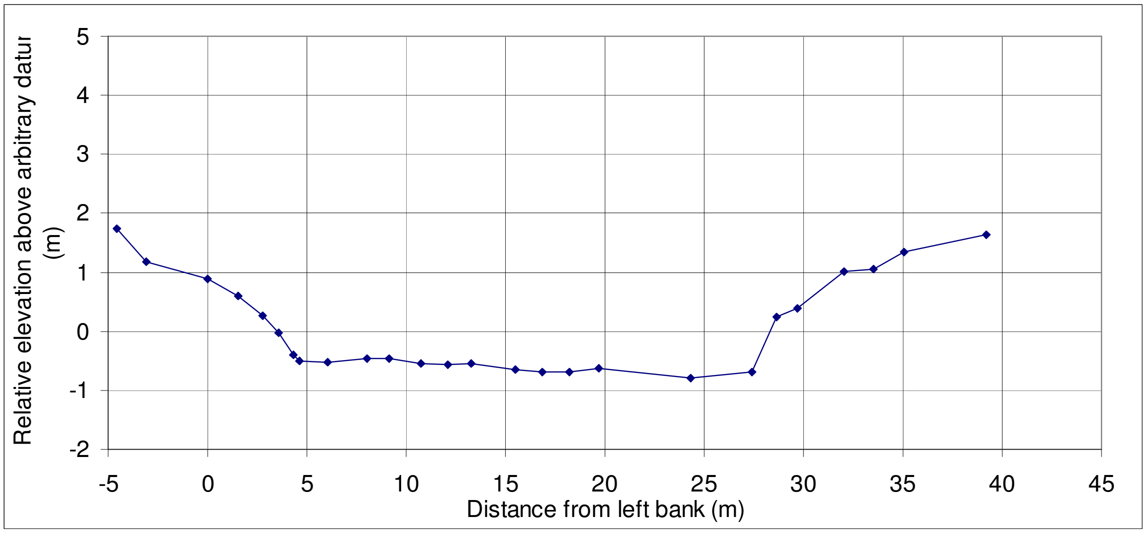

Figure B.28. Stanislaus River R10 cross section.

Figure B.29. Stanislaus River flow exceedance, see Chapter 3, Table 2 for a list of the gages used and the dates of the pre- and post-dam periods.

Table B.21. Background data for Tuolumne River bedload transport calculation site, II-10	
Site Name	II-10
Location	3.1 km downstream of La Grange Dam
Gravel tracer?	no
Roughness, n	0.0365 (Manning-Gauckler n)
Floodplain, n	0.1
Floodplain extent (using cross section stationing)	<67 m, >96 m

Table B.22. Grain Size Distribution. See Chapter 3, Table 3 for the data source. Excluding 2mm grains.				
Size (mm)	**% Finer**		**Grain Size Statistics**	
180	100		**Geometric mean (mm)**	63.7
128	97.32		**Geometric standard deviation**	1.54
90	76.52		**D10 (mm)**	34.93
64	47.55		**D16 (mm)**	39.38
45	22.67		**D25 (mm)**	46.51
32	5.61		**D50 (mm)**	65.87
22.6	0.46		**D65 (mm)**	78.59
16	0.3		**D75 (mm)**	88.41
8	0		**D84 (mm)**	102.16
			D90 (mm)	113.09

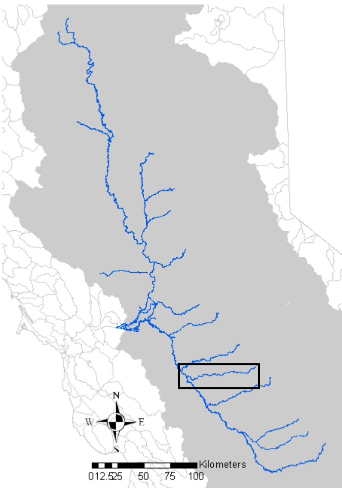

a

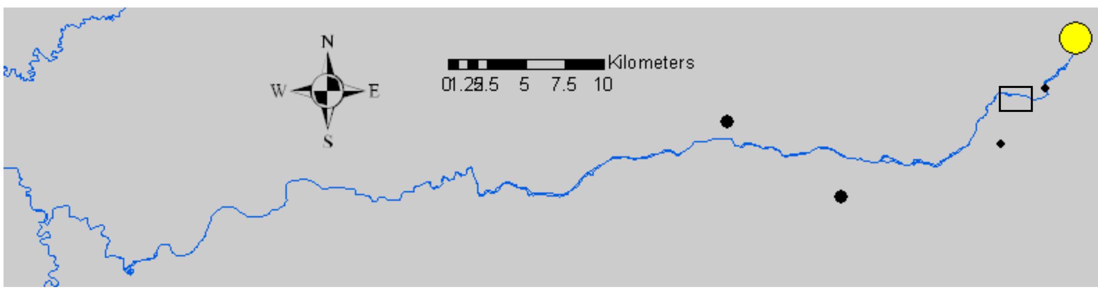

b

c

Figure B.30a-c. Location of Tuolumne River site II-10. Figure B.1a is the location of the site in the Sacramento-San Joaquin river system, with the box showing the location of Figure B.1b. Figure B.1b is a reach-scale map from New Don Pedro Dam (large yellow dot) down to the confluence with the San Joaquin River (La Grange Dam is the small black dot just downstream of New Don Pedro). Flow is right to left, with a box showing the location of figure B.1c. Figure B.1c is a recent aerial photograph, with the cross section line overlaid in white and New La Grange bridge on the left, and Old La Grange bridge on the right.

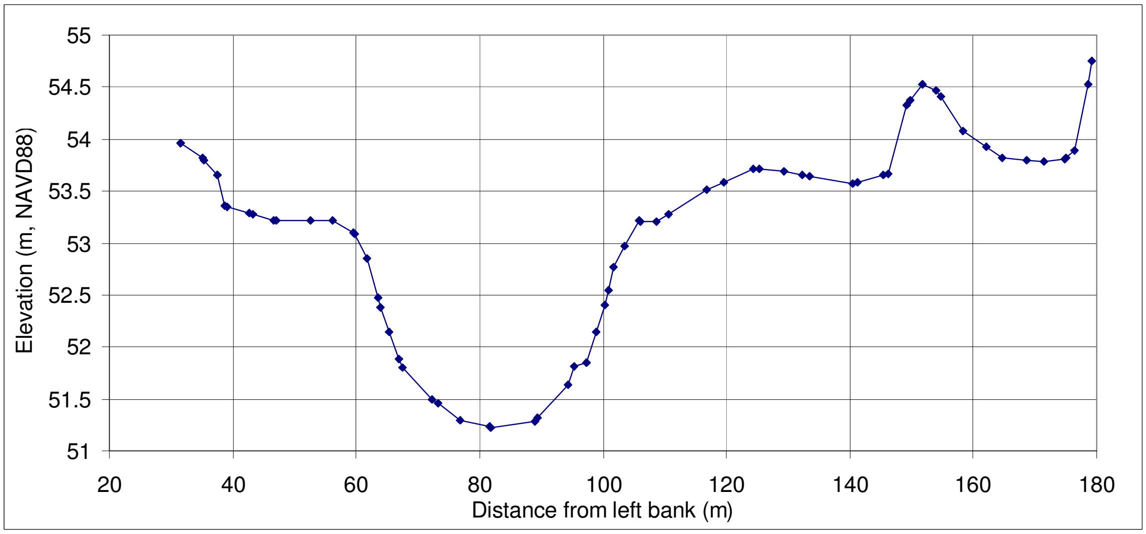

Figure B.31. Tuolumne River II-10 cross section.

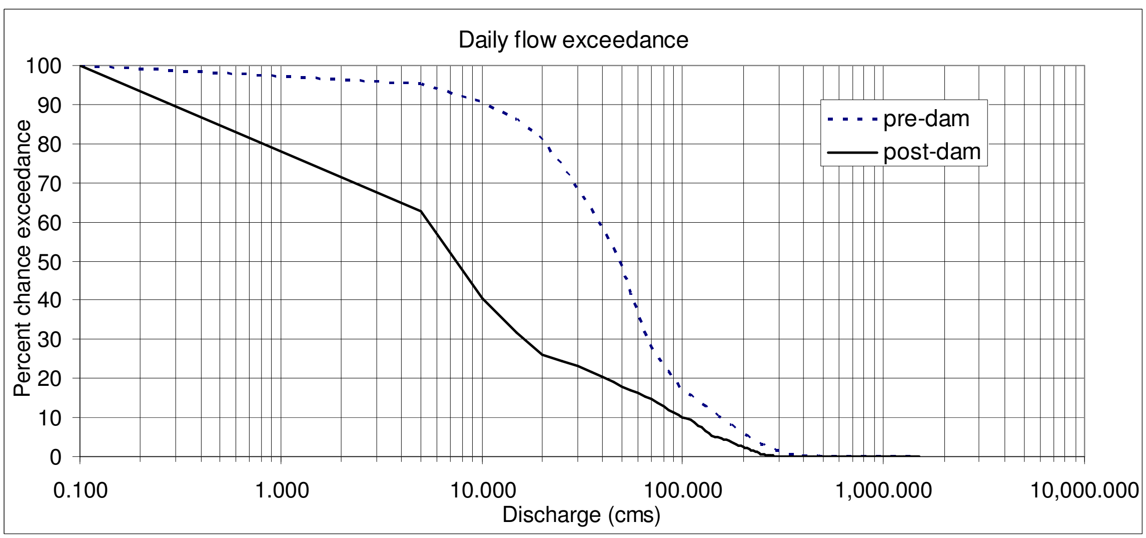

Figure B.32. Tuolumne River daily flow exceedance, see Chapter 3, Table 2 for a list of the gages used and the dates of the pre- and post-dam periods.

Table B.23. Background data for Merced River bedload transport calculation site, XS 144	
Site Name	XS 144
Location	13.8 km downstream of New Exchequer (0.3 km downstream of Crocker-Huffman Diversion Dam)
Gravel tracer?	no
Roughness, n	0.0365 (Manning-Gauckler n)
Floodplain, n	0.1
Floodplain extent (using cross section stationing)	<256 m, >290 m

Table B.24. Grain Size Distribution. See Chapter 3, Table 3 for the data source. Excluding 2mm grains.				
Size (mm)	**% Finer**		**Grain Size Statistics**	
512	100		**Geometric mean (mm)**	105.91
360	99.13		**Geometric standard deviation**	2.15
256	97.26		**D10 (mm)**	44.77
180	76.39		**D16 (mm)**	54.51
128	46.06		**D25 (mm)**	70.96
90	34.24		**D50 (mm)**	133.8
64	20.99		**D65 (mm)**	158.37
45	10.04		**D75 (mm)**	177.2
32	7.35		**D84 (mm)**	204.66
22.6	4.05		**D90 (mm)**	226.46
16	3.69			
11.6	2.98			
8	1.21			
4	0			

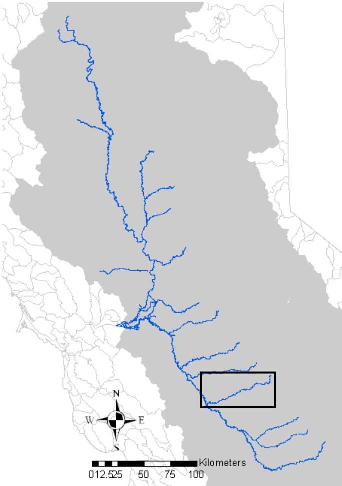

a

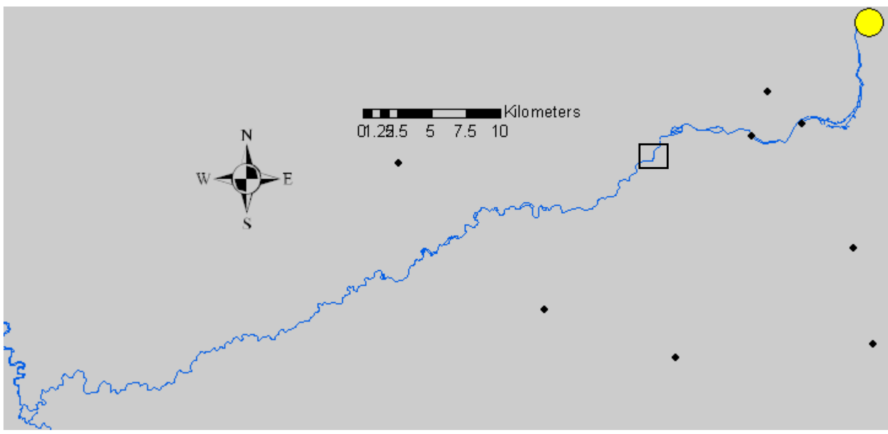

b


c

Figure B.33a-c. Location of Merced River site XS 144. Figure B.1a is the location of the site in the Sacramento-San Joaquin river system, with the box showing the location of Figure B.1b. Figure B.1b is a reach-scale map from New Exchequer Dam (yellow dot) down to the confluence with the San Joaquin River (small black dots downstream of New Exchequer are Merced Falls Dam and Crocker-Huffman Dams). Flow is right to left, with a box showing the location of figure B.1c. Figure B.1c is a recent aerial photograph, with the cross section line overlaid in white.

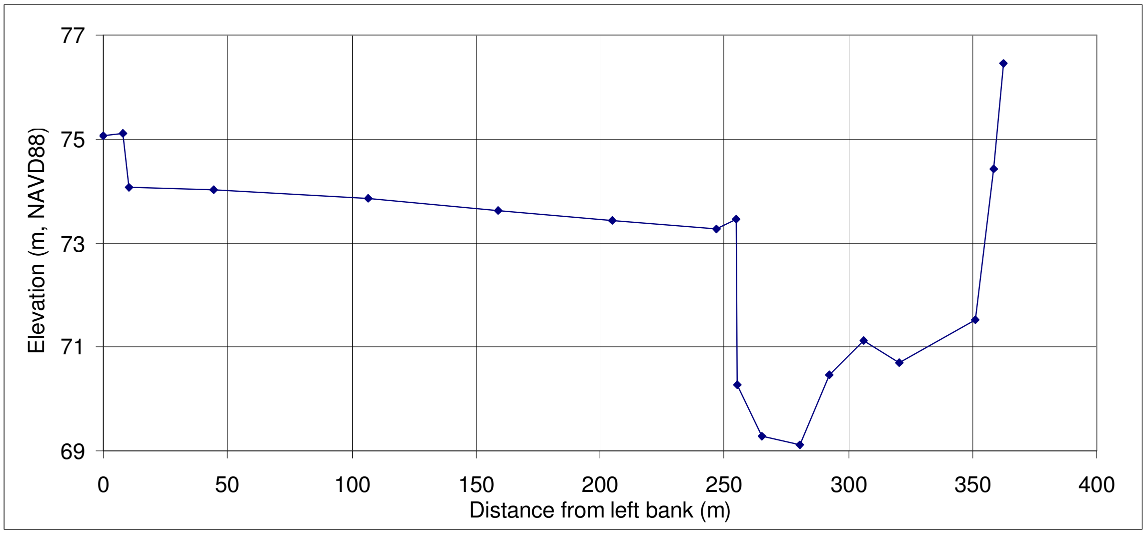

Figure B.34. Merced River XS 144 cross section.

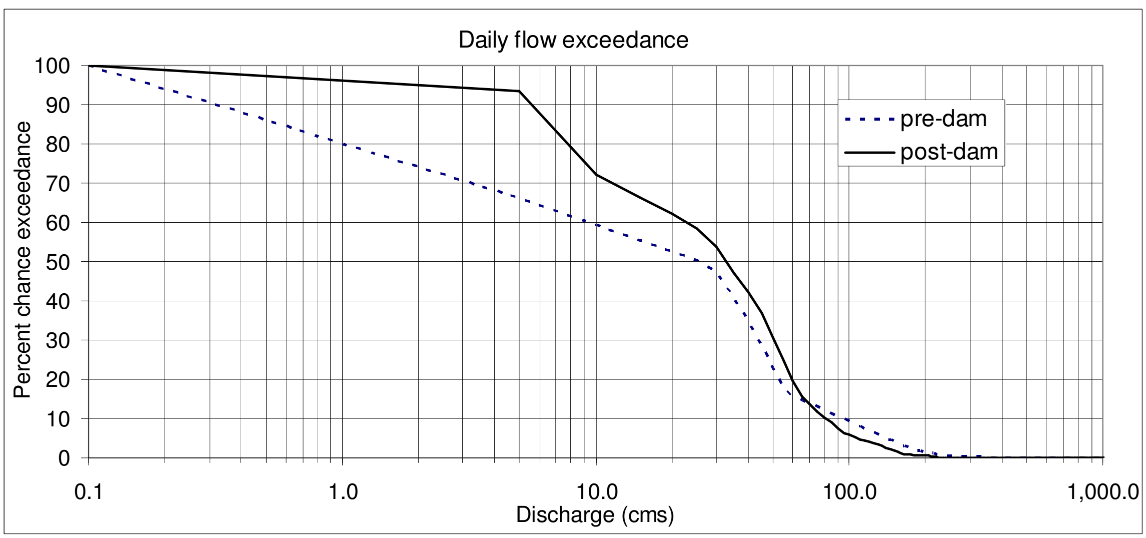

Figure B.35. Merced River daily flow exceedance, see Chapter 3, Table 2 for a list of the gages used and the dates of the pre- and post-dam periods.

Table B.25. Background data for San Joaquin River bedload transport calculation site, SJR1	
Site Name	SJR1
Location	1.51 km downstream of Friant Dam
Gravel tracer?	yes, WY2006
Roughness, n	0.0365 (Manning-Gauckler n)
Floodplain, n	0.1
Floodplain extent (using cross section stationing)	<138 m, >164 m

Table B.26. Grain Size Distribution. See Chapter 3, Table 3 for the data source. Excluding 2mm grains.				
Size (mm)	**% Finer**		**Grain Size Statistics**	
360	100		**Geometric mean (mm)**	46.67
256	99		**Geometric standard deviation**	3.02
180	98		**D10 (mm)**	10.07
128	75		**D16 (mm)**	13.19
90	62		**D25 (mm)**	19.49
64	54		**D50 (mm)**	55.59
45	44		**D65 (mm)**	97.62
32	33		**D75 (mm)**	128
22.6	28		**D84 (mm)**	146.27
16	21		**D90 (mm)**	159.87
11.3	12			
8	6			
5.6	4			
4	3			
2	0			

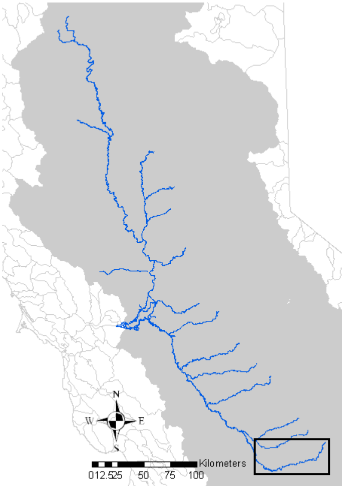

a

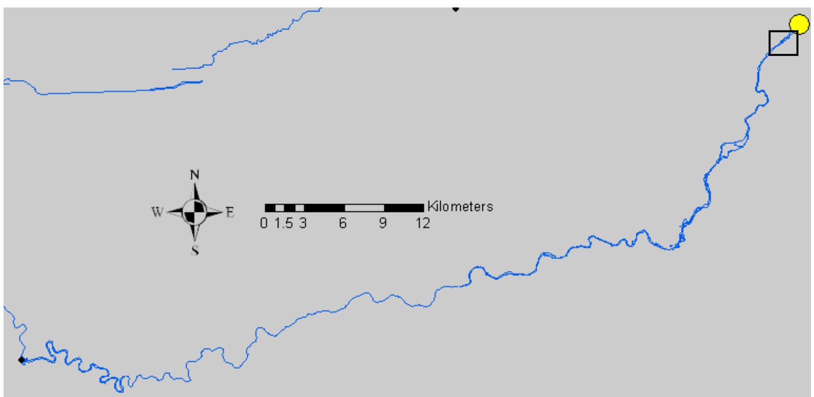

b

c

Figure B.36a-c. Location of San Joaquin River site SJR1. Figure B.1a is the location of the site in the Sacramento-San Joaquin river system, with the box showing the location of Figure B.1b. Figure B.1b is a reach-scale map from Friant Dam (yellow dot) down to the Mendota pool (small black dot in lower left corner). Flow is right to left, with a box showing the location of figure B.1c. Figure B.1c is a recent aerial photograph, with the cross section line overlaid in white, the North Fork Bridge is in the upper right corner.

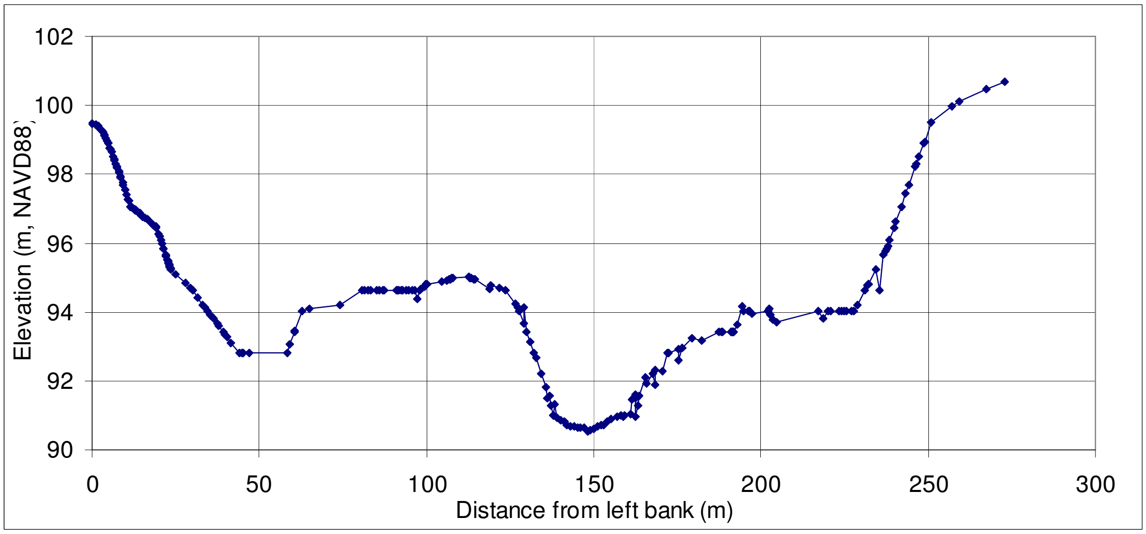

Figure B.37. San Joaquin River SJR1 cross section.

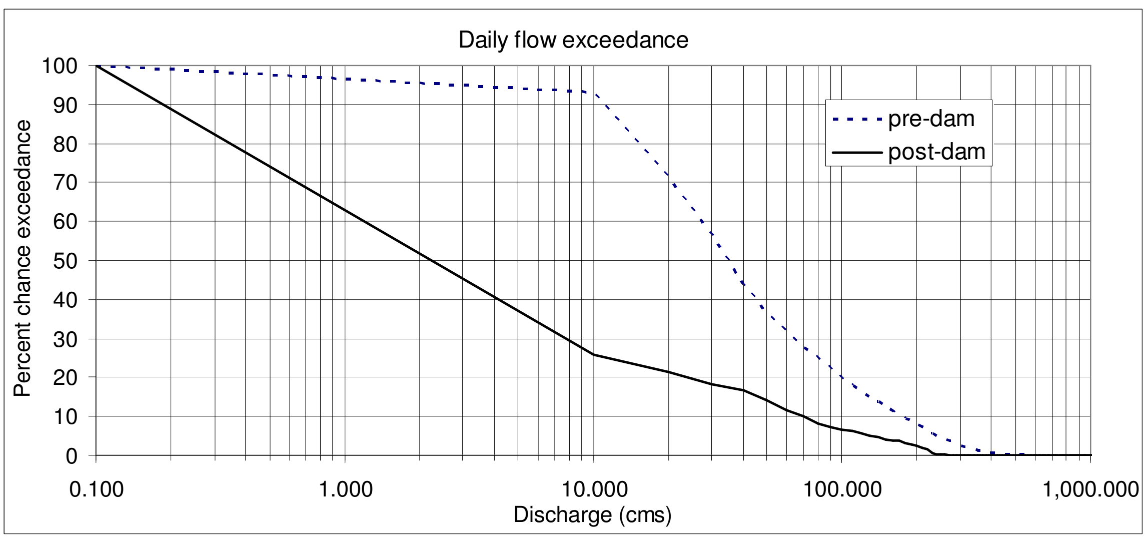

Figure B.38. San Joaquin River daily flow exceedance, see Chapter 3, Table 2 for a list of the gages used and the dates of the pre- and post-dam periods.